

**Role of cholesterol glucosylation in maintenance of
Helicobacter pylori morphology, cell wall integrity and
regulation of Mincle receptor response**

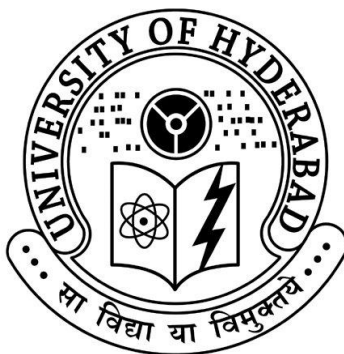
**Thesis Submitted to the University of Hyderabad
For the Degree of**

DOCTOR OF PHILOSOPHY

By

Majjid Ahmed Saleh Qaria

(Reg. No: 15LTPH10)



**Department of Biotechnology and Bioinformatics
School of Life Sciences
University of Hyderabad
Hyderabad-500046
INDIA**

November, 2018

University of Hyderabad

(A Central University by an Act of Parliament)

Department of Biotechnology and Bioinformatics

School of Life Sciences

P.O. Central University, Gachibowli, Hyderabad-500046



DECLARATION

The research work presented in the thesis entitled **“Role of cholesterol glucosylation in maintenance of *Helicobacter pylori* morphology, cell wall integrity and regulation of Mincle receptor response”** has been carried out by me at the Department of Biotechnology and Bioinformatics, School of Life Sciences, University of Hyderabad, Hyderabad, under the guidance of Professor Dr. Niyaz Ahmed. I hereby declare that this work is original and has not been submitted in part or full for any other degree or diploma of any other University or Institution.

Date:

Signature:

Name: Majjid Ahmed Saleh Qaria

Reg. No.: 10LTPM05

University of Hyderabad

(A Central University by an Act of Parliament)

Department of Biotechnology and Bioinformatics

School of Life Sciences

P.O. Central University, Gachibowli, Hyderabad-500046



CERTIFICATE

This is to certify that the thesis entitled **“Role of cholesterol glucosylation in maintenance of *Helicobacter pylori* morphology, cell wall integrity and regulation of Mincle receptor response”** submitted by Mr. Majjid Ahmed Saleh Qaria bearing registration number 15LTPH10 in partial fulfillment of the requirements for award of Doctor of Philosophy in the Department of Biotechnology and Bioinformatics, School of Life Sciences is a bonafide work carried out by him under my supervision and guidance.

This thesis is free from plagiarism and has not been submitted previously in part or in full to this or any other University or Institution for award of any degree or diploma.

Parts of this thesis have been:

A. Published and/or under Consideration in the following journals:

Majjid A. Qaria, Naveen Kumar, Arif Hussain, Shamsul Qumar, Sankara N. Doddam, Ludovico P. Sepe, Niyaz Ahmed. The role of cholesteryl- α -glucosides transferase and cholesteryl glucosides in maintenance of *Helicobacter pylori* morphology, cell wall integrity and resistance to antibiotics, mBio (accepted manuscript)

B. Presented in the following conferences:

Delivered oral presentation in International conference on Immunology (Major Breakthroughs and Advances in Immunology of Human Diseases) held during 26th-28th of September 2018 at School of Bioengineering, SRM Institute of Science and Technology, Chennai, India. (International).

Further, the student has passed the following courses towards fulfillment of course work requirements for the award of Ph.D.

S. No.	Course code	Subject	Credits	Remarks
1	BT-801	Analytical Techniques	4	Pass
2	BT-802	Research Ethics, Data Analysis and Biostatistics	3	Pass
3	BT-803	Lab Work and Seminar	5	Pass

Prof. Niyaz Ahmed

Research supervisor
Dept. of Biotechnology and Bioinformatics

Head

Dept. of Biotechnology and Bioinformatics

Dean

School of Life Sciences

*Dedicated to
my beloved family*

Acknowledgement

For Almighty ALLAH is all praise as befits for the strength and the light that he bestowed me to finish this research.

Here comes the day to thank my family who gave me unconditional love, encouragement and support to pursue my dreams and them patience to bear the pain of separation.

I express my deepest gratitude and sincere regards to my supervisor Prof. Niyaz Ahmed for his excellent guidance, paramount mentorship, and unwavering support that has helped me to overcome challenges during my work. I especially thank him for being open to new ideas and allowing one to pursue them. You are always a source of inspiration to me, I have learnt a lot from him both directly and indirectly which would definitely help me in the future. I thank you for the spellbinding way of delivering the talks and your scientific vision and sharing with us your experience in and out of lab. I am extremely indebted to you for the encouragement, motivation and keeping lab energetic by conducting a conclusive discussions and enjoying the lab members parties.

I would like to thank Dr. Nooruddin Khan and Prof. P. Prakash Babu for their accessibility as doctoral committee member to evaluate my PhD progress per semester. I acknowledge the present and former Heads of Dept. of Biotechnology and Bioinformatics and Deans of School of Life Sciences for allowing me to use the general facility of the school.

I would like to thank all my PBL family members Dr. Arif, Dr. Shankar, Naveen Kumar for them immense support in all possible way and providing a friendly atmosphere to pursue my Ph.D. work. I would like to express my sincere thanks to Dr. Nishanth, Dr. Amit Dr. Shivendar, Dr. Savita, Dr. Vidhyulatha, and Samshul for helping me and guiding me and troubleshoot the research problems during my PhD. I would like to acknowledge Priya, Kishore, Sabiha, Dr. Mohammed Majid, Dr. Ramani, Arya Suresh, Sumeet Tiwari, Shveta and Arun for their co-operation and providing friendly atmosphere in the lab.

*My heartfelt thanks to Prof. Dr. Thomas F Meyer for giving all research support and his valuable contributions to our *H. pylori* research group, Max Planck Institute of Infection Biology, Berlin, Germany. Also, I sincerely thank Dr. Ludo Vico for helping me during my research.*

Majjid Qaria

INDEX

	Page No.
Abbreviations	I-II
Chapter 1: Introduction	1-34
Chapter 2: Objective-1	35-67
Chapter 3: Objective-2	68-87
Chapter 4: Objective-3	88-100
Summary and conclusions	101-103
Publication	104

ABBREVIATIONS

BCA	: Bicinchoninic Acid
bp	: Base pair
BSA	: Bovine serum albumin
cagA	: Cytotoxin associated gene A
cDNA	: complementary Deoxyribonucleic Acid
CFU	: Colony forming units
CLR	: C-type lectin receptor
CRD	: Carbohydrate-recognition domain
DNA	: Deoxyribonucleic acid
dNTP	: Deoxyribonucleotide triphosphate
DU	: Duodenal ulcer
GAPDH	: Glyceraldehyde 3-phosphate dehydrogenase
SabA	: Sialic-acid binding adhesin
GU	: Gastric ulcer
αCG	: cholesteryl- α -D-glucopyranoside
αCAG	: cholesteryl-6-O-tetradecanoyl- α -D-glucopyranoside (α CAG)
APC	: Antigen-presenting cell
αCPG	: cholesteryl-6-O-phosphatidyl- α -D-glucopyranoside
IFNγ	: Interferon gamma
CGT	: cholesteryl- α -glucosyl transferase
T4SS	: type IV secretion system
MβCD	: Methyl- β -cyclodextrin
ACGal	: cholesteryl 6-O-acyl- β -D-galactopyranoside
CGal	: cholesterol- β -D-galactopyranoside
csds	: cell shape determinants
FC	: Flow cytometry
OD	: Optical Density
qRT-PCR	: Quantitative real time PCR
KDa	: kilo Dalton
LPS	: Lipopolysaccharides

MALT	: Mucosa-Associated Lymphoid Tissue
Mincle	: Macrophage inducible C-type lectin
LipoLLA	: liposomal linolenic acid
ml	: Millilitre
mM	: millimolar
mRNA	: Messenger RNA
FSC	: Forward scatter
SSC	: Side scatter
DTT	: Dithiothreitol
oC	: Degree centigrade
PAGE	: Polyacrylamide gel electrophoresis
PAGE	: Polyacrylamide gel electrophoresis
PAMP	: Pathogen-associated molecular pattern
PBS	: Phosphate buffered saline
PCR	: Polymerase chain reaction
TDB	: trehalose dibehenate
PMA	: Phorbol 12-myristate 13-acetate
PRR	: Pattern-recognition receptor
Syk	: spleen tyrosine kinase
RNA	: Ribonucleic acid
ROS	: Reactive oxygen species
rpm	: Revolutions per minute
SDS	: Sodium dodecyl sulfate
DMEM	: Dulbecco's Modified Eagle's Medium
MOI	: Multiplicity of infection
TDM	: Trehalose-6-6'-dimycolate
TLR	: Toll-like receptor
TNF	: Tumor necrosis factor
VacA	: Vacuolating cytotoxin A

Chapter 1

Introduction

What is *Helicobacter pylori*?

Helicobacter pylori (*H. pylori*) is a helical-shaped, microaerophilic and Gram negative bacterium which was first diagnosed in gastric mucosa of patients suffering from gastritis and peptic ulcer, it was then successfully cultured by the two Australian doctors; Barry J Marshall and Robin Warren, (Marshall and Warren 1984). Noticeably, this discovery contradicted the previously held scientific belief that stomach is a germ free organ and this discovery resulted in the award of Noble prize 2005 to Marshall and Warren in Physiology and Medicine. Chronic infection of *H. pylori* in humans is prevalent in more than half of the world's population (Hooi et al. 2017) and represents a major risk that causes gastritis and peptic ulcer, which may develop into mucosa-associated lymphoid tissue (MALT) lymphoma and finally can transform into gastric adenocarcinoma. More than 20% of all malignancies in humans are associated with infections and the major bacterial cause for human cancer till date is *H. pylori* (De Martel et al. 2012). Gastric cancer is the third major cause of cancer related deaths and fifth most common cancer after prostate cancer (Díaz et al. 2018). However, only few infected people are prone to develop serious clinical symptoms of *H. pylori* infection which in turn is determined by several factors which particularly depends on the host immune status such as presence of particular receptors and efficiency of inflammatory responses. Clinical outcome of *H. pylori* infection also depend on environmental determinants along with the strain specificity that affect the pathogenicity of the strains (strain diversity) (Backert, Neddermann, Maubach, & Naumann, 2016).

Prevalence and geographical distribution

H. pylori is the predominant human infection globally that colonizes over 50% of world's population with huge difference in its geographical distribution.

The highest prevalence of *H. pylori* is found in Africa with around 79.1% and the least in Northern America and Oceania at 24.4% (Hooi et al., 2017) (Figure 1.1). The prevalence is high in rural areas compared to urban which reflect the differences in the level of sanitation, socioeconomic status, urbanization, and facility to access clean water (Cardenas, Mulla, Ortiz, & Graham, 2006). Interestingly, the prevalence of *H. pylori* vary between populations even in the same country. Moreover, *H. pylori* prevalence varies between different ethnic groups residing in the same country. For instance, in United States the *H. pylori* infection in non-whites was found ranging from 34.5% to 61.6% and that in non-Hispanic whites ranges from 18.4% to 26.2% (James E. Everhart, 2000). Similarly, Malaysian population comprise of Malay, Chinese and Indians ethnic groups, the *H. pylori* prevalence in Malay is (19.9%), Indians (50.7%) and Chinese (40%) (Goh & Parasakthi, 2001).

H. pylori is being recognized as a Group I carcinogen by WHO which is responsible for the development of gastric adenocarcinoma. Almost 89% cases of Gastric cancer are attributed to *H. pylori* infection (Group., 2014). Previously, it has been shown that complete eradication of *H. pylori* infection reduced the gastric cancer incidences from 25% to 16.67% in China (Yeh, Kuntz, Ezzati, & Goldie, 2009).

In developed countries like Canada, US, and Northern Europe *H. pylori* prevalence is low with constant infection rates compared to Africa, Latin America, India and Eastern Europe. This is possibly a result of improved hygiene, sanitation and active elimination of carrier state by the use of antimicrobial therapies (Torres et al., 2000). Furthermore, *H. pylori* shows high prevalence rates of 58 to 62% in India in patients with dyspeptic symptoms (Eusebi, Zagari, & Bazzoli, 2014).

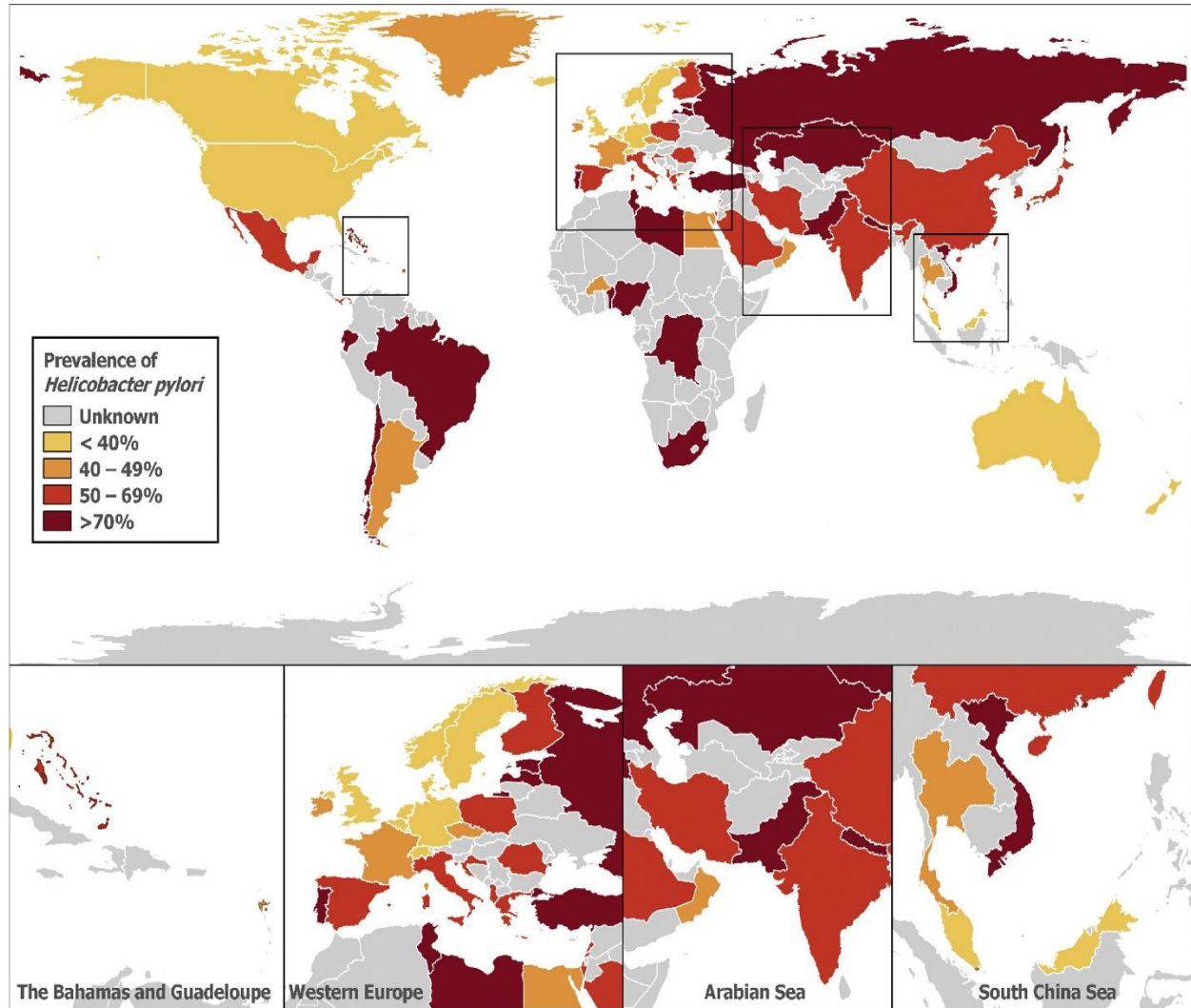


Figure 1.1: Choropleth map represents the global prevalence of *H. pylori*. Certain regions are magnified to display the smaller countries (Hooi et al., 2017).

Dynamics of *H. pylori* transmission

H. pylori infection can be transmitted through following routes:

- i. **Iatrogenic:** Transmission of *H. pylori* through iatrogenic mode is the most frequent, and fast in which the endoscopes which comes in contact with gastric mucosa of *H. pylori* infected individuals are applied for another person (Akamatsu, Tabata, Hirong, Kawakami, & Uyeda, 1996). Moreover, *H. pylori* infections are also reported to be transmitted from an infected individual to the staff members especially the technicians who execute endoscopy and the gastroenterologists (Lin, Lambert, Schembri, Nicholson, & Korman, 1994).
- ii. **Faecal-oral:** Lin et al., have reported to recover *H. pylori* bacterium from the faeces of young children (Lin et al., 1994) while isolation of *H. pylori* from adult faeces was reported not very frequently (Namavar et al., 1995). Numerous studies have established the relation between the seroprevalence of hepatitis A virus and *H. pylori*, suggesting similar (faecal-oral) mode of transmission for both the pathogens. (Bui, Brown, Harris, & Oren, 2016). Furthermore, *H. pylori* have been detected and cultured in drinking water samples. Hence, public water system has been considered as an source for *H. pylori* infection (Santiago, Moreno, & Ferrús, 2015).
- iii. **Oral–oral:** Transmission of *H. pylori* from infected individuals by oral-oral route is another transmission method but not well established although there are several studies that have attempted to detect and isolate *H. pylori* from the oral cavities (Yee, 2017). For example, *Loster et al.* detected *H. pylori* in dentist's oral cavity by culture method from sub-gingival dental plaque and observed that 57% of study subjects were culture were positive for *H. pylori* (Loster et al., 2009).

Colonization of the mucosal tissue

There are different factors that are critical during *H. pylori* colonization in the mucosa tissue of stomach (Figure 1.2). The two most studied and key essential factors are:

i. Production of Urease

H. pylori is not an acid-loving organism and the production of urease enzyme is one of the characteristic strategy of *H. pylori* to neutralize the acidic environment of the gastric lumen. The presence of urease and its activation is indispensable for the successful colonization of gastric mucosa by *H. pylori* (K. A. Eaton & Krakowka, 1994). It has been shown that in the presence of urea *H. pylori* can tolerate pH as low as 2.5 while in the absence of urea it can tolerate a pH range between 8.0 and 4.0 (Meyer-Rosberg, Scott, Rex, Melchers, & Sachs, 1996). It harbors a cluster of seven genes which control and regulate the biosynthesis process of urease enzyme (Turbett, Hoj, Horne, & Mee, 1992), and it's composed of a complex structure of twelve subunits of UreA and UreB. (Ha et al., 2001). *H. pylori* urease is a hydrolase enzyme that hydrolyses urea to CO₂ and NH₃. Unlike other ureases that are produced by bacterial species, *H. pylori* urease has strong affinity to urea with a Km value of 0.8 Mmol/L that enables the *H. pylori* urease to act on even very little quantities of urea (as low as 5 Mmol/L). Utilization of urea and production of NH₃ creates acid-neutralizing capacity empowering *H. pylori* to maintain the right pH in its periplasm and surrounding microenvironment. Consequently, regulating the proton motive force (Dunn, Campbell, Perez-Perez, & Blaser, 1990). This acid adaptation strategy of *H. pylori* for maintaining a neutral pH intracellularly while the pH of the surrounding vicinity is still in low pH, is a peculiar feature to *H. pylori*. This is vital for existence of *H. pylori* in the acidic gastric juice.

Moreover, generation of NH_3 by the urease enzyme in non-acidic environments could elevate the native pH above pH 7.0, which may be a reason why *H. pylori* does not colonize in niches other than the Gut. Moreover, it has been demonstrated that *H. pylori* is intolerant to alkaline environment (Clyne, Labigne, & Drumm, 1995).

ii. Ability to penetrate the mucus

Motility is the second critical key factor for gastric colonization by *H. pylori*. *H. pylori* features 2 to 6 unipolar flagella that confer motility to *H. pylori*. *H. pylori* flagella length range between 3-5 μm , with bulb-like structures that are mostly present at the end of the filaments (Geis, Lying, Suerbaum, Mai, & Opferkuch, 1989). *H. pylori* flagella sheath will be shielded by proteins and lipopolysaccharide and it is suggested that the bacterial outer membrane will be extended to protect the flagellar filaments from the gastric acid in the stomach (Geis et al., 1989). Previously, it has been shown that *H. pylori* mutants that lacked flagella have failed to colonize the stomach of animal models (K. Eaton, Morgan, & Krakowka, 1992). For instance, FlaA and FlaB proteins are essential for the proper movement of *H. pylori*. Deletion of FlaA has impaired the motility of *H. pylori* to a greater extent than that of FlaB mutant (Josenhans, Labigne, & Suerbaum, 1995). Furthermore, it was reported that the protein auto-inducer 2 (AI-2) encoded by *luxS* gene regulates the expression of flagellar genes (Rader, Campagna, Semmelhack, Bassler, & Guillemin, 2007). This has also been supported by the evidence that *luxS* mutants were less motile and less infectious compared to the wild-type strain (Osaki et al., 2006).

***H. pylori*'s penetration into gastric mucus**

The epithelial lining of the GI tract is shielded by heavy viscoelastic layer (300 μm) (Atuma, Strugala, Allen, & Holm, 2001). The, *H. pylori* has to penetrate the dense and viscoelastic mucus layer in order to reach the underlying epithelium for colonization. *H. pylori* can quickly lose motility in the very acidic gastric lumen (Thomsen, Gavin, & Tasman-Jones, 1990). The ability of *H. pylori* to elevate the pH by utilizing urea, reduces the viscoelasticity of the mucus permitting the bacterium to move faster through the mucus layer (Celli et al., 2009). Helical-rod shape has been suggested to enhance the velocity of *H. pylori* through viscous mucus in a corkscrew fashion. *csdI* is one of the *H. pylori* cell shape determining genes which codes for a metallopeptidase. Deletion of *csdI* has altered the morphology of *H. pylori* from native helical-rod to curved-rod morphology and the *csdI* mutant exhibited less velocity in gel-like medium and were inefficient in colonizing the mice stomach compared to the wild-type strains (Sycuro et al., 2010). Similarly, *csd4* deletion which results in straight rod-shaped morphology impairs the colonization efficiency and the motility of bacteria compared to the wild-type morphologies (Sycuro et al., 2012). *H. pylori* isogenic mutants with rod shaped morphology showed reduced swimming rates by 7-21% in purified porcine gastric mucus (Martínez et al., 2016).

Living within gastric mucus

H. pylori establishes microcolonies in the secreted gastric mucus present on the epithelial cells of the gastric mucosa (Hidaka et al., 2001). Moreover, It has been observed that *H. pylori* lives in close proximity to MUC5AC which is the main gel forming mucin secreted by gastric epithelial cells *in vivo* (Van den Brink et al., 2000).

It has been reported that lower mucus neck cells that are present in the antral glands secrete MUC6 which express α -1,4GlcNAc-capped core 2-branched O-glycan on the surface. MUC6 has shown to inhibit the formation of cholesteryl- α -D-glucopyranoside, one of essential cell wall components and inhibit the growth of *H. pylori* (Kawakubo et al., 2004; H. Lee et al., 2008).

Interaction with gastric epithelial cells

It has been believed that *H. pylori* colonizes the gastric mucus by interacting with gastric epithelial cells. A number of proteins have been identified to play an important play in the adherence to the host cells and for further interaction.

BabA

BabA is one of the well-studied adhesins of *H. pylori*. BabA is a 78 kDa outer membrane protein which attaches *H. pylori* to fucosylated structures on host cells, including Lewis^b blood group antigen and H-1 type (Ilver et al., 1998). BabA is a heterogeneous protein, with various polymorphisms among strains and binds to Lewis^b at different levels (Hennig, Mernaugh, Edl, Cao, & Cover, 2004).

Sialic-acid binding adhesin (SabA)

In addition to BabA adhesion, SabA is a protein which binds *H. pylori* to sialylated ligands of gastric mucin, epithelial cells and neutrophils, which trigger a nonopsonic response by neutrophils and brings about phagocytosis of the bacterial cells (Unemo et al., 2005). Moreover, it has been shown that expression of *sabA* influences the acid production in the stomach (Yamaoka et al., 2006). The expression of SabA will be reduced in the acidic environment (Goodwin et al., 2008).

Another mechanism used by *H. pylori* is to regulate the expression of sabA gene duplication that enhances the production of the SabA protein, which in turn results in stronger adherence of *H. pylori* to cells in vitro (Talarico, Whitefield, Fero, Haas, & Salama, 2012). Therefore, the sabA gene is highly heterogenic allowing *H. pylori* to regulate its adherence strategies depending on the microenvironmental conditions.

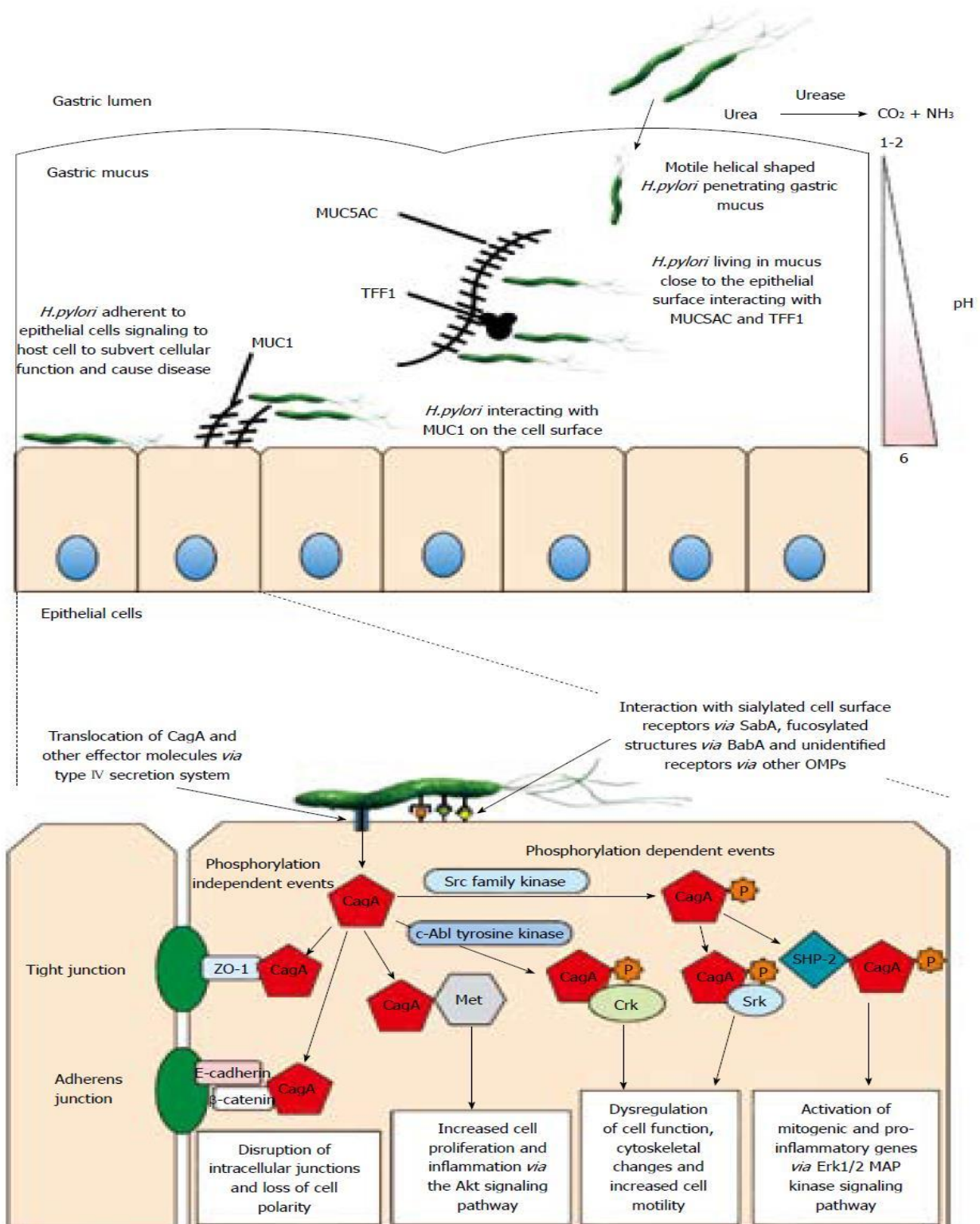


Figure 1.2: Colonization strategies and establishment of gastric mucosal infection by *H. pylori* (Dunne, Dolan, & Clyne, 2014).

Virulence strategies of *H. pylori*

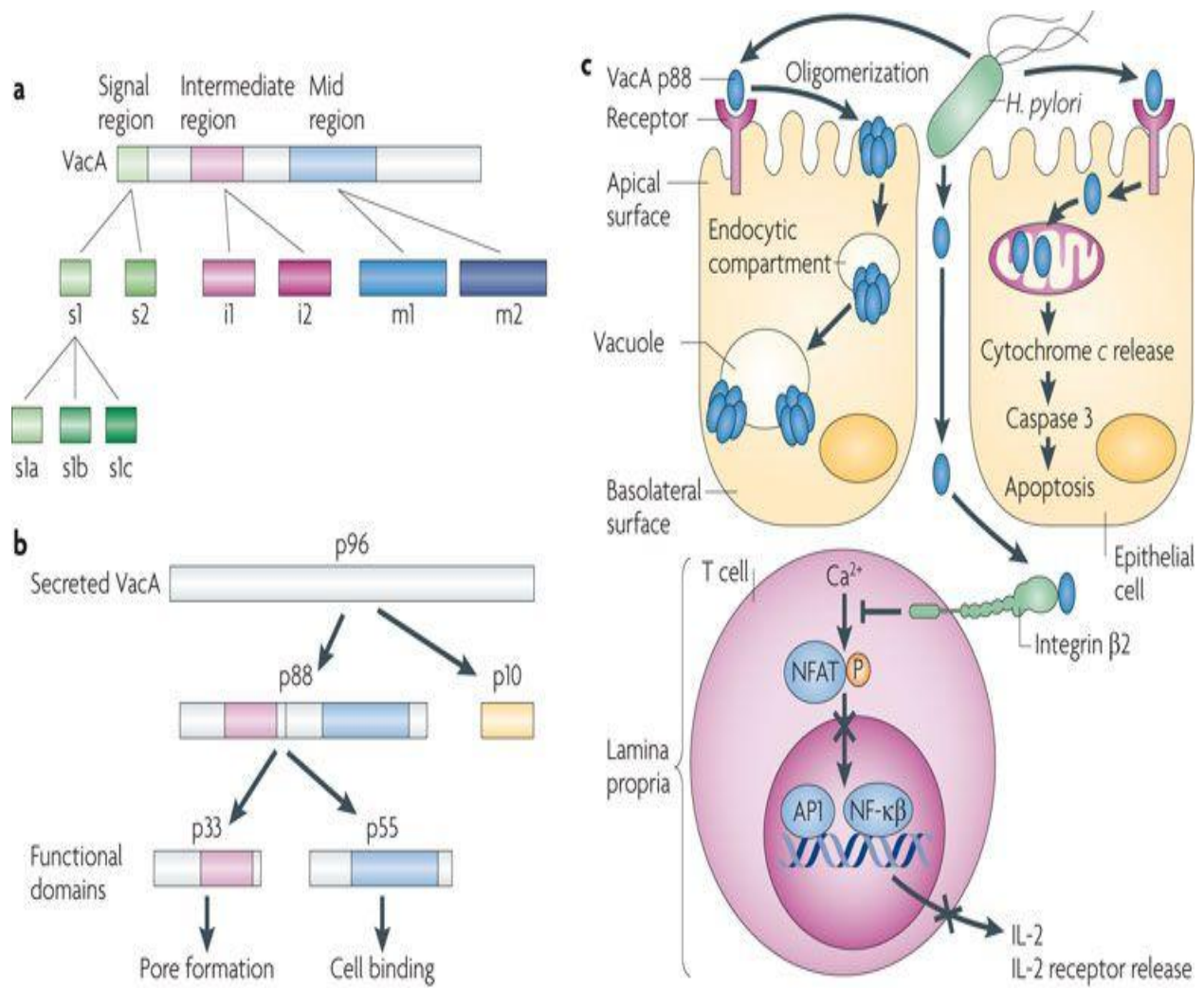
Cytotoxin-associated gene A (CagA)

H. pylori's major virulence factor CagA is a product of *cagA* gene. It is one the best characterized virulence gene in *H. pylori*. CagA produced by some of *H. pylori* strains is partially responsible for the symptoms of the infection (Covacci et al., 1993). Upon adherence of *H. pylori* strains the CagA protein is expressed and is injected into the epithelial cells *via* Type IV secretion system (T4SS) that is coded by multiple loci located in pathogenicity-island called *cagPAI*. After the translocation of CagA into host epithelial cells, it will be phosphorylated by host gastric epithelial cell kinases and finally it disrupts the host cell signaling pathways (Odenbreit et al., 2000). The *cagPAI* encompass around 30 genes, most of which are required for synthesis of the T4SS (Censini et al., 1996). The CagL protein is highly conserved in *H. pylori* and is involved in formation of the end of the pilus in the T4SS. CagL has an arginine- glycine- aspartate (RGD) motif that binds to the $\alpha 5 \beta 1$ integrin which is presents on the surface of host cells and facilitate the translocation of CagA into host cells. (Kwok et al., 2007). Furthermore, it has been shown that Non-CagPAI proteins are required for CagA translocation process. For instance, HopQ an *H. pylori* outer membrane protein is needed for introduction of CagA into the host cells. In addition, HopQ is required for the subsequent intracellular activity of CagA (Belogolova et al., 2013). Phosphorylation is required for CagA activity, this happens at EPIYA motifs present on the 145 kDa protein and triggers a robust immune response. In addition, the number of EPIYA motifs variey between the *H. pylori* strains and it has been observed that the strains with more number of motifs are more virulent and biologically active (Asahi et al., 2000; Higashi et al., 2002).

The E-cadherin and β -catenin complex that are commonly present in the adherent junctions of epithelial cells. CagA interaction with E-cadherin disrupts the complex irrespective of the CagA phosphorylation and results in the deregulation of β -catenin protein and its cytoplasmic accumulation this has been observed to induce carcinogenesis (Murata-Kamiya et al., 2007).

Vacuolating cytotoxin A (VacA)

VacA is the second most studied virulence factor in *H. pylori* and is genetically diverse. *vacA* encodes a primary toxin with a molecular weight of around 140 kDa, while the post-transnationally modified VacA toxin is made up of p55 and p33 domains which combine and form an oligomeric structure. This protein structure has an anion-selection channel which inserts into host epithelial cells and induces the secretion of organic anions and bicarbonates into the host cytoplasm (Szabò et al., 1999). This strategy helps *H. pylori* to obtain essential metabolic exudates for bacterial growth. Moreover, VacA has the ability to infuse the endosomes via endocytosis, in which the VacA endocytosed channel permit anions to pass into the late endosomes, which results into building up of weak bases. Consequently, it results in water influx and formation of large vacuole. (Palframan, Kwok, & Gabriel, 2012; Terebiznik et al., 2006). Furthermore, it has been reported that cell treatment by VacA essentially targets mitochondria and induces ER stress by section of cytochrome C and initiating apoptosis (Akazawa et al., 2013). Most *H. pylori* strains harbor *vacA*, but exhibits strain specific differences in the signal sequence (s1a, s1b, s1c, and s2), intermediate region (i1, i2, and i3) and mid-region (m1, m1T, and m2). The genotypes can be categorized in two subtypes according to the combination of these three regions; s1/m1 which is most active and abruptly damages the cells in an acute manner, in comparison with the s2/m2 which is less virulent (Cover, Tummuru, Cao, Thompson, & Blaser, 1994; Ferreira et al., 2012) (Figure1.3).



Nature Reviews | Cancer

Figure1.3: Structure and functions of *H. pylori* VacA (Polk & Peek Jr, 2010).

Lipopolysaccharide (LPS)

LPS of *H. pylori* unlike LPS of the other Gram negative bacteria, is less toxic, less pyrogenic, and less responsive to the innate system of the human host (Muotiala, Helander, Pyhälä, Kosunen, & Moran, 1992). The LPS of *H. pylori* contains O-Lewis antigens (Lewis a, Lewis b, Lewis x and Lewis y). Similarly, Lewis antigens are also expressed on the surface of human gastric epithelial cells, which enables antigenic mimicry, helping *H. pylori* to escape the immune recognition (Appelmelk, Monteiro, Martin, Moran, & Vandenbroucke-Grauls, 2000). Furthermore, these Lewis antigens help bacteria to get more carbon source and exudates by inducing inflammation of gastric epithelium. Anti-Lex (Lewis-x) antibodies produced as a result of Lewis antigen expression by *H. pylori* binds to *H. pylori* as well as to the gastric epithelium causing gastric autoimmune responses leading to enhanced inflammation and injury of the epithelium (Appelmelk et al., 2000). Lewis antigens of *H. pylori* have also been shown to undergo phase variation and to play a role in attachment of *H. pylori* to the gastric epithelium, thus providing a dynamic adherence nature to the bacteria (Edwards et al., 2000).

The structure of *H. pylori* LPS comprises the same primary structure as present in other Gram-negative LPS, which comprises of three domains; the variable outer most O-antigens, conserved and core oligosaccharide and hydrophobic domain lipid A. O-antigens contributes to antigenicity, the lipid A domain communicates with receptors on immune cells that has potent endotoxic capabilities and core oligosaccharide that induces permeability in the cells (Yamaoka, 2008). *H. pylori* LPS has two specific functions, Lewis antigens that mimic the host antigens and facilitate immune evasion (Monteiro, 2001), and the distinctive structure of its lipid A-core, which provides protection from the host produced cationic antimicrobial peptides (CAMPs) (Cullen et al., 2011).

O-antigen biosynthesis in *H. pylori* occur *via* a novel Wzk-dependent pathway where short individual undecaprenyl pyrophosphate (Und-PP)-linked O-antigen units are built in the cytoplasm and transported to the periplasm and then polymerized by only the Wzk flippase which is specific to *H. pylori* (Hug et al., 2010) (Figure 1.4).

H. pylori has unusual feature where it constitutively modifies lipid A upon specific environmental signals (Stead, Zhao, Raetz, & Trent, 2010). It is one of the strategies of *H. pylori* which has been evolved to disguise the host immune system, as it leads to low immune responses, helping the bacteria to evade the innate immunity and enable long term persistence (Atherton & Blaser, 2009).

H. pylori mutants of lipid A synthesis genes such as lpxE/F have shown a 1020-fold higher sensitivity to polymyxin B and different naturally occurring CAMPs, and a 10-fold higher induction of TLR4 receptors. Strikingly, the lpxE/F mutants also failed to establish infection in the murine stomach, demonstrating the substantial role of a dephosphorylated lipid A domain of *H. pylori* LPS (Cullen et al., 2011).

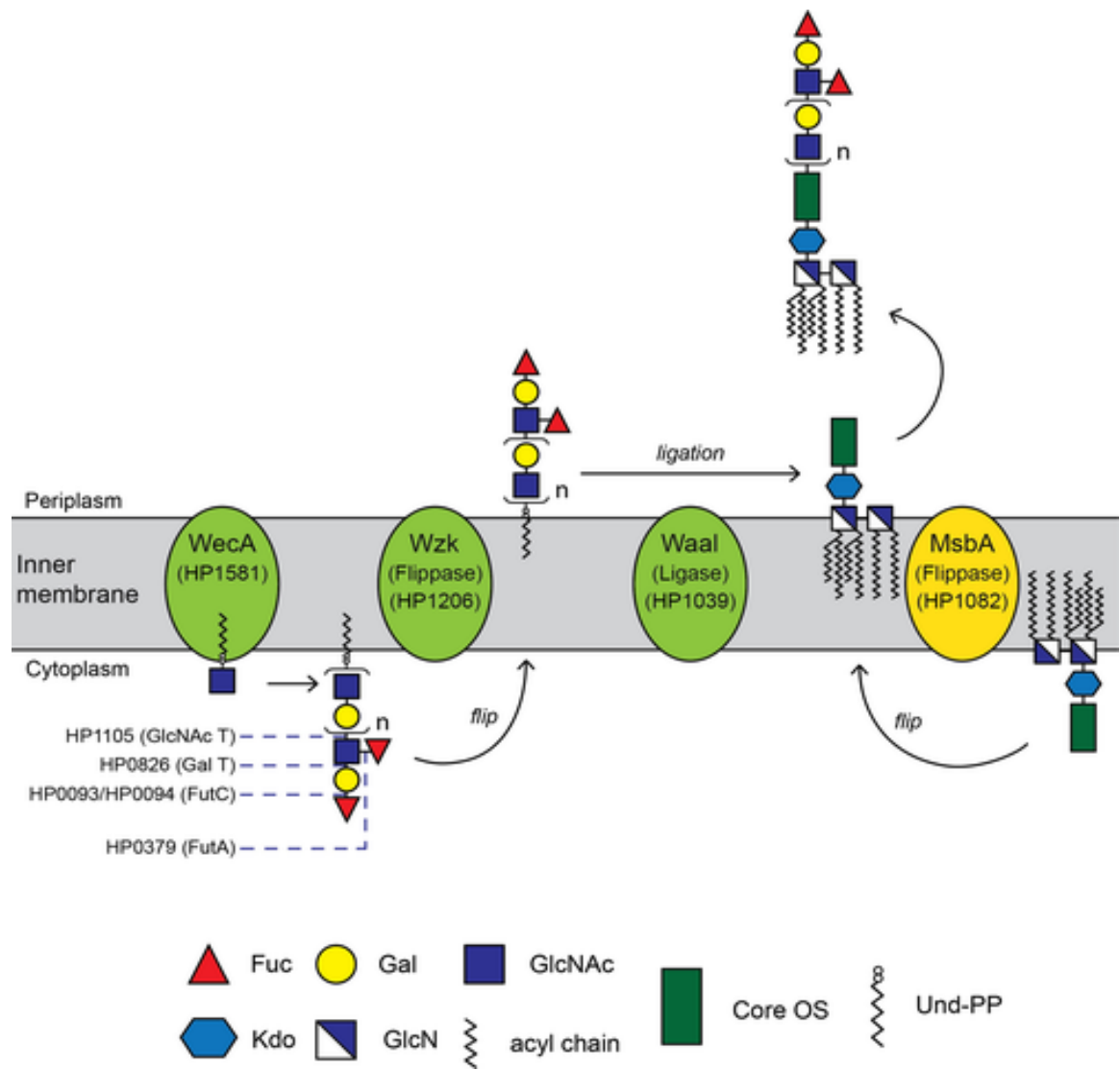


Figure1.4: Synthesis and O-antigen ligation with lipid A-core process in *H. pylori* (Li et al., 2016).

Pathogenesis of *H. pylori*

H. pylori infects more than 50% of world human population and causes histologic gastritis in all patients, wherein only 10 to 20% of infected people develops ulcer disease and 1 to 2% will likely develop gastric cancer. Moreover, the severity and the incidences of disease inflicted by *H. pylori* is controlled by different host and environmental factors (Ernst & Gold, 2000; Kuipers, 1999; Kuipers, Thijs, & Festen, 1995) (Figure 1.5).

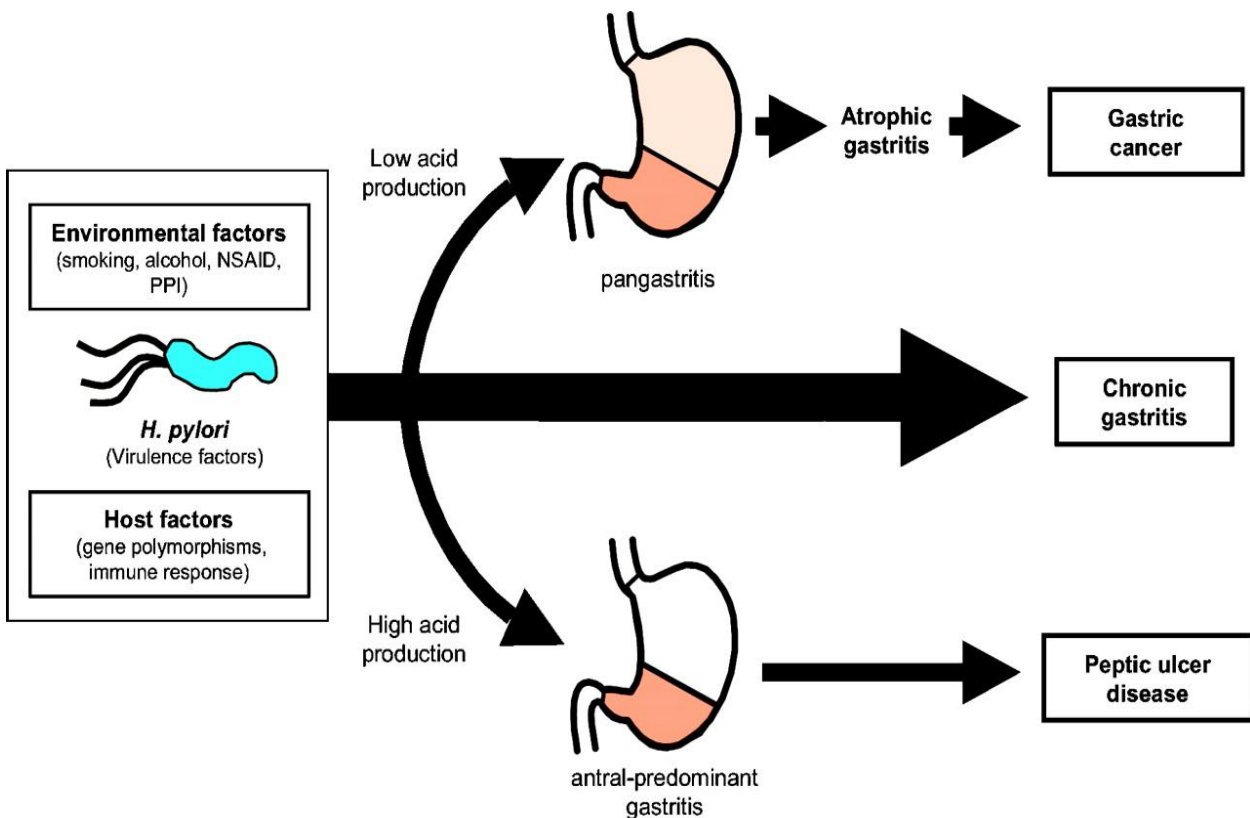


Figure 1.5: Schematic graph illustrating the factors that are responsible for gastric pathology and the subsequent disease consequences (Kusters, van Vliet, & Kuipers, 2006).

Acute gastritis: Acute infection of *H. pylori* is represented by significant inflammation of the distal and proximal stomach mucosa, momentary nonspecific dyspeptic symptoms, nausea, vomiting, and stomach fullness. These symptoms were based on reports of patients who either accidentally or deliberately consumed *H. pylori* or acquired infections through contaminated food or water (K. A. Eaton & Krakowka, 1994; Marshall, Armstrong, McGeachie, & Glancy, 1985; Sobala et al., 1991).

Chronic gastritis: Persistent infection of the *H. pylori* in the human Gut correlates with the distribution of gastritis and the level of acid secretion (Figure 1.5). Level of acid secretion has counteractive effects on *H. pylori*. *H. pylori* in specific infects gastric antrum, in the region where low acid-secretory layer of parietal cells exist. Such an infection is determined with an antrum-predominant gastric inflammation. In Patients who are acid secretion defective the bacteria are uniformly distributed within corpus and antrum together with adjoining contact with the gastric mucosa (E. J. Kuipers et al., 1995). The persistent inflammation of the corpus mucosa promotes hypochlorhydria, in parallel with local inflammatory factor responses such as interleukin-1(IL-1), which subsequently produces suppressive responses on parietal cell function, supported by reports which illustrated that eradication therapy has increased acid secretion in the patients (El-Omar et al., 1997; Ruiz, Correa, Fontham, & Ramakrishnan, 1996). Furthermore, the patients carrying proinflammatory genotype are at a greater risk of developing chronic gastritis, making them susceptible to intestinal metaplasia, atrophic gastritis and further to gastric cancer (El-Omar et al., 2000).

Peptic ulcer: Peptic ulcer is a mucosal deformity which is represented by a 0.5 cm diameter crossing the muscularis mucosa.

There are two types of ulcers; gastric ulcers and duodenal ulcers. Gastric ulcer mostly occur in the region between corpus and antrum mucosa while the duodenal ulcers arise in the duodenal bulb region (van Zanten, Dixon, & Lee, 1999). Gastric ulcers and duodenal ulcers are linked to *H. pylori* infection, wherein it was reported that 95% of duodenal ulcers and 85% of gastric ulcers were culture positive for *H. pylori* (E. Kuipers, J. Thijs, et al., 1995).

Progression of atrophic gastritis to IM and gastric cancer

Chronic *H. pylori* infection causes atrophic gastritis and develops into intestinal metaplasia (IM) in 50% of infected individuals. which is characterized by the damage of gastric glands, destruction of the gastric mucosal structure and fibrosis (E. Kuipers, A. Pena, et al., 1995). Intestinal metaplasia and loss of gastric gland progresses with time multifocally and increases the possibility of gastric cancer development from 5 to 90 folds based on the severity of gastric atrophy (Slipponen, Kekki, Haapakoski, Ihamäki, & Siurala, 1985).

Moreover, development of cancer by *H. pylori* infection is dependent on host susceptibility and bacterial virulence that stimulate chronic inflammatory responses. For instance, the possibility of developing gastric cancer increases in patients infected with CagA-positive *H. pylori* strains (Parsonnet, Friedman, Orentreich, & Vogelmann, 1997). Similarly, patients with a genetic tendency to produce higher IL-1 in response to infections are more prone to develop gastric cancers (El-Omar et al., 2000).

MALT lymphoma. Almost all MALT diseases develops in response to *H. pylori* infection as the lymphoid tissue is damaged in gastric mucosa. Unusually high titer of monoclonal population of B cells occur in gastric mucosa and gradually multiply and progress towards MALT lymphoma (Eidt, Stolte, & Fischer, 1994).

***H. pylori* infection diagnosis and treatment**

Several diagnostic tests have been established to identify *H. pylori* infection with varying levels of specificity and sensitivity (Table 1.1). There are two types of diagnostic tests for *H. pylori*; invasive tests, that include culture from biopsies, gastric samples for histology and non-invasive tests, which includes peripheral specimens, such as stools, blood, urine, saliva, or breathe samples for detecting urease activity, bacterial antigens, or detection of antibodies.

Treatment of *H. pylori* is mostly the triple therapy regimen which include two antibiotics like amoxicillin and clarithromycin with either a bismuth compound or a proton pump inhibitor (Kusters et al., 2006).

Table 1.1: Methods of *H. pylori* diagnosis

Diagnostic test	Sensitivity and specificity rate
<i>Invasive methods</i>	
Rapid urease (CLO) test	>90%
Culture biopsy	>95%
Histology	>95%
<i>Noninvasive methods</i>	
Fecal antigen test	>90%
Urea breath test	>95%
Serology	80-90%

***H. pylori* cholesteryl glucosides**

Cholesterol is the most abundant sterol in the mammalian cells, more than 90% of cholesterol is present in the cell membrane. It is one of the vital molecule in eukaryotic physiology, and also indispensable for some of the prokaryotes like *Mycobacterium tuberculosis* (Pandey & Sassetti, 2008). Moreover, it has been shown that cholesterol depletion inhibits the invasion of host cells by *Chlamydia trachomatis* (Stuart, Webley, & Norkin, 2003).

***H. pylori* have a unique structures of lipids**

H. pylori has unique constituents of cholesteryl glucosides (CGs); cholesteryl- α -D-glucopyranoside (α CG), cholesteryl-6-O-tetradecanoyl- α -D-glucopyranoside (α CAG), and cholesteryl-6-O-phosphatidyl- α -D-glucopyranoside (α CPG) which is the unique feature of this bacterium (Mahmudul Haque, Hirai, Yokota, & Oguma, 1995; Hirai et al., 1995). Presence of CGs are a general characteristic feature for *Helicobacter spp.* Its percentage varies from species to species which ranges from 7%-29% (M. Haque et al., 1996). Interestingly, *H. pylori* has unique lipids like 3-OH 14:0 and 3-OH C19:0 which enables it to survive in the acidic environment (Lambert, Patton, Barrett, & Moss, 1987).

H. pylori do not have genes for cholesterol synthesis but it obtains cholesterol from the surrounding environment (Tomb et al., 1997). Ansorg et al., studied the affinity of *H. pylori* to cholesterol from different sources like egg yolk and he observed that rich cholesterol sources attract *H. pylori* (Ansorg, Müller, Von Recklinghausen, & Nalik, 1992). Moreover, *H. pylori* has displayed the ability to sense cholesterol and thrive in high concentration of cholesterol when it was grown in hermetic tubes with different concentrations of cholesterol.

Also, *H. pylori* associates with epithelial cell and extracts cholesterol which results in the destruction of lipid raft of the cell. Furthermore, cholesterol extraction from host cells will take place only in the presence of cholesteryl- α -glucosyl transferase (CGT) which is encoded by *hp0421* gene and deletion of this gene results in the loss of all CGs variants (Lebrun et al., 2006; Wunder et al., 2006).

Crystal structure of CGT protein has been studied and submitted to RCSB PDB protein repository with accession number [<https://www.rcsb.org/structure/3QHP>] (3QHP) (S. J. Lee, Lee, & Suh, 2011). The synthesis of CGT takes place in the cytoplasm in an inactive form, which is further activated once it gets exported to the beneath of inner membrane.(Hoshino et al., 2011).

Role of cholesterol and CGs in pathogenicity of *H. pylori*

Several studies have investigated the substantial role of cholesterol glucosylation in *H. pylori* virulence and pathogenicity. CagA is an oncoprotein that is deposited into the cytosol of gastric epithelial cells through type IV secretion system (T4SS) and VacA toxin that alters endosome maturation and finally results in epithelial cell vacuolation, are the two main virulence mechanisms of *H. pylori* (Roesler, Rabelo-Gonçalves, & Zeitune, 2014). Remarkably, a decreased translocation of Phosphorylated CagA via T4SS in cholesterol-depleted AGS cell was observed which later reduced humming bird phenotype and decreased the induction of IL-8 expression (Wang, Cheng, Cheng, Lai, & Wang, 2012). Additionally, depletion of cholesterol from AGS cells before infection with *H. pylori* resulted in attenuated VacA toxin, thereby abrogating the vacuolation of AGS cells (Patel et al., 2002).

Moreover, depletion of cholesterol from AGS cells by using Methyl- β -cyclodextrin (M β CD) leads to decreased expression of NF- κ B and IL-8 which is a consequence of the disruption of α 5 β 1 integrin that is present in cholesterol rich microdomains in the outer membrane of the host cell surface. α 5 β 1 integrin is essential for NOD1 recognition of peptidoglycan and consequent induction of NF- κ B-dependent responses to *H. pylori* (Hutton et al., 2010).

Furthermore, *H. pylori* cultured in the absence of cholesterol showed susceptibility to certain antibiotics, bile salts and ceragenins (McGee et al., 2011; Trainor, Horton, Savage, Testerman, & McGee, 2011).

Cholesterol glucosylation and escape of host Immune response by *H. pylori*

Another strategy employed by *H. pylori* for immune evasion is glucosylation of the host cholesterol and incorporating it into its membrane in order to disguise the host immune system. High amount of cholesterol enhance phagocytosis of *H. pylori* by antigen-presenting cells (APC), like dendritic cells (DC) and macrophages and promote antigen-specific T cell responses. Cholesterol glucosylation by *H. pylori* delays internalization. Free cholesterol facilitates phagocytosis of *H. pylori* by macrophages and *H. pylori* incubated with cholesterol increases T-cell response. *In vivo*, cholesterol mediates T-cell dependent protection in mice fed with high cholesterol diet, histological studies showed infiltration for neutrophils and lymphocytes and upregulation of interferon- γ regulated genes but when the ratio of cholesteryl glucosides is higher than the cholesterol it protects the *H. pylori* from phagocytosis. Furthermore, *hp0421* mutant were cleared from mice stomach after 48 hours in contrary to the wild and reconstituted strains (Morey et al., 2018; Wunder et al., 2006). Usually inhibition of IL-2 by *H. pylori* is mediated by γ -glutamyl transpeptidase GGT and VacA (Gebert, Fischer, Weiss, Hoffmann, &

Haas, 2003; Schmees et al., 2007). Beigier, et al., showed that GGT and VacA IL-2 and IL-10 inhibition is attenuated in *H. pylori* after coating bacteria with cholesterol. Moreover, IL-4 was suppressed in VacA dependent manner and reverted back when bacteria were coated with cholesterol (Beigier-Bompadre et al., 2011). *H. pylori* mediates a direct inhibition of human CD41 T-cell proliferation while the immune response in iNKT mutant mice was lower when it was infected by wild-type *H. pylori* compared to *hp0421* mutant together with significant reduction in the cytokine responses by TH₁ and TH₂ cells (Ito et al., 2013).

One of the plausible strategies that *H. pylori* employs to modulate the autophagy is to arrest the phagosome maturation, but surprisingly this strategy have been restricted in *hp0421* mutant strains (Du et al., 2016; Lai et al., 2018). More recently, Pau Morey et al., reported that extraction of cholesterol by *H. pylori* from epithelial cells inhibits assembly of IFN- γ and other cytokines. The *hp0421* mutant fails to establish infections in *in vivo* animal models, which points towards the ineffectiveness of T-cell based vaccine against *H. pylori* (Morey et al., 2018) (Figure1.6).

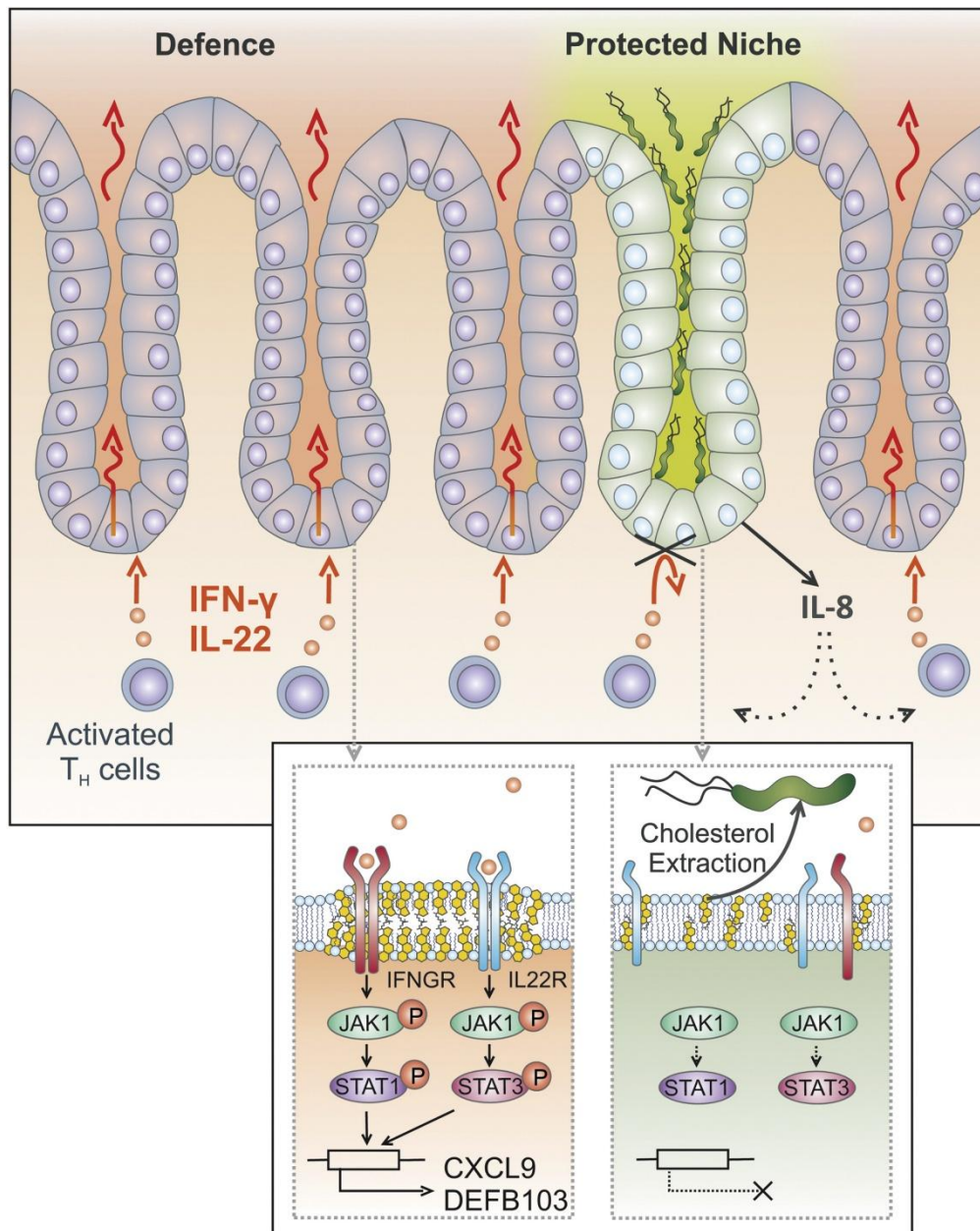


Figure 1.6: The cholesterol-dependent abrogation of immune response to *H. pylori* (Morey et al., 2018).

Objectives of the study

We hypothesize that CGs might play critical role in the maintenance of typical *H. pylori* morphology and permeability of *H. pylori* cell wall. Furthermore, we attempted to investigate the role of cholesterol glucosylation in *H. pylori* with regard to resistance to antibiotics, lipopolysaccharide profile and regulation of Mincle expression.

In order to address the above questions, the following objectives were framed:

1. To study the morphology of *H. pylori* population grown in the absence of cholesterol and deletion of *hp0421*.
2. To determine the role of *H. pylori* CGs in cell wall permeability, antibiotic resistance, LPS profiles and biofilm formation.
3. To analyze the role of *H. pylori* CGs in Mincle receptor regulation.

References

- Akamatsu, T., Tabata, K., Hironga, M., Kawakami, H., & Uyeda, M. (1996). Transmission of *Helicobacter pylori* infection via flexible fiberoptic endoscopy. *Am J Infect Control*, 24(5), 396-401.
- Akazawa, Y., Isomoto, H., Matsushima, K., Kanda, T., Minami, H., Yamaguchi, N., . . . Takeshima, F. (2013). Endoplasmic reticulum stress contributes to *Helicobacter pylori* VacA-induced apoptosis. *PLoS One*, 8(12), e82322.
- Ansorg, R., Müller, K.-D., Von Recklinghausen, G., & Nalik, H. P. (1992). Cholesterol binding of *Helicobacter pylori*. *Zentralblatt für Bakteriologie*, 276(3), 323-329.
- Appelmek, B. J., Monteiro, M. A., Martin, S. L., Moran, A. P., & Vandenbroucke-Grauls, C. M. (2000). Why *Helicobacter pylori* has Lewis antigens. *Trends in microbiology*, 8(12), 565-570.
- Asahi, M., Azuma, T., Ito, S., Ito, Y., Suto, H., Nagai, Y., . . . Omata, M. (2000). *Helicobacter pylori* CagA protein can be tyrosine phosphorylated in gastric epithelial cells. *Journal of Experimental Medicine*, 191(4), 593-602.
- Atherton, J. C., & Blaser, M. J. (2009). Coadaptation of *Helicobacter pylori* and humans: ancient history, modern implications. *The Journal of clinical investigation*, 119(9), 2475-2487.
- Atuma, C., Strugala, V., Allen, A., & Holm, L. (2001). The adherent gastrointestinal mucus gel layer: thickness and physical state in vivo. *American Journal of Physiology-Gastrointestinal and Liver Physiology*, 280(5), G922-G929.
- Backert, S., Neddermann, M., Maubach, G., & Naumann, M. (2016). Pathogenesis of *Helicobacter pylori* infection. *Helicobacter*, 21 Suppl 1, 19-25. doi: 10.1111/hel.12335
- Beigier-Bompadre, M., Moos, V., Belogolova, E., Allers, K., Schneider, T., Churin, Y., . . . Aebischer, T. (2011). Modulation of the CD4+ T-cell response by *Helicobacter pylori* depends on known virulence factors and bacterial cholesterol and cholesterol α -glucoside content. *Journal of Infectious Diseases*, 204(9), 1339-1348.
- Belogolova, E., Bauer, B., Pompaiah, M., Asakura, H., Brinkman, V., Ertl, C., . . . Machuy, N. (2013). *Helicobacter pylori* outer membrane protein HopQ identified as a novel T4SS-associated virulence factor. *Cellular microbiology*, 15(11), 1896-1912.
- Bui, D., Brown, H. E., Harris, R. B., & Oren, E. (2016). Serologic Evidence for Fecal-Oral Transmission of *Helicobacter pylori*. *Am J Trop Med Hyg*, 94(1), 82-88. doi: 10.4269/ajtmh.15-0297
- Cardenas, V. M., Mulla, Z. D., Ortiz, M., & Graham, D. Y. (2006). Iron deficiency and *Helicobacter pylori* infection in the United States. *Am J Epidemiol*, 163(2), 127-134. doi: 10.1093/aje/kwj018
- Celli, J. P., Turner, B. S., Afdhal, N. H., Keates, S., Ghiran, I., Kelly, C. P., . . . Erramilli, S. (2009). *Helicobacter pylori* moves through mucus by reducing mucin viscoelasticity. *Proceedings of the National Academy of Sciences*, 106(34), 14321-14326.
- Censini, S., Lange, C., Xiang, Z., Crabtree, J. E., Ghiara, P., Borodovsky, M., . . . Covacci, A. (1996). cag, a pathogenicity island of *Helicobacter pylori*, encodes type I-specific and disease-associated virulence factors. *Proceedings of the National Academy of Sciences*, 93(25), 14648-14653.
- Clyne, M., Labigne, A., & Drumm, B. (1995). *Helicobacter pylori* requires an acidic environment to survive in the presence of urea. *Infect Immun*, 63(5), 1669-1673.
- Covacci, A., Censini, S., Bugnoli, M., Petracca, R., Burrone, D., Macchia, G., . . . Figura, N. (1993). Molecular characterization of the 128-kDa immunodominant antigen of *Helicobacter pylori* associated with cytotoxicity and duodenal ulcer. *Proceedings of the National Academy of Sciences*, 90(12), 5791-5795.
- Cover, T. L., Tummuru, M., Cao, P., Thompson, S. A., & Blaser, M. J. (1994). Divergence of genetic sequences for the vacuolating cytotoxin among *Helicobacter pylori* strains. *Journal of Biological Chemistry*, 269(14), 10566-10573.

- Cullen, T. W., Giles, D. K., Wolf, L. N., Ecobichon, C., Boneca, I. G., & Trent, M. S. (2011). Helicobacter pylori versus the host: remodeling of the bacterial outer membrane is required for survival in the gastric mucosa. *PLoS pathogens*, 7(12), e1002454.
- Du, S.-Y., Wang, H.-J., Cheng, H.-H., Chen, S.-D., Wang, L. H.-C., & Wang, W.-C. (2016). Cholesterol glucosylation by Helicobacter pylori delays internalization and arrests phagosome maturation in macrophages. *Journal of Microbiology, Immunology and Infection*, 49(5), 636-645.
- Dunn, B. E., Campbell, G. P., Perez-Perez, G. I., & Blaser, M. J. (1990). Purification and characterization of urease from Helicobacter pylori. *J Biol Chem*, 265(16), 9464-9469.
- Dunne, C., Dolan, B., & Clyne, M. (2014). Factors that mediate colonization of the human stomach by Helicobacter pylori. *World Journal of Gastroenterology: WJG*, 20(19), 5610.
- Eaton, K., Morgan, D., & Krakowka, S. (1992). Motility as a factor in the colonisation of gnotobiotic piglets by Helicobacter pylori. *Journal of medical microbiology*, 37(2), 123-127.
- Eaton, K. A., & Krakowka, S. (1994). Effect of gastric pH on urease-dependent colonization of gnotobiotic piglets by Helicobacter pylori. *Infect Immun*, 62(9), 3604-3607.
- Edwards, N. J., Monteiro, M. A., Faller, G., Walsh, E. J., Moran, A. P., Roberts, I. S., & High, N. J. (2000). Lewis X structures in the O antigen side-chain promote adhesion of Helicobacter pylori to the gastric epithelium. *Molecular microbiology*, 35(6), 1530-1539.
- Eidt, S., Stolte, M., & Fischer, R. (1994). Helicobacter pylori gastritis and primary gastric non-Hodgkin's lymphomas. *Journal of Clinical Pathology*, 47(5), 436-439.
- El-Omar, E. M., Carrington, M., Chow, W.-H., McColl, K. E., Bream, J. H., Young, H. A., . . . Rothman, N. (2000). Interleukin-1 polymorphisms associated with increased risk of gastric cancer. *Nature*, 404(6776), 398.
- El-Omar, E. M., Oien, K., El-Nujumi, A., Gillen, D., Wirz, A., Dahill, S., . . . McColl, K. (1997). Helicobacter pylori infection and chronic gastric acid hyposecretion. *Gastroenterology*, 113(1), 15-24.
- Ernst, P. B., & Gold, B. D. (2000). The disease spectrum of Helicobacter pylori: the immunopathogenesis of gastroduodenal ulcer and gastric cancer. *Annual Reviews in Microbiology*, 54(1), 615-640.
- Eusebi, L. H., Zagari, R. M., & Bazzoli, F. (2014). Epidemiology of Helicobacter pylori infection. *Helicobacter*, 19 Suppl 1, 1-5. doi: 10.1111/hel.12165
- Ferreira, R. M., Machado, J. C., Letley, D., Atherton, J. C., Pardo, M. L., Gonzalez, C. A., . . . Figueiredo, C. (2012). A novel method for genotyping Helicobacter pylori vacA intermediate region directly in gastric biopsy specimens. *Journal of clinical microbiology*, JCM. 02087-02012.
- Gebert, B., Fischer, W., Weiss, E., Hoffmann, R., & Haas, R. (2003). Helicobacter pylori vacuolating cytotoxin inhibits T lymphocyte activation. *Science*, 301(5636), 1099-1102.
- Geis, G., Leying, H., Suerbaum, S., Mai, U., & Opferkuch, W. (1989). Ultrastructure and chemical analysis of Campylobacter pylori flagella. *Journal of clinical microbiology*, 27(3), 436-441.
- Goh, K. L., & Parasakthi, N. (2001). The racial cohort phenomenon: seroepidemiology of Helicobacter pylori infection in a multiracial South-East Asian country. *Eur J Gastroenterol Hepatol*, 13(2), 177-183.
- Goodwin, A. C., Weinberger, D. M., Ford, C. B., Nelson, J. C., Snider, J. D., Hall, J. D., . . . Forsyth, M. H. (2008). Expression of the Helicobacter pylori adhesin SabA is controlled via phase variation and the ArsRS signal transduction system. *Microbiology*, 154(8), 2231-2240.
- Group., I. A. f. R. o. C. H. p. W. (2014). Helicobacter pylori Eradication as a Strategy for Preventing Gastric Cance. (*IARC Working Group Reports, No. 8*). Lyon, France: International Agency for Research on Cancer,, Available from: <http://www.iarc.fr/en/publications/pdfsonline/wrk/wrk8/index.php>.
- Ha, N. C., Oh, S. T., Sung, J. Y., Cha, K. A., Lee, M. H., & Oh, B. H. (2001). Supramolecular assembly and acid resistance of Helicobacter pylori urease. *Nat Struct Biol*, 8(6), 505-509. doi: 10.1038/88563

- Haque, M., Hirai, Y., Yokota, K., Mori, N., Jahan, I., Ito, H., . . . Oguma, K. (1996). Lipid profile of *Helicobacter* spp.: presence of cholesteryl glucoside as a characteristic feature. *J Bacteriol*, 178(7), 2065-2070.
- Haque, M., Hirai, Y., Yokota, K., & Oguma, K. (1995). Steryl glycosides: a characteristic feature of the *Helicobacter* spp.? *Journal of bacteriology*, 177(18), 5334-5337.
- Hennig, E. E., Mernaugh, R., Edl, J., Cao, P., & Cover, T. L. (2004). Heterogeneity among *Helicobacter pylori* strains in expression of the outer membrane protein BabA. *Infect Immun*, 72(6), 3429-3435.
- Hidaka, E., Ota, H., Hidaka, H., Hayama, M., Matsuzawa, K., Akamatsu, T., . . . Katsuyama, T. (2001). *Helicobacter pylori* and two ultrastructurally distinct layers of gastric mucous cell mucins in the surface mucous gel layer. *Gut*, 49(4), 474-480.
- Higashi, H., Tsutsumi, R., Fujita, A., Yamazaki, S., Asaka, M., Azuma, T., & Hatakeyama, M. (2002). Biological activity of the *Helicobacter pylori* virulence factor CagA is determined by variation in the tyrosine phosphorylation sites. *Proceedings of the National Academy of Sciences*, 99(22), 14428-14433.
- Hirai, Y., Haque, M., Yoshida, T., Yokota, K., Yasuda, T., & Oguma, K. (1995). Unique cholesteryl glucosides in *Helicobacter pylori*: composition and structural analysis. *J Bacteriol*, 177(18), 5327-5333.
- Hooi, J. K. Y., Lai, W. Y., Ng, W. K., Suen, M. M. Y., Underwood, F. E., Tanyingoh, D., . . . Ng, S. C. (2017). Global Prevalence of *Helicobacter pylori* Infection: Systematic Review and Meta-Analysis. *Gastroenterology*, 153(2), 420-429. doi: 10.1053/j.gastro.2017.04.022
- Hoshino, H., Tsuchida, A., Kametani, K., Mori, M., Nishizawa, T., Suzuki, T., . . . Kobayashi, M. (2011). Membrane-associated activation of cholesterol α -glucosyltransferase, an enzyme responsible for biosynthesis of cholesteryl- α -D-glucopyranoside in *Helicobacter pylori* critical for its survival. *Journal of Histochemistry & Cytochemistry*, 59(1), 98-105.
- Hug, I., Couturier, M. R., Rooker, M. M., Taylor, D. E., Stein, M., & Feldman, M. F. (2010). *Helicobacter pylori* lipopolysaccharide is synthesized via a novel pathway with an evolutionary connection to protein N-glycosylation. *PLoS Pathog*, 6(3), e1000819. doi: 10.1371/journal.ppat.1000819
- Hutton, M. L., Kaparakis-Liaskos, M., Turner, L., Cardona, A., Kwok, T., & Ferrero, R. L. (2010). *Helicobacter pylori* exploits cholesterol-rich microdomains for induction of NF- κ B-dependent responses and peptidoglycan delivery in epithelial cells. *Infect Immun*, 78(11), 4523-4531.
- Ilver, D., Arnqvist, A., Ögren, J., Frick, I.-M., Kersulyte, D., Incecik, E. T., . . . Borén, T. (1998). *Helicobacter pylori* adhesin binding fucosylated histo-blood group antigens revealed by retagging. *Science*, 279(5349), 373-377.
- Ito, Y., Vela, J. L., Matsumura, F., Hoshino, H., Tyznik, A., Lee, H., . . . Kobayashi, M. (2013). *Helicobacter pylori* cholesteryl α -glucosides contribute to its pathogenicity and immune response by natural killer T cells. *PLoS One*, 8(12), e78191.
- James E. Everhart, G. I. P.-P., and Geraldine McQuillan, Deanna Kruszon-Moran, Tommie Sue Tralka, (2000). Seroprevalence and Ethnic Differences in *Helicobacter pylori* Infection among Adults in the United States. *The Journal of Infectious Diseases*.
- Josenhans, C., Labigne, A., & Suerbaum, S. (1995). Comparative ultrastructural and functional studies of *Helicobacter pylori* and *Helicobacter mustelae* flagellin mutants: both flagellin subunits, FlaA and FlaB, are necessary for full motility in *Helicobacter* species. *Journal of bacteriology*, 177(11), 3010-3020.
- Kawakubo, M., Ito, Y., Okimura, Y., Kobayashi, M., Sakura, K., Kasama, S., . . . Nakayama, J. (2004). Natural antibiotic function of a human gastric mucin against *Helicobacter pylori* infection. *Science*, 305(5686), 1003-1006.

- Kuipers, E. (1999). Exploring the link between *Helicobacter pylori* and gastric cancer. *Aliment Pharmacol Ther*, 13, 3-11.
- Kuipers, E., Pena, A., Festen, H., Meuwissen, S., Uytterlinde, A., Roosendaal, R., . . . Nelis, G. (1995). Long-term sequelae of *Helicobacter pylori* gastritis. *The Lancet*, 345(8964), 1525-1528.
- Kuipers, E., Thijs, J., & Festen, H. (1995). The prevalence of *Helicobacter pylori* in peptic ulcer disease. *Aliment Pharmacol Ther*, 9, 59-69.
- Kuipers, E. J., Uytterlinde, A. M., Pena, A. S., Hazenberg, H. J., Bloemena, E., Lindeman, J., . . . Meuwissen, S. G. (1995). Increase of *Helicobacter pylori*-associated corpus gastritis during acid suppressive therapy: implications for long-term safety. *American Journal of Gastroenterology*, 90(9), 1401-1406.
- Kusters, J. G., van Vliet, A. H., & Kuipers, E. J. (2006). Pathogenesis of *Helicobacter pylori* infection. *Clin Microbiol Rev*, 19(3), 449-490. doi: 10.1128/CMR.00054-05
- Kwok, T., Zabler, D., Urman, S., Rohde, M., Hartig, R., Wessler, S., . . . König, W. (2007). *Helicobacter* exploits integrin for type IV secretion and kinase activation. *Nature*, 449(7164), 862.
- Lai, C. H., Huang, J. C., Cheng, H. H., Wu, M. C., Huang, M. Z., Hsu, H. Y., . . . Chu, Y. T. (2018). *Helicobacter pylori* cholesterol glucosylation modulates autophagy for increasing intracellular survival in macrophages. *Cellular microbiology*, e12947.
- Lambert, M. A., Patton, C. M., Barrett, T. J., & Moss, C. W. (1987). Differentiation of *Campylobacter* and *Campylobacter*-like organisms by cellular fatty acid composition. *Journal of clinical microbiology*, 25(4), 706-713.
- Lebrun, A. H., Wunder, C., Hildebrand, J., Churin, Y., Zahringer, U., Lindner, B., . . . Warnecke, D. (2006). Cloning of a cholesterol- α -glucosyltransferase from *Helicobacter pylori*. *J Biol Chem*, 281(38), 27765-27772. doi: 10.1074/jbc.M603345200
- Lee, H., Wang, P., Hoshino, H., Ito, Y., Kobayashi, M., Nakayama, J., . . . Fukuda, M. (2008). α 1, 4GlcNAc-capped mucin-type O-glycan inhibits cholesterol α -glucosyltransferase from *Helicobacter pylori* and suppresses *H. pylori* growth. *Glycobiology*, 18(7), 549-558.
- Lee, S. J., Lee, B. I., & Suh, S. W. (2011). Crystal structure of the catalytic domain of cholesterol- α -glucosyltransferase from *Helicobacter pylori*. *Proteins: Structure, Function, and Bioinformatics*, 79(7), 2321-2326.
- Li, H., Liao, T., Debowski, A. W., Tang, H., Nilsson, H. O., Stubbs, K. A., . . . Benghezal, M. (2016). Lipopolysaccharide Structure and Biosynthesis in *Helicobacter pylori*. *Helicobacter*, 21(6), 445-461.
- Lin, S. K., Lambert, J. R., Schembri, M. A., Nicholson, L., & Korman, M. G. (1994). *Helicobacter pylori* prevalence in endoscopy and medical staff. *J Gastroenterol Hepatol*, 9(4), 319-324.
- Loster, B. W., Czesnikiewicz-Guzik, M., Bielanski, W., Karczewska, E., Loster, J. E., Kalukin, J., . . . Konturek, S. J. (2009). Prevalence and characterization of *Helicobacter pylori* (*H. pylori*) infection and colonization in dentists. *J Physiol Pharmacol*, 60 Suppl 8, 13-18.
- Marshall, B. J., Armstrong, J. A., McGeachie, D. B., & Glancy, R. J. (1985). Attempt to fulfil Koch's postulates for pyloric *Campylobacter*. *The medical journal of Australia*, 142(8), 436-439.
- Martínez, L. E., Hardcastle, J. M., Wang, J., Pincus, Z., Tsang, J., Hoover, T. R., . . . Salama, N. R. (2016). *Helicobacter pylori* strains vary cell shape and flagellum number to maintain robust motility in viscous environments. *Molecular microbiology*, 99(1), 88-110.
- McGee, D. J., George, A. E., Trainor, E. A., Horton, K. E., Hildebrandt, E., & Testerman, T. L. (2011). Cholesterol enhances *Helicobacter pylori* resistance to antibiotics and LL-37. *Antimicrob Agents Chemother*, 55(6), 2897-2904. doi: 10.1128/AAC.00016-11
- Meyer-Rosberg, K., Scott, D. R., Rex, D., Melchers, K., & Sachs, G. (1996). The effect of environmental pH on the proton motive force of *Helicobacter pylori*. *Gastroenterology*, 111(4), 886-900.

- Monteiro, M. A. (2001). *Helicobacter pylori*: a wolf in sheep's clothing: the glyco-type families of *Helicobacter pylori* lipopolysaccharides expressing histo-blood groups: structure, biosynthesis, and role in pathogenesis.
- Morey, P., Pfannkuch, L., Pang, E., Boccellato, F., Sigal, M., Imai-Matsushima, A., . . . Schlaermann, P. (2018). *Helicobacter pylori* Depletes Cholesterol in Gastric Glands to Prevent Interferon Gamma Signaling and Escape the Inflammatory Response. *Gastroenterology*, 154(5), 1391-1404. e1399.
- Muotiala, A., Helander, I. M., Pyhälä, L., Kosunen, T. U., & Moran, A. (1992). Low biological activity of *Helicobacter pylori* lipopolysaccharide. *Infect Immun*, 60(4), 1714-1716.
- Murata-Kamiya, N., Kurashima, Y., Teishikata, Y., Yamahashi, Y., Saito, Y., Higashi, H., . . . Azuma, T. (2007). *Helicobacter pylori* CagA interacts with E-cadherin and deregulates the β -catenin signal that promotes intestinal transdifferentiation in gastric epithelial cells. *Oncogene*, 26(32), 4617.
- Namavar, F., Roosendaal, R., Kuipers, E. J., de Groot, P., van der Bijl, M. W., Pena, A. S., & de Graaff, J. (1995). Presence of *Helicobacter pylori* in the oral cavity, oesophagus, stomach and faeces of patients with gastritis. *Eur J Clin Microbiol Infect Dis*, 14(3), 234-237.
- Odenbreit, S., Püls, J., Sedlmaier, B., Gerland, E., Fischer, W., & Haas, R. (2000). Translocation of *Helicobacter pylori* CagA into gastric epithelial cells by type IV secretion. *Science*, 287(5457), 1497-1500.
- Osaki, T., Hanawa, T., Manzoku, T., Fukuda, M., Kawakami, H., Suzuki, H., . . . Kurata, S. (2006). Mutation of *luxS* affects motility and infectivity of *Helicobacter pylori* in gastric mucosa of a Mongolian gerbil model. *Journal of medical microbiology*, 55(11), 1477-1485.
- Palframan, S. L., Kwok, T., & Gabriel, K. (2012). Vacuolating cytotoxin A (VacA), a key toxin for *Helicobacter pylori* pathogenesis. *Frontiers in cellular and infection microbiology*, 2, 92.
- Pandey, A. K., & Sasseti, C. M. (2008). Mycobacterial persistence requires the utilization of host cholesterol. *Proc Natl Acad Sci U S A*, 105(11), 4376-4380. doi: 10.1073/pnas.0711159105
- Parsonnet, J., Friedman, G., Orentreich, N., & Vogelstein, H. (1997). Risk for gastric cancer in people with CagA positive or CagA negative *Helicobacter pylori* infection. *Gut*, 40(3), 297-301.
- Patel, H. K., Willhite, D. C., Patel, R. M., Ye, D., Williams, C. L., Torres, E. M., . . . Blanke, S. R. (2002). Plasma Membrane Cholesterol Modulates Cellular Vacuolation Induced by the *Helicobacter pylori* Vacuolating Cytotoxin. *Infect Immun*, 70(8), 4112-4123. doi: 10.1128/iai.70.8.4112-4123.2002
- Polk, D. B., & Peek Jr, R. M. (2010). *Helicobacter pylori*: gastric cancer and beyond. *Nature Reviews Cancer*, 10(6), 403.
- Rader, B. A., Campagna, S. R., Semmelhack, M. F., Bassler, B. L., & Guillemin, K. (2007). The quorum-sensing molecule autoinducer 2 regulates motility and flagellar morphogenesis in *Helicobacter pylori*. *Journal of bacteriology*, 189(17), 6109-6117.
- Roesler, B. M., Rabelo-Gonçalves, E. M., & Zeitune, J. M. (2014). Virulence factors of *Helicobacter pylori*: a review. *Clinical Medicine Insights: Gastroenterology*, 7, CGast. S13760.
- Ruiz, B., Correa, P., Fontham, E. T., & Ramakrishnan, T. (1996). Antral atrophy, *Helicobacter pylori* colonization, and gastric pH. *American journal of clinical pathology*, 105(1), 96-101.
- Santiago, P., Moreno, Y., & Ferrús, M. A. (2015). Identification of viable *Helicobacter pylori* in drinking water supplies by cultural and molecular techniques. *Helicobacter*, 20(4), 252-259.
- Schmees, C., Prinz, C., Treptau, T., Rad, R., Hengst, L., Volland, P., . . . Gerhard, M. (2007). Inhibition of T-cell proliferation by *Helicobacter pylori* γ -glutamyl transpeptidase. *Gastroenterology*, 132(5), 1820-1833.
- Sipponen, P., Kekki, M., Haapakoski, J., Ihamäki, T., & Siurala, M. (1985). Gastric cancer risk in chronic atrophic gastritis: statistical calculations of cross-sectional data. *Int J Cancer*, 35(2), 173-177.

- Sobala, G., Crabtree, J., Dixon, M., Schorah, C., Taylor, J., Rathbone, B., . . . Axon, A. (1991). Acute *Helicobacter pylori* infection: clinical features, local and systemic immune response, gastric mucosal histology, and gastric juice ascorbic acid concentrations. *Gut*, 32(11), 1415-1418.
- Stead, C. M., Zhao, J., Raetz, C. R., & Trent, M. S. (2010). Removal of the outer Kdo from *Helicobacter pylori* lipopolysaccharide and its impact on the bacterial surface. *Molecular microbiology*, 78(4), 837-852.
- Stuart, E. S., Webley, W. C., & Norkin, L. C. (2003). Lipid rafts, caveolae, caveolin-1, and entry by *Chlamydiae* into host cells. *Experimental cell research*, 287(1), 67-78.
- Sycuro, L. K., Pincus, Z., Gutierrez, K. D., Biboy, J., Stern, C. A., Vollmer, W., & Salama, N. R. (2010). Peptidoglycan crosslinking relaxation promotes *Helicobacter pylori*'s helical shape and stomach colonization. *Cell*, 141(5), 822-833.
- Sycuro, L. K., Wyckoff, T. J., Biboy, J., Born, P., Pincus, Z., Vollmer, W., & Salama, N. R. (2012). Multiple peptidoglycan modification networks modulate *Helicobacter pylori*'s cell shape, motility, and colonization potential. *PLoS pathogens*, 8(3), e1002603.
- Szabò, I., Brutsche, S., Tombola, F., Moschioni, M., Satin, B., Telford, J. L., . . . Zoratti, M. (1999). Formation of anion-selective channels in the cell plasma membrane by the toxin VacA of *Helicobacter pylori* is required for its biological activity. *The EMBO journal*, 18(20), 5517-5527.
- Terebiznik, M., Vazquez, C., Torbicki, K., Banks, D., Wang, T., Hong, W., . . . Jones, N. (2006). *Helicobacter pylori* VacA toxin promotes bacterial intracellular survival in gastric epithelial cells. *Infect Immun*, 74(12), 6599-6614.
- Thomsen, L., Gavin, J., & Tasman-Jones, C. (1990). Relation of *Helicobacter pylori* to the human gastric mucosa in chronic gastritis of the antrum. *Gut*, 31(11), 1230-1236.
- Tomb, J.-F., White, O., Kerlavage, A. R., Clayton, R. A., Sutton, G. G., Fleischmann, R. D., . . . Dougherty, B. A. (1997). Corrections: The complete genome sequence of the gastric pathogen *Helicobacter pylori*. *Nature*, 389(6649), 412.
- Torres, J., Perez-Perez, G., Goodman, K. J., Atherton, J. C., Gold, B. D., Harris, P. R., . . . Munoz, O. (2000). A comprehensive review of the natural history of *Helicobacter pylori* infection in children. *Arch Med Res*, 31(5), 431-469.
- Trainor, E. A., Horton, K. E., Savage, P. B., Testerman, T. L., & McGee, D. J. (2011). Role of the HefC efflux pump in *Helicobacter pylori* cholesterol-dependent resistance to ceragenins and bile salts. *Infect Immun*, 79(1), 88-97. doi: 10.1128/IAI.00974-09
- Turbett, G. R., Hoj, P. B., Horne, R., & Mee, B. J. (1992). Purification and characterization of the urease enzymes of *Helicobacter* species from humans and animals. *Infect Immun*, 60(12), 5259-5266.
- Unemo, M., Aspholm-Hurtig, M., Ilver, D., Bergström, J., Borén, T., Danielsson, D., & Teneberg, S. (2005). The sialic acid binding SabA adhesin of *Helicobacter pylori* is essential for nonopsonic activation of human neutrophils. *Journal of Biological Chemistry*.
- Van den Brink, G., Tytgat, K., Van der Hulst, R., Van der Loos, C., Einerhand, A., Büller, H., & Dekker, J. (2000). *H. pylori* colocalises with MUC5AC in the human stomach. *Gut*, 46(5), 601-607.
- van Zanten, S. J. V., Dixon, M. F., & Lee, A. (1999). The gastric transitional zones: neglected links between gastroduodenal pathology and *helicobacter* ecology. *Gastroenterology*, 116(5), 1217-1229.
- Wang, H. J., Cheng, W. C., Cheng, H. H., Lai, C. H., & Wang, W. C. (2012). *Helicobacter pylori* cholesteryl glucosides interfere with host membrane phase and affect type IV secretion system function during infection in AGS cells. *Mol Microbiol*, 83(1), 67-84. doi: 10.1111/j.1365-2958.2011.07910.x
- Wunder, C., Churin, Y., Winau, F., Warnecke, D., Vieth, M., Lindner, B., . . . Meyer, T. F. (2006). Cholesterol glucosylation promotes immune evasion by *Helicobacter pylori*. *Nat Med*, 12(9), 1030-1038. doi: 10.1038/nm1480
- Yamaoka, Y. (2008). *Helicobacter pylori: molecular genetics and cellular biology*: Horizon Scientific Press.

- Yamaoka, Y., Ojo, O., Fujimoto, S., Odenbreit, S., Haas, R., Gutierrez, O., . . . Graham, D. Y. (2006). *Helicobacter pylori* outer membrane proteins and gastroduodenal disease. *Gut*, 55(6), 775-781.
- Yee, J. K. C. (2017). Are the view of *Helicobacter pylori* colonized in the oral cavity an illusion? *Exp Mol Med*, 49(11), e397. doi: 10.1038/emm.2017.225
- Yeh, J. M., Kuntz, K. M., Ezzati, M., & Goldie, S. J. (2009). Exploring the cost-effectiveness of *Helicobacter pylori* screening to prevent gastric cancer in China in anticipation of clinical trial results. *Int J Cancer*, 124(1), 157-166. doi: 10.1002/ijc.23864

Chapter 2

Objective 1: To study the morphology of *H. pylori* population grown in the absence of cholesterol and deletion of *hp0421*.



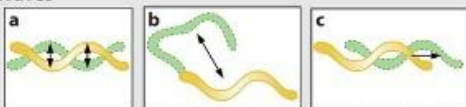
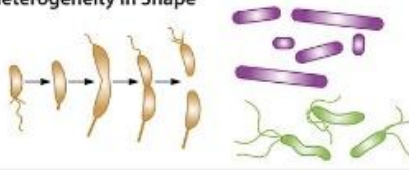
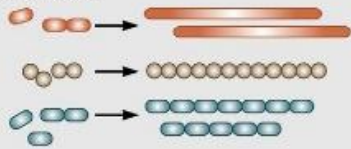
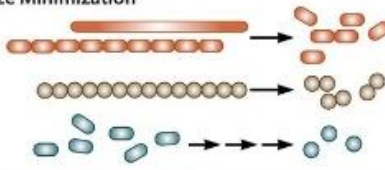

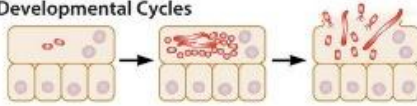


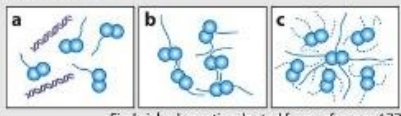
INTRODUCTION

Bacteria have diverse morphologies and recent studies made great progress in understanding mechanisms that are responsible for distinct morphological features of bacteria and the role of the bacterial morphology in virulence and colonization (Young, 2006). Bacteria are diverse in their cell shapes, some exhibit coccoid form and other extend as rods with varying degree of helicities and curvatures. On the other hand some bacteria develop unusual shapes like stars that is the result of the extensions of prosthecae via polar growth. (Table 2.1). Interestingly, bacterial morphology changes in response to the surroundings conditions or during their life phases. The current understanding about the mechanisms that are involved in bacterial shape comes from the comprehensive studies that focused on model bacteria which represent the most common shapes. For example, the most studied vibrioid or curved-rod is (*Caulobacter crescentus*), coccoid (*Staphylococcus aureus*) and rod (*Escherichia coli*). More recently, the studies that analyzed the infection models of pathogenic bacteria have explored the morphological diversity between mutants having altered shapes and exhibited an alteration in their virulence properties and colonization abilities (Yang et al., 2016). The above observations suggests that the bacterial cell morphology may be involved in the pathogenicity or that the host environment influences on selecting morphological distinctiveness.

Probably, one of the well-known model organism is *Caulobacter crescentus*. *C. crescentus* have a distinct crescent shape that is controlled by one protein called crescentin which is coded by *creS*. The deletion of *creS* results in straight-rod cells (Ausmees, Kuhn, & Jacobs-Wagner, 2003). Furthermore, Persat, et al., have shown that the straight-rod mutant's surface colonization ability have been affected compared to the native curve-rods (Persat, Stone, & Gitai, 2014).

With regard to the curved rod like pathogens such as; *Vibrio parahaemolyticus* and *Vibrio cholerae* that do not have a gene like *creS* homolog, demonstrate that there are alternative mechanisms that regulate the vibrioid shape. The helical shape of bacteria have arisen during evolution of bacteria. For example, the human bacterial pathogens like spirochetes (*Borrelia spp.*) and e.g., *Treponema* and the proteobacteria such as *Campylobacter jejuni* and *Helicobacter spp.* Several reports have observed that when helical spirochetes and proteobacteria lose their helical cell shape their motility and colonization abilities are greatly affected (Yang et al., 2016). For instance, *Campylobacter jejuni* is one of the helical shaped bacteria and a pathogen that cause enteritis in humans. The characteristic helical-shape of *C. jejuni* is controlled by *pgpI* (peptidoglycan peptidase 1). Moreover, *pgpI* mutants exhibited rod-shaped morphology which is in contrast to the native helical form of wild-type. Interestingly, the rod-shaped *pgpI* mutant have shown less colonization ability in chicks by more than three times compare to wild-type (Friedrich et al., 2012). Likewise, there are few bacteria which are known to possess glycolipids in their cell envelope. These include bacteria in the genera of *Helicobacter*, *Mycoplasma* and *Borrelia*. For example, *Borrelia burgdorferi*, is a spirochetes and one of human pathogens that cause Lyme disease. Cholesterol is required for *B. burgdorferi* to grow as it cannot synthesize cholesterol internally and it has developed the ability to acquire sterols from the vicinity (Johnson, 1977). Lipid contents were determined in *Borrelia* by high performance thin layer chromatography (HPLC) and eleven types of lipids were identified. Among these, two glycolipids contain cholesterol, cholesteryl 6-O-acyl- β -D-galactopyranoside (ACGal) and cholesterol- β -D-galactopyranoside (CGal), where cholesterol molecules are linked to galactose. The glycolipids comprises about 50–60% of the total lipids of bacterium (Hossain, Wellensiek, Geyer, & Lochnit, 2001).

Table 2.1: Morphological variations and the functional consequences in different bacteria (Yang, Blair, & Salama, 2016)

Morphological Feature/Shape	Example Organism(s)	Functional Consequence
Curvature 	<i>Caulobacter crescentus</i> <i>Vibrio cholerae</i> <i>Vibrio parahaemolyticus</i>	Cell curvature enhances surface colonization in aquatic environments with moderate flow.
Helical 	<i>Helicobacter pylori</i> <i>Campylobacter jejuni</i> <i>Spirochetes</i> sp. <i>Spirochaeta aurantia</i> <i>Leptospira interrogans</i>	Helical shape increases torque, which can enhance speed and facilitate escape from viscous solutions.
Waves  <p>Waves schematic adapted from reference 48.</p>	<i>Spirochetes</i> sp. <i>Borrelia burgdorferi</i> <i>Treponema pallidum</i>	Flat-wave morphology allows alternative motility in gel-like media: a) wriggling b) lunging c) translocating
Heterogeneity in Shape 	<i>Caulobacter crescentus</i> <i>Helicobacter pylori</i> <i>Mycobacterium tuberculosis</i>	Asymmetric growth and division can contribute towards directional motility, daughter cells with differing cell fates, and the formation of heterogeneous populations with varying susceptibility to antibiotics and other stresses. Increase/enhance successful adaptation to different host environments.
Filamentation 	<i>Legionella pneumophila</i> <i>Streptococcus pneumoniae</i> <i>Uropathogenic Escherichia coli</i>	Evade phagocytosis-mediated killing (harder to engulf long filaments). Filaments can promote slow, ligand-mediated uptake and invasion. Increase/enhance attachment to host surfaces/cells. Promote/facilitate the development of antibiotic resistance (promote/enhance the emergence of beneficial mutations in response to stress).
Size Minimization 	<i>Moraxella catarrhalis</i> <i>Neisseria meningitidis</i> <i>Salmonella typhimurium</i> <i>Streptococcus pneumoniae</i>	Cell size minimization helps to avoid complement-mediated killing by the host. Mucosa-associated bacterial lineages show size minimization from rods to cocci.
Swarm Cell Differentiation 	<i>Pseudomonas aeruginosa</i> <i>Proteus mirabilis</i> <i>Vibrio parahaemolyticus</i>	Surface sensing via rotational inhibition of a polar flagellum elicits genetic reprogramming events that can lead to cell elongation and expression of factors which promote swarming motility.
Developmental Cycles 	<i>Uropathogenic Escherichia coli</i> <i>Chlamydia</i> sp. <i>Rickettsia</i> sp.	Morphological changes associated with developmental cycles provide a mechanism for bacterial pathogens to grow intracellularly, subvert host immunity and facilitate subsequent rounds of invasion and infection. <i>Chlamydia</i> sp. and <i>Rickettsia</i> sp. developmental cycles are not pictured here.
Bacterial Appendage Number & Placement Flagella 	<i>Borrelia burgdorferi</i> <i>Campylobacter jejuni</i> <i>Helicobacter pylori</i>	Flagella placement determines distinct modes of motility and morphological characteristics crucial for nutrient and niche acquisition.
Stalks or Prosthecae 	<i>Asticcacaulis biprosthecium</i> <i>Asticcacaulis excentricus</i> <i>Caulobacter crescentus</i>	Stalks increase overall surface area and can allow for enhanced nutrient acquisition. Stalk elongation allows bacteria to physically separate from competitors.
Fimbriae or Pili  <p>Fimbrial schematic adapted from reference 177.</p>	<i>Neisseria meningitidis</i> <i>Uropathogenic Escherichia coli</i>	Pili can facilitate a number of different functions depending on how many are present: a) competence (single pilus) b) self-aggregation (two pili) c) crosstalk with host cells (dashed lines) (three or more pili)

LaRocca et al., reported that ACGal glycolipids that were gold labeled antibodies were observed directly under the transmission electron microscope (TEM) (Timothy J LaRocca et al., 2010). Moreover, cholesterol was chelated from *B. burgdorferi* membrane by methyl- β -cyclodextrin (M β CD) and swapped by ergosterol, cholesterol, dihydrocholesterol, and stigmasterol in model membrane studies they were shown to be raft-promoting that supported development of microdomains identical to the membrane microdomains in *B. burgdorferi* before sterol exchange. Moreover, substitution of sterols with zymosterol, lanosterol, desmosterol and cholesterol formate were shown to have a moderate ability to form rafts in model membrane in *B. burgdorferi*, while when it was substituted with androsterol and coprostanol no microdomains were detected. Similarly, the spiral morphology of *B. burgdorferi* varied based on the type of sterol that have been substituted after cholesterol depletion by M β CD. When sterol was exchanged in *B. burgdorferi* with strong raft-forming sterols, the cells exhibited smooth surface with native planar wave morphology, when it was exchanged with sterols that did not support formation of membrane ordered domains it totally lost its planar wave shape, forming a tightly curled morphology or straight cells. Interestingly, spirochete sterol when depleted with M β CD without sterol replacement formed coiled structures (T. J. LaRocca et al., 2013). Therefore, cholesterol containing glycolipids are crucial in maintaining the native spiral morphology of bacteria such as *B. burgdorferi*.

Morphology of *H. pylori*

H. pylori belongs to the Epsilon proteobacteria bacteria class, which almost includes curved and helical organisms. *H. pylori* is a helical shape bacteria and there are studies which have analyzed the morphology and identified some determinants that control the native helical morphology of *H. pylori*.

Sycuro et al., identified four genes that are required in the maintenance of *H. pylori*'s native helical morphology and they are called cell shape determinants (*csds*). Three genes (*csd1-3*) were identified as peptidoglycan endopeptidase homologs and the gene which control curved cell morphology (*ccmA*) homolog which is responsible for the straight rod shape in *Proteus mirabilis*. Moreover, deletion of these genes results in variable morphological alterations in *H. pylori*. For instance, deletion of *csd1* led to formation of rod shaped cells compared to native helical shape. Similarly, *csd3* mutants exhibited variable curved rod, 'c'-shaped cells and loss of helical shape (L. K. Sycuro et al., 2010). Furthermore, *csd5* a putative scaffolding protein and *csd4* which codes for DL-carboxypeptidase of peptidoglycan protein were identified. The *csd4* and *csd5* mutants showed that the helical shape was perturbed and resulted in slight changes in length and width of cells (Laura K Sycuro et al., 2012). Later it was observed that the Csd4 enzyme is involved in generation of *H. pylori* helical shape, as the glutamine-zinc ligand that split the cell wall tripeptides. (Chan et al., 2015).

H. pylori undergoes morphological changes from spiral to coccoid under different stress conditions like variations in temperature, oxygen level and increased culture duration. Previously, it has been reported that lipid contents drastically changes during helical to coccoid transition in *H. pylori* where α CAG levels increases while phosphatidyl ethanolamine and α CG level decreases. The α CPG scarcely presented in the spiral form in the log phase, but subsequently increases during the coccoid conversion in lag phase (Shimomura, Hayashi, Yokota, Oguma, & Hirai, 2004).

Here in this study, we tried to decipher the morphological changes in *H. pylori* grown in the absence of cholesterol. We also investigated the morphological changes of *hp0421* mutants of *H. pylori* strain 26695 [*Hp26695* (human strain)] and *H. pylori* strain 76 [*Hp76* (mice strain)] by various approaches like confocal microscopy, flow cytometry and quantitative morphology analysis by CellTool software package.

MATERIAL AND METHODS

Bacterial strains and cholesterol loading

Human adapted strain *Hp26695* and its mutant *Hp26695Δ0421* were grown on GC agar medium (Difco) enriched with 10% decomplexed horse serum, and contained nystatin and 2.5 µg/ml, vancomycin 1 µg/ml, trimethoprim, 10 µg/ml and 1X of vitamin mixture (Table 2.2) as described previously (Tenguria et al., 2014). For resistance selection an aliquot of 4 µg/ml kanamycin was added as marker for *Hp26695Δ0421*. Mice adapted strain *Hp76*, its mutant *Hp76Δ0421* and reconstituted *Hp76Δ0421* were a gift from Thomas F Meyer, Max Planck Institute for Infection Biology, Germany. *Hp76* strains were maintained as described previously (Wunder et al., 2006) and explained in (Table 2.3). Antibiotics were excluded in experiments such as antibiotic resistance determination and aztreonam filamentation assay. Further, *Hp26695* were grown in absence of cholesterol and the procedures were modified from earlier described method(s) (Testerman, McGee, & Mobley, 2001). Briefly, *Hp26695* wild-type were grown on (chemically defined medium) Ham's F-12 (Gibco) enriched with 1 mg/ml BSA with or without 1 mM of water-soluble cholesterol (250 µM cholesterol with 4 mM MβCD) (Sigma). For agar plates, Ham's F-12 medium was prepared (2x) and mixed with 30 g per liter agar at 1:1 ratio. To visualize the cell elongation, 2 µg/ml of aztreonam antibiotic was added to media. All the strains were incubated at humidified microaerophilic conditions at 5% O₂ and 5% CO₂.

Glycerol stocks of *H. pylori*

H. pylori culture with 10^9 CFU cells were collected from GC plates and suspended in 3 ml Brain heart infusion (BHI) broth supplemented with 10% decomplexed horse serum and 20% glycerol. It was then aliquoted in 50 μ l volumes in screw cap cryotubes each labeled and preserved in -80 (Oskouei, Bekmen, Ellidokuz, & Yilmaz, 2010).

Table 2.2: Vitamin Mixture Composition [Light sensitive]

Ser. No.	component	Final concentration	Made	Cat. No.
1	L-glutamine	0.68mM	Sigma	G8540
2	Cysteine Chloride	1.48mM	Sigma	C6852
3	Iron(III) nitrate	0.5 μ M	Sigma	216828
4	Thiamine Chloride	0.088 μ M	Sigma	T1270
5	NAD (Nicotinamide Adenine dinucleotide)	3.76 μ M	Sigma	N3014
6	Vitamin B12	0.073 μ M	Sigma	V6629
7	Adenine	27.1 μ M	Sigma	A8626
8	Uracil	44.6 μ M	Sigma	U0750
9	L- Argine Monohydrate	7.12 μ M	Sigma	A6969
Prepared as 500X, dissolved in autoclaved double distilled water and filtered by Millix-GV syringe filter 0.22 μ m and the aliquots were stored at -20c.				

Table 2.3: *Hp76* Strains growth media and selective markers

Strain	Media	Supplementation	Antibiotics µg/ml
<i>Helicobacter pylori</i> P76 (<i>Hp76</i>)	GC base agar 4 g/100ml (BD)	10% of decomplexed Horse Serum (Gibco) and 1x Vitamin mixture (Table 2.2).	Vancomycin 10, Nystatin 1, Trimethoprim 5, and Streptomycin 200.
<i>Helicobacter Pylori</i> <i>P76Δ421</i> (<i>Hp76Δ421</i>)	GC base agar 4 g/100ml (BD)	10% of decomplexed Horse Serum (Gibco) and 1x Vitamin mixture (Table 2.2).	Vancomycin 10, Nystatin 1, Trimethoprim 5, Streptomycin 400, and Chloramphenicol 4.
<i>Helicobacter pylori</i> <i>P76Δ421</i> -reconstituted (<i>Hp76Δ421</i> - reconstituted)	GC base agar 4 g/100ml (BD)	10% of decomplexed Horse Serum (Gibco) and 1x Vitamin mixture (Table 2.2).	Vancomycin 10, Nystatin 1, Trimethoprim 5, Streptomycin 400, Chloramphenicol 4, and Kanamycin 8.

Generation of *Hp26695Δ421*

Construct design

The gene *hp0421* (GeneID 900074) which code for cholesterol α -glucosyl transferase in *H. pylori* has a size of around 1.17 kb. Knockout in *Hp26695* was generated by homologous recombination as described previously (Lebrun et al., 2006). Two pairs of primers corresponding to a PCR product surrounding the *hp0421* upstream (PCR1) which flanked 400bp region and downstream (PCR2) which span 500bp were designed (Figure 2.1A).

In addition the internal primers (PCR1 reverse and PCR2 forward) carry the corresponding target sequence of XhoI and NcoI *hp0421*-US-F 5' GTGGATTATGACTCTTTAGAGACTTG 3' *hp0421*-US-F 5' GTGGATTATGACTCTTTAGAGACTTG 3', *hp0421*-US-R 5' GTGCCATGGCTCGAGTTAACTACTCTTCTTTAAAATTGAAT 3', *hp0421*-DS-F 5' GTGCCATGGCTCGAGTGAAAGGATAAAAAATGCAAGAA 3', *hp0421*-DS-R 5' CCAATTTTAGGGCAGGCTAAAAAC 3', *kanR*-F 5'GATCCATGGCTCGAGTTTTCTACGGGGTCTGACG 3' and *kanR*-R 5' GTGCCATGGCTCGAGCTTAGAAAACTCATCGAGCATCAAATGA 3'. All steps of construct designing were performed using Cloning Manger software (Figure 2.1B).

Construct amplification

Annealing temperature of the primer was standardized by gradient PCR from 46°C to 62°C (Figure 2.2A). Amplification of upstream, downstream and kanamycin resistant cassette by using Q5 High-Fidelity DNA polymerase (NEB) was performed. The reaction mixture and thermocycling conditions are mentioned in. 3 µl of PCR products were resolved on 1.5% agarose gel and the DNA concentration were measured by nanodrop spectrophotometry. The amplified products were stored at -20.

PCR1 and PCR2 restriction digestion

PCR1 and PCR2 products were subjected to digestion by XhoI in order to ligate the two fragments and generate PCR3 fragment. The restriction digestion mixture was prepared as mentioned in (Table 1.4). The mixture was mixed gently and spun for seconds and incubated for 2 hours at 37°C. Then XhoI was heat inactivated for 20 minutes at 65°C.

A *Helicobacter pylori* 26695 chromosome, complete genome

NCBI Reference Sequence: NC_000915.1

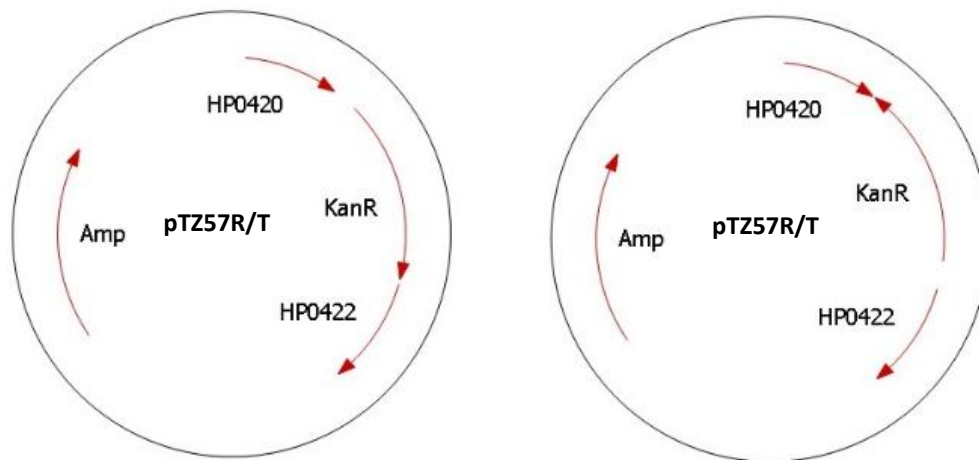
[GenBank](#) [FASTA](#)**B****Figure 2.1:** (A) genome map represent the position of *hp0421* in *H. pylori* strain 26695(B) Virtual clone of *hp0421* knockout construct designed by Cloning Manager softwarehttp://www.scied.com/pr_cmpro.htm.

Table 2.4: Restriction digestion reaction mixture

Components	Volume in μl
Nuclease free-water	18
10X buffer R	2
Template	10 (0.5 μg)
XhoI 10U/ μl	2

Cleaning-up the digested products from the enzymatic and salt contaminants using gel extraction columns (QIAGEN, 28706)

The digested fragments were resolved on agarose gel and the respective bands of PCR1 and PCR2 were excised under UV transilluminator. QG buffer (3:1 v/wt) were added to the excised gel of PCR1 and PCR2, and 1 volume of Isopropanol was mixed properly and then transferred into the elution QIAquick spin column. Spin column centrifuged for 1 min at 10000 rpm to bind DNA. Then, 0.75 ml of buffer PE was added to the column, left for 3 min. To elute DNA, 50 μl of H₂O was added to the middle of the column membrane followed by centrifugation at maximum speed for 1 min.

Ligation of PCR1 & PCR2 by T4 ligase and generation of PCR3

The PCR1 and PCR2 ligation mixture were mixed in order to generate PCR3 using T4 ligase. The ligation mixture was kept at 25°C for 1 hour followed by 65° C for 10 min. the ligated PCR3 was amplified using *hp0421*-US-F 5' GTGGATTATGACTCTTTAGAGACTTG 3', *hp0421*-DS-R 5' CCAATTTTAGGGCAGGCTAAAAAC 3' primers and Q5 High-Fidelity DNA polymerase.

The amplified products were loaded on 1.2% agarose gel (Figure 2.2B). To confirm the PCR3 fragment ligation and amplification PCR3 fragment was digested by XhoI as mentioned above and loaded on 1.5% agarose gel (Figure 2.2C). PCR3 products were loaded on 1% agarose gel, the corresponding band was excised and purified as mentioned previously using QIAquick spin column. In order to clone PCR3 into pTZ57R/T vector, purified PCR3 products were subjected for 3' A-tailing.

TA cloning of PCR3 in pTZ57R/T vector

The PCR3 products were ligated into pTZ57R/T vector at 1:3 (vector:insert) ratio using InsTAclone PCR Cloning Kit (Thermo Scientific). The mixture was incubated for overnight at 16°C followed by T4 ligase inactivation at 65°C for 10 minutes. *E. coli* DH5 α ultracomptent cells were thawed in ice and mixed with 2.5 μ l of ligation mixture and kept in ice for 30 min. The transformation mixture was kept at 42°C for 90 sec then immediately transformed into ice for 1 minutes. 0.5 ml of Luria-Bertani (LB) broth was added to the transformed cells and incubated at 37°C for 1 hour. Transformed cells were pelleted down at 6000 rpm for 5 min, mixed with 100 μ l of LB broth and plated on LB agar medium containing 100 μ g/ml of ampicillin.

Plasmid purification by alkaline lysis using QIAGEN kit and insert confirmation

The overnight cultures of transformed bacterial cells were pelleted down at 10000 rpm for 3 min, pellet was resuspended in 250 μ l of P1 solution containing RNaseA 20 μ g/ml and incubated for 20 minutes. 250 μ l of P2 solution were added and mixed gently until the solution became clear and incubated for 5 min.

350 µl of P3 solution were added, mixed gently by turn upside down the tubes 5 times, equal amounts of Isopropanol were added and incubated in -80°C for 30 minutes. The mixture was pelleted down for 12 minutes at 13000 rpm and the pellet removed. Followed by adding 1 ml of 70% ethanol to the supernatant and centrifuged at 13000 rpm. The pellet was left upside down on the bench till it dried from the ethanol and resuspend in 50 µl of desalted water. The plasmid were resolved on agarose gel. The plasmid was double digested using XhoI and BamHI and fragment size was checked on agarose gel. The *E. coli* that carried PCR3 insert were expanded and plasmids were purified as mentioned above. The plasmid concentration was quantified by nanodrop®.

Insertion of *kanR* cassette into pTZ57R/T-PCR3 plasmid

The purified plasmid carrying PCR3 was digested by XhoI followed by treatment with FastAP to remove phosphate group and inhibit self-ligation of the plasmid by adding 1 µl of FastAP and incubated for 10 min at 37°C followed by inactivation for 5 min at 75°C. The amplified *kanR* cassette was digested by XhoI and cleaned-up using QIAquick spin column as mentioned above. Then, *kanR* cassette was ligated to the pTZ57R/T-PCR3 plasmid and transformed into *E. coli* DH5α as mentioned above. The transformed bacterial cells were incubated overnight on LB agar containing 4 µg/ml kanamycin then 5 colonies were selected for plasmid isolation. To check the orientation of kanamycin resistance cassette the construct was double digested at one internal site and one external site as mentioned in (Table 2.5) and incubated at 37°C for 2 hours. The digestion mixtures were resolved on 2% agarose gel and visualized under UV illuminator.

Table 2.5: pTZ57R/T-PCR3 double-digestion reaction mixture

Components	Volume in μl
Nuclease free-water	18
2X Tango Buffer	4
Template	10 (0.5 μg)
XhoI 10U/ μl	2
BamHI	2

Natural transformation of pTZ57R/T-PCR3 into *H. pylori*

H. pylori were cultured on three plates of GC medium and collected into 3 ml of BHI broth. *H. pylori* cell paste was mixed with 3 $\mu\text{g}/\text{ml}$ of pTZ57R/T-PCR3 plasmid and 200 μl of mixture was aliquoted into 24 well plates and incubated in microaerophilic condition for 3 hours. The transformation paste were grown on GC agar medium containing 4 $\mu\text{g}/\text{ml}$ kanamycin for 3 days. Few colony were selected and checked for the absence of the plasmid (sensitivity to Amp) and for the presence of the resistance cassette inserted in the genome. Also, we performed a PCR with one primer internal to the cassette and one on the genome of *H. pylori* to ensure that the recombination took place in the correct locus.

Analysis of *H. pylori* cell morphology by flow cytometry (FC)

Flow cytometry is an efficient technique to analyze *H. pylori* whole population and the method we followed was modified from (L. K. Sycuro et al., 2013).

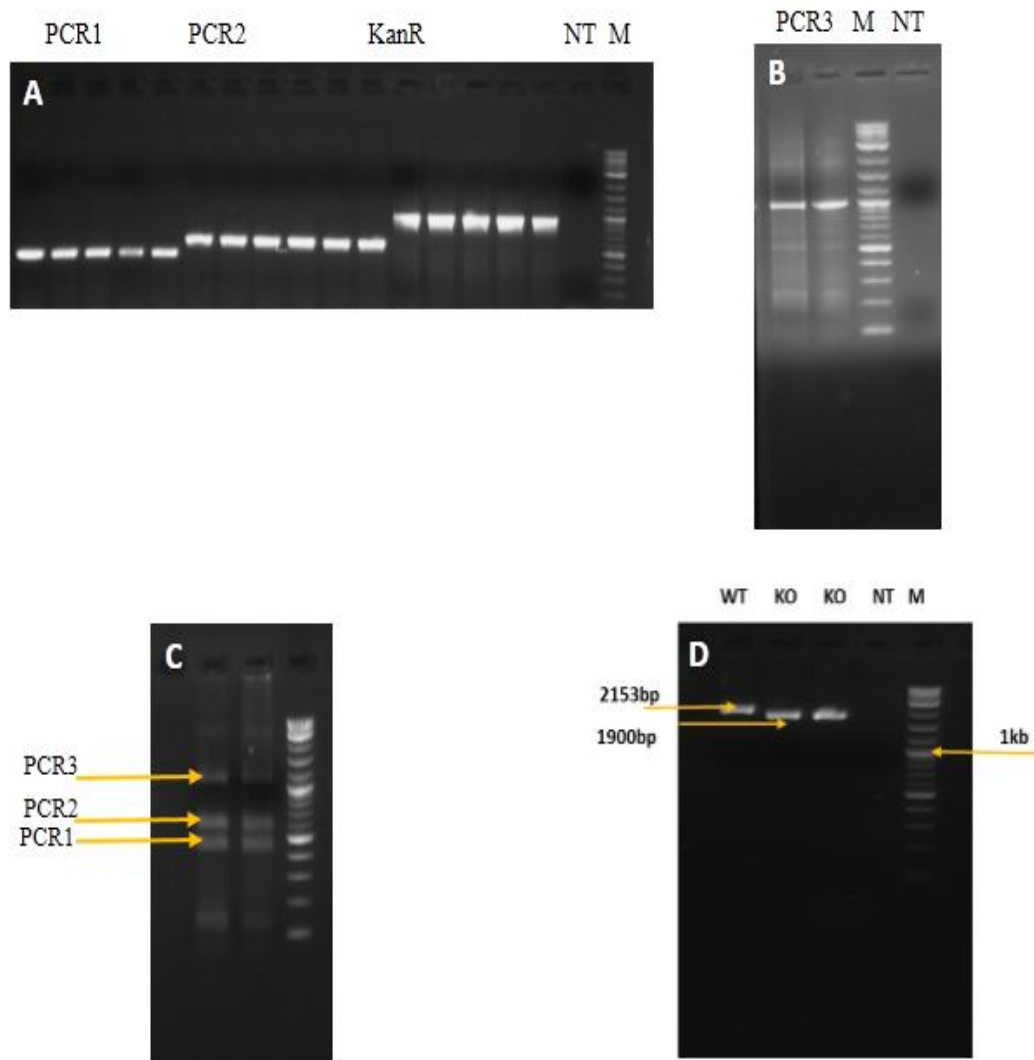


Figure 2.2: *hp0421* knockout generation in *H. pylori* strain 26695; 1.5% agarose gel shows, (A) The amplified PCR1, PCR2 and KanR fragments at different annealing temperature (B) PCR3 amplified fragment after ligation, (C) PCR3 digestion by XhoI and (D) Complete construct amplified from wild-type and *hp0421* mutant.

For cholesterol absence based selection, *Hp26695* strain was grown on chemically defined medium. For *hp0421* mutants, *Hp26695* strains and *Hp76* strains were all grown for 48-72 hours on GC agar (BD Biosciences). The bacterial cells were resuspended in 1 ml of filtered PBS through Millix-GV syringe filter 0.22 μm . The bacterial suspension was adjusted to 0.4 O.D₅₅₀ and acquired by flow cytometry.

H. pylori* morphological analysis upon deletion of *hp0421

H. pylori were grown on GC agar for 48 hours, washed by PBS (pH 7.0) with 10% glycerol thrice and the cells were adjusted to O.D₅₅₀ of 0.2. Cells were mounted on glass slides and cell population were captured using confocal microscope by employing transmitted light mode (Carl Zeiss Model: LSM 880). The image optimization was carried out in Adobe Photoshop 7 (Figure 2.2A). The quantitative analysis of processed images to measure the *x-size*, *y-size* and aspect ratio of *H. pylori* cells were done individually by CellTool software package as described previously (Pincus & Theriot, 2007; L. K. Sycuro et al., 2010). Briefly, the shape of each cell as image contours and smoothed using CellTool software package (Figure 2.2B). The individual contours were aligned in one plot and we plotted shape modes based on the variance from the standard deviations from mean in each shape mode and percentage of variance in each mode was calculated (Figure 2.2C). After that, all shape models were plotted in the normalized position based on standard deviations from the mean of curvature, width and length of cells (Figure 2.2D). Subsequently, one model was plotted which represents all populations (Figure 2.2E). Based on the mean model of cell population the shape of *Hp26695* wild-type, *Hp26695* Δ 421, *Hp76* wild-type, *Hp76* Δ 421 and *Hp76* Δ 421-reconstituted were analyzed and the individual cell's *x-size*, *y-size* and aspect ratio was quantified to display the variation in morphology between strains.

Analysis of *H. pylori* Cell wall fluidity by flow cytometry

To determine the fluorescence intensity of ethidium bromide (EtBr) in-fluxed into the bacterial cells flow cytometry was employed. The staining and measurement procedures for EtBr influx were modified from previous study (Paixão et al., 2009).

Briefly, for cholesterol absence based selection, *Hp26695* strain was grown on chemically defined medium. For *hp0421* mutants, *Hp26695* strains and *Hp76* strains were all grown for 48-72 hours on GC agar (BD Biosciences). Bacterial cells were collected and washed thrice with PBS at pH 7.4 (Gibco). A total of 10^6 cells were resuspended in 1 ml PBS or in 1 ml PBS containing 5 µg of EtBr filtered by Millix-GV syringe filter 0.22 µm (Merck-Millipore). All the tubes were incubated at 37° C with gentle mixing inside a hybridization rotor for 5 to 30 min followed by FC analysis on a BD FACS Canto II system (BD Biosciences).

Measurement of EtBr fluorescence intensity was performed by flow cytometry with excitation wavelength set at 488 nm and the fluorescence emission at 585 nm. The data were analyzed by using FlowJo LLC software.

Quantitative-PCR and gene expression analysis

The method for qRT-PCR analysis was described previously (Doddam, Peddireddy, & Ahmed, 2017). Briefly, using TriZOL, (Invitrogen) RNA was isolated from 108 cells of *H. pylori* strains. Subsequently, 3µg of RNA was converted to cDNA using random hexamers and SuperScript-III (Invitrogen) according to the manufacturer's instructions.

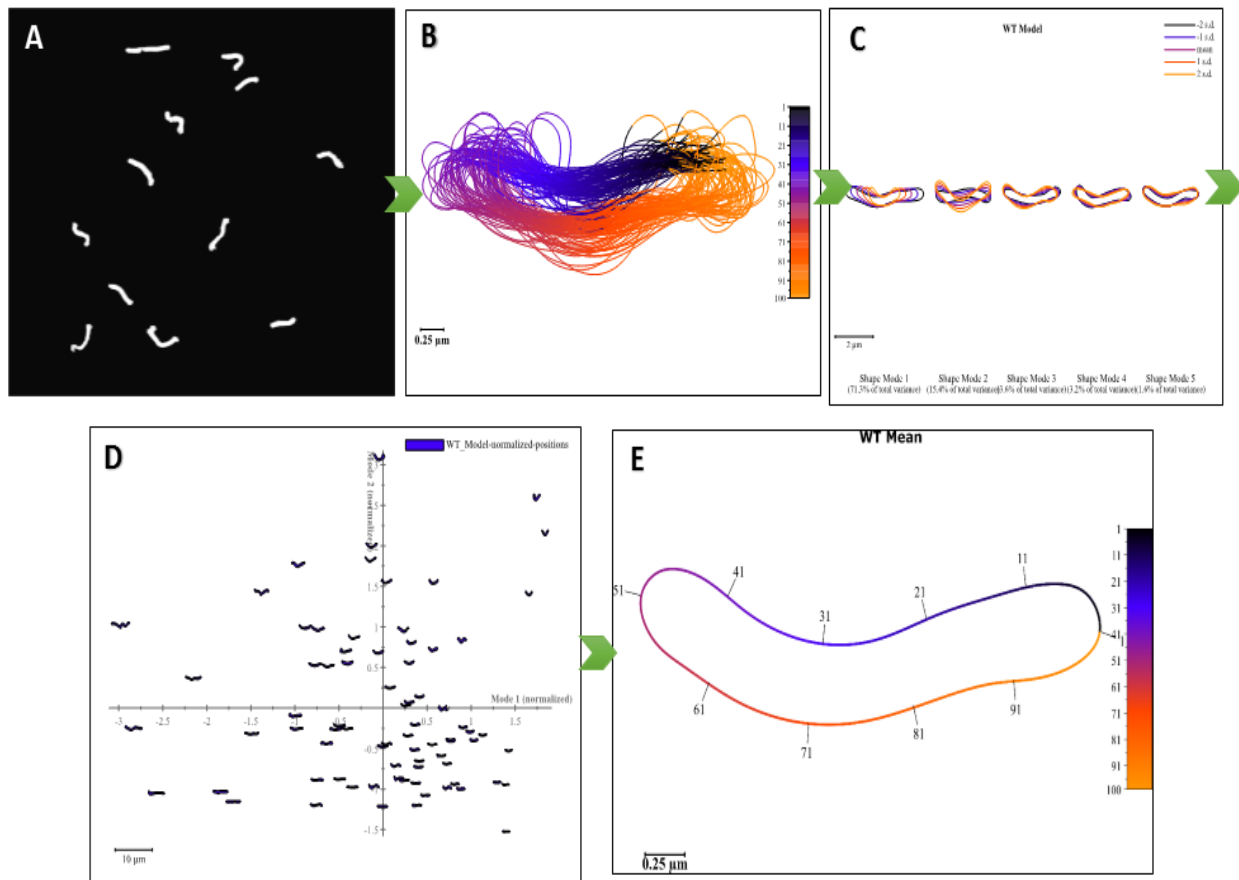


Figure 2.2: Steps followed for morphological quantitative analysis of *H. pylori* strains by CellTool software; (A) confocal image of *H. pylori* cells were executed by Adobe Photoshop 7, (B) The individual cell contours were aligned (C) Shape models were plotted based on the variance from mean, (D) Plot represent the normalized positions for all individual cells (E) Plot represent the mean model of the cell population.

For qRT-PCR, 40 ng of the first transcribed DNA strand was amplified by using SYBR® Fast qPCR Mix (Takara, Japan) with primers targeting *cds3*-F 5' CTAAACATGGCAGCTTGATCC 3' *cds3*-R 5' AATGGATTTCACACCTTCC 3', *cds1*-F 5' GGATGAATTTTGTAGACGATTTGC 3' *cds1*-R 5' CCCTCTTCTTTTCTTCTTCAGG 3', *wzx*-F 5' AAACCTCAAAGACAACCACGAAG 3' *wzx*-R 5' CGACCGCTAAAATCAACAAG 3', *wecA*-F 5' ATGGTGCTTGGGTTTATGGTG 3' *wecA*-R 5' GGCTTTCTGGCGTTTTATTTG 3' genes and *16S* *rRNA*-F 5' GGTAATCCGTAGAGATCAAGAG 3', *16S* *rRNA*-R 5' ACAACTAGCATCCATCGTTTAGG 3' as an internal control. For *luxS*, *H. pylori* strains were grown for 2 days in 2 ml of Brucella broth and RNA was isolated from planktonic and sessile bacterial cells and targeted with primers *luxS*-F 5' TTTGATTGTCAAATACGATGTGC 3' *luxS*-R 5' TGTGAGATAAAATCCCGTTTGG 3'.

Treatment of *H. pylori* cells with filamenting drug aztreonam

To induce bacterial cell elongation, 2 µg/ml of aztreonam antibiotic was added to Brucella agar medium and incubated at humidified microaerophilic conditions at 5% O₂ and 5% CO₂. *H. pylori* 48 hour culture was washed thrice by PBS (pH 7.0) containing 10% glycerol and the cells were adjusted to OD₅₅₀ 0.2. Cells were mounted on glass slides and imaged by confocal microscopy by employing transmitted light mode (Carl Zeiss Model: LSM 880).

RESULTS

Loss of CGs alter the morphology of *H. pylori*

To decipher the role of CGs on *H. pylori* morphology, the wild-type (*Hp76*), knock out (*Hp76Δ421*) and *Hp76Δ421* reconstituted strains morphologies were captured under confocal microscope by employing transmitted light mode. *Hp76Δ421* indeed exhibited morphological deformities wherein most cells displayed coiled ‘c’-shape as a dominant morphology along with coccoid and rod-shaped bacteria (Figure 2.3A), whereas *Hp76* strain exhibited the native helical shape (Figure 2.3B). Interestingly, the reconstitution of *Hp76Δ421* strain resulted in the recovery of the cell morphology (Figure 2.3C). To study the morphology of *Hp26695* strain in absence of cholesterol, *Hp26695* wild-type were grown either in the presence or absence of cholesterol. The confocal images revealed remarkable variation in morphology of *Hp26695* cells that were grown in absence of cholesterol (Figure 2.4A). The altered shapes that were observed included ‘c’ shape, rod and coccoid forms in contrast to the bacteria grown in the presence of cholesterol which exhibited normal helical shape (Figure 2.4B).

Furthermore, we performed quantitative morphological analysis of confocal microscopy images of wild-type (*Hp76*), knockout (*Hp76Δ421*) and *Hp76Δ421*-reconstituted strains using CellTool software package. It was revealed that the distribution of cell populations of *Hp76Δ421* according to the *x-size* and *y-size* of cell population was bimodal and notably the size of cells varied as a result of variable cell shapes, whereas the *Hp76* population distribution was narrower, due to the consistency of cell shapes (Figure 2.3D).

Moreover, the aspect ratio which represents the width/length ratio of individual cell presented significantly uneven distribution of *Hp76Δ421* cell population due to inconsistencies and distortion in the shape of *Hp76Δ421* cells, mainly because of 'c' shaped cells compared to the wild-type cells which demonstrated native distribution for the aspect ratio (Figure 2.3E). Moreover, the morphology quantitative analysis of *Hp76Δ421* reconstituted strain shown that cells restored the wild-type like morphology and cell population distribution based on aspect ratio, *x-size* and *y-size* was comparable to the wild-type strain. To ensure that the morphological alteration was not strain specific. Similar morphological quantitative analysis was performed on *Hp26695* strains. Morphology analysis of *Hp26695*, *Hp26695Δ421* was in concordance with the results obtained in case of *Hp76* strains (Figure 2.4C & D).

In order to manifest the morphological changes of *Hp76*, *Hp76Δ421* and *Hp76Δ421* reconstituted strains, they were grown in the presence of aztreonam, an antibiotic that induces pronounced filamentation in *H. pylori* by inhibiting septal peptidoglycan synthesis. Under these conditions, the *Hp76Δ421* exhibited morphological changes such as loss of curvatures and stunted filamentation (Figure 2.3F) compared to wild-type cells which exhibited typical curvatures and elongated filaments (Figure 2.3G). Remarkably, *Hp76Δ421* reconstituted strain restored the curvature and wild-type-like morphologies (Figure 2.3H).

Moreover, to confirm that the deletion of *hp0421* did not interfere with *csd1* and *csd3* expression, the genes that are responsible for the native curvature and length of *H. pylori*, we analyzed their relative mRNA expression using qRT-PCR of *H. pylori* wild-type and *hp0421* mutant strains. According to our observation there was no significant influence on the *csd1* and *csd3* mRNA expression levels due to the deletion of *hp0421* gene (Figure 2.4E & F).

Overall, we observed adverse morphological changes of *H. pylori* upon deletion of *hp0421* or by cholesterol depletion in growth media which indicates that the lack of CGs remarkably impairs the morphology of *H. pylori*.

The morphological changes following CG's absence are attributed to a 'c' shaped bacterial population

The flow cytometry analysis appears to be an efficient and rapid technique to detect the cell shape of *H. pylori* at population level (L. K. Sycuro et al., 2013). As *H. pylori* is dependent on exogenous cholesterol for synthesis of CGs the strain Hp26695 was grown under microaerophilic conditions with and without cholesterol to analyze the morphological changes by FC. Forward scatter (FSC) usually represent the cell size while side scatter (SSC) roughly correlates with cell complexity, granularity and the absorbance of cell wall. We observed that Hp26695 strain cultured in the absence of cholesterol exhibited much higher FSC that corresponded with the increased bulk width of the bacterial cell, represented by 'c'-shaped cells compared to the cells cultured in presence of cholesterol.

Moreover, *Hp26695* grown in the absence of cholesterol displayed slightly higher side scatter (SSC) value, which indicates that cells presented higher granularity or complexity (Figure 2.5A). Notably, *Hp26695* strain grown for 72 hours in the absence of cholesterol also displayed remarkably higher FSC and SSC values compared to those grown up to only 48 hours (Figure 2.5B). Furthermore, the mean values of FSC and SSC in both conditions were higher in *H. pylori* grown in the absence of cholesterol. To analyze the morphology of *hp0421* mutant, the *Hp26695* and *Hp26695Δ421* cell populations were acquired by flow cytometry. The strain *Hp26695Δ421* displayed higher FSC and SSC values in both 48 hours and 72 hour culture populations, in comparison to the wild-type strain (Figure 2.5C & D).

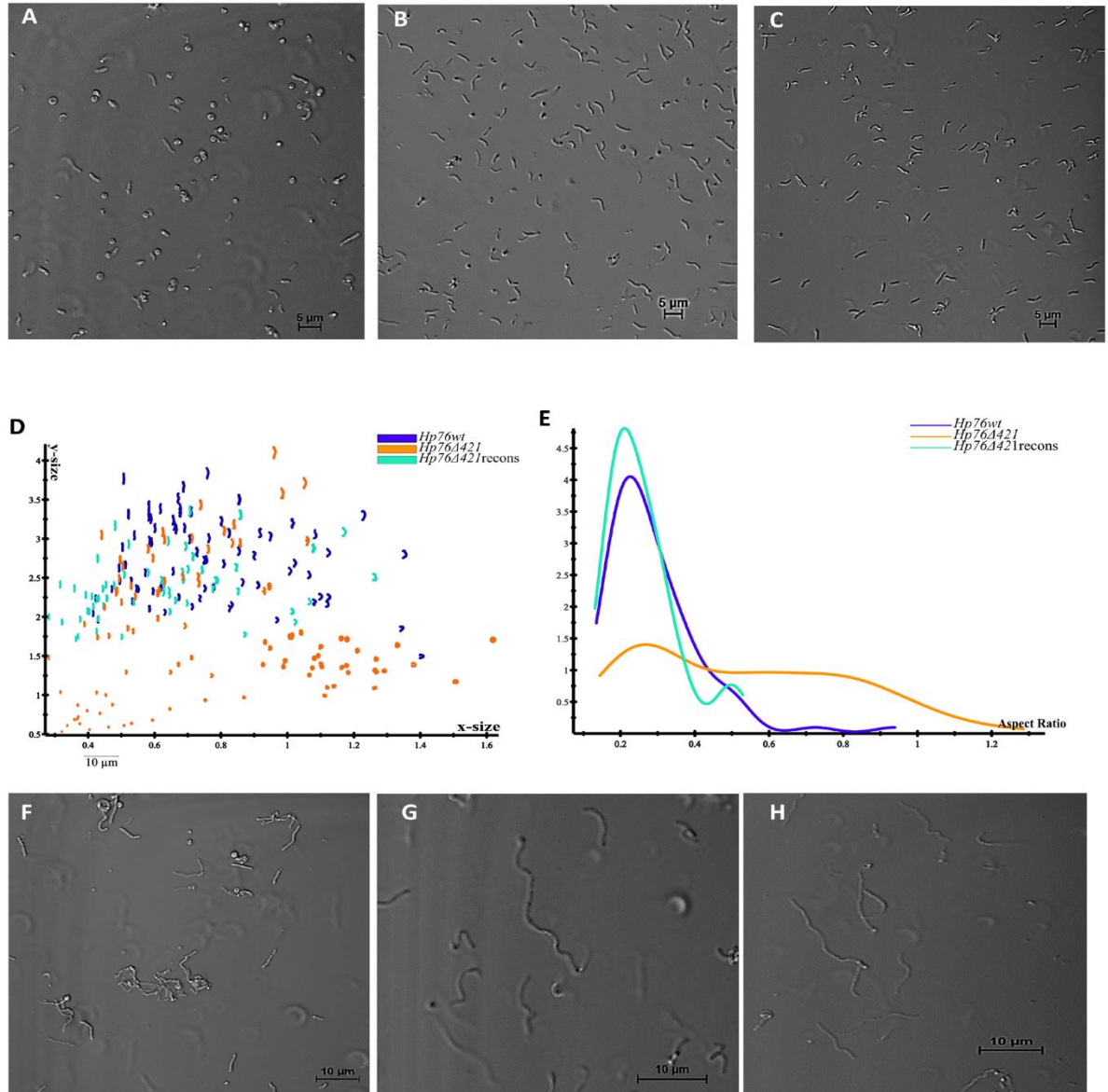


Figure 2.3: Deletion of *hp0421* gene perturbs *H. pylori* cell morphology; confocal microscopy profiles depicting morphological patterns of (A) *Hp76Δ421*, (B) *Hp76* and (C) *Hp76Δ421*-reconstituted strain. (D) Scatter plots arraying *Hp76*, *Hp76Δ421* and *Hp76Δ421*-reconstituted cells based on *x*-size and *y*-size analyses performed using CellTool software. (E) CellTool analysis output based on plots representing the distribution of *Hp76*, *Hp76Δ421* and *Hp76Δ421*-reconstituted cell populations according to the

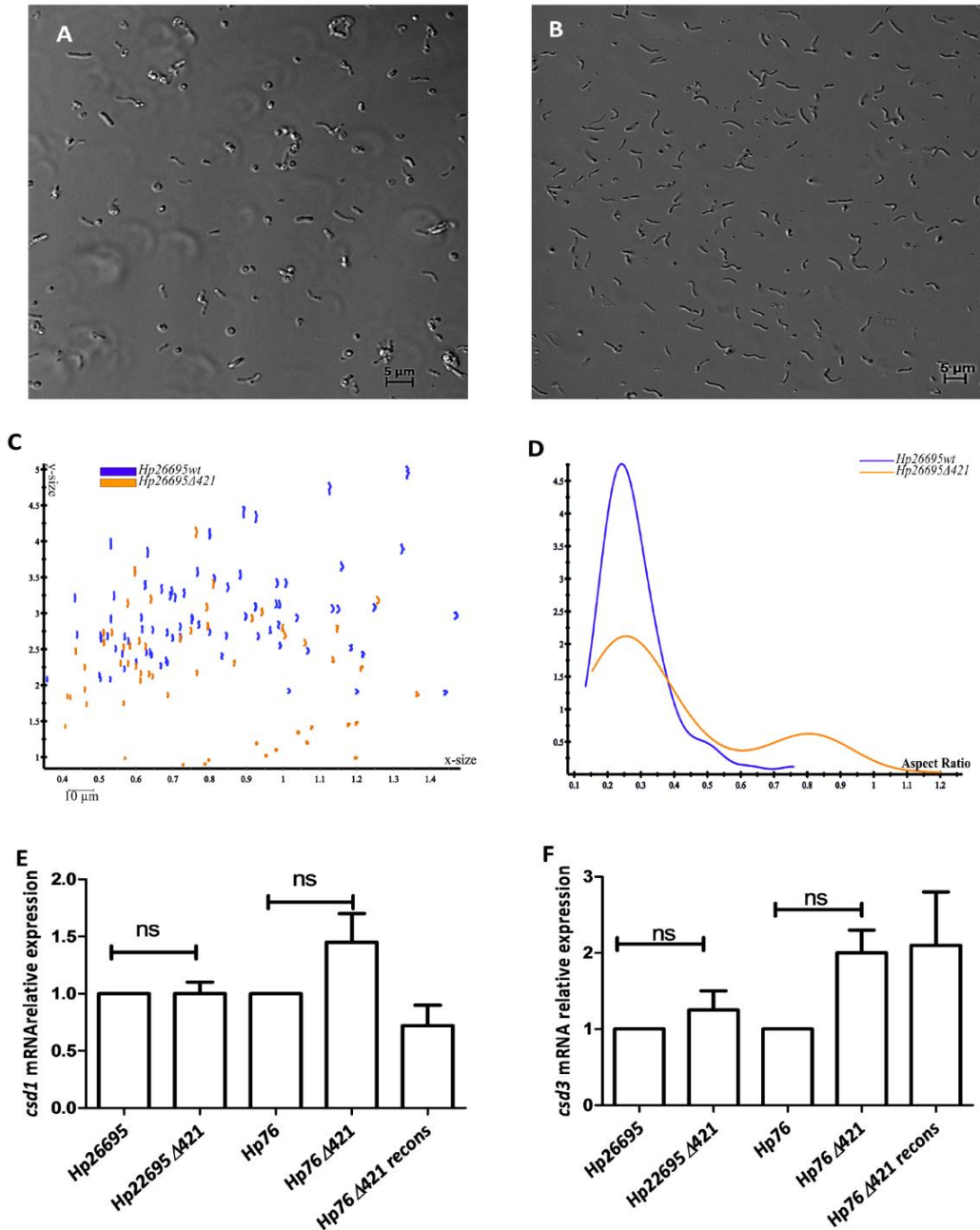


Figure 2.4: Morphology of *H. pylori* entailing the absence of cholesterol in culture and upon deletion of *hp0421*; confocal microscopy images depicting *H. pylori* cultured in absence (A) and presence of cholesterol (B). Shown in (C) are the scatter plots arraying *Hp26695* and *Hp26695* Δ 421 cell populations by *x*-size and *y*-size as analyzed by CellTool. Graphical profiles (D) representative of the distribution of *Hp26695* and *Hp26695* Δ 421 cell populations according to the aspect ratio and as analyzed by CellTool are shown. RNA isolated from and the relative mRNA expression analyses of *Hp26695* and *Hp76* strains log phase culture as quantified by qRT-PCR entailing gene loci *csd1* and *csd3* are shown in panels E and F. (ns denotes non-significant differences at $p \geq 0.05$).

Furthermore, the cell population morphology analysis for mice-adapted strain, *Hp76* strains were subjected for analysis by flow cytometry. As expected the *Hp76Δ421* exhibited higher FSC and SSC mean compare to *Hp76* which is in accordance with the observation recorded for *Hp26695* and *Hp26695Δ421* strains. Interestingly, the mean values of FSC and SSC in *Hp76Δ421* reconstituted cell population was similar to the results from *Hp76* cell population which indicates that *Hp76Δ421* reconstituted strain cells have restored the native morphology and cell wall integrity (Figure 2.6A and B). Taken together, these observations suggest that the alterations in morphology of *Hp26695Δ421* and *Hp76Δ421* or of wild-type strains cultured in the absence of cholesterol are due to the presence of ‘c’ shaped cell population which is also evident by the higher FCS values. Moreover, *H. pylori* that lack CGs displayed alteration in cell wall integrity and cell granularity which correlates with higher SSC values observed.

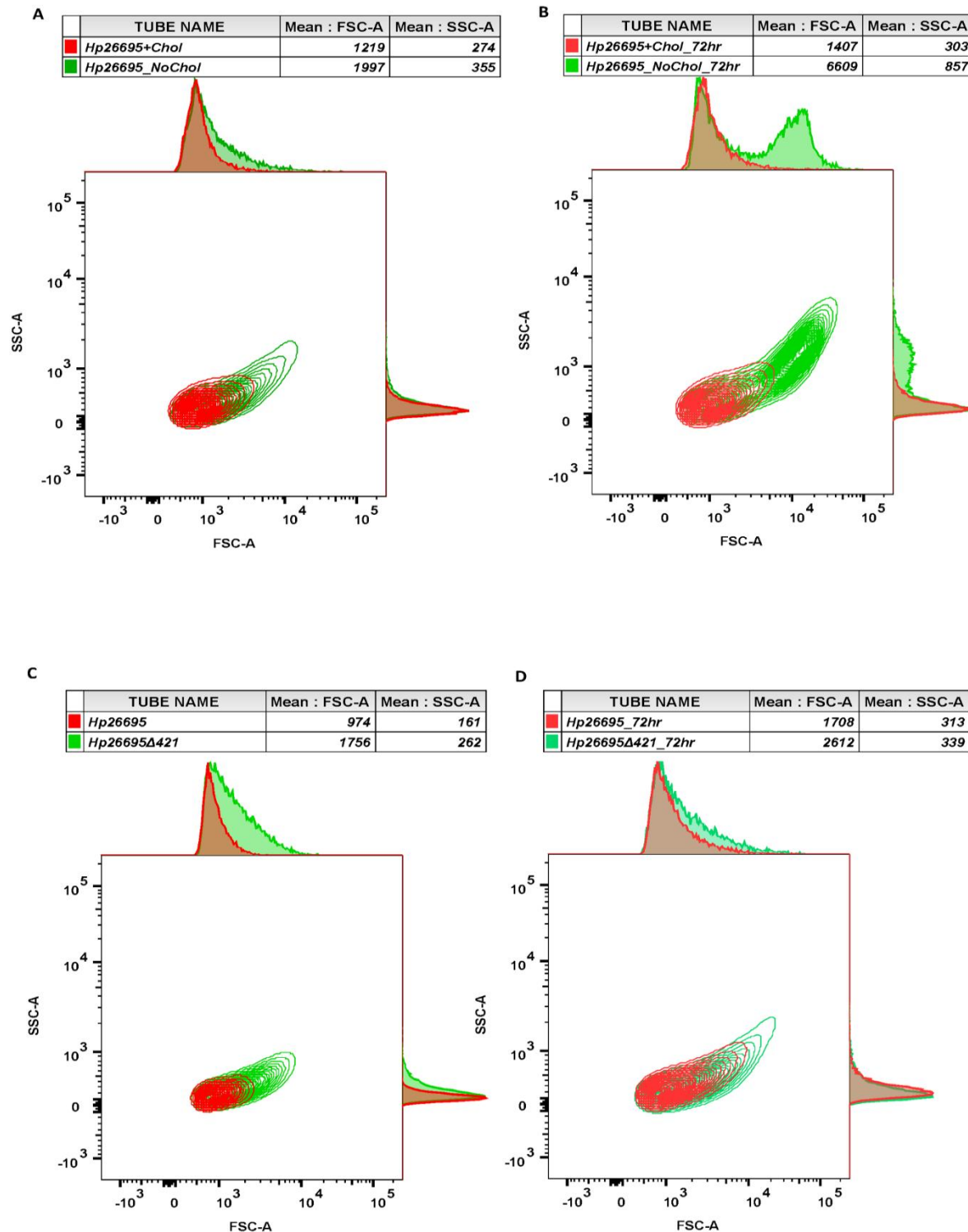


Figure 2.5: Flow cytometry analysis of *H. pylori* cell populations based on their shape; Representative contour plots of *H. pylori* populations depicted based on flow cytometry analyses. SSC on the y-axis and FSC as plotted on the x-axis are presented with mean and median. (A) *Hp26695* grown with or without cholesterol for 48 hours and (B) 72 hours. Similarly depicted are (un-supplemented) *Hp26695* and *Hp26695Δ421* (C) grown for 48 hours and (D) grown for 72 hours.

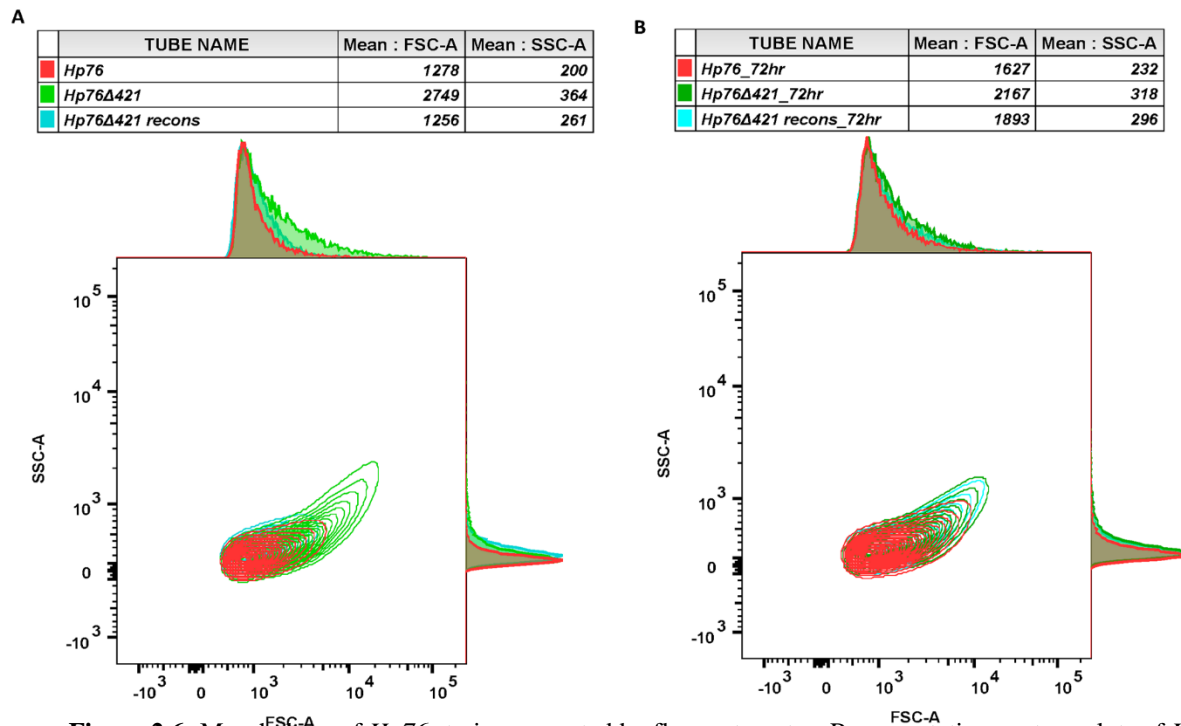


Figure 2.6: Morphology of *Hp76* strains presented by flow cytometry. Representative contour plots of *H. pylori* populations when analyzed by flow cytometry; FSC and SSC are shown on the *x-axis* and *y-axis*, respectively, with mean. *Hp76Δ421* displayed high FSC and SSC compared to the *Hp76* and *Hp76Δ421*-reconstituted strains grown for 48 (A) and for 72 hour (B).

DISCUSSION

H. pylori belongs to the Epsilon proteobacteria which display helical-shape as a default morphology. In this work, we analyzed the possible role of CGs in the maintenance of native helical-shape of *H. pylori*. CGs are one of the unique characters of *H. pylori* that are present adequately in *H. pylori* membrane (Hirai et al., 1995). Presence of membrane lipids is suggested to be an important component that maintains eukaryotic cell structures and morphology (Frolov, Shnyrova, & Zimmerberg, 2011). Lipid presence in prokaryotes membrane is uncommon feature and only few organisms possess lipids in their cell envelop such as *Helicobacter pylori*, *Mycoplasma spp.* and *Borrelia burgdorferi* (Bramkamp & Lopez, 2015). Given this, we observed that the presence of CGs is essential factor in maintenance of the native helical morphology of *H. pylori*, irrespective of the strain type and growth duration. Whereas, lack of CGs remarkably distorted the shape of *H. pylori* cells to variable shape and size, with coiled and ‘c’-shaped cells being the dominant. A previous studies by Sycuro et al., observed similar morphological alterations like ‘c’ shaped and rod shaped cells upon deletion of *csds* genes, such as peptidoglycan endopeptidase genes *csd1* and *csd3* in *H. pylori* (L. K. Sycuro et al., 2010). However, we found that there was no effect on the gene expression levels of *csd1* and *csd3* upon deletion of the *hp0421*. Moreover, CGs are one of the main constituents of *H. pylori* cell wall which comprise around 25% of the total cell wall lipids (Haque et al., 1996). Given this, our results strongly suggests that depletion of CGs leads to alteration of lipid raft components of the *H. pylori* cell wall which disrupts its integrity. Since lipid rafts are required in maintaining the architecture of cell wall and order of cell wall domains, absence of the CGs may be linked to change in the normal helical shape of *H. pylori*.

In fact, in a study on *Borrelia burgdorferi* when cell wall cholesterol was depleted by M β CD without substitution by other sterols, as a result *Borrelia burgdorferi* was converted into coiled spirochetes (T. J. LaRocca et al., 2013). These data support the previous observations which demonstrated that the GCs contents were altered when *H. pylori* morphology undergoes transformation from helical to coccoid form (Shimomura et al., 2004). Our results are in line with this observation which supports that the lack of sterols alters the morphology of *H. pylori*. Moreover, the morphology analysis suggests that the lack of CGs remarkably altered the size and curvature of *H. pylori* cells; these results point at the possibility that CGs are part of lipid rafts in the cell wall and they play a substantial role in maintaining the typical helical shape and size of *H. pylori* cells. It should be considered that the helical shape of *H. pylori* is a key strategy in the process of invasion of gastric niches. This is of particular significance given the reports that the colonization rates in mice stomach by the helical rod-shaped *H. pylori* were higher compared to *csd1* and *csd3* mutants that were curved and rod-shaped (L. K. Sycuro et al., 2010). Similarly, Wunder *et al.*, reported that *hp0421* mutant(s) failed to colonize C57BL/6 mice and were cleared from the gastric tissue (Wunder et al., 2006). These results demonstrate that the changes morphology in *H. pylori*, due to the absence of CGs negatively influence the colonization potential of *H. pylori*. We speculate that this could be a result of direct or indirect interaction between the CGs and the peptidoglycans that altered the order of cell wall domains.

REFERENCES

- Ausmees, N., Kuhn, J. R., & Jacobs-Wagner, C. (2003). The bacterial cytoskeleton: an intermediate filament-like function in cell shape. *Cell*, 115(6), 705-713.
- Bramkamp, M., & Lopez, D. (2015). Exploring the existence of lipid rafts in bacteria. *Microbiology and molecular biology reviews*, 79(1), 81-100.
- Chan, A. C., Blair, K. M., Liu, Y., Fridrich, E., Gaynor, E. C., Tanner, M. E., . . . Murphy, M. E. (2015). Helical shape of *Helicobacter pylori* requires an atypical glutamine as a zinc ligand in the carboxypeptidase Csd4. *Journal of Biological Chemistry*, 290(6), 3622-3638.
- Doddam, S. N., Peddireddy, V., & Ahmed, N. (2017). Mycobacterium tuberculosis DosR Regulon Gene Rv2004c Encodes a Novel Antigen with Pro-inflammatory Functions and Potential Diagnostic Application for Detection of Latent Tuberculosis. *Front Immunol*, 8, 712. doi: 10.3389/fimmu.2017.00712
- Fridrich, E., Biboy, J., Adams, C., Lee, J., Ellermeier, J., Gielda, L. D., . . . Gaynor, E. C. (2012). Peptidoglycan-modifying enzyme Pgp1 is required for helical cell shape and pathogenicity traits in *Campylobacter jejuni*. *PLoS pathogens*, 8(3), e1002602.
- Frolov, V. A., Shnyrova, A. V., & Zimmerberg, J. (2011). Lipid polymorphisms and membrane shape. *Cold Spring Harbor perspectives in biology*, a004747.
- Haque, M., Hirai, Y., Yokota, K., Mori, N., Jahan, I., Ito, H., . . . Oguma, K. (1996). Lipid profile of *Helicobacter* spp.: presence of cholesteryl glucoside as a characteristic feature. *J Bacteriol*, 178(7), 2065-2070.
- Hirai, Y., Haque, M., Yoshida, T., Yokota, K., Yasuda, T., & Oguma, K. (1995). Unique cholesteryl glucosides in *Helicobacter pylori*: composition and structural analysis. *J Bacteriol*, 177(18), 5327-5333.
- Hossain, H., Wellensiek, H.-J., Geyer, R., & Lochnit, G. (2001). Structural analysis of glycolipids from *Borrelia burgdorferi*. *Biochimie*, 83(7), 683-692.
- Johnson, R. C. (1977). The spirochetes. *Annual Reviews in Microbiology*, 31(1), 89-106.
- LaRocca, T. J., Crowley, J. T., Cusack, B. J., Pathak, P., Benach, J., London, E., . . . Benach, J. L. (2010). Cholesterol lipids of *Borrelia burgdorferi* form lipid rafts and are required for the bactericidal activity of a complement-independent antibody. *Cell host & microbe*, 8(4), 331-342.
- LaRocca, T. J., Pathak, P., Chiantia, S., Toledo, A., Silvius, J. R., Benach, J. L., & London, E. (2013). Proving lipid rafts exist: membrane domains in the prokaryote *Borrelia burgdorferi* have the same properties as eukaryotic lipid rafts. *PLoS Pathog*, 9(5), e1003353. doi: 10.1371/journal.ppat.1003353
- Lebrun, A. H., Wunder, C., Hildebrand, J., Churin, Y., Zahringer, U., Lindner, B., . . . Warnecke, D. (2006). Cloning of a cholesterol- α -glucosyltransferase from *Helicobacter pylori*. *J Biol Chem*, 281(38), 27765-27772. doi: 10.1074/jbc.M603345200
- Oskoueï, D. D., Bekmen, N., Ellidokuz, H., & Yilmaz, Ö. (2010). Evaluation of different cryoprotective agents in maintenance of viability of *Helicobacter pylori* in stock culture media. *Brazilian Journal of Microbiology*, 41(4), 1038-1046.
- Paixão, L., Rodrigues, L., Couto, I., Martins, M., Fernandes, P., De Carvalho, C. C., . . . Viveiros, M. (2009). Fluorometric determination of ethidium bromide efflux kinetics in *Escherichia coli*. *J Biol Eng*, 3(1), 18.
- Persat, A., Stone, H. A., & Gitai, Z. (2014). The curved shape of *Caulobacter crescentus* enhances surface colonization in flow. *Nature communications*, 5, 3824.

- Pincus, Z., & Theriot, J. A. (2007). Comparison of quantitative methods for cell-shape analysis. *J Microsc*, 227(Pt 2), 140-156. doi: 10.1111/j.1365-2818.2007.01799.x
- Shimomura, H., Hayashi, S., Yokota, K., Oguma, K., & Hirai, Y. (2004). Alteration in the composition of cholesteryl glucosides and other lipids in *Helicobacter pylori* undergoing morphological change from spiral to coccoid form. *FEMS Microbiol Lett*, 237(2), 407-413. doi: 10.1016/j.femsle.2004.07.004
- Sycuro, L. K., Pincus, Z., Gutierrez, K. D., Biboy, J., Stern, C. A., Vollmer, W., & Salama, N. R. (2010). Peptidoglycan crosslinking relaxation promotes *Helicobacter pylori*'s helical shape and stomach colonization. *Cell*, 141(5), 822-833. doi: 10.1016/j.cell.2010.03.046
- Sycuro, L. K., Rule, C. S., Petersen, T. W., Wyckoff, T. J., Sessler, T., Nagarkar, D. B., . . . Salama, N. R. (2013). Flow cytometry-based enrichment for cell shape mutants identifies multiple genes that influence *Helicobacter pylori* morphology. *Mol Microbiol*, 90(4), 869-883. doi: 10.1111/mmi.12405
- Sycuro, L. K., Wyckoff, T. J., Biboy, J., Born, P., Pincus, Z., Vollmer, W., & Salama, N. R. (2012). Multiple peptidoglycan modification networks modulate *Helicobacter pylori*'s cell shape, motility, and colonization potential. *PLoS pathogens*, 8(3), e1002603.
- Tenguria, S., Ansari, S. A., Khan, N., Ranjan, A., Devi, S., Tegtmeyer, N., . . . Ahmed, N. (2014). *Helicobacter pylori* cell translocating kinase (CtkA/JHP0940) is pro-apoptotic in mouse macrophages and acts as auto-phosphorylating tyrosine kinase. *Int J Med Microbiol*, 304(8), 1066-1076. doi: 10.1016/j.ijmm.2014.07.017
- Testerman, T. L., McGee, D. J., & Mobley, H. L. (2001). *Helicobacter pylori* growth and urease detection in the chemically defined medium Ham's F-12 nutrient mixture. *J Clin Microbiol*, 39(11), 3842-3850. doi: 10.1128/JCM.39.11.3842-3850.2001
- Wunder, C., Churin, Y., Winau, F., Warnecke, D., Vieth, M., Lindner, B., . . . Meyer, T. F. (2006). Cholesterol glucosylation promotes immune evasion by *Helicobacter pylori*. *Nat Med*, 12(9), 1030-1038. doi: 10.1038/nm1480
- Yang, D. C., Blair, K. M., & Salama, N. R. (2016). Staying in shape: the impact of cell shape on bacterial survival in diverse environments. *Microbiology and molecular biology reviews*, 80(1), 187-203.
- Young, K. D. (2006). The selective value of bacterial shape. *Microbiology and molecular biology reviews*, 70(3), 660-703.

Chapter 3

Objective 2: To determine the role of *H. pylori* CGs in cell wall permeability, antibiotic resistance, LPS profiles and biofilm formation.

INTRODUCTION

Cell-envelope is the shield that protect the bacterial cell and the first region of contact between pathogens and host. The organization of *H. pylori* cell envelope is identical to the other gram-negative bacteria. In vitro studies have revealed that *H. pylori* cell-envelop in general is negatively charged and it has a hydrophilic surface character (Smith, Drumm, Neumann, Policova, & Sherman, 1990). Separation of outer and inner membranes of *H. pylori* has been reported to be difficult as they are very connected (Doig & O'Toole, 1997). Furthermore, unlike *Escherichia coli* *H. pylori* (1-6)-anhydro-*N*-acetylmuramic acid and having peptidoglycan composed of a muropeptides with pentapeptide side chain ending with glycine (Costa et al., 1999). Similar to other bacteria the peptidoglycan synthesized in the cytoplasm followed by integration into the membrane by the penicillin-binding proteins (PBPs) (Krishnamurthy et al., 1999). Several genes that involve in synthesis of *H. pylori* peptidoglycan have been identified as cell shape determinants csds (explained in details in chapter 2).

Remarkably, *H. pylori* has a characteristic composition of lipids and fatty acids which is the major feature that excludes *H. pylori* from the genus *Campylobacter* (GOODWIN et al., 1989). The gas-liquid chromatography (GC) analysis of four strains of *H. pylori* fatty acid compositions resulted in identification of several fatty acids like palmitic acid, myristic acid, linoleic acid, and stearic. The most membrane abundant fatty acids was myristic acid (31 to 45%), followed by 19-carbon cyclopropane (20 to 24%) (Geis, Leying, Suerbaum, & Opferkuch, 1990).

H. pylori has most abundantly (lipid by weight) phospholipids 73.4%, then 20.6% glycolipids, and is 6% neutral lipids. The main phosphides are cardiolipin, phosphatidylethanolamine, and phosphatidylglycerol. CGs are uncommon in bacteria and animals, but they have been identified in 13 out of 15 *Helicobacter* species studied (Haque et al., 1996).

It has been observed that the mechanisms disturbing the properties of the bacterial outer membrane lipid bilayer itself will have an influence on the Gram-negative bacteria sensitivity to certain types of antibiotics. Like-wise, perturbing the bacterial LPS pattern such as targeting LPS synthesizing enzymes have rendered the bacterial sensitivity to certain hydrophilic and hydrophobic antibiotics, leading to the possibility of combinatorial drug therapy (Delcour, 2009). Several studies have determined the effects of permeabilizers on bacteria resistance to antibiotics. For instance, Sung W. J. et al., have investigated the effect of liposomal linolenic acid (LipoLLA) nanoparticles, which is a permeabilizing and effective bactericidal agents, against *H. pylori*. They observed that LipoLLA permeabilizes *H. pylori* membranes, and actively work in a dose-dependent manner (Jung, Thamphiwatana, Zhang, & Obonyo, 2015). Interestingly, Hildebrandt *et al.*, observed that *Hp26695* cultured in the absence of cholesterol develops an aberrant LPS which are determined by dephosphorylation of lipid A at the 1-position compare to the one grown in presence of cholesterol. *H. pylori* LPS usually presents Lewis Y and/or X antigens. The quantification of Lewis Y and Lewis X antigens by whole-cell ELISA shown that the expression of these genes markedly increased when 26695, SS1, or G27 strains were grown in cholesterol containing media (Hildebrandt & McGee, 2009). Furthermore, *H. pylori* cultivated in the absence of cholesterol showed susceptibility to certain antibiotics, bile salts and ceragenins (McGee et al., 2011; Trainor, Horton, Savage, Testerman, & McGee, 2011).

MATERIAL AND METHODS

H. pylori cell wall fluidity analysis by flow cytometry

For cholesterol based selection, *Hp26695* strain was grown on chemically defined medium Ham's-F12 as explained in the previous chapter. The strains *Hp26695* wild-type, *Hp26695* Δ 0421, *Hp76* strains were grown for 48-72 hours on Brucella agar (BD Biosciences). The staining and measurement procedures for EtBr influx were followed from a previous study with minor modifications (Paixao et al., 2009). Briefly, bacterial cells were suspended and washed thrice with PBS at pH 7.4 (Gibco, USA). A total of 10^6 cells were resuspended in 1 ml PBS or in 1 ml PBS [containing 5 μ g of EtBr filtered through a Millix-GV syringe filter 0.22 μ m (Merck-Millipore, USA)]. All the tubes were incubated at 37° C with gentle mixing inside a hybridization rotor for 5 to 30 min followed by FC analysis on a BD FACS Canto II system (BD Biosciences). EtBr fluorescence intensity was measured by flow cytometry analysis with excitation wavelength set at 488 nm and the fluorescence emission at 585 nm. The data were analyzed by using FlowJo LLC software.

Quantitative-PCR and gene expression analysis

The method for qRT-PCR analysis was followed as described previously (Doddam, Peddireddy, & Ahmed, 2017). Briefly, RNA was isolated from 10^8 cells of *H. pylori* strains by TRIzol (Invitrogen). Subsequently, 3 μ g of RNA was converted to cDNA using random hexamers and SuperScript-III (Invitrogen) according to the manufacturer's instructions.

For qRT-PCR, 40 ng of the first transcribed DNA strand was amplified by using SYBR® Fast qPCR Mix (Takara) with primers corresponding to *wzx*-F 5' AAACTCAAAGACAACCACGAAG 3' *wzx*-R 5' CGACCGCTAAAATCAACAAG 3', *wecA*-F 5' ATGGTGCTTGGGTTTATGGTG 3' *wecA*-R 5' GGCTTTCTGGCGTTTTATTTTG 3' genes and *16S-rRNA*-F 5' GGTAATCCGTAGAGATCAAGAG 3', *16S-rRNA*-R 5' ACAACTAGCATCCATCGTTTAGG 3' used as an internal control. For *luxS*, *H. pylori* strains were cultured in Brucella broth (BB) for 2 days and RNA was isolated from planktonic and sessile bacterial cells using the primers *luxS*-F 5' TTTGATTGTCAAATACGATGTGC 3' *luxS*-R 5' TGTGAGATAAAATCCCGTTTGG 3'.

Determination of antibiotic resistance among *hp0421* mutant and *H. pylori* wild-type

Hp26695 and *Hp76* strains grown on Brucella agar medium were suspended and washed with PBS and resuspended in BHI broth media. About 50 µl of cell suspension which contains approximately 10⁸ *H. pylori* was spread on Brucella agar medium and antibiotic impregnated discs corresponding to colistin, amoxicillin, fosfomycin, clarithromycin, Azithromycin, Gentamycin, tetracycline, ciprofloxacin and rifampicin (HiMedia) were placed on the agar plate. Subsequently, based on the above screened antibiotics, the strips corresponding to clarithromycin (0.016-256 mcg/ml), amoxicillin (0.016 - 256 mcg/ml) fosfomycin (0.064-1024 mcg/ml), polymyxin-B (0.016-256 mcg/ml), colistin (0.016-256 mcg/ml), tetracycline (0.016-256 mcg/ml) and ciprofloxacin (0.002-31 mcg/ml) were selected for MIC test. The E-MIC strips were placed on Brucella agar plates and incubated for 3 days. The susceptibility was defined by breakpoints defined as per Clinical and Laboratory Standards Institute (CLSI) (PA, 2016).

Biofilm formation by *H. pylori* hp0421 mutant strains

The biofilm formation assay was performed using a modified protocol as described previously (Hussain et al., 2012; Yonezawa et al., 2009). In brief, *Hp26695* and *Hp76* cells were collected from BHI agar and washed with PBS. Inoculums at an OD₅₅₀ of 0.2 were seeded in 12 well plates, each well contain 2ml of BB with 7% of decomplexed horse serum (Gibco) and sterilized glass coverslips were used to cover the wells and also to enhance the attachment of *H. pylori* at the air-liquid interface. The cultures were incubated under microaerophilic conditions at 37°C for 2 to 6 days. Subsequently, the coverslips were washed with PBS followed by 0.1% crystal violet staining. The coverslips were further rinsed with PBS, dried and the associated dye was dissolved in acetone and ethanol (2:8) and the crystal violet dye absorbance was measured by microplate reader at 594 nm.

Lipopolysaccharides purification and visualization

Purification of lipopolysaccharides from *H. pylori* strains was performed according to the previously described method of Hong *et al.* with slight modifications (Hong, Cunneen, & Reeves, 2012). Briefly, the bacterial lawns were collected and washed thrice in 1ml PBS (pH 7.4) and pelleted down at 10000 rpm for 10 min. The pellets were lysed with lysis buffer (60 mM Tris-HCl pH 6.8, 2% SDS) and incubated at 98° C for 10 min and the whole lysate protein was quantified by BCA bicinchoninic acid assay (Thermo Fischer Scientific). LPS were extracted by adding 45% hot phenol to the lysate, vortexed vigorously and incubated at 70° C for 30 min. The mixtures were centrifuged at 16000g for 15 min and the upper phase layer was collected in 2 ml tubes and LPS were precipitated by adding 75% cold ethanol and 10 mM sodium acetate. The tubes were then incubated at -20° C overnight followed by centrifugation at 16000g for 15 min.

To remove DNA and RNA contaminants, 3 μ l of buffer 2 (10 mM MgCl₂, 50 mM NaCl, 1 mM DTT, 10 mM Tris-HCl, pH 7.9@25°C) (NEB), 0.5 mg/ml DNaseI (amplification grade) (Sigma) and 0.5 mg/ml RNase A (Invitrogen) were added, incubated for 1 hour at 37° C and treatment with 0.5 mg/ml Proteinase K (Amresco) for 1 hr at 56° C. The LPS was re-extracted by adding 50% phenol followed by vigorous vortexing and centrifugation. The pellet was finally precipitated by cold ethanol, dissolved in 50 μ l of deionized water and preserved at -80 °C. For visualization of LPS, 10 μ l from each tube were loaded on 15% SDS gel and stained with dual silver stain (Keenan, Allardyce, & Bagshaw, 1997). The LPS units were been quantified by Limulus amebocyte lysate (LAL) chromogenic endotoxin quantitation kit (Pierce) according to the manufacturer's instructions.

Statistical analysis

The statistical analyses for *Hp26695* strains were performed using student's *t-test* and one-way ANOVA followed by Tukey's multiple comparison tests for *Hp76* strains. The data are presented as mean \pm the standard errors (of mean) from three independent experiments.

RESULTS

Lack of CGs enhanced *H. pylori* cell wall permeability

H. pylori CGs comprise around 25% of total cell wall lipids (Haque et al., 1996). Hence, to study whether the depletion of CGs has any effect on *H. pylori* cell wall permeability, we measured the influx of ethidium bromide (EtBr) among wild-type and knockout strains by flow cytometry. Bacterial strains were incubated with EtBr and the median fluorescence intensity (MFI) was measured. We observed that *Hp26695* strain grown in absence of cholesterol showed higher MFI compared to the bacteria grown in the presence of cholesterol (Figure 3.1A), indicating a higher influx of EtBr in bacterial cultured in the absence of cholesterol. We also measured EtBr fluorescence intensity between the strains *Hp26695* and *Hp26695Δ421*; the MFI was considerably higher in *Hp26695Δ421* as compared to the wild type (Fig. 3.1B). To determine the kinetics of EtBr influx in *Hp26695* and *Hp26695Δ421* strains, we measured the MFI of EtBr influx at 5, 10 and 30 minutes time intervals. The MFI of *Hp26695Δ421* was significantly higher through all the time intervals compared to the MFI observed for *Hp26695* (P value <0.05) (Fig. 3.1C).

To check the cell wall fluidity of lag phase cultures, the *Hp26695Δ421* and *Hp26695* strains were cultured for 72 hours and were observed for EtBr influx. As expected, the MFI was found to be remarkably higher in *Hp26695Δ421* compared to the *Hp26695* (P value <0.05) (Fig. 3.1D & 3.2A). Furthermore, we observed that *Hp76Δ421* exhibited higher MFI compared to *Hp76* and *Hp76Δ421*-reconstituted strain (Fig. 3.1E and 3.2B). We also measured the MFI for *Hp76* strains in 72 hours cultures and found that the influx rate was considerably higher in *Hp76Δ421* compared to *Hp76* and *Hp76Δ421*-reconstituted strains (P value <0.05) (Fig. 3.1F, 3.2C and D). Overall, from these observations, we anticipate that the lack of CGs would likely perturbs the cell wall permeability of *H. pylori* by damaging the cell wall integrity.

Cholesteryl glucosides perturbation in *H. pylori* renders bacteria sensitive to antibiotics

To decipher the effect of loss of CGs in *H. pylori* on antibiotics resistance, we determined the minimum inhibitory concentrations (MICs) of certain antibiotics entailing *Hp26695* and *Hp76* strains. For this, the strains were grown on Brucella agar plates in the presence of MIC E-strips belonging to different antibiotics. *Hp26695* and *Hp76* strains were resistant to fosfomycin, polymyxin-B, colistin, tetracycline and ciprofloxacin. Moreover, *Hp26695Δ421* was more sensitive to amoxicillin compared to *Hp26695* while both strains were sensitive to clarithromycin. Interestingly, *Hp26695Δ421* and *Hp76Δ421* strains on the other hand, were found to be sensitive to all the above antibiotics tested (Figure 3.4A) and (Table 3.1). The increased sensitivity of *Hp26695Δ421* and *Hp76Δ421* strains was understandable as these strains demonstrated an increase in cell wall permeability due to the loss of CGs. Overall, it appears that the deletion of *hp0421* perturbs the cell wall integrity of *H. pylori* which in turn leads to increased susceptibility to all the antibiotics tested.

Lack of CGs disrupts LPS structure

In order to detect the changes in O-antigen expression due to CGs disruption, we isolated lipopolysaccharides from *Hp76*, *Hp76Δ421* and *Hp76Δ421*-reconstituted strain and visualized by silver stained SDS gel. Depletion of CGs resulted in the disruption of O-antigens as observed by silver staining of *Hp76Δ421* LPS in which the O-antigens were absent when compared to *Hp76* LPS profile. Consequently, the O-antigens and core LPS were partially restored in the *Hp76Δ421*-reconstituted strain (Fig. 3.3A).

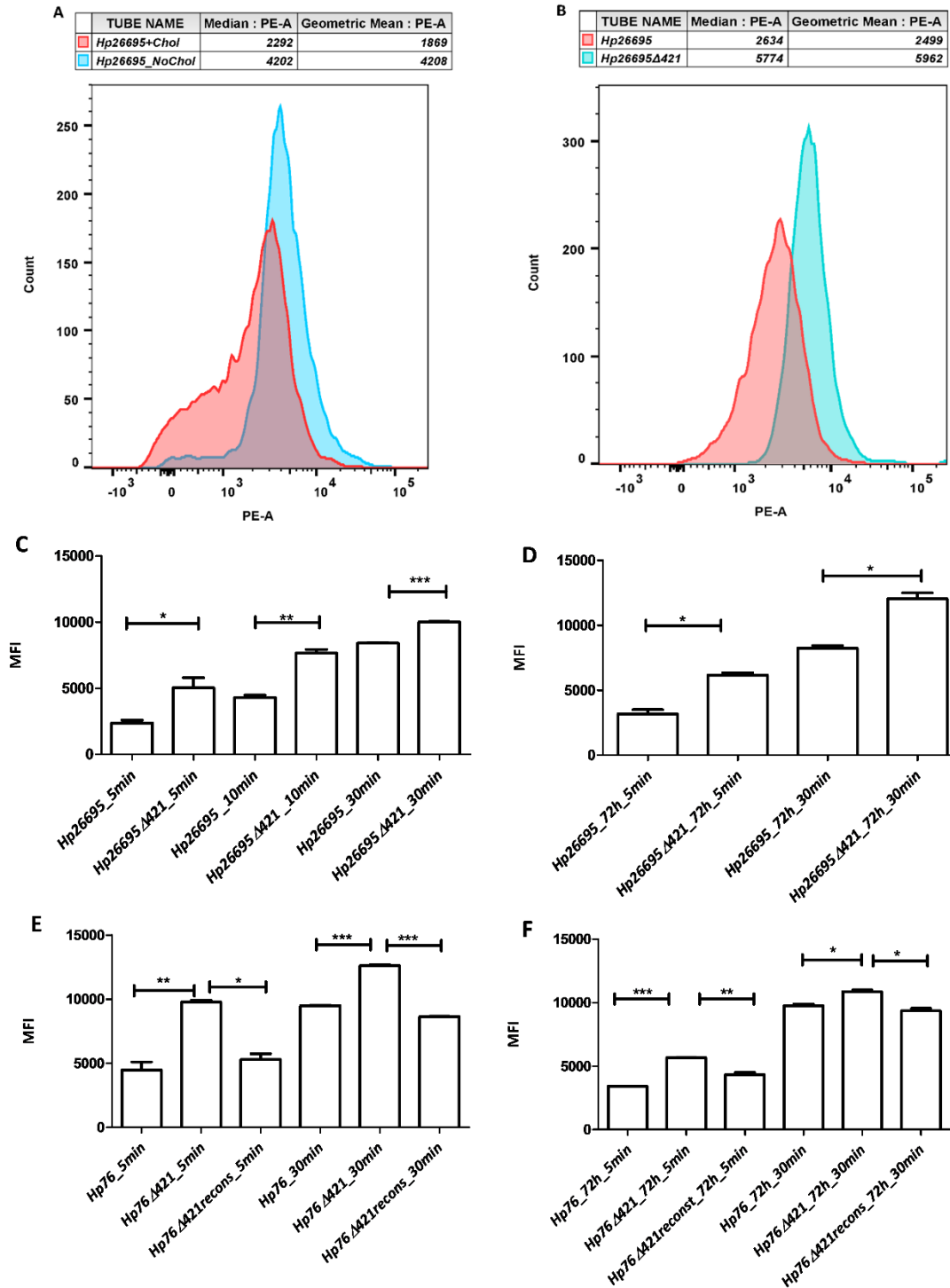


Figure 3.1: Absence of cholesteryl glucosides increased *H. pylori* cell wall permeability: Flow cytometry analysis based on influx rates of EtBr as depicted in the form of PE-A histograms delineating the median fluorescence intensity (MFI) for (A) *Hp26695* grown in presence and absence of cholesterol. Also depicted are (B) influx rates of EtBr for *Hp26695* and *Hp26695Δ421* grown for 48 hours. Bars in panels C to F represent MFIs when analyzed by student's *t*-test and one-way ANOVA for different wild type, knockout and reconstituted strains (as annotated) when treated /incubated with EtBr for 5, 10 and 30 minutes using cultures grown either at 48 hours or 72 hours (* denotes $p < 0.05$, ** denotes $p \leq 0.01$ and *** denotes $p \leq 0.001$).

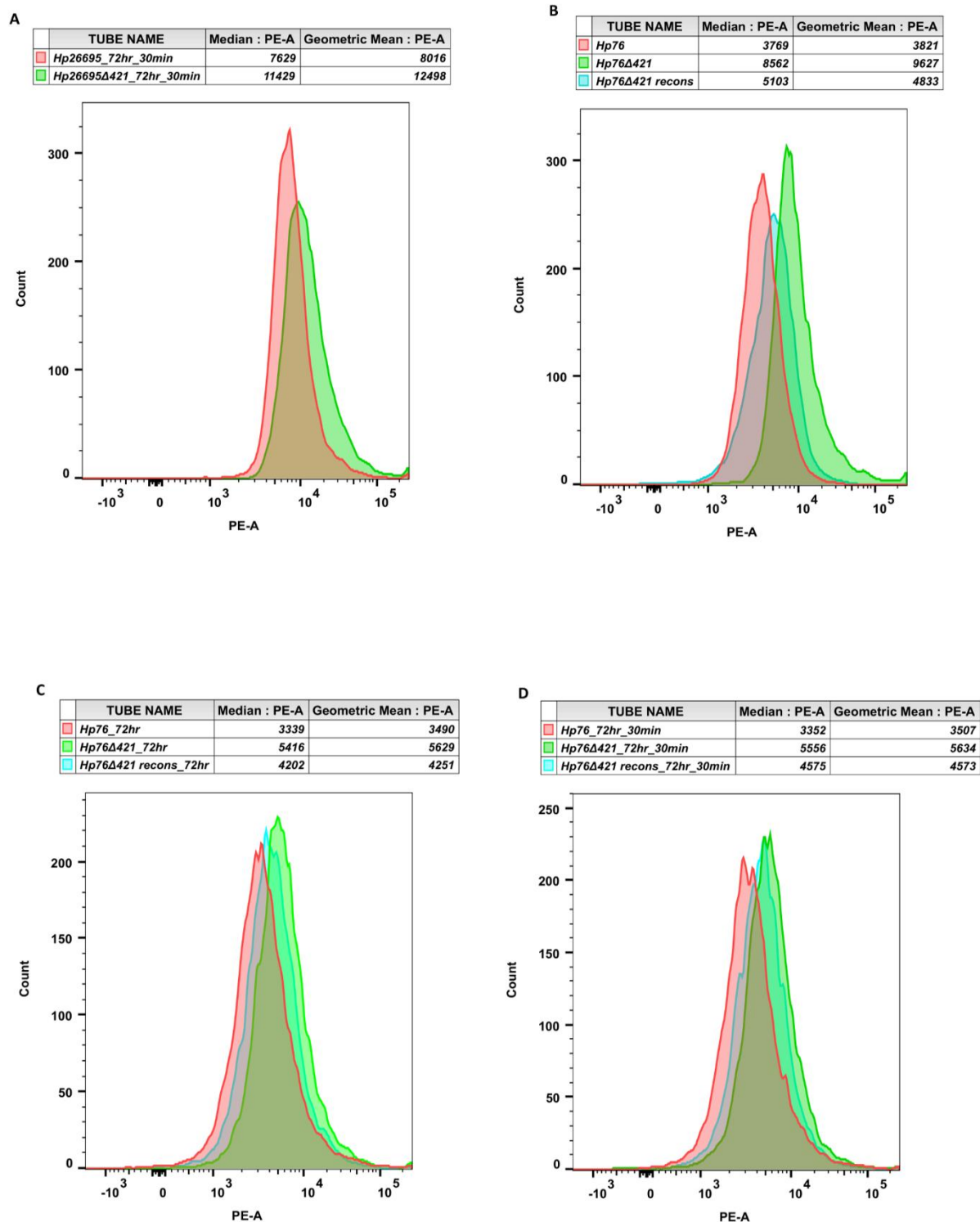


FIG 3.2: The absence of cholesteryl glucosides caused increased cell wall permeability. PE-A histograms delineating the influx rates of EtBr represented as MFI for (A) *Hp26695* strains grown for 72 hours and incubated with EtBr for 30min, (B) *Hp76* strains grown for 48 hours and incubated with EtBr for 5min, (C) *Hp76* strains grown for 72 hours and incubated with EtBr for 5min, (D) *Hp76* strains grown for 48 hours and incubated with EtBr for 30min.

Moreover we investigated whether the deletion of *hp0421* in *Hp26695* and *Hp76* strains had any effect on the transcription of *wecA* and *wzk* genes. We found no influence on *wecA* and *wzk* mRNA expression levels of these two genes in both wild-type and *Hp26695* Δ 421 and *Hp76* Δ 421 (Fig. 3.3C and 3.3D). This observation rules out the possibility that the alteration in LPS profile was due to alterations in the expression of these O-antigen synthesis genes. Thus, the lack of CGs most likely disrupted the normal components of *H. pylori* LPS.

Table 3.1: MICs of wild-type, Δ 421 mutants, and Δ 421-reconstituted *H. pylori* strains

Antibiotic. mcg/ml	<i>Hp26695</i>	<i>Hp26695</i> Δ 421	<i>Hp76</i>	<i>Hp76</i> Δ 421	<i>Hp76</i> Δ 421 recons
Fosfomycin	≥ 1024 (R)	$\leq 1.5 \pm 0.5$ (S)	≥ 1024 (R)	$\leq 0.064 \pm 2$ (S)	≥ 1024 (R)
Colistin	≥ 256 (R)	$\leq 12 \pm 3$ (S)	≥ 256 (R)	$\leq 10 \pm 5$ (S)	≥ 256 (R)
Polymyxin B	≥ 256 (R)	$\leq 8 \pm 4$ (S)	≥ 256 (R)	$\leq 10 \pm 4$ (S)	≥ 256 (R)
Ciprofloxacin	$\leq 0.38 \pm 0.5$ (R)	$\leq 0.064 \pm 0.02$ (S)	$\leq 0.50 \pm 0.5$ (R)	$\leq 0.19 \pm 0.2$ (S)	$\leq 0.047 \pm 0.08$ (R)
Tetracycline	$\leq 10 \pm 3$ (R)	$\leq 0.01 \pm 0.02$ (S)	$\leq 0.50 \pm 0.1$ (R)	$\leq 0.01 \pm 0.09$ (S)	$\leq 0.38 \pm 0.18$ (R)
Amoxicillin	$\leq 0.47 \pm 0.01$ (S)	$\leq 0.016 \pm 0.01$ (S)	$\leq 0.016 \pm 0.01$ 0.01 (S)	$\leq 0.016 \pm 0.01$ (S)	$\leq 0.016 \pm 0.01$ (S)
Clarithromycin	≤ 0.001 (S)	≤ 0.001 (S)	≤ 0.001 (S)	≤ 0.001 (S)	≤ 0.001 (S)

The letters in parentheses after the MIC indicate whether the strain is resistant (R) or sensitive (S) to the indicated antibiotic.

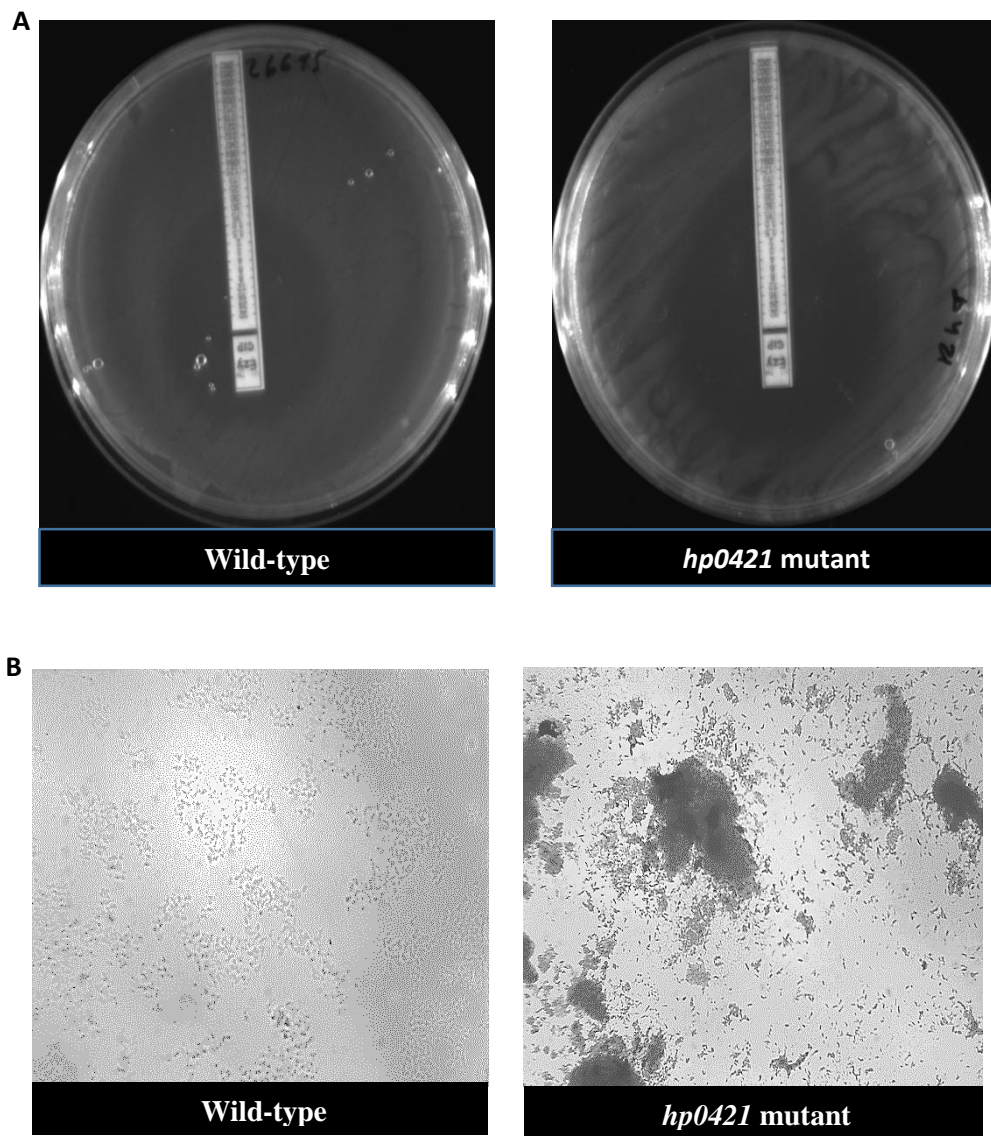


Figure 3.4: Lack of CGs in *H. pylori*: (A) Caused an increase in susceptibility against ciprofloxacin and (B) enhanced the aggregation of *H. pylori* on glass coverslip which were placed in broth media

Deletion of *hp421* enhances *H. pylori* cell aggregation

H. pylori produce biofilms on stomach mucosa in order to circumvent the gut's harsh environment and it was stated that the deletion of the *luxS* gene increases the biofilm formation (Cole, Harwood, Lee, She, & Guiney, 2004). We observed that *Hp26695Δ421* and *Hp76Δ421* tended to aggregate in the liquid cultures in contrast to the wild-type cultures that appeared turbid in their growth. So, we investigated the effect of *hp0421* deletion on the biofilm formation in *Hp26695* and *Hp76* strains. Biofilm formation was visualized under the microscope on glass coverslips (Figure 3.4B).

Hp26695Δ421 and *Hp76Δ421* demonstrated biofilm formation on the third day while wild-types formed biofilm on the fifth day. Moreover, crystal violet absorbance assay revealed the biofilm formation in *Hp26695Δ421* and *Hp76Δ421* to be significantly denser than in *Hp26695*, *Hp76* and *Hp76Δ421*-reconstituted strains (Figure 3.3B). The results showed that *Hp26695Δ421* and *Hp76Δ421* tended to aggregate and adhere strongly to the surface of the coverslip at the air-liquid interface. Hence, perhaps, the lack of CGs enhances aggregation of bacterial cells and promotes biofilm formation in *H. pylori*. Moreover, we analyzed the expression of the *luxS* gene in the above strains to check if its expression is affected by the deletion of *hp0421*. We observed that deletion of *hp0421* did not influence *luxS* mRNA expression levels in both wild-type and *Hp26695Δ421* and *Hp76Δ421* strains (Fig 3.3E).

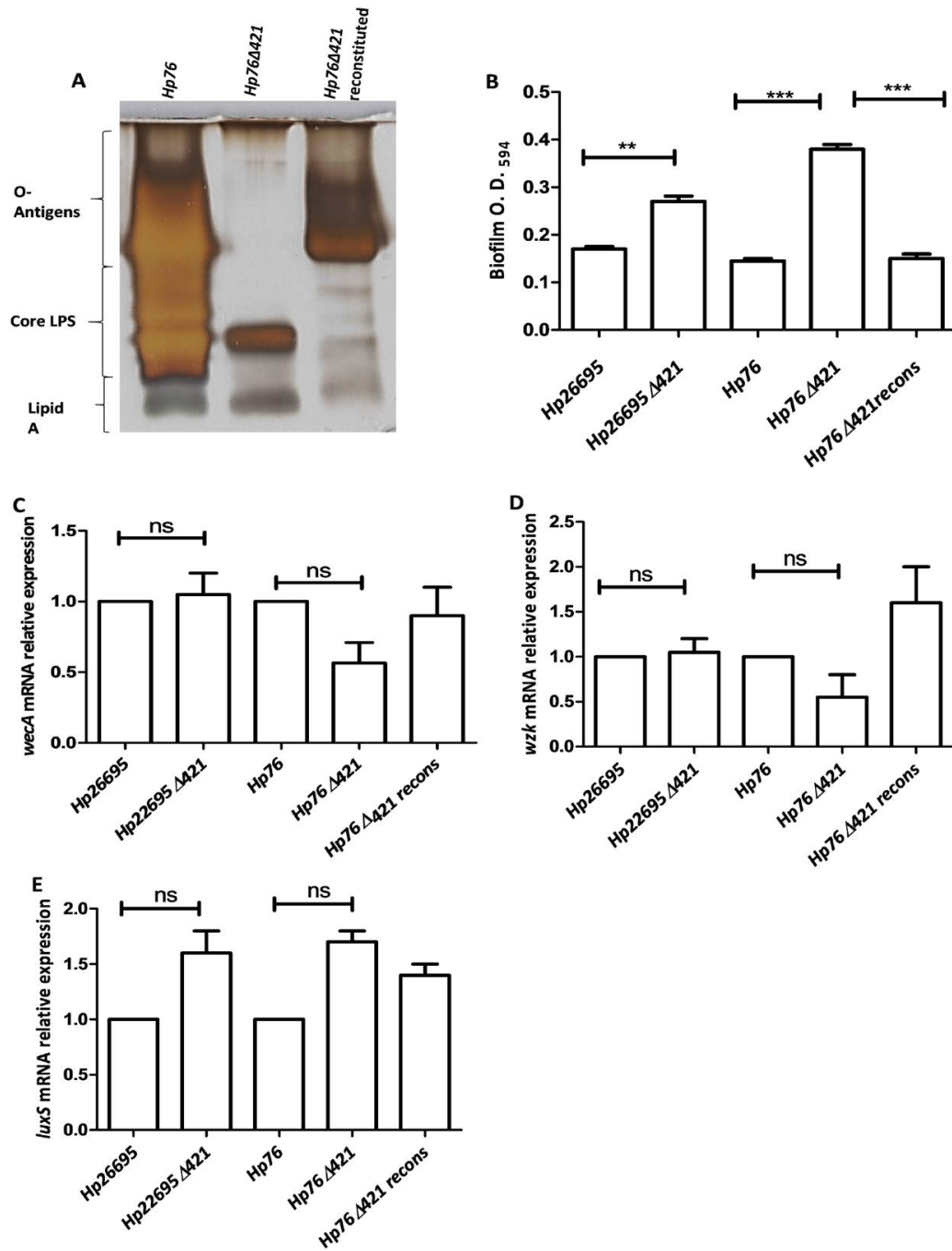


Figure 3.3: Analysis of LPS expression and biofilm formation (A) (15%) SDS-PAGE gel double silver stained depicting profiles of LPS from *Hp76*, *Hp76Δ421* and *Hp76Δ421*-reconstituted strain; (B) bar graph representing quantification of biofilm formation by *H. pylori* after 5 days of incubation. (C, D) qRT-PCR analyses of *wecA* and *wzk* genes by using RNA isolated from wild-type (*Hp26695*, *Hp76*), knockout (*Hp26695Δ421*, *Hp76Δ421*), and *Hp76Δ421*reconstituted strain(s) grown for 48 hr; (E) relative mRNA expression of *luxS* from 2 day old broth cultures (ns denotes non-significant difference(s), * denotes $p < 0.05$, ** denotes $p \leq 0.01$ and *** denotes $p \leq 0.001$).

DISCUSSION

Beside the substantial role of CGs in maintenance of *H. pylori* native helical morphology, the deletion of *hp0421* gene which results in loss of all CGs variants in the cell wall, which could lead to higher cell wall permeability. Likewise, when *H. pylori* 26695 strain was grown without cholesterol, the bacterial outer membrane permeability was significantly higher. Thus, this may indicate the critical role of CGs in the formation of intact cell wall units of *H. pylori* to maintain its integrity. In an alternative scenario, the CGs are probably required to preserve the tight pack of the outer membrane of *H. pylori*. Sterols in the membrane are believed to support the cell membrane integrity. For example, in *B. burgdorferi* the depletion of membrane cholesterol by M β CD and substitution with different sterol analogues increased the permeability of the membrane at varying levels based on the type of sterols, while the depletion of cholesterol without substitution with any sterols caused significant increase in the permeability of the membrane (LaRocca et al., 2013). Also, in yeast, the deletion of essential genes of sterol biosynthesis was reported to increase the cell membrane permeability (Dupont, Beney, Ferreira, & Gervais, 2011). Our findings are in line with these and other reports and suggest that CGs interact with peptidoglycan domains to maintain the architecture of *H. pylori* cell wall. The permeabilization of *H. pylori* cell wall has far reaching implications for therapeutic interventions.

Further, we observed that *Hp76 Δ 421* exhibited aberrant LPS expression profile with loss of O-antigens and lack of core LPS. Our observations suggest that the perturbation of the architecture of *H. pylori* cell wall as a result to the lack of CGs reduced the LPS expression. On the other hand, this might have occurred due to the alterations in the structure of cell wall affecting the O-antigen biosynthesis enzymes that are present in the cell wall. It is relevant in this context that the deletion of *hp0421* did not affect the mRNA expression of essential LPS synthesis genes *wecA* and *wzk*.

Alternatively, the alterations in the structure and composition of the cell wall due to the lack of CGs may result in the dysregulation of the transfer of LPS units through membranes. Our observations appear to be in correlation with the report of Hildebrandt *et al.*, who observed that depletion of cholesterol leads to the development of aberrant LPS in *Hp26695*, which depends on lipid-A phosphorylation (Hildebrandt & McGee, 2009).

Furthermore, we observed that lack of CGs reverted the resistance of *H. pylori* to antibiotics. The increased susceptibility to the antibiotics due to the deletion of *hp0421* may be the result of permeabilization of the cell wall, facilitating antibiotics to penetrate passively through *H. pylori* cells. The bacterial cell wall is the first line of defense against antibiotics, detergents and host defense elements. The membrane/cell wall permeabilization could be an effective method to control bacterial infections by enhancing antibiotic action/delivery (Delcour, 2009). Secondly, our study suggest that disruption of LPS and/or influencing the outer membrane charge as a result to the lack of CGs decreased the resistance of *H. pylori* to certain antibiotics like polymyxin and colistin. Disruption of lipid A gene encoding *lp_{XEHP}*, in *H. pylori*, has been shown to dramatically decrease the polymyxin resistance from MIC > 250 µg/ml to MIC, 10 µg/ml (Tran et al., 2006). Similarly, we believe that the deletion of *hp0421* might possibly affect the LPS structure thus influencing the outer membrane charge and cell wall integrity and eventually increasing the sensitivity of *H. pylori* to certain antibiotics. Inhibition of CGs synthesis may not kill the bacteria directly, but rather render the pathogens incapable of establishing successful infection by hindering their colonization potential and fitness advantage (resistance towards antibiotics).

Moreover, our study suggest that the tendency of *Hp26695Δ421* and *Hp76Δ421* to aggregate on the surface of coverslips is probably due to the changes in the properties of LPS. Modifications in LPS have been shown to enhance bacterial auto-aggregation and biofilm formation (Nakao,

Ramstedt, Wai, & Uhlin, 2012). Alternatively, the changes in the cell wall properties and morphology may triggered stress-related genes, including quorum sensing gene *luxS*. Similarly, the changes in the membrane structure of *Pseudomonas aeruginosa* were previously reported to alter quorum sensing (Baysse et al., 2005). However, according to our observation there was no changes in the mRNA expression levels of *luxS*.

REFERENCES

- Bayse, C., Cullinane, M., Denervaud, V., Burrowes, E., Dow, J. M., Morrissey, J. P., . . . O'Gara, F. (2005). Modulation of quorum sensing in *Pseudomonas aeruginosa* through alteration of membrane properties. *Microbiology*, 151(Pt 8), 2529-2542. doi: 10.1099/mic.0.28185-0
- Cole, S. P., Harwood, J., Lee, R., She, R., & Guiney, D. G. (2004). Characterization of Monospecies Biofilm Formation by *Helicobacter pylori*. *Journal of bacteriology*, 186(10), 3124-3132. doi: 10.1128/jb.186.10.3124-3132.2004
- Costa, K., Bacher, G., Allmaier, G., Dominguez-Bello, M. G., Engstrand, L., Falk, P., . . . García-del Portillo, F. (1999). The Morphological Transition of *Helicobacter pylori* Cells from Spiral to Coccoid Is Preceded by a Substantial Modification of the Cell Wall. *Journal of bacteriology*, 181(12), 3710-3715.
- Delcour, A. H. (2009). Outer membrane permeability and antibiotic resistance. *Biochim Biophys Acta*, 1794(5), 808-816. doi: 10.1016/j.bbapap.2008.11.005
- Doddam, S. N., Peddireddy, V., & Ahmed, N. (2017). Mycobacterium tuberculosis DosR Regulon Gene Rv2004c Encodes a Novel Antigen with Pro-inflammatory Functions and Potential Diagnostic Application for Detection of Latent Tuberculosis. *Front Immunol*, 8, 712. doi: 10.3389/fimmu.2017.00712
- Doig, P., & O'Toole, P. W. (1997). Molecular Characterization of *H. pylori* Surface Antigens *Helicobacter pylori* Protocols (pp. 177-189): Springer.
- Dupont, S., Beney, L., Ferreira, T., & Gervais, P. (2011). Nature of sterols affects plasma membrane behavior and yeast survival during dehydration. *Biochim Biophys Acta*, 1808(6), 1520-1528. doi: 10.1016/j.bbamem.2010.11.012
- Geis, G., Leying, H., Suerbaum, S., & Opferkuch, W. (1990). Unusual fatty acid substitution in lipids and lipopolysaccharides of *Helicobacter pylori*. *Journal of clinical microbiology*, 28(5), 930-932.
- GOODWIN, C. S., ARMSTRONG, J. A., CHILVERS, T., PETERS, M., COLLINS, M. D., SLY, L., . . . HARPER, W. E. (1989). Transfer of *Campylobacter pylori* and *Campylobacter mustelae* to *Helicobacter* gen. nov. as *Helicobacter pylori* comb. nov. and *Helicobacter mustelae* comb. nov., respectively. *International Journal of Systematic and Evolutionary Microbiology*, 39(4), 397-405.
- Haque, M., Hirai, Y., Yokota, K., Mori, N., Jahan, I., Ito, H., . . . Oguma, K. (1996). Lipid profile of *Helicobacter* spp.: presence of cholesteryl glucoside as a characteristic feature. *J Bacteriol*, 178(7), 2065-2070.
- Hildebrandt, E., & McGee, D. J. (2009). *Helicobacter pylori* lipopolysaccharide modification, Lewis antigen expression, and gastric colonization are cholesterol-dependent. *BMC Microbiol*, 9, 258. doi: 10.1186/1471-2180-9-258
- Hong, Y., Cunneen, M. M., & Reeves, P. R. (2012). The Wzx translocases for *Salmonella enterica* O-antigen processing have unexpected serotype specificity. *Mol Microbiol*, 84(4), 620-630. doi: 10.1111/j.1365-2958.2012.08048.x
- Hussain, A., Ewers, C., Nandanwar, N., Guenther, S., Jadhav, S., Wieler, L. H., & Ahmed, N. (2012). Multiresistant uropathogenic *Escherichia coli* from a region in India where urinary tract infections are endemic: genotypic and phenotypic characteristics of sequence type 131 isolates of the CTX-M-15 extended-spectrum-beta-lactamase-producing lineage. *Antimicrob Agents Chemother*, 56(12), 6358-6365. doi: 10.1128/AAC.01099-12
- Jung, S. W., Thamphiwatana, S., Zhang, L., & Obonyo, M. (2015). Mechanism of antibacterial activity of liposomal linolenic acid against *Helicobacter pylori*. *PLoS One*, 10(3), e0116519.

- Keenan, J. I., Allardyce, R. A., & Bagshaw, P. F. (1997). Dual silver staining to characterise *Helicobacter* spp. outer membrane components. *J Immunol Methods*, 209(1), 17-24.
- Krishnamurthy, P., Parlow, M. H., Schneider, J., Burroughs, S., Wickland, C., Vakil, N. B., . . . Phadnis, S. H. (1999). Identification of a novel penicillin-binding protein from *Helicobacter pylori*. *Journal of bacteriology*, 181(16), 5107-5110.
- LaRocca, T. J., Pathak, P., Chiantia, S., Toledo, A., Silvius, J. R., Benach, J. L., & London, E. (2013). Proving lipid rafts exist: membrane domains in the prokaryote *Borrelia burgdorferi* have the same properties as eukaryotic lipid rafts. *PLoS Pathog*, 9(5), e1003353. doi: 10.1371/journal.ppat.1003353
- McGee, D. J., George, A. E., Trainor, E. A., Horton, K. E., Hildebrandt, E., & Testerman, T. L. (2011). Cholesterol enhances *Helicobacter pylori* resistance to antibiotics and LL-37. *Antimicrob Agents Chemother*, 55(6), 2897-2904. doi: 10.1128/AAC.00016-11
- Nakao, R., Ramstedt, M., Wai, S. N., & Uhlin, B. E. (2012). Enhanced biofilm formation by *Escherichia coli* LPS mutants defective in Hep biosynthesis. *PLoS One*, 7(12), e51241. doi: 10.1371/journal.pone.0051241
- PA, W. (2016). CLSI. Methods for Antimicrobial Dilution and Disk Susceptibility Testing of Infrequently Isolated or Fastidious Bacteria, 3rd ed CLSI guidelines M45. Clinical and laboratory Standards Institute
- Paixao, L., Rodrigues, L., Couto, I., Martins, M., Fernandes, P., de Carvalho, C. C., . . . Viveiros, M. (2009). Fluorometric determination of ethidium bromide efflux kinetics in *Escherichia coli*. *J Biol Eng*, 3, 18. doi: 10.1186/1754-1611-3-18
- Smith, J., Drumm, B., Neumann, A., Policova, Z., & Sherman, P. (1990). In vitro surface properties of the newly recognized gastric pathogen *Helicobacter pylori*. *Infect Immun*, 58(9), 3056-3060.
- Trainor, E. A., Horton, K. E., Savage, P. B., Testerman, T. L., & McGee, D. J. (2011). Role of the HefC efflux pump in *Helicobacter pylori* cholesterol-dependent resistance to ceragenins and bile salts. *Infect Immun*, 79(1), 88-97. doi: 10.1128/IAI.00974-09
- Tran, A. X., Whittimore, J. D., Wyrick, P. B., McGrath, S. C., Cotter, R. J., & Trent, M. S. (2006). The lipid A 1-phosphatase of *Helicobacter pylori* is required for resistance to the antimicrobial peptide polymyxin. *J Bacteriol*, 188(12), 4531-4541. doi: 10.1128/JB.00146-06
- Yonezawa, H., Osaki, T., Kurata, S., Fukuda, M., Kawakami, H., Ochiai, K., . . . Kamiya, S. (2009). Outer membrane vesicles of *Helicobacter pylori* TK1402 are involved in biofilm formation. *BMC Microbiol*, 9, 197. doi: 10.1186/1471-2180-9-197

Chapter 4

Objective 3: To analyze the role of *H. pylori* CGs in Mincle receptor regulation.

INTRODUCTION

The first line of body defense is the innate immunity that identifies any non self, non-specific molecular patterns of pathogens. One category of the innate immune receptors are C-type lectin receptors (CLRs) that contain members of transmembrane and soluble receptors. These receptors possess a carbohydrate recognition domain (CRD) as a characteristic feature or a homologous domain (Zelensky & Gready, 2005). Furthermore, Transmembrane CLRs can function as pattern recognition receptors (PRRs), which mean that it has the ability to recognize and internalize a pathogen, and subsequently degrade and present the constituent molecules as an antigens which will be recognized by innate immune defense system and subsequently induce adaptive immunity (Geijtenbeek & Gringhuis, 2009). One of plausible example of transmembrane CLRs that identify a wide range of foreign and self-molecule as part of innate immune response is Mincle (Patin, Orr, & Schaible, 2017). One of the most studied molecules that are recognized by Mincle receptor is the ‘cord factor’ trehalose dibehenate (TDB) which is a part of *M. tuberculosis* membrane. TDB trigger a strong immune response and has potent immune modulating properties (Ishikawa et al., 2009; Schoenen et al., 2010).

Mincle is composed of 219 amino acids and a carbohydrate recognition domain (CRD) which is categorized under type II transmembrane protein which and present at its extracellular region that are present in various cells including macrophages, DCs and neutrophils (Matsumoto et al., 1999). The ligand binding site expressed on cell surface side, its ligand include cholesterol and protein, the signal transduces via the Fc receptor γ -chain molecule (FC- γ) with tyrosine- based activation motif immune receptor that has (Yamasaki et al., 2008). Mincle downstream signaling pathway involves activation of spleen tyrosine kinase (Syk) which subsequently activates Card9-Bcl10-

MALT1 complex where the latter target (NF- κ B). Subsequently, the transcription factor NF- κ B induces the expression of various cytokines such as interleukin-6 (IL-6) and tumor necrosis factor (TNF), interleukin-10 (IL-10) (Werninghaus et al., 2009). TNF and IL-6 responses act as a pro-inflammatory while induction of IL-10 is considered as anti-inflammatory and results in downregulation of IL-12p40 that interferes with pro-inflammatory cytokine secretion (Patin et al., 2016). Induction of Mincle receptor triggers a defensive TH1 cell mediated immunity when induced by cord factor and initiates TH17 responses (Figure 4.1) (van Dissel et al., 2014). Recently, there are number of studies that have shown that lipid derivatives induce Mincle signaling and trigger inflammatory responses (Kiyotake et al., 2015; Kostarnoy et al., 2017). Moreover, Kiyotake R. et al., analysed ligands that trigger the human-Mincle by mass spectrophotometry (MS) and it revealed that free cholesterol, cholesterol crystals, cholesterol intermediate induced hMincle expression while endogenous steroids such as testosterone, cortisone, estradiol, progesterone, aldosterone, bile acid cholestanoic acid, and yeast ergosterol did not induce hMincle expression (Kiyotake et al., 2015).

Mincle is a PRRs which recognizes the pathogen-associated molecular patterns (PAMPs) of bacteria and fungi mainly glycolipids (Richardson & Williams, 2014). Previously, it was shown that *H. pylori* induces Mincle expression and triggers anti-inflammatory responses through IL-10 production in order to escape clearance by the host immune system (Devi, Rajakumara, & Ahmed, 2015)

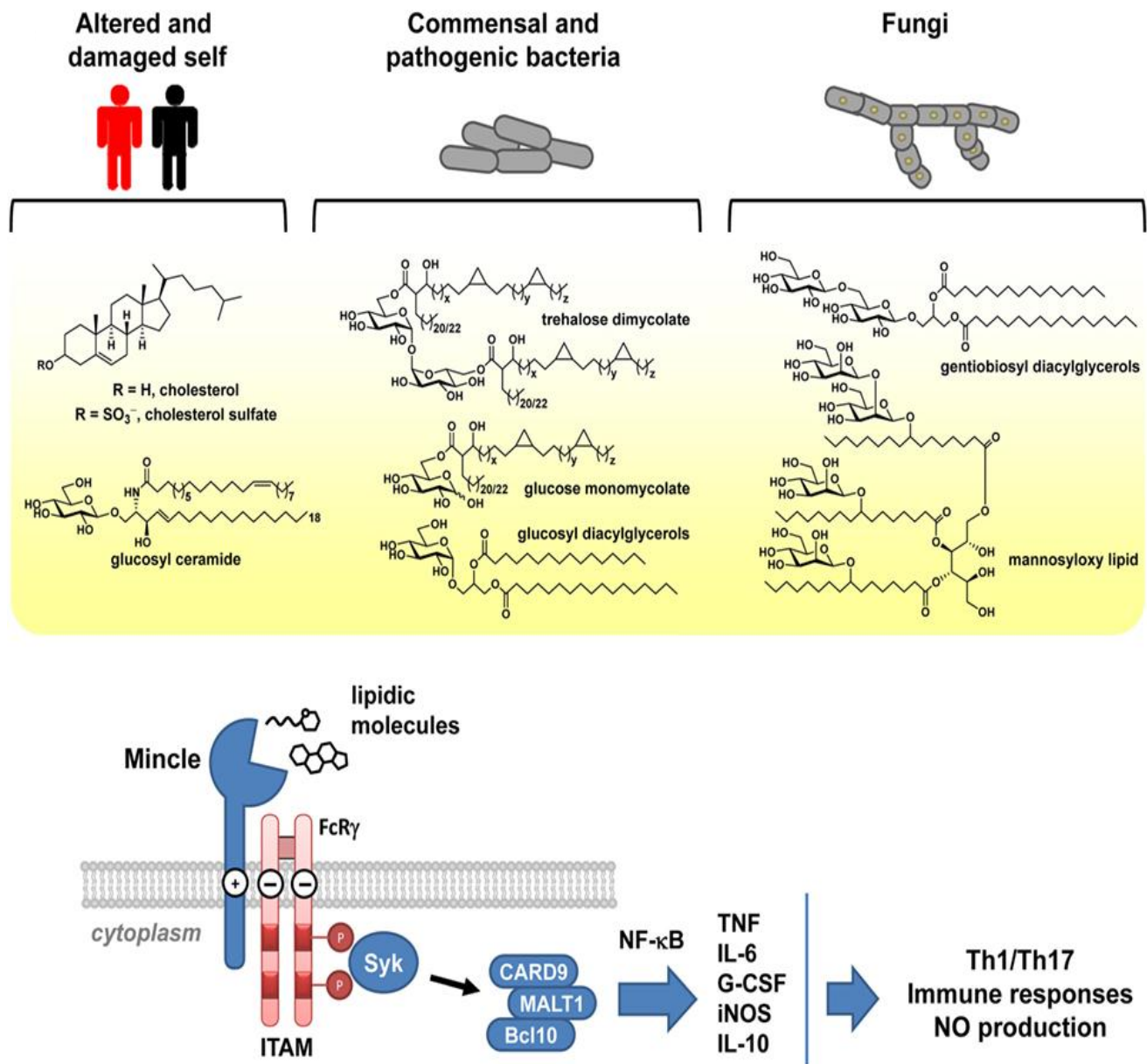


Figure 4.1: Signaling via Mincle, some of glycolipids ligands that induce Mincle and the signaling pathway through Mincle which triggers secretion of chemokines, cytokines, and activate T-cell immune responses (Williams, 2017).

MATERIAL AND METHODS

Culture of Macrophage cell lines

The human monocyte THP-1 cells and RAW 264.7 cells were obtained from National Centre for Cell Sciences, Pune, India. THP-1 cells were cultivated in RPMI-1640 medium and RAW 264.7 cells were cultivated in Dulbecco's Modified Eagle's Medium (DMEM) (Gibco) enriched with 10% (v/v) decompemented fetal bovine serum (FBS) (Invitrogen), 1% of 100X anti-mycotic/antibiotic solution which contains Amphotericin B, Penicillin, Streptomycin (Gibco) and were incubated in microaerophilic conditions with 5% O₂ and 5% CO₂ at 37°C. To differentiate THP-1 cells from monocytes to macrophages 50 ng/mL PMA (phorbol 12-myristate 13-acetate) were added (Sigma) and incubated for 48 hours. After cell differentiation and adherence, the culture media was replaced by fresh media with 10% decompemented FBS and was further incubated for another 12-24 hours before infection.

Infection assay

THP-1 cells and RAW 264.7 cell infection assay was modified from (Devi et al., 2015; Menaker, Ceponis, & Jones, 2004). Briefly, *H. pylori* strains lawns were collected from GC agar plates in 1X PBS and were washed twice with 1X PBS. Macrophage-like THP-1 cells in serum and antibiotic free RPMI-1640 medium were infected with *Hp26695* and *Hp26695Δ421* strains (human-adapted strain) at multiplicity of infection (MOI) of 100 i for 12 hour. Similarly, RAW 264.7 cells were grown till they reached 70% confluency and infected by *Hp76* wild-type, *Hp76Δ421* and *Hp76Δ421*-reconstituted strains (mice-adapted strain) for 12 hour.

Quantitative-PCR and gene expression analysis

The method for qRT-PCR analysis was described previously (Doddam, Peddireddy, & Ahmed, 2017). Briefly, RNA was isolated from 10^8 cells of *H. pylori* strains by TriZOL (Invitrogen). Subsequently, 3µg of RNA was converted to cDNA using random hexamers and SuperScript-III (Invitrogen) referring to the manufacturer's instructions. For qRT-PCR, 40 ng of the first transcribed DNA strand was amplified using SYBR[®] Fast qPCR Mix (TaKaRa) with primers corresponding to Mincle receptor expression in THP-1 cells by using primers Mincle-F 5' AAACACAATGCACAGAGAGAGG 3', Mincle-R 5' ACACATCTGGTGATGAAACAGG 3', together with GAPDH-F 5' GAGTCAACGGATTTGGTCGT 3' GAPDH-R 5' GACAAGCTTCCCGTTCTCAG 3', as internal control. For RAW 264.7 cells the primers used were Mincle-F 5' AGGAAGAAAGGCAGGAAAAAGG 3', Mincle-R 5' GAAACAGCCACTGAGAAACAGG 3', together with β -actin-F 5' GCTACAGCTTCACCACCACAG 3', β -actin-R 5' GGTCTTACGGATCAACGTC 3' as internal control.

Statistical analysis

The statistical analyses for Hp26695 strains were performed using student's t-test and one-way ANOVA followed by Tukey's multiple comparison tests for Hp76 strains. The data are presented as mean \pm the standard errors (of mean) from three independent experiments. The data represented the standard error of mean of three independent experiments.

RESULTS

Mincle induction reduces in THP-1 and RAW 264.7 cells upon infection by *hp0421* mutants

THP-1 cells are human macrophage cells that express Mincle receptor. We observed that *Hp26695* wild-type strain significantly induced Mincle expression compared to uninfected cells when tested at 12 hour post infection. Moreover, Mincle relative mRNA expression in THP-1 cells infected by *Hp26695Δ421* was remarkably reduced compared to the cells that were infected by *Hp26695* wild-type (Figure 4.2). Similarly, expression of Mincle relative mRNA expression was considerably induced upon infection by *Hp76* wild-type compared to uninfected RAW 264.7 cells. Furthermore, Mincle expression was reduced significantly in RAW 264.7 cells upon infection by *Hp76Δ421* strain compared to Mincle expression after infection with wild-type strain. Interestingly, infection of RAW 264.7 cells by *Hp76Δ421*-reconstituted strain induced Mincle expression similar to the induction of Mincle by wild-type strain (Figure 4.3). Overall, infection of macrophage cells by *H. pylori* strains induces Mincle expression while infection by *hp0421* mutants demonstrated reduced Mincle expression compared to wild-type and reconstituted strains.

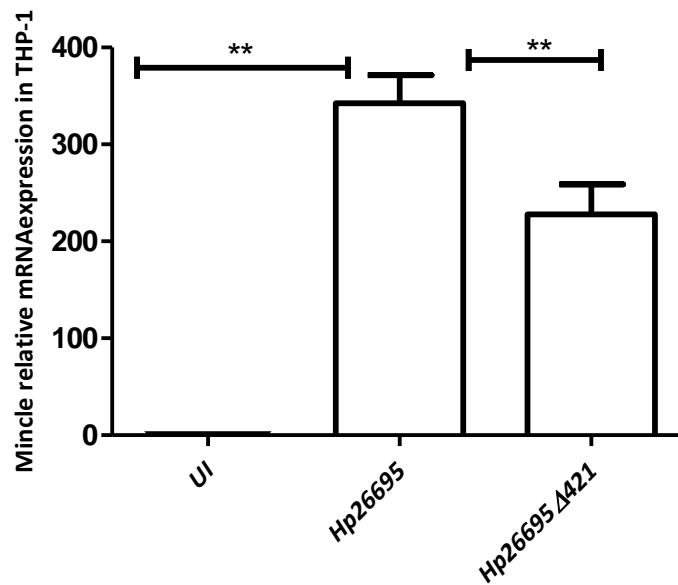


Figure 4.2: Deletion of *hp0421* in *Hp26695* resulted in decreased expression of Mincle receptor in THP1 cells; THP-1 cells were infected by *Hp26695* strains for 12 hours at MOIs of 100. Mincle relative mRNA expression levels were analyzed by qRT-PCR. The expression of Mincle gene was reduced significantly in THP-1 cells upon infection by *Hp26695*Δ421 strains compared to wild-type. (As annotated). ** denotes $p \leq 0.01$.

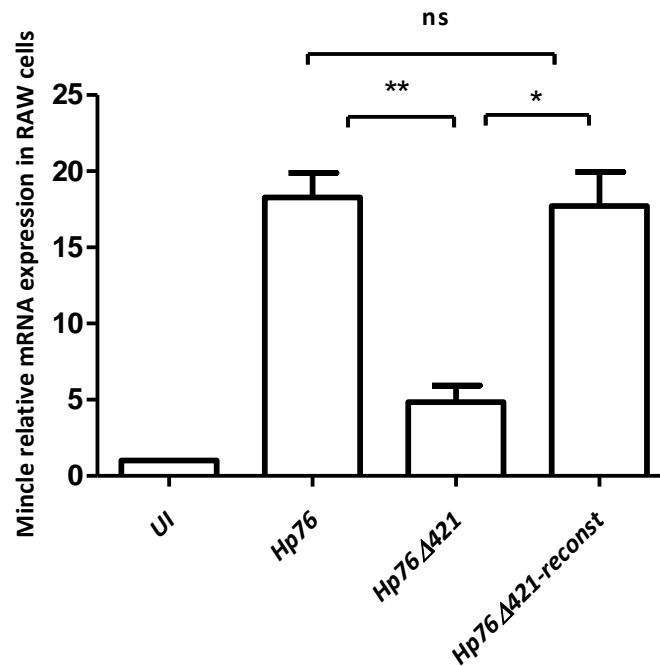


Figure 4.3: Deletion of *hp0421* in *Hp76* strain resulted in decreased expression of mMincle in RAW 264.7 cells; RAW 264.7 cells were infected by *Hp76* strains for 12 hours at MOI of 100. Mincle mRNA expression levels were detected by qRT-PCR. The expression of mMincle gene was reduced significantly in RAW 264.7 cells upon infection by *Hp76* Δ 421 strain compared to infection with wild-type and reconstituted strains. Data were analyzed by one-way ANOVA followed by Tukey's multiple comparison tests. (ns denotes non-significant difference(s), * denotes $p < 0.05$, ** and denotes $p \leq 0.01$).

DISCUSSION

Evading the responses of innate immune system is a key strategy in prolong colonization of *H. pylori*. *H. pylori* achieves this by its ability to regulate the host innate immune responses and their signaling pathways. Mincle predominantly expressed by macrophages are critical in mounting host defense responses against the invading pathogens. Mincle receptor mainly recognizes the glycolipids present on the pathogens. *H. pylori* CGs are a glycolipids which are the characteristic feature of this bacterium. Our study suggest that may CGs work as a ligands in order to induce Mincle receptor expression in macrophages obtained from human and mice as it was evident from the *in vitro* investigates performed. The reduction of Mincle expression in mice-macrophages and human-macrophages upon infection by *hp0421* mutants that lack CGs indicates that the presence of CGs is required to upregulate Mincle expression in macrophage cells. Restoration of Mincle expression comparable to the Mincle expression level in cells infected with wild-type and *Hp76Δ421*-reconstituted provides a strong evidence that CGs could perhaps play a significant role in induction of Mincle receptor. In line with this, previous studies have also demonstrated that the glycolipids present on some pathogens are responsible for Mincle receptor induction. For example Mycobacterial trehalose-6-6'-dimycolate (TDM) which is present on *M. tuberculosis* outer membrane is a potent trigger that induces immune response upon interaction with Mincle receptor (Söldner, Horn, & Sticht, 2018). Furthermore, the glycolipid α -Glucosyl diacylglycerides from *Streptococcus pneumonia* was shown to induce Mincle expression in Mincle reporter cell line (Behler-Janbeck et al., 2016). Overall, our results indicate that *H. pylori* CGs induces Mincle receptor response in animals and modulates host immune response through Mincle expression. These observations provide important insights into the innate immune responses provoked by *H.*

pylori which could be useful in targeting immune based control of infections and *H. pylori* eradication therapies.

REFERENCES

- Behler-Janbeck, F., Takano, T., Maus, R., Stolper, J., Jonigk, D., Tarrés, M. T., . . . Timmer, M. S. (2016). C-type lectin Mincle recognizes glucosyl-diacylglycerol of *Streptococcus pneumoniae* and plays a protective role in pneumococcal pneumonia. *PLoS pathogens*, 12(12), e1006038.
- Devi, S., Rajakumara, E., & Ahmed, N. (2015). Induction of Mincle by *Helicobacter pylori* and consequent anti-inflammatory signaling denote a bacterial survival strategy. *Sci Rep*, 5, 15049. doi: 10.1038/srep15049
- Doddam, S. N., Peddireddy, V., & Ahmed, N. (2017). Mycobacterium tuberculosis DosR Regulon Gene Rv2004c Encodes a Novel Antigen with Pro-inflammatory Functions and Potential Diagnostic Application for Detection of Latent Tuberculosis. *Front Immunol*, 8, 712. doi: 10.3389/fimmu.2017.00712
- Geijtenbeek, T. B., & Gringhuis, S. I. (2009). Signalling through C-type lectin receptors: shaping immune responses. *Nature Reviews Immunology*, 9(7), 465.
- Ishikawa, E., Ishikawa, T., Morita, Y. S., Toyonaga, K., Yamada, H., Takeuchi, O., . . . Yamasaki, S. (2009). Direct recognition of the mycobacterial glycolipid, trehalose dimycolate, by C-type lectin Mincle. *Journal of Experimental Medicine*, 206(13), 2879-2888.
- Kiyotake, R., Oh-Hora, M., Ishikawa, E., Miyamoto, T., Ishibashi, T., & Yamasaki, S. (2015). Human Mincle binds to cholesterol crystals and triggers innate immune responses. *Journal of Biological Chemistry*, jbc. M115. 645234.
- Kostarnoy, A. V., Gancheva, P. G., Lepenies, B., Tukhvatulin, A. I., Dzharullaeva, A. S., Polyakov, N. B., . . . Bobrov, M. A. (2017). Receptor Mincle promotes skin allergies and is capable of recognizing cholesterol sulfate. *Proceedings of the National Academy of Sciences*, 114(13), E2758-E2765.
- Matsumoto, M., Tanaka, T., Kaisho, T., Sanjo, H., Copeland, N. G., Gilbert, D. J., . . . Akira, S. (1999). A novel LPS-inducible C-type lectin is a transcriptional target of NF-IL6 in macrophages. *The Journal of Immunology*, 163(9), 5039-5048.
- Menaker, R. J., Ceponis, P. J., & Jones, N. L. (2004). *Helicobacter pylori* induces apoptosis of macrophages in association with alterations in the mitochondrial pathway. *Infect Immun*, 72(5), 2889-2898.
- Patin, E. C., Orr, S. J., & Schaible, U. E. (2017). Macrophage inducible C-type lectin as a multifunctional player in immunity. *Front Immunol*, 8, 861.
- Patin, E. C., Willcocks, S., Orr, S., Ward, T. H., Lang, R., & Schaible, U. E. (2016). Mincle-mediated anti-inflammatory IL-10 response counter-regulates IL-12 in vitro. *Innate immunity*, 22(3), 181-185.
- Richardson, M. B., & Williams, S. J. (2014). MCL and Mincle: C-type lectin receptors that sense damaged self and pathogen-associated molecular patterns. *Front Immunol*, 5, 288.
- Schoenen, H., Bodendorfer, B., Hitchens, K., Manzanero, S., Werninghaus, K., Nimmerjahn, F., . . . Ruland, J. (2010). Cutting edge: Mincle is essential for recognition and adjuvanticity of the mycobacterial cord factor and its synthetic analog trehalose-dibehenate. *The Journal of Immunology*, ji_0904013.
- Söldner, C. A., Horn, A. H., & Sticht, H. (2018). Interaction of Glycolipids with the Macrophage Surface Receptor Mincle—a Systematic Molecular Dynamics Study. *Sci Rep*, 8(1), 5374.
- van Dissel, J. T., Joosten, S. A., Hoff, S. T., Soonawala, D., Prins, C., Hokey, D. A., . . . Andreasen, L. V. (2014). A novel liposomal adjuvant system, CAF01, promotes long-lived Mycobacterium tuberculosis-specific T-cell responses in human. *Vaccine*, 32(52), 7098-7107.
- Werninghaus, K., Babiak, A., Groß, O., Hölscher, C., Dietrich, H., Agger, E. M., . . . Finger, K. (2009). Adjuvanticity of a synthetic cord factor analogue for subunit Mycobacterium tuberculosis

- vaccination requires FcRγ–Syk–Card9–dependent innate immune activation. *Journal of Experimental Medicine*, 206(1), 89-97.
- Williams, S. J. (2017). Sensing Lipids with Mincle: Structure and Function. *Front Immunol*, 8, 1662.
- Yamasaki, S., Ishikawa, E., Sakuma, M., Hara, H., Ogata, K., & Saito, T. (2008). Mincle is an ITAM-coupled activating receptor that senses damaged cells. *Nature immunology*, 9(10), 1179.
- Zelensky, A. N., & Gready, J. E. (2005). The C-type lectin-like domain superfamily. *The FEBS journal*, 272(24), 6179-6217.

Summary and conclusions

SUMMARY AND CONCLUSION

Infection of the human stomach caused by *Helicobacter pylori* is very common as the pathogen colonizes more than half of the world's population. It is associated with varied outcomes of infection, such as peptic ulcer disease, gastric ulcers, mucosa-associated lymphoid tissue lymphoma, and is generally considered as a risk factor for the development of gastric adenocarcinoma. Cholesteryl glucosides (CGs) constitute a vital component of the cell wall of *H. pylori* and contribute to its pathogenicity and virulence. The gene, *hp0421*, encodes cholesteryl- α -glucosides transferase (CGT), which demonstrates critical enzymatic functions entailing the integration of unique CGs into the cell wall of *H. pylori*. Deletion of this gene leads to the depletion of CGs and their variants. Herein, we report that the deletion of *hp0421* and consequent deficiency of cholesterol alters morphology, shape and cell wall composition of *H. pylori* cells, as demonstrated by high-resolution confocal microscopy and flow cytometry analyses of two different type strains of *H. pylori*, their isogenic knockouts as well as a reconstituted strain.

Moreover, measurement of ethidium bromide (EtBr) influx by flow cytometry showed that lack of CGs increased cell wall permeability. Antimicrobial susceptibility testing revealed that the *hp0421* isogenic knockouts, *Hp26695 Δ 421* and *Hp76 Δ 421*, were sensitive to antibiotics, such as fosfomycin, polymyxin-B, colistin, tetracycline and ciprofloxacin, in contrast to the wild-type strains that were resistant to the above antibiotics also the isogenic knockouts tended to form denser biofilms compared to their wild-type strains. Lipid profile analysis of both *Hp76* and *Hp76 Δ 421* strains showed an aberrant profile of lipopolysaccharides (LPS) in the *Hp76 Δ 421* strain.

Taken together, we herein provide a set of mechanistic evidences to demonstrate that CGs play critical roles in the maintenance of typical spiral morphology of *H. pylori* and its cell wall integrity, and any alteration in CGs content affects the characteristic morphological features and renders the *H. pylori* susceptible to various antibiotics.

Helicobacter pylori is an important cause of chronic gastritis leading to peptic ulcer and is a major risk factor for gastric malignancies. Failure in the eradication of *H. pylori* infection and increasing antibiotic resistance are two major problems in preventing *H. pylori* colonization. Hence, a deeper understanding of the bacterial survival strategies is needed to tackle the increasing burden of *H. pylori* infection by an appropriate intervention. Our study demonstrated that the lack of cholesteryl glucosides (CGs) remarkably altered the morphology of *H. pylori* and increased permeability of the bacterial cell wall. Further, this study highlighted the substantial role of CGs in maintaining the typical *H. pylori* morphology that is essential for maintaining its pathogenic potential. We also demonstrated that the loss of CGs in *H. pylori* renders the bacterium susceptible to different antibiotics.

Evading the responses of innate immune system is a key strategy in prolong colonization of *H. pylori*. *H. pylori* achieves this by its ability to regulate the host innate immune responses and their signaling pathways. Mincle receptors are predominantly expressed by macrophages and are critical in mounting host defense responses against the invading pathogens. Mincle receptor mainly recognizes the glycolipids present on the pathogens. *H. pylori* CGs are a glycolipids and are a characteristic feature of this bacterium. Our observations indicate that *H. pylori* CGs act as ligands for Mincle receptors and induce Mincle receptor upregulation and modulates host immune response through Macrophage-Mincle expression. These observations provide important insights into the innate immune responses triggered by *H. pylori*.

In conclusion, in this study, we have evidenced the role of CGs in the maintenance of *H. pylori* native helical morphology and the lack of CGs remarkably resulted in variable shape and size of *H. pylori* cells dominated by 'c' shaped cells. Moreover, the cell wall permeability increased irrespective of the duration of culture and the strain type of *H. pylori*. Further, we showed that lack of CGs perturbed the structure of cell wall components like LPS, which on one hand, would attenuate the virulence of *H. pylori* and, on the other hand, would render *H. pylori* susceptible to antibiotics to which it was otherwise resistant. CGs could be a promising target for drugs aiming at the eradication of *H. pylori* infection. The functional roles of CGs in *H. pylori* that we report here significantly extends the previous understanding on the role of cholesterol glucosylation in *H. pylori* immune evasion and pathogenicity. Future studies are needed to determine whether inhibition of *H. pylori* specific CGs constitutes a target for the development of new therapeutic molecules for *H. pylori* induced inflammation and malignancies.

Publications



Roles of Cholesteryl- α -Glucoside Transferase and Cholesteryl Glucosides in Maintenance of *Helicobacter pylori* Morphology, Cell Wall Integrity, and Resistance to Antibiotics

Majjid A. Qaria,^a Naveen Kumar,^{a*} Arif Hussain,^a Shamsul Qumar,^a Sankara N. Doddam,^a Ludovico P. Sepe,^b Niyaz Ahmed^{a,c}

^aPathogen Biology Laboratory, Department of Biotechnology and Bioinformatics, University of Hyderabad, Hyderabad, India

^bDepartment of Molecular Biology, Max-Planck Institute for Infection Biology, Berlin, Germany

^cInternational Centre for Diarrheal Disease Research, Bangladesh, Dhaka, Bangladesh

ABSTRACT Infection of the human stomach caused by *Helicobacter pylori* is very common, as the pathogen colonizes more than half of the world's population. It is associated with varied outcomes of infection, such as peptic ulcer disease, gastric ulcers, and mucosa-associated lymphoid tissue lymphoma, and is generally considered a risk factor for the development of gastric adenocarcinoma. Cholesteryl glucosides (CGs) constitute a vital component of the cell wall of *H. pylori* and contribute to its pathogenicity and virulence. The *hp0421* gene, which encodes cholesteryl- α -glucoside transferase (CGT), appears critical for the enzymatic function of integrating unique CGs into the cell wall of *H. pylori*, and deletion of this gene leads to depletion of CGs and their variants. Herein, we report that the deletion of *hp0421* and consequent deficiency of cholesterol alter the morphology, shape, and cell wall composition of *H. pylori* cells, as demonstrated by high-resolution confocal microscopy and flow cytometry analyses of two different type strains of *H. pylori*, their isogenic knockouts as well as a reconstituted strain. Moreover, measurement of ethidium bromide (EtBr) influx by flow cytometry showed that lack of CGs increased cell wall permeability. Antimicrobial susceptibility testing revealed that the *hp0421* isogenic knockout strains, the *Hp26695Δ421* and *Hp76Δ421* strains, were sensitive to antibiotics, such as fosfomycin, polymyxin B, colistin, tetracycline, and ciprofloxacin, in contrast to the wild-type strains that were resistant to the above antibiotics and tended to form denser biofilms. Lipid profile analysis of both *Hp76* and *Hp76Δ421* strains showed an aberrant profile of lipopolysaccharides (LPS) in the *Hp76Δ421* strain. Taken together, we herein provide a set of mechanistic evidences to demonstrate that CGs play critical roles in the maintenance of the typical spiral morphology of *H. pylori* and its cell wall integrity, and any alteration in CG content affects the characteristic morphological features and renders the *H. pylori* susceptible to various antibiotics.

IMPORTANCE *Helicobacter pylori* is an important cause of chronic gastritis leading to peptic ulcer and is a major risk factor for gastric malignancies. Failure in the eradication of *H. pylori* infection and increasing antibiotic resistance are two major problems in preventing *H. pylori* colonization. Hence, a deeper understanding of the bacterial survival strategies is needed to tackle the increasing burden of *H. pylori* infection by an appropriate intervention. Our study demonstrated that the lack of cholesteryl glucosides (CGs) remarkably altered the morphology of *H. pylori* and increased permeability of the bacterial cell wall. Further, this study highlighted the substantial role of CGs in maintaining the typical *H. pylori* morphology that is essential for maintaining its pathogenic potential. We also demonstrated that the loss of CGs in *H. pylori* renders the bacterium susceptible to different antibiotics.

Received 1 October 2018 Accepted 22 October 2018 Published XXX

Citation Qaria MA, Kumar N, Hussain A, Qumar S, Doddam SN, Sepe LP, Ahmed N. 2018. Roles of cholesteryl- α -glucoside transferase and cholesteryl glucosides in maintenance of *Helicobacter pylori* morphology, cell wall integrity, and resistance to antibiotics. mBio 9:e01523-18. <https://doi.org/10.1128/mBio.01523-18>.

Editor Indranil Biswas, KUMC

Copyright © 2019 Qaria et al. This is an open-access article distributed under the terms of the [Creative Commons Attribution 4.0 International license](https://creativecommons.org/licenses/by/4.0/).

Address correspondence to Niyaz Ahmed, niyaz.ahmed@icddr.org.

* Present address: Naveen Kumar, Department of Molecular Biology, Max-Planck Institute for Infection Biology, Berlin, Germany.

This article is a direct contribution from a Fellow of the American Academy of Microbiology. Solicited external reviewers: Yoshio Yamaoka, Oita University Faculty of Medicine; Mun Fai Loke, University of Malaya; Motiur Rahman, Oxford University Clinical Research Unit; Mrutyunjay Suar, KIIT Deemed to be University.

Solicited external reviewers: Yoshio Yamaoka, Oita University Faculty of Medicine; Mun Fai Loke, University of Malaya.

KEYWORDS *H. pylori*, cholesteryl glucosides, morphology, membrane permeability, antibiotic susceptibility, biofilm formation, *Helicobacter pylori*, antibiotic resistance, cell wall integrity

Helicobacter pylori is a highly prevalent human pathogen that colonizes more than 50% of the world's population. The infection generally results in acute or chronic gastritis and progresses to more severe outcomes such as peptic ulcer disease, mucosa-associated lymphoid tissue (MALT) lymphoma, and gastric adenocarcinoma (1). Due to the global distribution of *H. pylori*, it is generally held that smart bacterial strategies might contribute to the adaptation of this bacterium to its preferred host (2).

H. pylori has through the course of its evolution and adaptation resorted to a number of strategies to establish persistent infections within gastric and duodenal niches and to evade the host immune system (3). Apart from molecular strategies, some of the structural features, such as the helical shape of the bacilli, which has been suggested to provide a mechanical convenience for penetrating the viscous mucous layer of the stomach, aid in its pathological prowess (4). Another strategy employed by *H. pylori* for immune evasion is glucosylation of exogenous cholesterol in order to evade the host immune system (5).

Although *H. pylori* cannot synthesize sterols, the bacteria have the ability to utilize exogenous cholesterol from the living vicinity. It is known that pathogens, such as *Mycobacterium tuberculosis*, can utilize cholesterol as an energy source (6), while other organisms, such as *Borrelia burgdorferi* and *Mycoplasma* sp. have the ability to incorporate exogenous cholesterol from their environment and convert it into glycolipids to incorporate into their cell walls (7, 8). Similarly, *H. pylori* absorbs cholesterol from host epithelial cells, as it assimilates the secreted lipid and then carries out glucosylation of the exogenous cholesterol to produce three components of cholesteryl glucosides (CGs), cholesteryl- α -D-glucopyranoside, cholesteryl-6-O-tetradecanoyl- α -D-glucopyranoside, and cholesteryl-6-O-phosphatidyl- α -D-glucopyranoside, which is a characteristic feature of *H. pylori* (9). The glucosylation of cholesterol into CGs in *H. pylori* is mediated by the enzyme cholesterol- α -glucosyltransferase (CGT) which is encoded by the gene *hp0421* (Gene ID 900074), and deletion of this gene results in the loss of all three CGs (10). CGT is primarily synthesized in cytoplasm in an inactive form and becomes activated when it is bound to the cell membrane (11). Previously, it has been reported that CG content varies in *H. pylori* when it undergoes morphological changes from the spiral to coccoid form (12).

Morphological alterations in *H. pylori* were reported upon deletion of cell shape determinants (*csd*) such as peptidoglycan endopeptidase genes, *csd1* and *csd3*. Mutation of these two genes results in rod-shaped and "c"-shaped cells (13). Interestingly, Hildebrandt and McGee observed that the *Hp26695* strain grown in the absence of cholesterol develops an aberrant LPS (14). There are several genes reported to be involved in synthesis of LPS in *H. pylori*, such as *wecA* and *wzk*, which particularly play essential roles in the synthesis of LPS O antigens (15). Furthermore, *H. pylori* grown in the absence of cholesterol showed susceptibility to certain antibiotics, bile salts, and ceragenins (16, 17).

In this study, we investigated the underlying changes in cell morphology, cell integrity, and antimicrobial susceptibility upon deletion of *hp0421* in *H. pylori*. Our data provide evidence for the loss of typical *H. pylori* morphology, increase in cell wall permeability, increased sensitivity to antibiotics, and an altered O-antigen expression profile upon deletion of *hp0421*. These findings suggest that loss of cholesteryl glucosides in *H. pylori* impairs the normal morphology, physiology, and virulence of *H. pylori*.

RESULTS

Loss of cholesteryl- α -glucosides distorts *H. pylori* morphology. We consistently observed morphological changes of *H. pylori* upon deletion of *hp0421* or by cholesterol depletion in growth media.

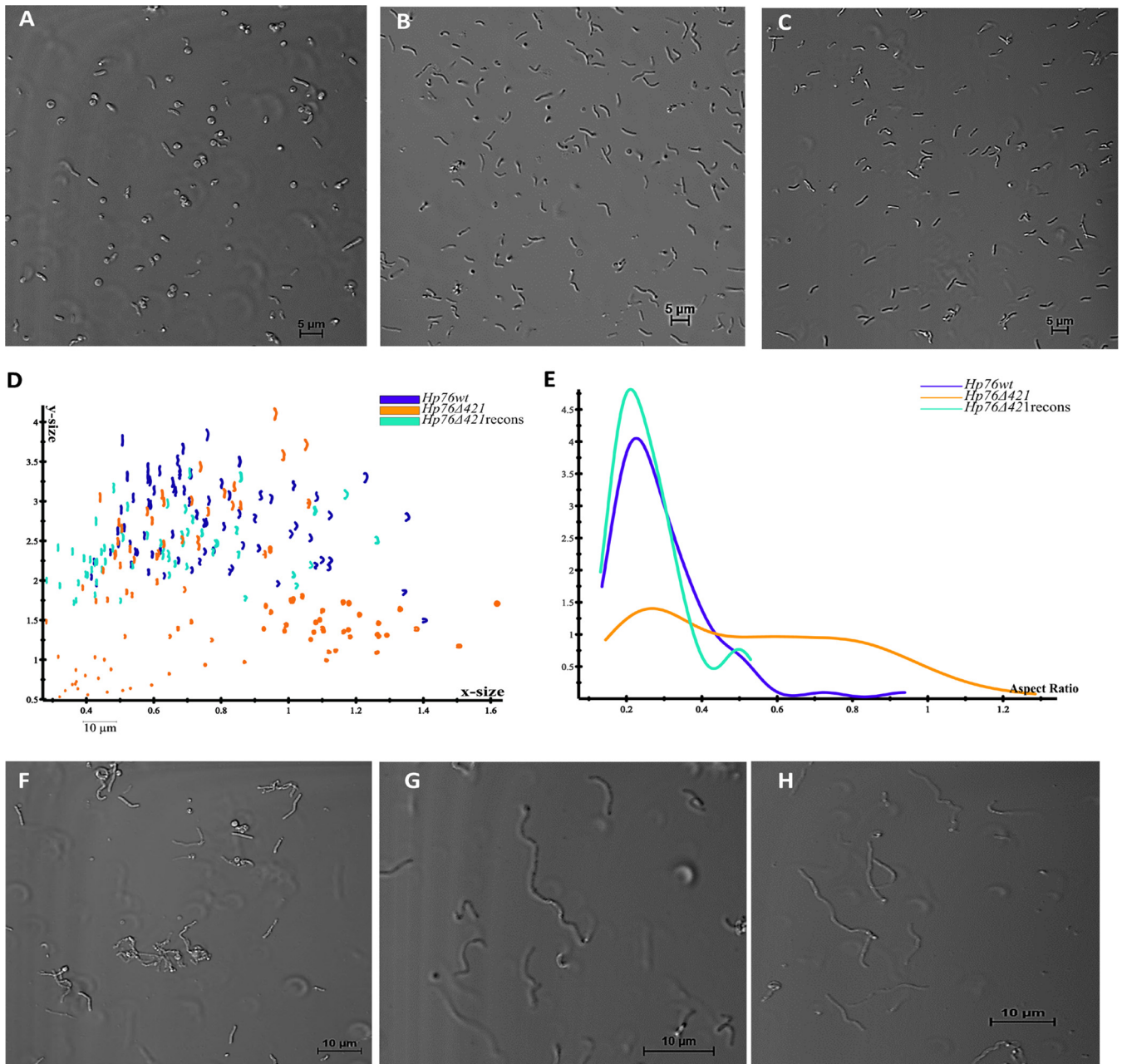


FIG 1 Deletion of the *hp0421* gene perturbs *H. pylori* cell morphology. (A to C) Confocal microscopy profiles depicting morphological patterns of the *Hp76Δ421* (A), *Hp76* (B), and *Hp76Δ421*-reconstituted (C) strains. (D) Scatter plots arraying *Hp76*, *Hp76Δ421*, and *Hp76Δ421*-reconstituted cells based on x-size and y-size analyses performed using CellTool software. (E) CellTool analysis output based on plots representing the distribution of *Hp76*, *Hp76Δ421*, and *Hp76Δ421*-reconstituted cell populations according to the aspect ratio. (F to H) Confocal microscopy images for *Hp76Δ421* (F), *Hp76* (G), and *Hp76Δ421*-reconstituted (H) cells when the cells were treated with the filamenting drug aztreonam.

To investigate the effect of CGs on *H. pylori* morphology, the wild-type (*Hp76*) and knockout (*Hp76Δ421*) strain morphologies were visualized with a confocal microscope by employing transmitted light. The *Hp76Δ421* strain indeed exhibited morphological deformities wherein most cells displayed the coiled “c”-shaped form along with coccoid and rod-shaped bacteria (Fig. 1A), whereas the *Hp76* strain exhibited the normal helical shape (Fig. 1B). Consequently, the reconstitution of the *Hp76Δ421* strain resulted in the recovery of the cell morphology (Fig. 1C). The *Hp26695* strain with or without cholesterol supplementation revealed remarkable variation in the morphology of *H. pylori* cells (see Fig. S1A in the supplemental material). The altered shapes that were observed

included “c” shapes, rods, and coccoid forms in contrast to the normal helical shape observed in bacteria grown in the presence of cholesterol (Fig. S1B).

Furthermore, we performed quantitative morphological analysis of confocal microscopy images of wild-type (*Hp76*), knockout (*Hp76Δ421*) and *Hp76Δ421*-reconstituted strains using the CellTool software package. It was revealed that the distribution of cell populations of the *Hp76Δ421* strain was bimodal as a result of variable cell shapes, whereas the *Hp76* population distribution was narrower, due to the consistency of cell shapes (Fig. 1D). Moreover, the aspect ratio of cell populations presented significantly uneven distribution due to inconsistencies in the shape of *Hp76Δ421* cells compared to the wild-type cells which demonstrated normal distribution for the aspect ratio (Fig. 1E). Moreover, the reconstitution of *Hp76Δ421* resulted in a wild-type-like cell population distribution. To ensure that the morphological alteration was not dependent on the *H. pylori* strain used, a similar analysis was performed on *Hp26695* strains. The results of morphology analysis of *Hp2669* and *Hp26695Δ421* strains were in concordance with the results obtained for *Hp76* strains (Fig. S1C and D).

In order to manifest the morphological changes of *H. pylori*, *Hp76* *Hp76Δ421*, and *Hp76Δ421* reconstituted strains were grown in the presence of aztreonam, an antibiotic that induces pronounced filamentation in *H. pylori* by inhibiting septal peptidoglycan synthesis. Under these conditions, the *Hp76Δ421* strain exhibited morphological changes such as loss of curvature and stunted filamentation (Fig. 1F) compared to wild-type cells, which exhibited typical curvature and elongated filaments (Fig. 1G). The *Hp76Δ421* reconstituted strain restored the wild-type-like morphologies (Fig. 1H). Moreover, to confirm that the deletion of *hp0421* did not interfere with *csd1* and *csd3* expression, we analyzed their mRNA expression and found that there was no effect on the gene expression levels of *csd1* and *csd3* (Fig. S1E and F). Overall, lack of CGs remarkably impaired the morphology of *H. pylori*.

The morphological changes following CG's absence are attributed to a “c”-shaped bacterial population. Flow cytometry analysis appears to be an efficient and rapid technique to detect the cell shape of *H. pylori* at the population level (18). As *H. pylori* is dependent on exogenous cholesterol for synthesis of CGs, the *Hp26695* strain was grown under microaerophilic conditions with and without cholesterol to analyze the morphological changes by flow cytometry.

We observed that the *Hp26695* strain grown in the absence of cholesterol exhibited much higher forward scatter (FSC) due to the increased bulk width of the bacterial cell, which represents “c”-shaped cells compared to the cells grown in cholesterol-containing medium. Moreover, *Hp26695* cells grown in the absence of cholesterol have displayed slightly higher side scatter (SSC) value, which indicates that cells presented higher granularity or complexity (Fig. 2A). Notably, the *Hp26695* strain grown for 72 h in the absence of cholesterol also displayed remarkably higher FSC and SSC values compared to the strain grown only for 48 h (Fig. 2B). In line with the above results, the *Hp26695Δ421* strain also displayed higher FSC and SSC values in both 48-h and 72-h culture populations compared to the wild-type strain (Fig. 2C and D). Furthermore, the population shape outcomes of *Hp76* and *Hp76Δ421* strains as analyzed by flow cytometry were in accordance with the observation recorded for *Hp26695* and *Hp26695Δ421* strains, and interestingly, the cell wall integrity was restored in *Hp76Δ421* reconstituted strain (Fig. S2A and B).

Taken together, these observations indicate that the changes in morphology of the *Hp26695Δ421* and *Hp76Δ421* strains or of wild-type strains grown in the absence of cholesterol are due to the presence of “c”-shaped cell population, which is also evidenced by the higher FSC values.

Deletion of *hp0421* results in cell wall fluidity. *H. pylori* CGs comprise more than 25% of total cell wall lipids (19). Hence, to study whether the depletion of CGs has any effect on *H. pylori* cell wall permeability, we measured the influx of ethidium bromide (EtBr) among wild-type and knockout strains by flow cytometry. Bacterial strains were incubated with EtBr, and the median fluorescence intensity (MFI) was measured. We

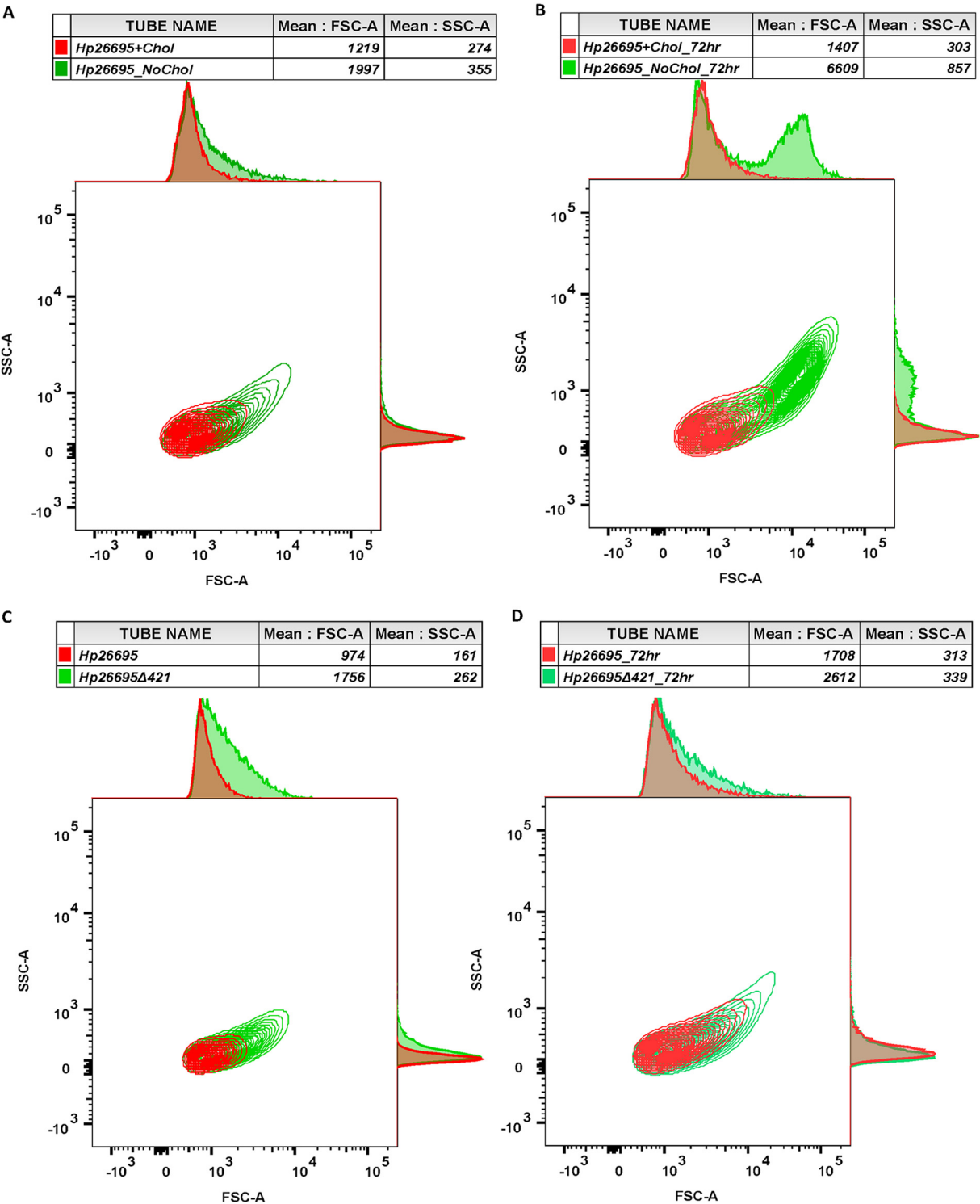


FIG 2 Flow cytometry analysis of *H. pylori* cell populations based on their shape. Representative contour plots of *H. pylori* populations depicted based on flow cytometry analyses. Forward scatter (FSC) plotted on the x axis and side scatter (SSC) on the y axis are presented with mean and median. (A and B) The *Hp26695* strain was grown in the presence and absence of cholesterol for 48 h (A) and 72 h (B). (C and D) The *Hp26695* and *Hp26695*Δ421 strains were grown (not supplemented) for 48 h (C) and 72 h (D).

observed that the *Hp26695* strain grown in the absence of cholesterol showed higher MFI than the strain grown in the presence of cholesterol (Fig. 3A), indicating a higher influx of EtBr in bacterial cultures grown in the absence of cholesterol. We also

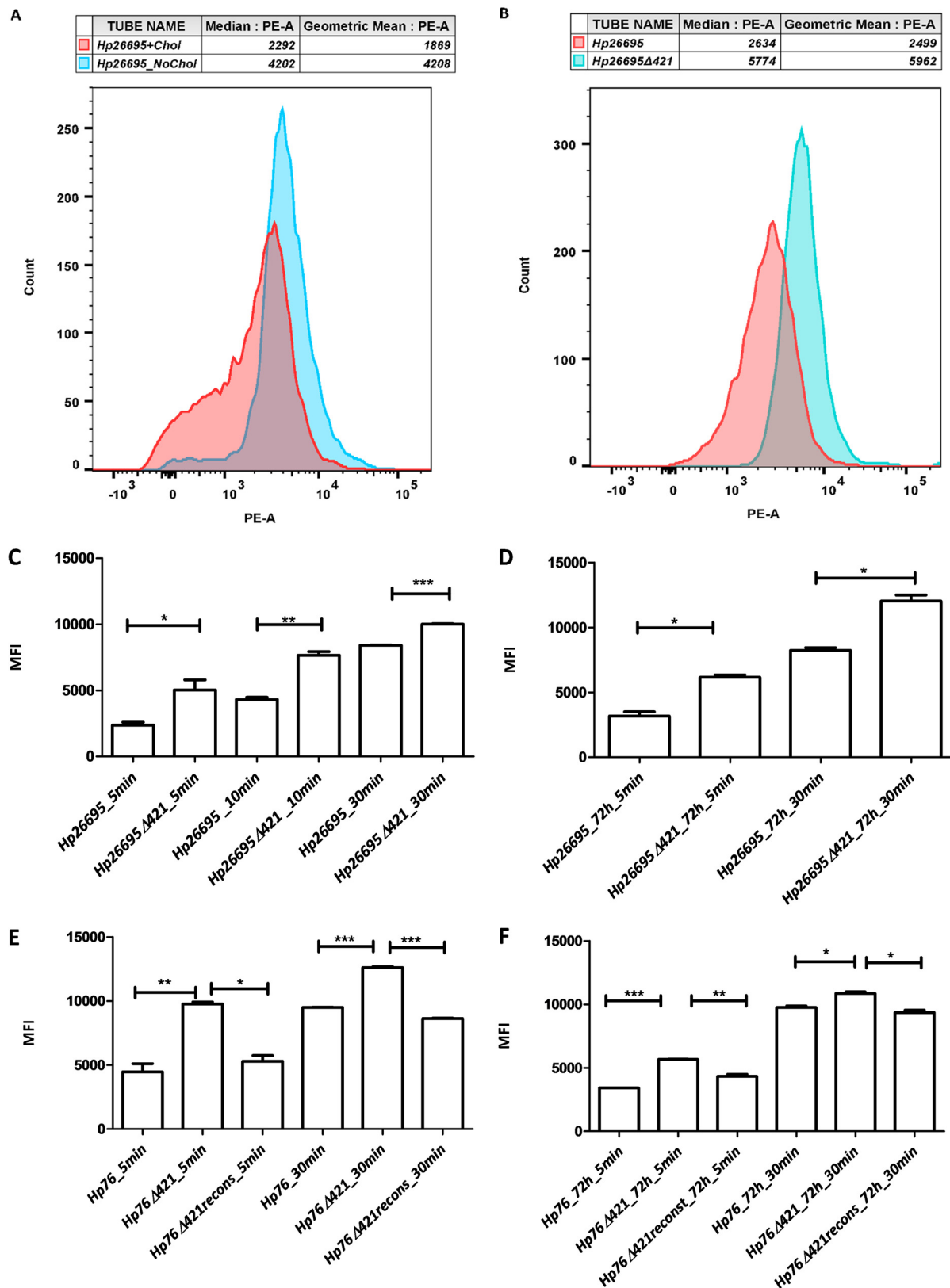


FIG 3 Absence of cholesteryl glucosides increased *H. pylori* cell wall permeability. (A and B) Flow cytometry analysis based on influx rates of EtBr as depicted in the form of PE-A histograms delineating the median fluorescence intensity (MFI) for *Hp26695* strain grown in the presence and absence of cholesterol (A). (B) Influx rates of EtBr for *Hp26695* and *Hp26695*Δ421 strains grown for 48 h. (C to F) The bars represent MFIs for 5, 10, and 30 min using cultures grown either at 48 h or 72 h (*, $P < 0.05$; **, $P \leq 0.01$; ***, $P \leq 0.001$).

measured EtBr fluorescence intensity between the *Hp26695* and *Hp26695Δ421* strains; the MFI was significantly higher in the *Hp26695Δ421* strain than in the wild type (Fig. 3B). To determine the kinetics of EtBr influx in *Hp26695* and *Hp26695Δ421* strains, we measured the MFI of EtBr influx at 5-, 10-, and 30-min time intervals. The MFI of the *Hp26695Δ421* strain was significantly higher through all the time intervals compared to the MFI observed for the *Hp26695* strain (*P* value of <0.05) (Fig. 3C).

In order to check the cell wall fluidity of lag-phase cultures, the *Hp26695Δ421* and *Hp26695* strains were cultured for 72 h and were observed for EtBr influx. As expected, the MFI was found to be significantly higher in the *Hp26695Δ421* strain than in the *Hp26695* strain (*P* value of <0.05) (Fig. 3D and Fig. S3A). Furthermore, we observed that the *Hp76Δ421* strain exhibited higher MFI than the *Hp76* strain and the *Hp76Δ421*-reconstituted strain (Fig. 3E and Fig. S3B). We also measured the MFI for *Hp76* strains in 72-h cultures and found that the influx rate was significantly higher in the *Hp76Δ421* strain than in the *Hp76* and *Hp76Δ421*-reconstituted strains (*P* value of <0.05) (Fig. 3F and Fig. S3C and D). Overall, from these observations, we anticipate that the lack of CGs would likely perturb the cell wall permeability of *H. pylori* by damaging the cell wall integrity.

Lack of CGs disrupts LPS structure. In order to detect the changes in O-antigen expression due to disruption of CGs, we isolated lipopolysaccharides from *Hp76*, *Hp76Δ421*, and *Hp76Δ421*-reconstituted strains and visualized them by silver-stained SDS-polyacrylamide gel electrophoresis. Depletion of CGs resulted in the disruption of O antigens as observed by silver staining of *Hp76Δ421* LPS in which the O antigens were absent compared to the *Hp76* LPS profile. Consequently, the O antigens and core LPS were partially restored in the *Hp76Δ421*-reconstituted strain (Fig. 4A). Moreover, we investigated whether the deletion of *hp0421* in *Hp26695* and *Hp76* strains had any effect on the transcription of *wecA* and *wzk* genes. We found no significant differences in the gene expression levels for these two genes in both wild-type and *Hp26695Δ421* and *Hp76Δ421* strains (Fig. 4C and D). This observation rules out the possibility that the alteration in LPS profile was due to changes in the expression of these O-antigen synthesis genes. Thus, the lack of CGs most likely disrupted the normal components of *H. pylori* LPS.

Cholesteryl glucoside perturbation in *H. pylori* renders bacteria sensitive to antibiotics. To investigate the effect of loss of CGs in *H. pylori* on antibiotic resistance, we determined the MICs of several antibiotics on *Hp26695* and *Hp76* strains. For this, the strains were grown on brucella agar plates in the presence of MIC E-strips belonging to different antibiotics. *Hp26695* and *Hp76* strains were found to be resistant to fosfomycin, polymyxin B, colistin, tetracycline, and ciprofloxacin. Moreover, the *Hp26695Δ421* strain was more sensitive to amoxicillin than the *Hp26695* strain, while both strains were sensitive to clarithromycin. Interestingly, the *Hp26695Δ421* and *Hp76Δ421* strains, on the other hand, were found to be sensitive to all of the above antibiotics tested (Table 1). The increased sensitivity of *Hp26695Δ421* and *Hp76Δ421* strains was understandable, as these strains demonstrated an increase in cell wall permeability due to the loss of CGs. Overall, it appears that the deletion of *hp0421* perturbs the cell wall integrity of *H. pylori*, which in turn leads to increased susceptibility to all the antibiotics tested.

Deletion of *hp421* enhances *H. pylori* cell aggregation. *H. pylori* bacteria produce biofilms on stomach mucosa in order to circumvent the gut's harsh environment, and it was reported that deletion of the *luxS* gene increases the biofilm formation (20). We observed that *Hp26695Δ421* and *Hp76Δ421* strains tended to aggregate in the liquid cultures in contrast to the wild-type cultures that appeared turbid in their growth. Therefore, we investigated the effect of *hp0421* deletion on biofilm formation in the *Hp26695* and *Hp76* strains. Biofilm formation was visualized on glass coverslips with a microscope. The *Hp26695Δ421* and *Hp76Δ421* strains demonstrated biofilm formation on the third day, while the wild-type strain formed biofilm on the fifth day. Moreover, crystal violet absorbance assay revealed that the biofilms formed by *Hp26695Δ421* and

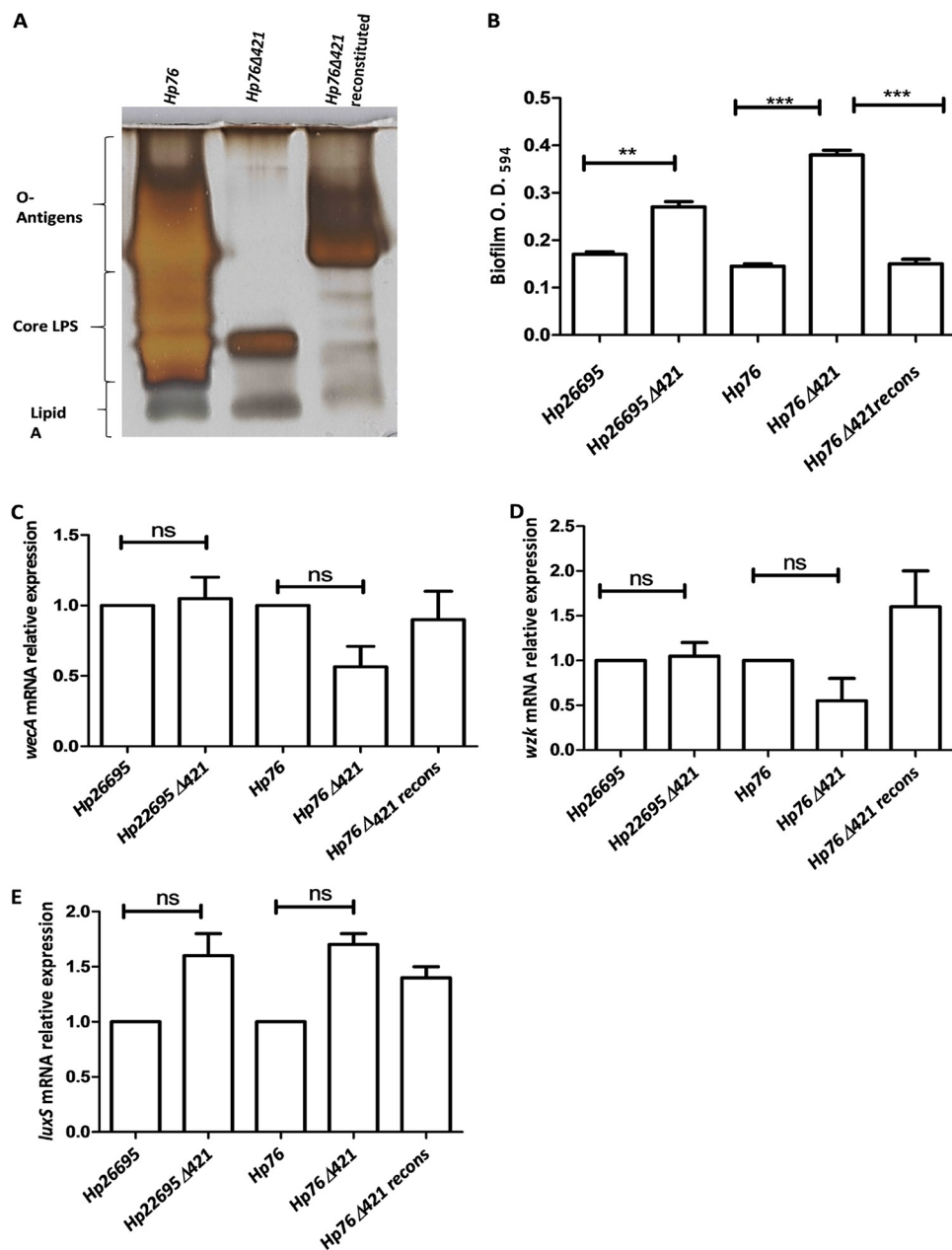


FIG 4 Analysis of LPS expression and biofilm formation. (A) Silver-stained SDS-PAGE gel (15%) depicting profiles of LPS from *Hp76*, *Hp76Δ421*, and *Hp76Δ421*-reconstituted strains. (B) Bar graph representing quantification of biofilm formation by *H. pylori* after 5 days of incubation. The *Hp26695* strain data were analyzed by Student's *t* test. The *Hp76* strain data were analyzed by one-way ANOVA followed by Turkey's multiple-comparison tests. (C and D) qRT-PCR analyses of *wecA* and *wzk* genes using RNA isolated from wild-type (*Hp26695* and *Hp76*), knockout (*Hp26695Δ421* and *Hp76Δ421*), and *Hp76Δ421*-reconstituted strains grown for 48 h. (E) Relative mRNA expression of *luxS* from 2-day-old broth cultures [ns, nonsignificant difference(s); *, $P < 0.05$; **, $P \leq 0.01$; ***, $P \leq 0.001$].

Hp76Δ421 strains were significantly denser than the biofilms formed by the *Hp26695*, *Hp76*, and *Hp76Δ421*-reconstituted strains (Fig. 4B). The results showed that the *Hp26695Δ421* and *Hp76Δ421* strains tended to aggregate and adhere strongly to the surface of the coverslip at the air-liquid interface. Hence, perhaps, the lack of CGs enhances aggregation of bacterial cells and promotes biofilm formation in *H. pylori*. Moreover, we determined the expression of the *luxS* gene in the above strains to check whether its expression is affected by the deletion of *hp0421*. We found no significant differences in the gene expression levels for *luxS* in both wild-type and *Hp26695Δ421* and *Hp76Δ421* strains (Fig. 4E).

TABLE 1 MICs of wild-type, $\Delta 421$ mutants, and $\Delta 421$ -reconstituted *H. pylori* strains

Antibiotic	MIC ($\mu\text{g/ml}$) of the following strain ^a :				
	<i>Hp26695</i>	<i>Hp26695</i> $\Delta 421$	<i>Hp76</i>	<i>Hp76</i> $\Delta 421$	<i>Hp76</i> $\Delta 421$ -reconstituted
Fosfomycin	$\geq 1,024$ (R)	$\leq 1.5 \pm 0.5$ (S)	$\geq 1,024$ (R)	$\leq 0.064 \pm 2$ (S)	$\geq 1,024$ (R)
Colistin	≥ 256 (R)	$\leq 12 \pm 3$ (S)	≥ 256 (R)	$\leq 10 \pm 5$ (S)	≥ 256 (R)
Polymyxin B	≥ 256 (R)	$\leq 8 \pm 4$ (S)	≥ 256 (R)	$\leq 10 \pm 4$ (S)	≥ 256 (R)
Ciprofloxacin	$\leq 0.38 \pm 0.5$ (R)	$\leq 0.064 \pm 0.02$ (S)	$\leq 0.50 \pm 0.5$ (R)	$\leq 0.19 \pm 0.2$ (S)	$\leq 0.047 \pm 0.08$ (R)
Tetracycline	$\leq 10 \pm 3$ (R)	$\leq 0.01 \pm 0.02$ (S)	$\leq 0.50 \pm 0.1$ (R)	$\leq 0.01 \pm 0.09$ (S)	$\leq 0.38 \pm 0.18$ (R)
Amoxicillin	$\leq 0.47 \pm 0.01$ (R)	$\leq 0.016 \pm 0.01$ (S)	$\leq 0.016 \pm 0.01$ (S)	$\leq 0.016 \pm 0.01$ (S)	$\leq 0.016 \pm 0.01$ (S)
Clarithromycin	≤ 0.001 (S)	≤ 0.001 (S)	≤ 0.001 (S)	≤ 0.001 (S)	≤ 0.001 (S)

^aThe letters in parentheses after the MIC indicate whether the strain is resistant (R) or sensitive (S) to the indicated antibiotic.

DISCUSSION

In the present study, we analyzed the possible role of CGs in *H. pylori* in the maintenance of normal spiral shaped bacillary morphology and cell wall integrity and investigated their role in sensitivity and resistance to antibiotics. We also studied the effect of loss of CGs on lipopolysaccharide profiles and on biofilm formation using *Hp26695* $\Delta 421$ and *Hp76* $\Delta 421$ (knockout) strains and their respective wild types. We observed the presence of CGs to be essential for maintaining the normal, spiral morphology of *H. pylori*, while the lack of CGs remarkably distorted the shape of *H. pylori* cells to variable structures, with coiled and "c"-shaped cells being dominant. A previous study also observed similar morphological alterations upon deletion of peptidoglycan endopeptidase genes *csd1* and *csd3* in *H. pylori* (13). However, we found that there was no effect on the gene expression levels of *csd1* and *csd3* upon deletion of the *hp0421* gene. Moreover, CGs are the major constituents of the *H. pylori* cell wall and comprise more than 25% of the total cell wall lipids (19). Given this, our results are strongly suggestive of CG depletion leading to alteration of lipid raft components of the *H. pylori* cell wall which could have disrupted its integrity. Since lipid rafts are required in maintaining the architecture of the cell wall and order of cell wall domains, absence of the CGs may be linked to change in the normal helical shape of *H. pylori*. In fact, a study on *Borrelia burgdorferi* wherein cell wall cholesterol depletion by methyl- β -cyclodextrins (M β CD) without substitution by other sterols resulted into coiled spirochetes (21). Our results are in line with this observation which supports that the lack of sterols alters the morphology of *H. pylori*. Moreover, the results of analysis of *H. pylori* morphology suggest that the lack of CGs remarkably altered the size and curvature of the cells; these results strongly point to the possibility that CGs are part of lipid rafts in the cell wall and that they play a crucial role in maintaining the typical helical shape and size of *H. pylori* cells. It should be noted that the helical shape of *H. pylori* is a major factor in the process of invasion of gastric niches. This is of particular significance given the reports that the colonization rates for the stomachs of mice by the helical rod-shaped *H. pylori* were higher than those of the *csd1* and *csd3* mutants that were curved and rod shaped (13). Similarly, Wunder et al. reported that *hp0421* mutant(s) failed to colonize C57BL/6 mice and were cleared from the gastric tissue (5). These results demonstrate that the changes in *H. pylori* morphology due to the absence of CGs negatively influence the colonization potential of *H. pylori*. We speculate that this could be a result of direct or indirect interaction between the CGs and the peptidoglycans that altered the order of cell wall domains.

The deletion of the *hp0421* gene results in depletion of CGs in the cell wall, which could lead to enhanced permeability. Likewise, when *H. pylori* was grown in the absence of cholesterol, bacterial cell permeability was significantly increased. Thus, this indicates the critical role of CGs in the formation of ordered cell wall units of *H. pylori* to maintain its integrity. In an alternative scenario, the CGs are probably required to maintain the tight pack of the outer wall/capsule of *H. pylori*. Sterols in the membrane are believed to support the cell membrane in *B. burgdorferi*, and the depletion of membrane cholesterol and substitution with different sterol analogues increased the

permeability of the membrane at different levels based on the type of sterols and the depletion of cholesterol by methyl- β -cyclodextrins (M β CD); lack of substitution with any sterols caused significant increase in the permeability of the membrane (21). Also, in yeast, the deletion of essential genes of sterol biosynthesis was reported to increase the cell membrane permeability (22). Our findings are in line with these and other reports and suggest that CGs interact with peptidoglycan domains in order to maintain the architecture of the *H. pylori* cell wall. The permeabilization of *H. pylori* cell wall has far-reaching implications for therapeutic interventions.

Further, we observed that the *Hp76 Δ 421* strain exhibited aberrant LPS expression profile with loss of O antigens and lack of core LPS. Our observations suggest that the perturbation of the architecture of the *H. pylori* cell wall due to the lack of CGs reduced LPS expression. On the other hand, this might have occurred due to the changes in the structure of the cell wall affecting the O-antigen biosynthesis enzymes that are present in the cell wall. It is relevant in this context that the deletion of *hp0421* did not affect the mRNA expression of essential LPS synthesis genes *wecA* and *wzk*. Alternatively, the changes in the structure and composition of the cell wall due to the lack of CGs may result in the dysregulation of the transfer of LPS units through membranes. Our observations appear to be in agreement with the report of Hildebrandt et al., who observed that depletion of cholesterol leads to the development of aberrant LPS in the *Hp26695* strain, which depends on lipid A phosphorylation (14).

Furthermore, we observed that lack of CGs reverted the resistance of *H. pylori* to antibiotics. The increased susceptibility to the antibiotics due to the deletion of *hp0421* may be the result of permeabilization of the cell wall, facilitating antibiotics to penetrate passively through *H. pylori* cells. The bacterial cell wall is the first line of defense against antibiotics, detergents, and host defense elements. The membrane/cell wall permeabilization could be an effective method to control bacterial infections by enhancing antibiotic action/delivery (23). Second, we suggest that disruption of LPS and/or influencing the outer membrane charge due to the lack of CGs decreased the resistance of *H. pylori* to certain antibiotics like polymyxin and colistin. Disruption of *lpx_{EHP}*, a gene encoding lipid A in *H. pylori*, has been shown to dramatically decrease the polymyxin resistance from a MIC of >250 μ g/ml to a MIC of 10 μ g/ml (24). Similarly, we believe that the deletion of *hp0421* might possibly affect the LPS structure thus influencing the outer membrane charge and cell wall integrity and eventually increasing the sensitivity of *H. pylori* to certain antibiotics. Inhibition of CG synthesis may not kill the bacteria directly but rather render the pathogens incapable of establishing successful infection by hindering their colonization potential and fitness advantage (resistance toward antibiotics).

Moreover, we suggest that the tendency of *Hp26695 Δ 421* and *Hp76 Δ 421* strains to aggregate on the surface of coverslips is probably due to changes in the properties of LPS. Modifications in LPS have been shown to enhance bacterial autoaggregation and biofilm formation (25). Alternatively, the changes in the cell wall properties and morphology may trigger stress-related genes, including the quorum-sensing gene *luxS*. Similarly, the changes in the membrane structure of *Pseudomonas aeruginosa* were previously reported to alter quorum sensing (26). However, we did not observe any changes in the mRNA expression levels of *luxS*.

In conclusion, in this study, we have shown the role of CGs in the maintenance of *H. pylori* native helical morphology, and the lack of CGs remarkably resulted in variable shape and size of *H. pylori* cells dominated by “c”-shaped cells. Moreover, the cell wall permeability increased irrespective of the duration of culture and the strain type of *H. pylori*. Further, we showed that lack of CGs perturbed the structure of cell wall components like LPS, which on one hand, would attenuate the virulence of *H. pylori* and, on the other hand, would render *H. pylori* susceptible to antibiotics to which it was otherwise resistant. CGs could be a promising target for drugs aiming at the eradication of *H. pylori* infection. The functional roles of CGs in *H. pylori* that we report here significantly extends the previous understanding on the role of cholesterol glucosylation in *H. pylori* immune evasion and pathogenicity. Future studies are needed to

TABLE 2 Primers used in this study

Target gene of the primer	Nucleotide sequence of the primer
<i>hp0421</i> US F	GTGGATTGACTCTTTAGAGACTTG
<i>hp0421</i> US R	GTGCCATGGCTCGAGTTAACTACTCTTCTTTAAATGAAT
<i>hp0421</i> DS F	GTGCCATGGCTCGAGTAAAGGATAAAAAATGCAAGAA
<i>hp0421</i> DS R	CCAATTTTAGGGCAGGCTAAAAAC
<i>wecA</i> F	ATGGTGCTTGGGTTTATGGTG
<i>wecA</i> R	GGCTTCTGGCGTTTATTTTG
<i>wzk</i> F	AAACTCAAAGACAACCACGAAG
<i>wzk</i> R	CGACCGCTAAATCAACAAG
16s rRNA F	GGTAAAATCCGTAGAGATCAAGAGG
16s rRNA R	ACAACCTAGCATCCATCGTTTAGG
<i>cds1</i> F	GGATGAATTTTAGACGATTGTC
<i>cds1</i> R	CCCTCTTCTTTTCTTCTTCAGG
<i>cds3</i> F	CTAAACATGGCAGCTTGATCC
<i>cds3</i> R	AATGGATTCAACCACCTTCC
<i>luxS</i> F	TTTGATTGTCAAATACGATGTGC
<i>luxS</i> R	TGTGAGATAAAATCCCGTTTGG

determine whether inhibition of *H. pylori*-specific CGs constitutes a target for the development of new therapeutic molecules for *H. pylori*-induced inflammation and malignancies.

MATERIALS AND METHODS

Bacterial strains and cholesterol loading. The human-adapted *Hp26695* strain and its mutant strain, the *Hp26695Δ0421* strain, were grown on GC agar medium (Difco, USA) supplemented with 10% horse serum, 2.5 μg/ml trimethoprim, 10 μg/ml vancomycin, and 1 μg/ml nystatin as described previously (27) (antibiotics were excluded in some experiments of antibiotic resistance determination and aztreonam filamentation assay). An aliquot of 4 μg/ml kanamycin was added as a resistance selection marker for *Hp26695Δ0421*. The mouse-adapted *Hp76* strain, its mutant strain (the *Hp76Δ0421* strain), and the reconstituted *Hp76Δ0421* strain were a gift from Thomas F. Meyer, Max Planck Institute for Infection Biology, Germany. *Hp76* strains were cultured as described previously (5). Further, the procedures to grow *Helicobacter pylori* in the absence of cholesterol were modified from earlier described method(s) (28). Briefly, the wild-type strains were grown on Ham's F-12 medium (Gibco, USA) (chemically defined) supplemented with 1 mg/ml BSA with or without 1 mM water-soluble cholesterol (250 μM cholesterol with 4 mM MβCD) (Sigma). For agar plates, Ham's F-12 medium was prepared (2×) and mixed with 30 g per liter agar at 1:1 ratio. For broth culture, the strains were grown in brucella broth medium with the use of CampyGen compact sachets (Oxoid, UK) inside a shaker-incubator to create a microaerophilic condition. To visualize cell elongation, 2 μg/ml of aztreonam antibiotic was added to the medium. All strains were incubated under humidified microaerophilic conditions with 5% O₂ and 5% CO₂.

Construction of *Hp26695Δ421* and *Hp76Δ421* strains. The cholesterol α-glucosyl transferase *hp0421* (Gene ID 900074) knockout in *Hp26695* was generated by homologous recombination as described previously (10). Briefly, two pairs of primers upstream (PCR1) and downstream (PCR2) of *hp0421* regions were designed with XhoI restriction enzyme sequence (Table 2). Ligated PCR1 and PCR2 were inserted by TA cloning into the pTZ57R/T plasmid, followed by transformation into *Escherichia coli* DH5α. The plasmids were purified by Plasmid Miniprep kit (Qiagen, Germany) and digested with XhoI. The kanamycin resistance cassette was inserted between PCR1 and PCR2 and subsequently cloned into *E. coli* DH5α. The purified plasmids were transformed into the *Hp26695* strain by natural transformation. The transformed bacteria were grown on GC agar kanamycin medium. Additionally, the absence of the pTZ57R/T plasmid was confirmed by sensitivity to ampicillin, and the presence of the knockout construct was confirmed by PCR and construct sequence analysis.

Cell wall fluidity and *H. pylori* cell morphology by flow cytometry. For cholesterol depletion-based selection, the *Hp26695* strain was grown on chemically defined medium. The wild-type *Hp26695*, *Hp26695Δ0421*, wild-type *Hp76*, *Hp76Δ421*, and *Hp76Δ421*-reconstituted strain were all grown for 48 to 72 h on brucella agar (BD Biosciences). The staining and measurement procedures for EtBr influx were modified from a previous study (29). Briefly, bacterial cells were collected and washed thrice with PBS at pH 7.4 (Gibco, USA). A total of 10⁶ cells were resuspended in 1 ml PBS or in 1 ml PBS (containing 5 μg of EtBr filtered through a 0.22-μm Millipore-GV syringe filter [Merck-Millipore, USA]). All tubes were incubated at 37°C with gentle mixing inside a hybridization rotor for 5 to 30 min, followed by flow cytometry analysis on a BD FACS Canto II system (BD Biosciences). To measure the influx rate, *Hp26695* and *Hp76* strains were incubated with 10 μg/ml EtBr for 1 h, followed by centrifugation at 6,000 rpm for 5 min. The pellets were resuspended in 1 ml of PBS or 1 ml of PBS with 0.4% of glucose. EtBr fluorescence intensity was measured by flow cytometry analysis with the excitation wavelength set at 488 nm and the fluorescence emission set at 585 nm. The data were analyzed by using FlowJo LLC software.

***H. pylori* morphology analysis upon deletion of *hp0421*.** *H. pylori* cultures grown for 48 h were washed by PBS (pH 7.0) with 10% glycerol thrice, and the cells were adjusted to an OD₅₅₀ of 0.2. Cells were mounted on glass slides and imaged by confocal microscope (model LSM 880; Carl Zeiss). The

image optimization was carried out in Adobe Photoshop 7. The quantitative analysis of processed images to measure the *x* size, *y* size, and aspect ratio of *H. pylori* cells were done individually by CellTool software package as described previously (30).

Quantitative PCR and gene expression analysis. The method for qRT-PCR analysis was described previously (31). Briefly, RNA was isolated from 10^8 cells of *H. pylori* strains by TRIzol (Invitrogen, USA). Subsequently, 3 μ g of RNA was converted to cDNA using SuperScript-III (Invitrogen, USA) and random hexamers according to the manufacturer's instructions. For qRT-PCR, 40 ng of the first transcribed DNA strand was amplified by using SYBR Fast qPCR Mix (TaKaRa, Japan) with primers targeting *cds3*, *cds1*, *wzx*, and *wecA* genes and 16S rRNA as an internal control. For *luxS*, *H. pylori* strains were grown in brucella broth for 2 days, and RNA was isolated from planktonic and sessile bacterial cells. The primer sequences are listed in Table 2.

Determination of antibiotic resistance among wild-type *H. pylori* and *hp0421* mutant. *Hp26695* and *Hp76* strains grown on brain heart infusion agar medium were collected and washed with PBS. About 50 μ l of 10^8 *H. pylori* cell suspension was spread on brain heart infusion agar medium and antibiotic-impregnated strips (HiMedia, India) corresponding to clarithromycin (0.016 to 256 μ g/ml), amoxicillin (0.016 to 256 μ g/ml), fosfomycin (0.064 to 1024 μ g/ml), polymyxin B (0.016 to 256 μ g/ml), colistin (0.016 to 256 μ g/ml), tetracycline (0.016 to 256 μ g/ml), and ciprofloxacin (0.002 to 31 μ g/ml) were placed on the plates and incubated for 3 days. The susceptibility was defined by breakpoints defined by the Clinical and Laboratory Standards Institute (CLSI) (32).

Biofilm formation by *H. pylori* *hp0421* mutant strains. Biofilm formation was assayed using a modified protocol as described previously (33, 34). Briefly, *Hp26695* and *Hp76* cells were collected from BHI agar and washed with PBS. Inocula at an OD₅₅₀ of 0.2 were seeded in 12-well plates, each well contained 2 ml of brucella broth with 7% decomplexed horse serum (Gibco, USA), and sterilized glass coverslips were used to cover the wells to allow adherence of *H. pylori* at the air-liquid interface. The cultures were incubated under microaerophilic conditions at 37°C for 2 to 6 days. After incubation, the coverslips were washed with PBS, followed by 0.1% crystal violet staining. The coverslips were further rinsed with PBS and dried. The associated dye was dissolved in acetone and ethanol (2:8), and the absorbance was measured by microplate reader at 594 nm.

Lipopolysaccharide purification and visualization. Purification of lipopolysaccharides from *H. pylori* strains was carried out according to the previously described method of Hong et al. with slight modifications (35). Briefly, the bacterial lawns were collected and washed with 1 ml PBS (pH 7.4), followed by centrifugation thrice at 10,000 rpm for 10 min each time. The pellets were resuspended in lysis buffer (60 mM Tris-HCl [pH 6.8], 2% SDS) and incubated at 98°C for 10 min, and the whole-lysate protein was quantified by BCA bicinchoninic acid assay (Thermo Fisher Scientific, USA). LPS was extracted by adding 45% hot phenol to the lysate, vortexed vigorously, and incubated at 70°C for 30 min. The mixtures were centrifuged at $16,000 \times g$ for 15 min, and the upper phase layer was collected in 2-ml tubes and LPS was precipitated by adding 75% cold ethanol and 10 mM sodium acetate. The tubes were then incubated at -20°C overnight, followed by centrifugation at $16,000 \times g$ for 15 min. To remove DNA and RNA contaminants, 3 μ l of buffer 2 (NEB, UK), 0.5 mg/ml DNase I (amplification grade) (Sigma, USA), and 0.5 mg/ml RNase A (Invitrogen, USA) were added, followed by incubation for 1 h at 37°C and treatment with 0.5 mg/ml proteinase K (Amresco, USA) for 1 h at 56°C. The LPS was reextracted by adding 50% phenol, followed by vigorous vortexing and centrifugation. The pellet was finally precipitated by cold ethanol, resuspended in 50 μ l of deionized water, and stored at -80°C. For visualization of LPS, 10 μ l from each tube was loaded on a 15% SDS gel and stained with dual silver stain (36). The LPS units were quantified by *Limulus* amoebocyte lysate (LAL) chromogenic endotoxin quantitation kit (Pierce, USA) according to the manufacturer's instructions.

Statistical analysis. The statistical analyses were performed using Student's *t* test and one-way ANOVA followed by Turkey's multiple-comparison tests. The data are the means and standard errors of the means from three independent experiments.

SUPPLEMENTAL MATERIAL

Supplemental material for this article may be found at <https://doi.org/10.1128/mBio.01523-18>.

FIG S1, TIF file, 2.1 MB.

FIG S2, TIF file, 0.5 MB.

FIG S3, TIF file, 1.1 MB.

ACKNOWLEDGMENTS

We thank all the members of the Pathogen Biology Lab for their constructive comments on the manuscript and suggestions, especially Savita Devi for helpful discussions and guidance she provided to M.A.Q.

The work of the International Centre for Diarrheal Disease Research, Bangladesh (icddr,b) is funded by core donors Sweden (SIDA), Canada (CIDA and GAC), United Kingdom (DIFID), and the Government of Bangladesh.

M.A.Q. designed and performed all experiments with assistance from N.K., A.H., S.Q., and L.P.S. and is the custodian of all data and serves as guarantor on this article. S.N.D.

participated in discussions, interpreted some of the results, and edited the draft manuscript. N.A. provided laboratory facilities and resources, interpreted and discussed results, edited the draft and final versions of the manuscript, and handled the peer review. All authors contributed to the development of the manuscript and its display items.

REFERENCES

- Kusters JG, van Vliet AH, Kuipers EJ. 2006. Pathogenesis of *Helicobacter pylori* infection. *Clin Microbiol Rev* 19:449–490. <https://doi.org/10.1128/CMR.00054-05>.
- Abadi ATB. 2017. Strategies used by *Helicobacter pylori* to establish persistent infection. *World J Gastroenterol* 23:2870. <https://doi.org/10.3748/wjg.v23.i16.2870>.
- Devi S, Rajakumara E, Ahmed N. 2015. Induction of Mincle by *Helicobacter pylori* and consequent anti-inflammatory signaling denote a bacterial survival strategy. *Sci Rep* 5:15049. <https://doi.org/10.1038/srep15049>.
- Sycuro LK, Wyckoff TJ, Biboy J, Born P, Pincus Z, Vollmer W, Salama NR. 2012. Multiple peptidoglycan modification networks modulate *Helicobacter pylori*'s cell shape, motility, and colonization potential. *PLoS Pathog* 8:e1002603. <https://doi.org/10.1371/journal.ppat.1002603>.
- Wunder C, Churin Y, Winau F, Warnecke D, Vieth M, Lindner B, Zahring U, Mollenkopf HJ, Heinz E, Meyer TF. 2006. Cholesterol glucosylation promotes immune evasion by *Helicobacter pylori*. *Nat Med* 12: 1030–1038. <https://doi.org/10.1038/nm1480>.
- Pandey AK, Sasseti CM. 2008. Mycobacterial persistence requires the utilization of host cholesterol. *Proc Natl Acad Sci U S A* 105:4376–4380. <https://doi.org/10.1073/pnas.0711159105>.
- Crowley JT, Toledo AM, LaRocca TJ, Coleman JL, London E, Benach JL. 2013. Lipid exchange between *Borrelia burgdorferi* and host cells. *PLoS Pathog* 9:e1003109. <https://doi.org/10.1371/journal.ppat.1003109>.
- Slutzky GM, Razin S, Kahane I, Eisenberg S. 1977. Cholesterol transfer from serum lipoproteins to mycoplasma membranes. *Biochemistry* 16: 5158–5163. <https://doi.org/10.1021/bi00642a032>.
- Hirai Y, Haque M, Yoshida T, Yokota K, Yasuda T, Oguma K. 1995. Unique cholesteryl glucosides in *Helicobacter pylori*: composition and structural analysis. *J Bacteriol* 177:5327–5333. <https://doi.org/10.1128/jb.177.18.5327-5333.1995>.
- Lebrun AH, Wunder C, Hildebrand J, Churin Y, Zahring U, Lindner B, Meyer TF, Heinz E, Warnecke D. 2006. Cloning of a cholesterol- α -glucosyltransferase from *Helicobacter pylori*. *J Biol Chem* 281: 27765–27772. <https://doi.org/10.1074/jbc.M603345200>.
- Hoshino H, Tsuchida A, Kametani K, Mori M, Nishizawa T, Suzuki T, Nakamura H, Lee H, Ito Y, Kobayashi M, Masumoto J, Fujita M, Fukuda M, Nakayama J. 2011. Membrane-associated activation of cholesterol α -glucosyltransferase, an enzyme responsible for biosynthesis of cholesteryl- α -D-glucopyranoside in *Helicobacter pylori* critical for its survival. *J Histochem Cytochem* 59:98–105. <https://doi.org/10.1369/jhc.2010.957092>.
- Shimomura H, Hayashi S, Yokota K, Oguma K, Hirai Y. 2004. Alteration in the composition of cholesteryl glucosides and other lipids in *Helicobacter pylori* undergoing morphological change from spiral to coccoid form. *FEMS Microbiol Lett* 237:407–413. <https://doi.org/10.1016/j.femsle.2004.07.004>.
- Sycuro LK, Pincus Z, Gutierrez KD, Biboy J, Stern CA, Vollmer W, Salama NR. 2010. Peptidoglycan crosslinking relaxation promotes *Helicobacter pylori*'s helical shape and stomach colonization. *Cell* 141:822–833. <https://doi.org/10.1016/j.cell.2010.03.046>.
- Hildebrandt E, McGee DJ. 2009. *Helicobacter pylori* lipopolysaccharide modification, Lewis antigen expression, and gastric colonization are cholesterol-dependent. *BMC Microbiol* 9:258. <https://doi.org/10.1186/1471-2180-9-258>.
- Hug I, Couturier MR, Rooker MM, Taylor DE, Stein M, Feldman MF. 2010. *Helicobacter pylori* lipopolysaccharide is synthesized via a novel pathway with an evolutionary connection to protein N-glycosylation. *PLoS Pathog* 6:e1000819. <https://doi.org/10.1371/journal.ppat.1000819>.
- McGee DJ, George AE, Trainor EA, Horton KE, Hildebrandt E, Testerman TL. 2011. Cholesterol enhances *Helicobacter pylori* resistance to antibiotics and LL-37. *Antimicrob Agents Chemother* 55:2897–2904. <https://doi.org/10.1128/AAC.00016-11>.
- Trainor EA, Horton KE, Savage PB, Testerman TL, McGee DJ. 2011. Role of the HefC efflux pump in *Helicobacter pylori* cholesterol-dependent resistance to ceragenins and bile salts. *Infect Immun* 79:88–97. <https://doi.org/10.1128/IAI.00974-09>.
- Sycuro LK, Rule CS, Petersen TW, Wyckoff TJ, Sessler T, Nagarkar DB, Khalid F, Pincus Z, Biboy J, Vollmer W, Salama NR. 2013. Flow cytometry-based enrichment for cell shape mutants identifies multiple genes that influence *Helicobacter pylori* morphology. *Mol Microbiol* 90:869–883. <https://doi.org/10.1111/mmi.12405>.
- Haque M, Hirai Y, Yokota K, Mori N, Jahan I, Ito H, Hotta H, Yano I, Kanemasa Y, Oguma K. 1996. Lipid profile of *Helicobacter* spp.: presence of cholesteryl glucoside as a characteristic feature. *J Bacteriol* 178: 2065–2070. <https://doi.org/10.1128/jb.178.7.2065-2070.1996>.
- Cole SP, Harwood J, Lee R, She R, Guiney DG. 2004. Characterization of monospecies biofilm formation by *Helicobacter pylori*. *J Bacteriol* 186: 3124–3132. <https://doi.org/10.1128/JB.186.10.3124-3132.2004>.
- LaRocca TJ, Pathak P, Chiantia S, Toledo A, Silvius JR, Benach JL, London E. 2013. Proving lipid rafts exist: membrane domains in the prokaryote *Borrelia burgdorferi* have the same properties as eukaryotic lipid rafts. *PLoS Pathog* 9:e1003353. <https://doi.org/10.1371/journal.ppat.1003353>.
- Dupont S, Beney L, Ferreira T, Gervais P. 2011. Nature of sterols affects plasma membrane behavior and yeast survival during dehydration. *Biochim Biophys Acta* 1808:1520–1528. <https://doi.org/10.1016/j.bbame.2010.11.012>.
- Delcour AH. 2009. Outer membrane permeability and antibiotic resistance. *Biochim Biophys Acta* 1794:808–816. <https://doi.org/10.1016/j.bbapap.2008.11.005>.
- Tran AX, Whittimore JD, Wyrick PB, McGrath SC, Cotter RJ, Trent MS. 2006. The lipid A 1-phosphatase of *Helicobacter pylori* is required for resistance to the antimicrobial peptide polymyxin. *J Bacteriol* 188: 4531–4541. <https://doi.org/10.1128/JB.00146-06>.
- Nakao R, Ramstedt M, Wai SN, Uhlin BE. 2012. Enhanced biofilm formation by *Escherichia coli* LPS mutants defective in Hep biosynthesis. *PLoS One* 7:e51241. <https://doi.org/10.1371/journal.pone.0051241>.
- Bayse C, Cullinane M, Denervaud V, Burrows E, Dow JM, Morrissey JP, Tam L, Trevors JT, O'Gara F. 2005. Modulation of quorum sensing in *Pseudomonas aeruginosa* through alteration of membrane properties. *Microbiology* 151:2529–2542. <https://doi.org/10.1099/mic.0.28185-0>.
- Tenguria S, Ansari SA, Khan N, Ranjan A, Devi S, Tegtmeyer N, Lind J, Backert S, Ahmed N. 2014. *Helicobacter pylori* cell translocating kinase (CtkA/JHP0940) is pro-apoptotic in mouse macrophages and acts as auto-phosphorylating tyrosine kinase. *Int J Med Microbiol* 304: 1066–1076. <https://doi.org/10.1016/j.ijmm.2014.07.017>.
- Testerman TL, McGee DJ, Mobley HL. 2001. *Helicobacter pylori* growth and urease detection in the chemically defined medium Ham's F-12 nutrient mixture. *J Clin Microbiol* 39:3842–3850. <https://doi.org/10.1128/JCM.39.11.3842-3850.2001>.
- Paixao L, Rodrigues L, Couto I, Martins M, Fernandes P, de Carvalho CC, Monteiro GA, Sansonetty F, Amaral L, Viveiros M. 2009. Fluorometric determination of ethidium bromide efflux kinetics in *Escherichia coli*. *J Biol Eng* 3:18. <https://doi.org/10.1186/1754-1611-3-18>.
- Pincus Z, Theriot JA. 2007. Comparison of quantitative methods for cell-shape analysis. *J Microsc* 227:140–156. <https://doi.org/10.1111/j.1365-2818.2007.01799.x>.
- Doddam SN, Peddireddy V, Ahmed N. 2017. Mycobacterium tuberculosis DosR regulon gene Rv2004c encodes a novel antigen with pro-inflammatory functions and potential diagnostic application for detection of latent tuberculosis. *Front Immunol* 8:712. <https://doi.org/10.3389/fimmu.2017.00712>.
- Clinical and Laboratory Standards Institute (CLSI). 2016. Methods for antimicrobial dilution and disk susceptibility testing of infrequently isolated or fastidious bacteria, 3rd ed. CLSI guideline M45. Clinical and Laboratory Standards Institute, Wayne, PA.

33. Hussain A, Ewers C, Nandanwar N, Guenther S, Jadhav S, Wieler LH, Ahmed N. 2012. Multiresistant uropathogenic *Escherichia coli* from a region in India where urinary tract infections are endemic: genotypic and phenotypic characteristics of sequence type 131 isolates of the CTX-M-15 extended-spectrum-beta-lactamase-producing lineage. *Antimicrob Agents Chemother* 56:6358–6365. <https://doi.org/10.1128/AAC.01099-12>.
34. Yonezawa H, Osaki T, Kurata S, Fukuda M, Kawakami H, Ochiai K, Hanawa T, Kamiya S. 2009. Outer membrane vesicles of *Helicobacter pylori* TK1402 are involved in biofilm formation. *BMC Microbiol* 9:197. <https://doi.org/10.1186/1471-2180-9-197>.
35. Hong Y, Cunneen MM, Reeves PR. 2012. The Wzx translocases for *Salmonella enterica* O-antigen processing have unexpected serotype specificity. *Mol Microbiol* 84:620–630. <https://doi.org/10.1111/j.1365-2958.2012.08048.x>.
36. Keenan JI, Allardyce RA, Bagshaw PF. 1997. Dual silver staining to characterise *Helicobacter* spp. outer membrane components. *J Immunol Methods* 209:17–24. [https://doi.org/10.1016/S0022-1759\(97\)00141-5](https://doi.org/10.1016/S0022-1759(97)00141-5).



SUPPLEMENTAL MATERIAL LEGENDS

[Author: Because the full supplemental material legends will appear in the HTML version of the article online, and because the copy editor may have made changes, we have reproduced the legends below. Feel free to enter your changes on this page and we will see that they are conveyed to the online article.]

FIG S1 Morphology of *H. pylori* in the absence of cholesterol in culture and upon deletion of *hp0421*. (A and B) Confocal microscopy images depicting *H. pylori* grown in the absence (A) and presence (B) of cholesterol. (C) Scatter plots showing *Hp26695* and *Hp26695Δ421* cell populations by *x* size and *y* size as analyzed by CellTool. (D) Graphical profiles representative of the distribution of *Hp26695* and *Hp26695Δ421* cell populations according to the aspect ratio and as analyzed by CellTool are shown. (E and F) RNA isolated from and the relative mRNA expression analyses of log-phase cultures of *Hp26695* and *Hp76* strains as quantified by qRT-PCR of *csd1* and *csd3* gene loci (ns denotes nonsignificant differences at $P \geq 0.05$).

FIG S2 Morphology of *Hp76* strains presented by flow cytometry. Representative contour plots of *H. pylori* populations when analyzed by flow cytometry; FSC and SSC are shown on the *x* and *y* axes, respectively, with mean and median. *Hp76Δ421* displayed high FSC and SSC compared to the *Hp76* and *Hp76Δ421*-reconstituted strains grown for 48 h (A) and 72 h (B).

FIG S3 The absence of cholesteryl glucosides caused increased cell wall permeability. (A to D) PE-A histograms delineating the influx rates of EtBr represented as MFI for different wild-type and knockout strains grown in culture for different periods and when treated with EtBr at different time points as shown.

AUTHOR QUERIES

AUTHOR PLEASE ANSWER ALL QUERIES

1

AQau—Please confirm the given-names and surnames are identified properly by the colors.
■ = Given-Name, ■ = Surname

AQA—(i) Proofread the entire article carefully to ensure that sense was not inadvertently changed incorrectly during processing of electronic file and editing. Check symbols (e.g., Greek symbols, diacritical marks, etc.) throughout. (ii) Running title OK? (top of page 3) If not, compose an appropriate running title (a limit of 54 characters plus spaces per ASM style).

AQfund—The table below includes funding information that you provided on the submission form when you submitted the manuscript. This funding information will not appear in the article, but it will be provided to CrossRef and made publicly available. Please check it carefully for accuracy and mark any necessary corrections. If you would like statements acknowledging financial support to be published in the article itself, please make sure that they appear in the Acknowledgments section. Statements in Acknowledgments will have no bearing on funding data deposited with CrossRef and vice versa.

Funder	Grant(s)	Author(s)	Funder ID
International Centre for Diarrhoeal Disease Research, Bangladesh (ICDDR,B)	Core Grant	Niyaz Ahmed	https://doi.org/10.13039/501100009054

AQB—Is “IO” correct here or should “IO” be changed to “10” or “L-O”?

AQC—Tables 1 and 2 renumbered per ASM style (ASM style for tables to be discussed in numerical order); check renumbering of tables and table citations throughout.

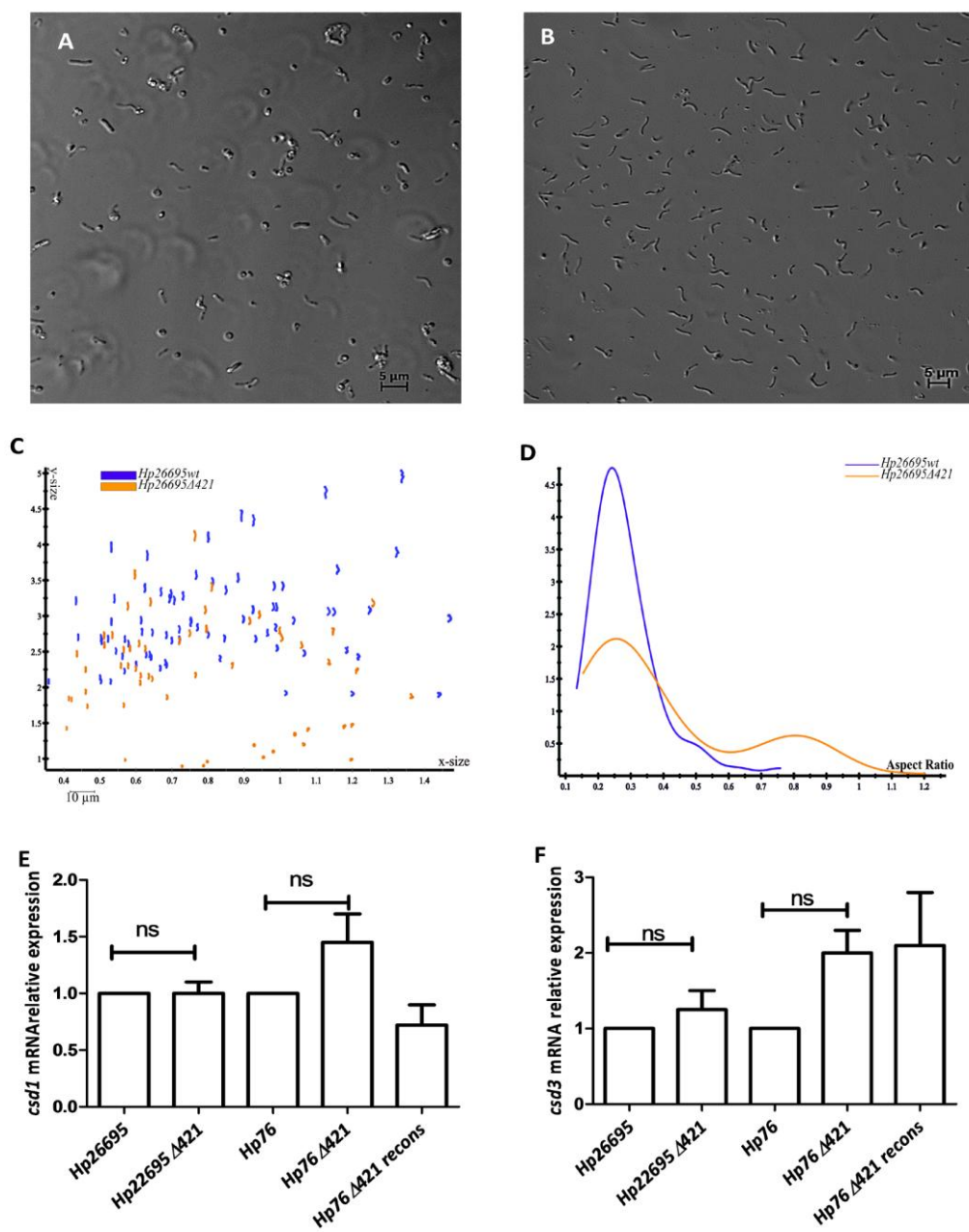


Figure S1

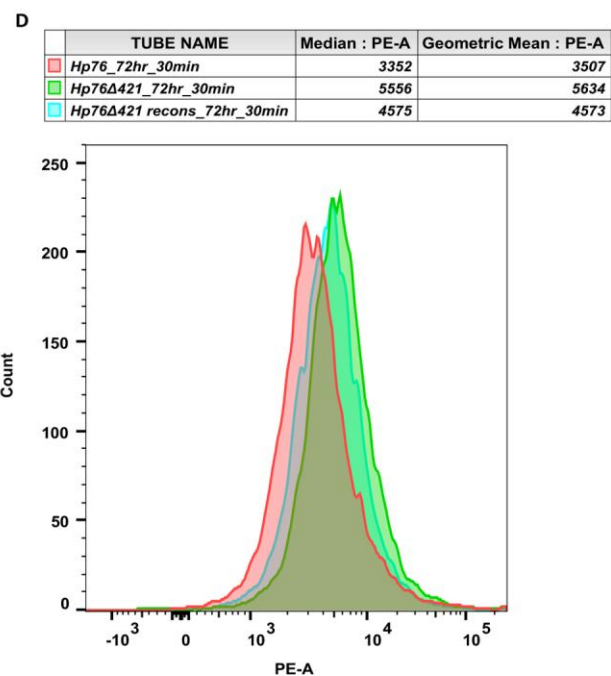
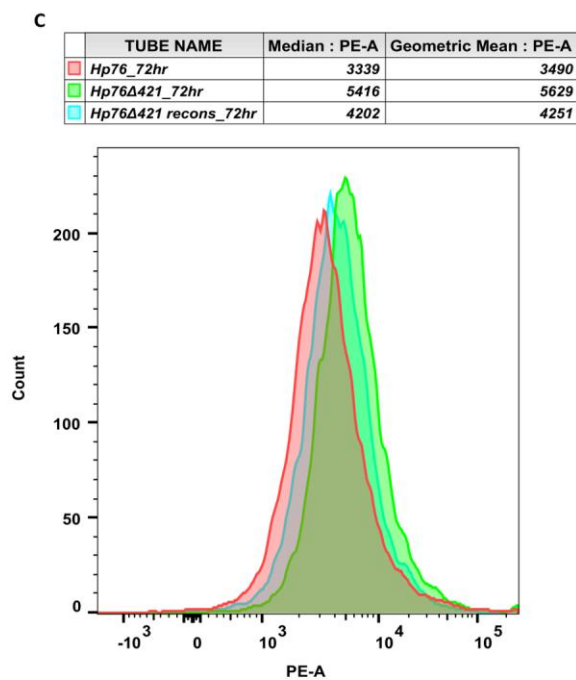
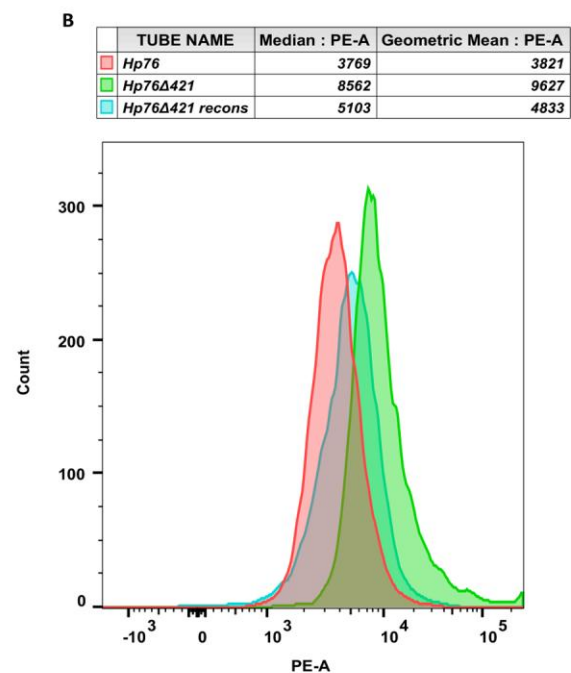
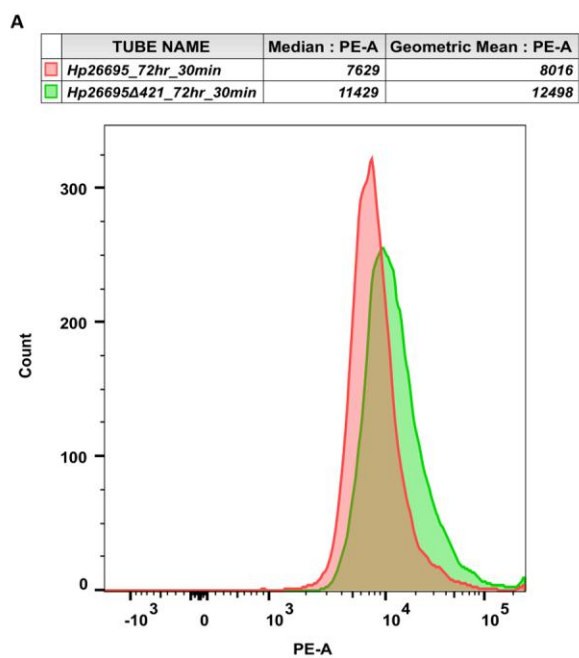
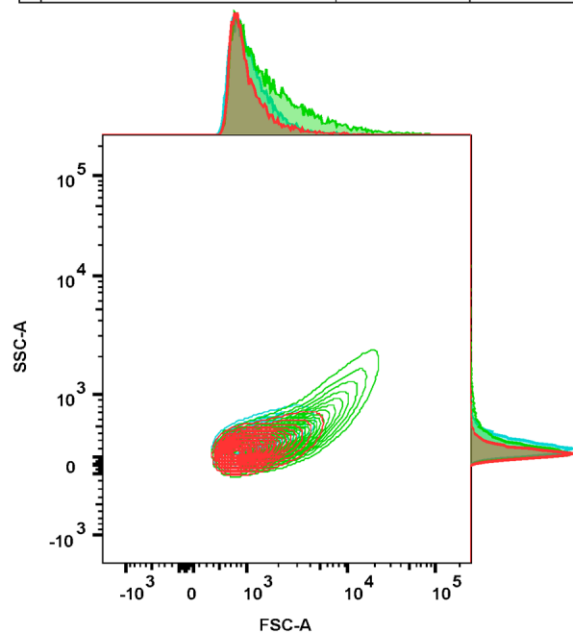


Figure S2

A

	TUBE NAME	Mean : FSC-A	Mean : SSC-A
■	<i>Hp76</i>	1278	200
■	<i>Hp76Δ421</i>	2749	364
■	<i>Hp76Δ421 recons</i>	1256	261



B

	TUBE NAME	Mean : FSC-A	Mean : SSC-A
■	<i>Hp76_72hr</i>	1627	232
■	<i>Hp76Δ421_72hr</i>	2167	318
■	<i>Hp76Δ421 recons_72hr</i>	1893	296

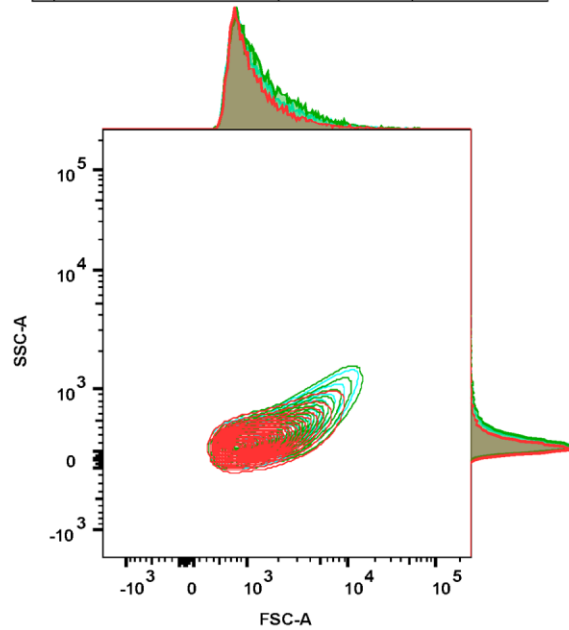


Figure S3

Role of cholesterol glucosylation in maintenance of *Helicobacter pylori* morphology, cell wall integrity and regulation of Mincle receptor response

by Majjid Ahmed Saleh Qaria

Submission date: 24-Nov-2018 05:41PM (UTC+0530)

Submission ID: 1044023877

File name: plagiarism_test.pdf (1.12M)

Word count: 15628

Character count: 85251

Chapter 1

Introduction

What is *Helicobacter pylori*?

Helicobacter pylori (³³*H. pylori*) is a helical-shaped, microaerophilic and Gram negative bacterium which was first diagnosed in gastric mucosa of patients suffering from gastritis and peptic ulcer, it was then successfully cultured by the two Australian doctors; Barry J Marshall and Robin Warren, (Marshall and Warren 1984). Noticeably, this discovery contradicted the previously held scientific belief that stomach is a germ free organ and this discovery resulted in the award of Noble prize 2005 to Marshall and Warren in Physiology and Medicine. Chronic infection of *H. pylori* in humans is prevalent in ⁹more than half of the world's population (¹⁸Hooi et al. 2017) and represents a major risk that causes gastritis and peptic ulcer, which may develop into ¹⁸mucosa-associated lymphoid tissue (MALT) lymphoma and finally can transform into gastric adenocarcinoma. More than 20% of all malignancies in humans are associated with infections and the major bacterial cause for human cancer till date is *H. pylori* (De Martel et al. 2012). ²Gastric cancer is the third major cause of cancer related deaths and fifth most common cancer after prostate cancer (Díaz et al. 2018). However, only few infected people are prone to develop serious clinical symptoms of *H. pylori* infection which in turn is determined by several factors which particularly depends on the host immune status such as presence of particular receptors and efficiency of inflammatory responses. Clinical outcome of *H. pylori* infection also depend on environmental determinants along with the strain specificity that affect the pathogenicity of the strains (strain diversity) [9].

Prevalence and geographical distribution

H. pylori is the predominant human infection globally that colonizes over 50% of world's population with huge difference in its geographical distribution. The highest prevalence of *H. pylori* is found in Africa with around 79.1% and the least in Northern America and Oceania at 24.4% [1] (Figure 1.1). The prevalence is high in rural areas compared to urban which reflect the

differences in the level of sanitation, socioeconomic status, urbanization, and facility to access clean water [10]. Interestingly, the prevalence of *H. pylori* vary between populations even in the same country. Moreover, *H. pylori* prevalence varies between different ethnic groups residing in the same country. For instance, in United States the *H. pylori* infection in non-whites was found ranging from 34.5% to 61.6% and that in non-Hispanic whites ranges from 18.4% to 26.2% [11]. Similarly, Malaysian population comprise of Malay, Chinese and Indians ethnic groups, the *H. pylori* prevalence in Malay is (19.9%), Indians (50.7%) and Chinese (40%) [12].

¹ *H. pylori* is being recognized as a Group I carcinogen by WHO which is responsible ² for the development of gastric adenocarcinoma. Almost 89% cases of Gastric cancer are attributed to *H. pylori* infection [13]. Previously, ³ it has been shown that complete eradication of *H. pylori* infection reduced the gastric cancer incidences from 25% to 16.67% in China [14].

In developed countries like Canada, US, and Northern Europe *H. pylori* prevalence is low with constant infection rates compared to Africa, Latin America, India and Eastern Europe. This is possibly a result of improved hygiene, sanitation and active elimination of carrier state by the use of antimicrobial therapies [15]. Furthermore, *H. pylori* shows high prevalence rates of 58 to 62% in India in patients with dyspeptic symptoms [16].

Dynamics of *H. pylori* transmission

H. pylori infection can be transmitted through following routes:

- i. **Iatrogenic:** Transmission of *H. pylori* through iatrogenic mode is the most frequent, and fast in which the endoscopes which comes in contact with gastric mucosa of *H. pylori* infected individuals are applied for another person [17]. Moreover, *H. pylori* infections are also reported to be transmitted from an infected individual to the staff members especially the technicians who execute endoscopy and the gastroenterologists [18].
- ii. **Faecal-oral:** Lin et al., have reported to recover *H. pylori* bacterium from the faeces of young children [18] while isolation of *H. pylori* from adult faeces was reported not very frequently [19]. Numerous studies have established the relation between the

Figure 1.1: Choropleth map represents the global prevalence of *H. pylori*. Certain regions are magnified to display the smaller countries [1].

seroprevalence of hepatitis A virus and *H. pylori*, suggesting similar (faecal-oral) mode of transmission for both the pathogens. [20]. Furthermore, *H. pylori* have been detected and cultured in drinking water samples. Hence, public water system has been considered as an source for *H. pylori* infection [21].

- iii. **Oral-oral:** Transmission of *H. pylori* from infected individuals by oral-oral route is another transmission method but not well established although there are several studies that

have attempted to detect and isolate *H. pylori* from the oral cavities [22]. For example, *Loster et al.* detected *H. pylori* in dentist's oral cavity by culture method from sub-gingival dental plaque and observed that 57% of study subjects were culture were positive for *H. pylori* [23].

Colonization of the mucosal tissue

There are different factors that are critical during *H. pylori* colonization in the mucosa tissue of stomach (Figure 1.2). The two most studied and key essential factors are:

i. Production of Urease

H. pylori is not an acid-loving organism and the production of urease enzyme is one of the characteristic strategy of *H. pylori* to neutralize the acidic environment of the gastric lumen. The presence of urease and its activation is indispensable for the successful colonization of gastric mucosa by *H. pylori* [24]. It has been shown that in the presence of urea *H. pylori* can tolerate pH as low as 2.5 while in the absence of urea it can tolerate a pH range between 8.0 and 4.0 [25]. It harbors a cluster of seven genes which control and regulate the biosynthesis process of urease enzyme [26], and it's composed of a complex structure of twelve subunits of UreA and UreB. [27]. *H. pylori* urease is a hydrolase enzyme that hydrolyses urea to CO₂ and NH₃. Unlike other ureases that are produced by bacterial species, *H. pylori* urease has strong affinity to urea with a Km value of 0.8 Mmol/L that enables the *H. pylori* urease to act on even very little quantities of urea (as low as 5 Mmol/L). Utilization of urea and production of NH₃ creates acid-neutralizing capacity empowering *H. pylori* to maintain the right pH in its periplasm and surrounding microenvironment. Consequently, regulating the proton motive force [28]. This acid adaptation strategy of *H. pylori* for maintaining a neutral pH intracellularly while the pH of the surrounding

vicinity ³ is still in low pH, is a peculiar feature to *H. pylori*. This is vital for existence of *H. pylori* in the acidic gastric juice. Moreover, generation of NH₃ by the urease enzyme in non-acidic environments could elevate the native pH above pH 7.0, which may be a reason why *H. pylori* does not colonize in niches other than the Gut. Moreover, ¹ it has been demonstrated that *H. pylori* is intolerant to alkaline environment [29].

ii. Ability to penetrate the mucus

Motility is the second critical key factor for gastric colonization by *H. pylori*. *H. pylori* features 2 to 6 unipolar flagella that confer motility to *H. pylori*. *H. pylori* flagella length range between 3-5 µm, with bulb-like structures that are mostly present at the end of the filaments [30]. *H. pylori* flagella sheath will be shielded by proteins and lipopolysaccharide and it is suggested that the bacterial outer membrane will be extended to protect the flagellar filaments from the gastric acid in the stomach [30]. Previously, it has been shown that *H. pylori* mutants that lacked flagella have failed to colonize the stomach of animal models [31]. For instance, FlaA and FlaB proteins are essential for the proper movement of *H. pylori*. Deletion of FlaA has impaired the motility of *H. pylori* to a greater extent than that of FlaB mutant [32]. Furthermore, it was reported that the protein auto-inducer 2 (AI-2) encoded by *luxS* gene regulates the expression of flagellar genes [33]. This has also been supported by the evidence that *luxS* mutants were less motile and less infectious ² compared to the wild-type strain [34].

***H. pylori*'s penetration into gastric mucus**

The epithelial lining of the GI tract is shielded by heavy viscoelastic layer (300 μ m) [35]. The, *H. pylori* has to penetrate the dense and viscoelastic mucus layer in order to reach the underlying epithelium for colonization. *H. pylori* can quickly lose motility in the very acidic gastric lumen [36]. The ability of *H. pylori* to elevate the pH by utilizing urea, reduces the viscoelasticity of the mucus permitting the bacterium to move faster through the mucus layer [37]. Helical-rod shape has been suggested to enhance the velocity of *H. pylori* through viscous mucus in a cork-screw fashion. *csdI* is one of the *H. pylori* cell shape determining genes which codes for a metallopeptidase. Deletion of *csdI* has altered the morphology of *H. pylori* from native helical-rod to curved-rod morphology and the *csdI* mutant exhibited less velocity in gel-like medium and were inefficient in colonizing the mice stomach compared to the wild-type strains [38]. Similarly, *csd4* deletion which results in straight rod-shaped morphology impairs the colonization efficiency and the motility of bacteria compared to the wild-type morphologies [39]. *H. pylori* isogenic mutants with rod shaped morphology showed reduced swimming rates by 7-21% in purified porcine gastric mucus [40].

Living within gastric mucus

H. pylori establishes microcolonies in the secreted gastric mucus present on the epithelial cells of the gastric mucosa [41]. Moreover, It has been observed that *H. pylori* lives in close proximity to MUC5AC which is the main gel forming mucin secreted by gastric epithelial cells *in vivo* [42]. It has been reported that lower mucus neck cells that are present in the antral glands secrete MUC6 which express α -1,4GlcNAc-capped core 2-branched O-glycan on the surface. MUC6 has shown to inhibit the formation of cholesteryl- α -D-glucopyranoside, one of essential cell wall components and inhibit the growth of *H. pylori* [43, 44].

Interaction with gastric epithelial cells

³ It has been believed ² that *H. pylori* colonizes the gastric mucus by interacting with gastric epithelial cells. A number of proteins have been identified to play an important play in the adherence to the host cells and for further interaction.

BabA

¹ **Figure 1.2:** Colonization strategies and establishment of gastric mucosal infection by *H. pylori* [3].

BabA is one of the well-studied adhesins of *H. pylori*. BabA is a 78 kDa outer membrane protein ¹ which attaches *H. pylori* to fucosylated structures on host cells, including Lewis^b blood group antigen and H-1 type [45]. BabA is a heterogeneous protein, with various polymorphisms among strains and binds to Lewis^b at different levels [46].

Sialic-acid binding adhesin (SabA)

In addition to BabA adhesion, SabA is a protein which binds *H. pylori* to sialylated ligands of gastric mucin, epithelial cells and neutrophils, which trigger a nonopsonic response by neutrophils and brings about phagocytosis of the bacterial cells [47]. Moreover, it has been shown that expression of *sabA* influences the acid production in the stomach [48]. The expression of SabA will be reduced in the acidic environment [49]. Another mechanism used by *H. pylori* ² is to regulate the expression of *sabA* gene duplication that enhances the ¹ production of the SabA protein, which in turn results in stronger adherence of *H. pylori* to cells *in vitro* [50]. Therefore, the *sabA* gene is

highly heterogenic allowing *H. pylori* to regulate its adherence strategies depending on the microenvironmental conditions.

³ Virulence strategies of *H. pylori*

Cytotoxin-associated gene A (CagA)

H. pylori's major virulence factor CagA is a product of *cagA* gene. It is one the best characterized virulence gene in *H. pylori*. CagA produced by some of ²⁰ *H. pylori* strains is partially responsible for the symptoms of the infection [51]. Upon adherence of *H. pylori* strains the CagA protein is expressed and is injected into the epithelial cells via Type IV secretion system (T4SS) that is coded by multiple loci located in pathogenicity island called *cagPAI*. After the translocation of CagA into host epithelial cells, it will be phosphorylated by host gastric epithelial cell kinases and finally it disrupts the host cell signaling pathways [52]. The *cagPAI* encompass around 30 genes, most of which are required for synthesis of the T4SS [53]. The CagL protein is highly conserved in *H. pylori* and is involved in formation of the end of the pilus in the T4SS. CagL has an arginine-glycine-aspartate (RGD) motif that binds to the $\alpha 5 \beta 1$ integrin which is presents on the surface of host cells and facilitate the translocation of CagA into host cells. [54]. Furthermore, it has been shown that Non-CagPAI proteins are required for CagA translocation process. For instance, HopQ an *H. pylori* outer membrane protein is needed for introduction of CagA into the host cells. In addition, HopQ is required for the subsequent intracellular activity of CagA [55]. Phosphorylation is required for CagA activity, this happens at EPIYA motifs present on the 145 kDa protein and triggers a robust immune response. In addition, the number of EPIYA motifs variey between the

23

H. pylori strains and it has been observed that the strains with more number of motifs are more virulent and biologically active [56, 57]. The E-cadherin and β -catenin complex that are commonly present in the adherent junctions of epithelial cells. CagA interaction with E-cadherin disrupts the complex irrespective of the CagA phosphorylation and results in the deregulation of β -catenin protein and its cytoplasmic accumulation this has been observed to induce carcinogenesis [58].

51

Vacuolating cytotoxin A (VacA)

VacA is the second most studied virulence factor in *H. pylori* and is genetically diverse. *vacA* encodes a primary toxin with a molecular weight of around 140 kDa, while the post-transnationally modified VacA toxin is made up of p55 and p33 domains which combine and form an oligomeric structure. This protein structure has an anion-selection channel which inserts into host epithelial cells and induces the secretion of organic anions and bicarbonates into the host cytoplasm [59]. This strategy helps *H. pylori* to obtain essential metabolic exudates for bacterial growth. Moreover, VacA has the ability to infuse the endosomes via endocytosis, in which the VacA endocytosed channel permit anions to pass into the late endosomes, which results into building up of weak bases. Consequently, it results in water influx and formation of large vacuole. [60, 61]. Furthermore, it has been reported that cell treatment by VacA essentially targets mitochondria and induces ER stress by section of cytochrome C and initiating apoptosis [62]. Most *H. pylori* strains harbor *vacA*, but exhibits strain specific differences in the signal sequence (s1a, s1b, s1c, and s2), intermediate region (i1, i2, and i3) and mid-region (m1, m1T, and m2). The genotypes can be categorized in two subtypes according to the combination of these three regions; s1/m1 which is most active and abruptly damages the cells in an acute manner, in comparison with the s2/m2 which is less virulent [63, 64] (Figure1.3).

Figure1.3: Structure and functions of *H. pylori* VacA [2].

Lipopolysaccharide (LPS)

LPS of *H. pylori* unlike LPS of the other Gram negative bacteria, is less toxic, less pyrogenic, and less responsive to the innate system of the human host [65]. The LPS of *H. pylori* contains O-Lewis antigens (Lewis a, Lewis b, Lewis x and Lewis y). Similarly, Lewis antigens are also expressed ³² on the surface of human gastric epithelial cells, which enables antigenic mimicry, helping *H. pylori* to escape the immune recognition [66]. Furthermore, these Lewis antigens help bacteria to get more carbon source and exudates by inducing inflammation of gastric epithelium. Anti-Lex (Lewis-x) antibodies produced as a result of Lewis antigen expression by *H. pylori* binds to *H. pylori* as well as to the gastric epithelium causing gastric autoimmune responses leading to enhanced inflammation and injury of the epithelium [66]. Lewis antigens of *H. pylori* have also been shown to undergo phase variation and to play a role in attachment of *H. pylori* to the gastric epithelium, thus providing a dynamic adherence nature to the bacteria [67].

The structure of *H. pylori* LPS comprises the same primary structure as present in other Gram-negative LPS, which comprises of three domains; the variable outer most O-antigens, conserved and core oligosaccharide and hydrophobic domain lipid A. O-antigens contributes to antigenicity, the lipid A domain communicates with receptors on immune cells that has potent endotoxic capabilities and core oligosaccharide that induces permeability in the cells [68]. *H. pylori* LPS has two specific functions, Lewis antigens that mimic the host antigens and facilitate immune evasion [69], and the distinctive structure of its lipid A-core, which provides protection from the host

produced cationic antimicrobial peptides (CAMPs) [70]. O-antigen biosynthesis in *H. pylori* occur via a novel Wzk-dependent pathway where short individual undecaprenyl pyrophosphate (Und-PP)-linked O-antigen units are built in the cytoplasm and transported to the periplasm and then polymerized by only the Wzk flippase which is specific to *H. pylori* [71] (Figure 1.4).

H. pylori has unusual feature where it constitutively modifies lipid A upon specific environmental signals [72]. It is one of the strategies of *H. pylori* which has been evolved to disguise the host immune system, as it leads to low immune responses, helping the bacteria to evade the innate immunity and enable long term persistence [73].

H. pylori mutants of lipid A synthesis genes such as lpxE/F have shown a 1020-fold higher sensitivity to polymyxin B and different naturally occurring CAMPs, and a 10-fold higher induction of TLR4 receptors. Strikingly, the lpxE/F mutants also failed to establish infection in the murine stomach, demonstrating the substantial role of a dephosphorylated lipid A domain of *H. pylori* LPS [70].

Figure1.4: Synthesis and O-antigen ⁷ligation with lipid A-core process in *H. pylori* [6].

Pathogenesis of *H. pylori*

H. pylori infects more than 50% of world human population and causes histologic gastritis in all patients, wherein only 10 to 20% of infected people develops ulcer disease and 1 to 2% will likely develop gastric cancer. Moreover, the severity and the incidences of disease inflicted by *H. pylori* is controlled by different host and environmental factors [74-76] (Figure 1.5).

Figure 1.5: Schematic graph illustrating the factors that are responsible for gastric pathology and the subsequent disease consequences [8].

Acute gastritis: Acute infection of *H. pylori* is represented by significant inflammation of the distal and proximal stomach mucosa, momentary nonspecific dyspeptic symptoms, nausea, vomiting, and stomach fullness. These symptoms were based on reports of patients who either accidentally or deliberately consumed *H. pylori* or acquired infections through contaminated food or water [24, 77, 78].

Chronic gastritis: Persistent infection of the *H. pylori* in the human Gut correlates with the distribution of gastritis and the level of acid secretion (Figure 1.5). Level of acid secretion has counteractive effects on *H. pylori*. *H. pylori* in specific infects gastric antrum, in the region where low acid-secreting layer of parietal cells exist. Such an infection is determined with an antrum-predominant gastric inflammation. In Patients who are acid secretion defective the bacteria are uniformly distributed within corpus and antrum together with adjoining contact with the gastric mucosa [79]. The persistent inflammation of the corpus mucosa promotes hypochlorhydria, in parallel with local inflammatory factor responses such as interleukin-1(IL-1), which subsequently produces suppressive responses on parietal cell function, supported by reports which illustrated that eradication therapy has increased acid secretion in the patients [80, 81]. Furthermore, the patients carrying proinflammatory genotype are at a greater risk of developing chronic gastritis, making them susceptible to intestinal metaplasia, atrophic gastritis and further to gastric cancer [82].

Peptic ulcer: Peptic ulcer is a mucosal deformity which is represented by a 0.5 cm diameter crossing the muscularis mucosa.

There are two types of ulcers; gastric ulcers and duodenal ulcers. Gastric ulcer mostly occur in the region between corpus and antrum mucosa while the duodenal ulcers arise in the duodenal bulb region [83]. Gastric ulcers and duodenal ulcers are linked to *H. pylori* infection, wherein it was reported that ¹95% of duodenal ulcers and 85% of gastric ulcers were culture positive for *H. pylori* [76].

Progression of atrophic gastritis to IM and gastric cancer

³Chronic *H. pylori* infection causes atrophic gastritis and develops into intestinal metaplasia (IM) in 50% of infected individuals, which is characterized by the damage of gastric glands, destruction of the gastric mucosal structure and fibrosis [84]. Intestinal metaplasia and loss of gastric gland progresses with time multifocally and increases the possibility of gastric cancer development from 5 to 90 folds based on the severity of gastric atrophy [85].

Moreover, development of cancer by *H. pylori* infection is dependent on ²host susceptibility and bacterial virulence that stimulate chronic inflammatory responses. For instance, the possibility of developing ³gastric cancer increases in patients infected with CagA-positive *H. pylori* strains [86]. Similarly, patients with a genetic tendency to produce higher IL-1 in response to infections are more prone to develop gastric cancers [82].

MALT lymphoma. Almost all MALT diseases develops in response to *H. pylori* infection as the lymphoid tissue is damaged in gastric mucosa. Unusually high titer of monoclonal population of B cells occur in gastric mucosa and gradually multiply and progress towards MALT lymphoma [87].

***H. pylori* infection diagnosis and treatment**

Several diagnostic tests have been established ³ to identify *H. pylori* infection with varying levels of specificity and sensitivity (Table 1.1). There are two types of diagnostic tests for *H. pylori*; invasive tests, that include culture from biopsies, gastric samples for histology and non-invasive tests, which includes peripheral specimens, such as stools, blood, urine, saliva, or breathe samples for detecting urease activity, bacterial antigens, or detection of antibodies.

Treatment of ⁹ *H. pylori* is mostly the triple therapy regimen which include two antibiotics like ⁴² amoxicillin and clarithromycin with either a bismuth compound or a proton pump inhibitor [8].

Table 1.1: Methods of *H. pylori* diagnosis

Diagnostic test	Sensitivity and specificity rate
<i>Invasive methods</i>	
Rapid urease (CLO) test	>90%
Culture biopsy	>95%
Histology	>95%
<i>Noninvasive methods</i>	
Fecal antigen test	>90%
Urea breath test	>95%
Serology	80-90%

***H. pylori* cholesteryl glucosides**

Cholesterol is the most abundant sterol in the mammalian cells, more than 90% of cholesterol is present in the cell membrane. It is one of the vital molecule in eukaryotic physiology, and also indispensable for some of the prokaryotes like *Mycobacterium tuberculosis* [88]. Moreover, it has

been shown that cholesterol depletion inhibits the invasion of host cells by *Chlamydia trachomatis* [89].

***H. pylori* have a unique structures of lipids**

H. pylori has unique constituents of ¹³cholesteryl glucosides (CGs); cholesteryl- α -D-glucopyranoside (α CG), cholesteryl-6-O-tetradecanoyl- α -D-glucopyranoside (α CAG), and cholesteryl-6-O-phosphatidyl- α -D-glucopyranoside (α CPG) which is the unique feature of this bacterium [90, 91]. Presence of CGs are a general characteristic feature for *Helicobacter spp.* Its percentage varies from species to species which ranges from 7%-29% [92]. Interestingly, *H. pylori* has unique lipids like 3-OH 14:0 and 3-OH C19:0 which enables it to survive in the acidic environment [93].

H. pylori do not have genes for cholesterol synthesis but it obtains cholesterol from the surrounding environment [94]. Ansorg et al., studied the affinity of *H. pylori* to cholesterol from different sources like egg yolk and he observed that rich cholesterol sources attract *H. pylori* [95]. Moreover, *H. pylori* has displayed the ability to sense cholesterol and thrive in high concentration of cholesterol when it was grown in hermetic tubes with different concentrations of cholesterol. Also, *H. pylori* associates with epithelial cell and extracts cholesterol which results in the destruction of lipid raft of the cell. Furthermore, cholesterol extraction from host cells will take place only in the presence of cholesteryl- α -glucosyl transferase (CGT) which is encoded by *hp0421* gene and deletion of this gene results in the loss of all CGs variants [96, 97].

Crystal structure of CGT protein has been studied and submitted to RCSB PDB protein repository with accession number [<https://www.rcsb.org/structure/3QHP> (3QHP)] [98]. The synthesis of

CGT takes place in the cytoplasm in an inactive form, which is further activated once it gets exported to the beneath of inner membrane.[99].

Role of cholesterol and CGs in pathogenicity of *H. pylori*

Several studies have investigated the substantial role of cholesterol glucosylation in *H. pylori* virulence and pathogenicity. CagA is an oncoprotein that is deposited into the cytosol of gastric epithelial cells through type IV secretion system (T4SS) and VacA toxin that alters endosome maturation and finally results in epithelial cell vacuolation, are the two main virulence mechanisms of *H. pylori* [100]. Remarkably, a decreased translocation of Phosphorylated CagA via T4SS in cholesterol-depleted AGS cell was observed which later reduced humming bird phenotype and decreased the induction of IL-8 expression [101]. Additionally, depletion of cholesterol from AGS cells before infection with *H. pylori* resulted in attenuated VacA toxin, thereby abrogating the vacuolation of AGS cells [102]. Moreover, depletion of cholesterol from AGS cells by using Methyl- β -cyclodextrin (M β CD) leads to decreased expression of NF- κ B and IL-8 which is a consequence of the disruption of $\alpha 5 \beta 1$ integrin that is present in cholesterol rich microdomains in the outer membrane of the host cell surface. $\alpha 5 \beta 1$ integrin is essential for NOD1 recognition of peptidoglycan and consequent induction of NF- κ B-dependent responses to *H. pylori* [103].

Furthermore, *H. pylori* cultured in the absence of cholesterol showed susceptibility to certain antibiotics, bile salts and ceragenins [104, 105].

Cholesterol glucosylation and escape of host Immune response by *H. pylori*

Another strategy employed by *H. pylori* for immune evasion is glucosylation of the host cholesterol and incorporating it into its membrane in order to disguise the host immune system. High amount of cholesterol enhance phagocytosis of *H. pylori* by antigen-presenting cells (APC),

like dendritic cells (DC) and macrophages and promote ³⁹ antigen-specific T cell responses. Cholesterol glucosylation by *H. pylori* delays internalization. Free cholesterol facilitates phagocytosis of *H. pylori* by macrophages and *H. pylori* incubated with cholesterol increases T-cell response. *In vivo*, cholesterol mediates T-cell dependent protection in mice fed with high cholesterol diet, histological studies showed infiltration for neutrophils and lymphocytes and upregulation of interferon- γ regulated genes but when the ratio of cholesteryl glucosides is higher than the cholesterol it protects the *H. pylori* from phagocytosis. Furthermore, *hp0421* mutant were cleared from mice stomach after 48 hours in contrary to the wild and reconstituted strains [7, 96]. Usually inhibition of IL-2 ² by *H. pylori* is mediated by ² γ -glutamyl transpeptidase GGT and VacA [106, 107]. Beigier, et al., showed that GGT and VacA IL-2 and IL-10 inhibition is attenuated in *H. pylori* after coating bacteria with cholesterol. Moreover, IL-4 was suppressed in VacA dependent manner and reverted back when bacteria were coated with cholesterol [108]. *H. pylori* mediates a direct inhibition of human CD41 T-cell proliferation while the immune response in iNKT mutant mice was lower when it was infected by wild-type *H. pylori* compared to *hp0421* mutant together with significant reduction in the cytokine responses by TH₁ and TH₂ cells [109]. One of the plausible strategies that *H. pylori* employs to modulate the autophagy is to arrest the phagosome maturation, but surprisingly this strategy have been restricted in *hp0421* mutant strains [110, 111]. More recently, Pau Morey et al., reported that extraction of cholesterol by *H. pylori* from epithelial cells inhibits assembly of IFN- γ and other cytokines. The *hp0421* mutant fails to establish infections in *in vivo* animal models, which points towards the ineffectiveness of T-cell based vaccine against *H. pylori* [7] (Figure1.6).

Figure 1.6: The cholesterol-dependent abrogation of ³immune response to *H. pylori* [7].

Objectives of the study

We hypothesize that CGs might play critical role ² in the maintenance of typical *H. pylori* morphology and permeability of *H. pylori* cell wall. Furthermore, we attempted to investigate the role of cholesterol glucosylation in *H. pylori* with regard to resistance to antibiotics, lipopolysaccharide profile and regulation of Mincle expression.

In order to address the above questions, the following objectives were framed:

1. To study the morphology of *H. pylori* population grown in the absence of cholesterol and deletion of *hp0421*.
2. ³ To determine the role of *H. pylori* CGs in cell wall permeability, antibiotic resistance, LPS profiles and biofilm formation.
3. To analyze ³ the role of *H. pylori* CGs in Mincle receptor regulation.

Chapter 2

Objective 1: To investigate the morphology of *H. pylori* population ⁴ grown in the absence of cholesterol and deletion of *hp0421*

INTRODUCTION

Bacteria have diverse morphologies and recent studies made great progress in understanding mechanisms that are responsible for distinct morphological features of bacteria and the role of the bacterial morphology in virulence and colonization [112]. Bacteria are diverse in their cell shapes, where some exhibit a coccoid form and other extend to rods with various helicities and curvatures. In addition, some bacteria develop unusual shapes like stars that is result of the extensions of prosthecae via polar growth. (Table 2.1). Interestingly, bacterial morphology can reforms in response to the surroundings conditions or during their life phases. The current understanding about the mechanisms that are involved in bacteria shape builds-up the comprehensive studies that focused on model bacteria which represent the most common shapes. For example, the most studied vibrioid or curved-rod is (*Caulobacter crescentus*), coccoid (*Staphylococcus aureus*) and rod (*Escherichia coli*). More recently, the studies that analyzing the infection models of pathogenic bacteria have explored the morphological diversity between mutants having altered shapes and exhibited an alteration in their virulence properties or colonization abilities [4]. This investigations has suggested that assumption that bacterial cell morphology may be involved in the pathogenicity or that the host environment influences an environment selection promoting morphological distinctiveness.

Probably, one of the well-known models organism *Caulobacter crescentus*. *C. crescentus* have a distinctive crescent shape that is controlled by a one protein called crescentin which coded by *creS*, . The deletion of *creS* results in straight-rod cells [113]. Furthermore, Persat, et al., shown that the straight-rods mutants surface colonization under moderate flow of water over the cells has been affected compare to the native curve-rods [114]. Regarding other examples of curved rods, like the pathogens *Vibrio parahaemolyticus* and *Vibrio cholerae* do not have a gene like *creS* homolog, demonstrating that there are an alternative mechanisms that control the vibrioid shape. The helical shape of bacteria have arisen during evolution of bacteria. For example, the human bacterial pathogens like spirochetes (*Borrelia* spp.) and e.g., *Treponema* and the proteobacteria such as *Campylobacter jejuni* and *Helicobacter* spp.

Table 2.1: Morphological variations and the functional consequences in different bacteria [4]

Several reports have observed that when helical spirochetes and proteobacteria loss helical cell shape and/or motility greatly affected the colonization abilities of these organisms [4]. For instance, *Campylobacter jejuni* is one of the helical shaped bacteria and a human pathogen that cause enteritis in humans. *C. jejuni* characteristic helical-shape is controlled by *pgp1* (peptidoglycan peptidase 1). Moreover, *pgp1* mutants exhibited rod-shaped morphology which is in contrast to the native helical form of wild-type. Interestingly, the rod-shaped *pgp1* mutant shown less colonization ability to chick by more than three times compare to wild-type [115]. Likewise, there are few bacteria which are known to possess glycolipids in their cell envelope. These include bacteria in the genera of *Helicobacter*, *Mycoplasma* and *Borrelia*. For example, *Borrelia burgdorferi*, is a spirochetes and one of human pathogens that cause Lyme disease. Cholesterol is required for *B. burgdorferi* to grow as it cannot synthesize cholesterol internally and it has developed the ability to acquire sterols from the vicinity [116]. Lipid contents were determined in *Borrelia* by high performance thin layer chromatography (HPLC) and eleven types of lipids were identified. Among these, two glycolipids contain cholesterol, ³⁸cholesteryl 6-O-acyl- β -D-galactopyranoside (ACGal) and cholesterol- β -D-galactopyranoside (CGal), where cholesterol molecules linked to galactose. The glycolipids comprises about 50–60% of the total lipids of bacterium [117]. LaRocca et al., reported that ACGal glycolipids that were gold labeled antibodies were observed directly under the transmission electron microscope (TEM) [118]. Moreover, cholesterol was chelated from *B. burgdorferi* membrane by methyl- β -cyclodextrin (M β CD) and swapped by ergosterol, cholesterol, dihydrocholesterol, and stigmasterol in model membrane studies they were shown to be raft-promoting that supported development of microdomains identical to the membrane microdomains in *B. burgdorferi* before sterol exchange. Moreover, substitution of sterols with zymosterol, lanosterol, desmosterol and cholesterol formate were shown to have an moderate ability to form rafts in model membrane in *B. burgdorferi*, while when it was substituted androsterol and coprostanol no microdomains were detected. Similarly, the spiral morphology of *B. burgdorferi* varied based on the type of sterol that have been substituted after cholesterol depletion by M β CD. When sterol was exchanged in *B. burgdorferi* with strong raft-forming sterols, the cells exhibited smooth surface with native planar wave morphology, but when it was swapped with sterols having an average sustenance to the membrane, while when it was

exchanged with sterols that didn't support forming of membrane ordered domain it totally lost its planar wave shape, forming a tightly curled morphology or straight cells. Interestingly, spirochetes sterol depleted with M β CD without sterol replacement formed coiled structure [119]. Therefore, cholesterol containing glycolipids are substantial in maintaining the native spiral morphology of bacteria such as *B. burgdorferi*.

Morphology of *H. pylori*

H. pylori belongs to the Epsilon proteobacteria bacteria class, which almost includes curved and helical organisms. *H. pylori* is a helical shape bacteria and there are studies which have analyzed the morphology and identified some determinants that control the native helical morphology of *H. pylori*. Sycuro et al., identified four genes that are required for the sustenance of *H. pylori* the native helical morphology and they called cell shape determinants (csds). Three genes (*csd1-3*) were identified as peptidoglycan endopeptidase homologs and the gene which control curved cell morphology (*ccmA*) homolog which is responsible for the straight rod shape in *Proteus mirabilis*. Moreover, deletion of these genes results in variable morphological alterations in *H. pylori*. For instance, deletion of *csd1* led to formation of rod shaped cells compare to native helical of wild-type. Similarly, *csd3* mutants exhibited variable curved rod, 'c'-shaped cells and loss of helical shape [120]. Furthermore, *csd5* a putative scaffolding protein and *csd4* which codes for DL-carboxypeptidase of peptidoglycan protein were identified. The *csd4* and *csd5* mutants showed that the helical shape was perturbed and slight changes in length and width of cells [39]. Later it was observed that the Csd4 enzyme is involved in generation of *H. pylori* helical shape, as the glutamine-zinc ligand that split the cell wall tripeptides. [121].

H. pylori undergoes morphological changes from spiral to coccoid under different stress conditions like variations in temperature, oxygen level and increased culture duration. Previously, it has been reported that lipid contents drastically changes during helical to coccoid transition in *H. pylori* where α CAG levels increases while phosphatidyl ethanolamine and α CG level decreases. The α CPG scarcely presented in the spiral form in the log phase, but subsequently increases during the coccoid conversion in lag phase [122].

Here in this study, we tried to decipher the morphological changes in ⁴*H. pylori* grown in the absence of cholesterol. We also investigated the morphological changes of hp0421 mutants of *H. pylori* strain 26695 [Hp26695 (human strain)] and *H. pylori* strain 76 [Hp76 (mice strain)] by

various approaches like confocal microscopy, flow cytometry and quantitative morphology analysis by CellTool software package.

MATERIAL AND METHODS

Bacterial strains and cholesterol loading

Human adapted strain *Hp26695* and its mutant *Hp26695Δ0421* were grown on GC agar medium (Difco) enriched with 10% decomplexed horse serum, and contained nystatin and 2.5 µg/ml, vancomycin 1 µg/ml, trimethoprim, 10 µg/ml and 1X of vitamin mixture (Table 2.2) as described previously [123]. For resistance selection an aliquot of 4 µg/ml kanamycin was added as marker for *Hp26695Δ0421*. Mice adapted strain *Hp76*, its mutant *Hp76Δ0421* and reconstituted *Hp76Δ0421* were a gift from Thomas F Meyer, Max Planck Institute for Infection Biology, Germany. *Hp76* strains were maintained as described previously [96] and explained in (Table 2.3). Antibiotics were excluded in experiments such as antibiotic resistance determination and aztreonam filamentation assay. Further, *Hp26695* were grown in absence of cholesterol and the procedures were modified from earlier described method(s) [124]. Briefly, *Hp26695* wild-type were grown on (chemically defined medium) Ham's F-12 (Gibco) enriched with 1 mg/ml BSA with or without 1 mM of water-soluble cholesterol (250 µM cholesterol with 4 mM MβCD) (Sigma). For agar plates, Ham's F-12 medium was prepared (2x) and mixed with 30 g per liter agar at 1:1 ratio. To visualize the cell elongation, 2 µg/ml of aztreonam antibiotic was added to media. All the strains were incubated at humidified microaerophilic conditions at 5% O₂ and 5% CO₂.

Glycerol stocks of *H. pylori*

H. pylori culture with 10⁹ CFU cells were collected from GC plates and suspended in 3 ml Brain heart infusion (BHI) broth supplemented with 10%decomplexed horse serum and 20% glycerol . It was then aliquoted in 50 µl volumes in screw cap cryotubes each labeled and preserved in -80 [125].

Table 2.2: Vitamin Mixture Composition [Light sensitive]

Ser. No.	component	Final concentration	Made	Cat. No.
1	L-glutamine	0.68mM	Sigma	G8540
2	Cysteine Chloride	1.48mM	Sigma	C6852
3	Iron(III) nitrate	0.5μM	Sigma	216828
4	Thiamine Chloride	0.088μM	Sigma	T1270
5	NAD (Nicotinamide Adenine dinucleotide)	3.76μM	Sigma	N3014
6	Vitamin B12	0.073μM	Sigma	V6629
7	Adenine	27.1μM	Sigma	A8626
8	Uracil	44.6μM	Sigma	U0750
9	L- Argine Monohydrate	7.12μM	Sigma	A6969

Prepared as 500X, dissolved in autoclaved double distilled water, filtered by Millipore GV syringe filter 0.22 μm and the aliquots were stored at -20c.

Table 2.3: *Hp76* Strains growth media and selective markers

Strain	Media	Supplementation	Antibiotics μg/ml
<i>Helicobacter pylori</i> P76 (<i>Hp76</i>)	GC base agar 4 g/100ml (BD)	10% of decomplexed Horse Serum (Gibco) and 1x Vitamin mixture (Table 2.2).	Vancomycin 10, Nystatin 1, Trimethoprim 5, and Streptomycin 200.
<i>Helicobacter Pylori</i> P76Δ421 (<i>Hp76Δ421</i>)	GC base agar 4 g/100ml (BD)	10% of decomplexed Horse Serum (Gibco) and 1x Vitamin mixture (Table 2.2).	Vancomycin 10, Nystatin 1, Trimethoprim 5, Streptomycin 400, and Chloramphenicol 4.
<i>Helicobacter pylori</i> P76Δ421-reconstituted (<i>Hp76Δ421-reconstituted</i>)	GC base agar 4 g/100ml (BD)	10% of decomplexed Horse Serum (Gibco) and 1x Vitamin mixture (Table 2.2).	Vancomycin 10, Nystatin 1, Trimethoprim 5, Streptomycin 400, Chloramphenicol 4, and Kanamycin 8.

Generation of *Hp26695Δ421*

Construct design

The gene *hp0421* (GeneID 900074) which code for cholesterol α -glucosyl transferase in *H. pylori* has a size of around 1.17 kb. Knockout in *Hp26695* was generated by homologous recombination as described previously [97]. Two pairs of primers corresponding to a PCR product surrounding the *hp0421* upstream (PCR1) which flanked 400bp region and downstream (PCR2) which span

500bp were designed (Figure 2.1A). In addition the internal primers (PCR1 reverse and PCR2 forward) carry the corresponding target sequence of XhoI and NcoI *hp0421*-US-F 5' GTGGATTATGACTCTTTAGAGACTTG 3' *hp0421*-US-F 5' GTGGATTATGACTCTTTAGAGACTTG 3', *hp0421*-US-R 5' GTGCCATGGCTCGAGTTAACTACTCTTCTTTAAATTGAAT 3', *hp0421*-DS-F 5' GTGCCATGGCTCGAGTGAAAGGATAAAAAATGCAAGAA 3', *hp0421*-DS-R 5' CCAATTTTAGGGCAGGCTAAAAAC 3', *kanR*-F 5'GATCCATGGCTCGAGTTTTCTACGGGGTCTGACG 3' and *kanR*-R 5' GTGCCATGGCTCGAGCTTAGAAAACTCATCGAGCATCAAATGA 3'. All steps of construct designing were performed using Cloning Manger software (Figure 2.1B).

Construct amplification

Annealing temperature of the primer was standardized by gradient PCR from 46°C to 62°C (Figure 2.2A). Amplification of upstream, downstream and kanamycin resistant cassette by using Q5 High-Fidelity DNA polymerase (NEB, M0491S) was performed. The reaction mixture and thermocycling conditions are mentioned in (Table 2.4 & 2.5). 3 µl of PCR products were resolved on 1.5% agarose gel and the DNA concentration were measured by nanodrop spectrophotometry. The amplified products were stored at -20.

PCR1 and PCR2 restriction digestion

PCR1 and PCR2 products were subjected to digestion by XhoI in order to ligate the two fragments and generate PCR3 fragment. The restriction digestion mixture was prepared as mentioned in (Table 1.6). The mixture was mixed gently and spun for seconds and incubated for 2 hours at 37°C. Then XhoI was heat inactivated for 20 minutes at 65°C.

A Helicobacter pylori 26695 chromosome, complete genome

NCBI Reference Sequence: NC_000915.1

[GenBank](#) [FASTA](#)



B

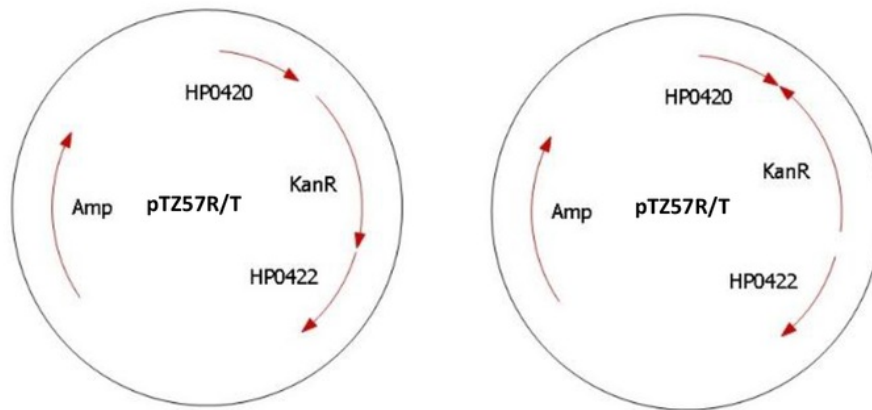


Figure 2.1: (A) genome map represent the position of *hp0421* in *H. pylori* strain 26695

(B) Virtual clone of *hp0421* knockout construct designed by Cloning Manager software

http://www.scied.com/pr_cmpro.htm.

Table 2.4: Restriction digestion reaction mixture

Components	Volume in μ l
Nuclease free-water	18
10X buffer R	2
Template	10 (0.5 μ g)
XhoI 10U/ μ l	2

Cleaning-up the digested products from the enzymatic and salt contaminants using gel extraction columns (QIAGEN, 28706)

The digested fragments were resolved on agarose gel and the respective bands of PCR1 and PCR2 were excised under UV transilluminator. QG buffer (3:1 v/wt) were added to the excised gel of PCR1 and PCR2, and 1 volume of Isopropanol was mixed properly and then transferred into the elution QIAquick spin column. Spin column centrifuged for 1 min at 10000 rpm to bind DNA. Then, 0.75 ml of buffer PE was added to the column, left for 3 min. To elute DNA, 50 μ l of H₂O was added to the middle of the column membrane followed by centrifugation at maximum speed for 1 min.

Ligation of PCR1 & PCR2 by T4 ligase and generation of PCR3

The PCR1 and PCR2 ligation mixture were mixed in order to generate PCR3 using T4 ligase. The ligation mixture was kept at 25°C for 1 hour followed by 65° C for 10 min. the ligated PCR3 was amplified using *hp0421*-US-F 5' GTGGATTATGACTCTTTAGAGACTTG 3', *hp0421*-DS-R 5' CCAATTTTAGGGCAGGCTAAAAAC 3' primers and Q5 High-Fidelity DNA polymerase. The amplified products were loaded on 1.2% agarose gel (Figure 2.2B). To confirm the PCR3 fragment ligation and amplification PCR3 fragment was digested by XhoI as mentioned above and loaded on 1.5% agarose gel (Figure 2.2C). PCR3 products were loaded on 1% agarose gel, the corresponding band was excised and purified as mentioned previously using QIAquick spin

column. In order to clone PCR3 into pTZ57R/T vector, purified PCR3 products were subjected for 3' A-tailing.

TA cloning of PCR3 in pTZ57R/T vector

The PCR3 products were ligated into pTZ57R/T vector at 1:3 (vector:insert) ratio using InsTAclone PCR Cloning Kit (Thermo Scientific). The mixture was incubated for overnight at 16°C followed by T4 ligase inactivation at 65°C for 10 minutes. *E. coli* DH5 α ultracompetent cells were thawed in ice and mixed with 2.5 μ l of ligation mixture and kept in ice for 30 min. The transformation mixture was kept at 42°C for 90 sec then immediately transformed into ice for 1 minutes. 0.5 ml of Luria-Bertani (LB) broth was added to the transformed cells and incubated at 37°C for 1 hour. Transformed cells were pelleted down at 6000 rpm for 5 min, mixed with 100 μ l of LB broth and plated on LB agar medium containing 100 μ g/ml of ampicillin.

Plasmid purification by alkaline lysis using QIAGEN kit and insert confirmation

The overnight cultures of transformed bacterial cells were pelleted down at 10000 rpm for 3 min, pellet was resuspended in 250 μ l of P1 solution containing RNase A 20 μ g/ml and incubated for 20 minutes. 250 μ l of P2 solution were added and mixed gently until the solution became clear and incubated for 5 min. 350 μ l of P3 solution were added, mixed gently by turn upside down the tubes 5 times, equal amounts of Isopropanol were added and incubated in -80°C for 30 minutes. The mixture was pelleted down for 12 minutes at 13000 rpm and the pellet removed. Followed by adding 1 ml of 70% ethanol to the supernatant and centrifuged at 13000 rpm. The pellet was left upside down on the bench till it dried from the ethanol and resuspend in 50 μ l of desalted water. The plasmid were resolved on agarose gel. The plasmid was double digested using XhoI and BamHI and fragment size was checked on agarose gel. The *E. coli* that carried PCR3 insert were expanded and plasmids were purified as mentioned above. The plasmid concentration was quantified by nanodrop[®].

Insertion of *kanR* cassette into pTZ57R/T-PCR3 plasmid

The purified plasmid carrying PCR3 was digested by XhoI followed by treatment with FastAP to remove phosphate group and inhibit self-ligation of the plasmid by adding 1 μ l of FastAP and

37

incubated for 10 min at 37°C followed by inactivation for 5 min at 75°C. The amplified *kanR* cassette was digested by XhoI and cleaned-up using QIAquick spin column as mentioned above. Then, *kanR* cassette was ligated to the pTZ57R/T-PCR3 plasmid and transformed into *E. coli* DH5 α as mentioned above. The transformed bacterial cells were incubated overnight on LB agar containing 4 μ g/ml kanamycin then 5 colonies were selected for plasmid isolation. To check the orientation of kanamycin resistance cassette the construct was double digested at one internal site and one external site as mentioned in (Table 2.9) and incubated at 37°C for 2 hours. The digestion mixtures were resolved on 2% agarose gel and visualized under UV illuminator.

Table 2.9: pTZ57R/T-PCR3 double-digestion reaction mixture

Components	Volume in μ l
Nuclease free-water	18
2X Tango Buffer	4
Template	10 (0.5 μ g)
XhoI 10U/ μ l	2
BamHI	2

Natural transformation of pTZ57R/T-PCR3 into *H. pylori*

H. pylori were cultured on three plates of GC medium and collected into 3 ml of BHI broth. *H. pylori* cell paste was mixed with 3 μ g/ml of pTZ57R/T-PCR3 plasmid and 200 μ l of mixture was aliquoted into 24 well plates and incubated in microaerophilic condition for 3 hours. The transformation paste were grown on GC agar medium containing 4 μ g/ml kanamycin for 3 days. Few colony were selected and checked for the absence of the plasmid (sensitivity to Amp) and for the presence of the resistance cassette inserted in the genome. Also, we performed a PCR with one primer internal to the cassette and one on the genome of *H. pylori* to ensure that the recombination took place in the correct locus.

Analysis of *H. pylori* cell morphology by flow cytometry (FC)

Flow cytometry is an efficient technique to analyze *H. pylori* whole population and the method we followed was modified from [126]. For cholesterol absence based selection, *Hp26695* strain was grown on chemically defined medium. For *hp0421* mutants, *Hp26695* strains and *Hp76* strains were all grown for 48-72 hours on GC agar (BD Biosciences). The bacterial cells were resuspended

in 1 ml of filtered PBS through Millix-GV syringe filter 0.22 μm . The bacterial suspension was adjusted to 0.4 O.D₅₅₀ and acquired by flow cytometry.

Figure 2.2: *hp0421* knockout generation in *H. pylori*³⁷ strain 26695; 1.5% agarose gel shows, (A) The amplified PCR1, PCR2 and KanR fragments at different annealing temperature (B) PCR3 amplified fragment after ligation, (C) PCR3 digestion by XhoI and (D) Complete construct amplified from wild-type and *hp0421* mutant.

H. pylori* morphological analysis upon deletion of *hp0421

H. pylori were grown on GC agar for 48 hours, washed by PBS (pH 7.0) with 10% glycerol thrice and the cells were adjusted to O.D₅₅₀ of 0.2. Cells were mounted on glass slides and cell population were captured using confocal microscope by employing transmitted light mode (Carl Zeiss Model: LSM 880). The image optimization was carried out in Adobe Photoshop 7 (Figure 2.2A). The quantitative analysis of processed images to measure the *x-size*, *y-size* and aspect ratio of *H. pylori* cells were done individually by CellTool software package as described previously [120, 127]. Briefly, the shape of each cell as image contours and smoothed using CellTool software package (Figure 2.2B). The individual contours were aligned in one plot and we plotted shape modes based on the variance from the standard deviations from mean in each shape mode and percentage of variance in each mode was calculated (Figure 2.2C). After that, all shape models were plotted in the normalized position based on standard deviations from the mean of curvature, width and length of cells (Figure 2.2D). Subsequently, one model was plotted which represents all populations (Figure 2.2E). Based on the mean model of cell population the shape of *Hp26695* wild-type, *Hp26695*Δ421, *Hp76* wild-type, *Hp76*Δ421 and *Hp76*Δ421-reconstituted were analyzed and the individual cell's *x-size*, *y-size* and aspect ratio was quantified to display the variation in morphology between strains.

Analysis of *H. pylori* Cell wall fluidity by flow cytometry

To determine the fluorescence intensity of ethidium bromide (EtBr) in-fluxed into the bacterial cells flow cytometry was employed. The staining and measurement procedures for EtBr influx were modified from previous study [128]. Briefly, for cholesterol absence based selection, *Hp26695* strain was grown on chemically defined medium. For *hp0421* mutants, *Hp26695* strains and *Hp76* strains were all grown for 48-72 hours on GC agar (BD Biosciences). Bacterial cells were collected and washed thrice with PBS at pH 7.4 (Gibco). A total of 10⁶ cells were resuspended in 1 ml PBS or in 1 ml PBS containing 5 µg of EtBr filtered by Millix-GV syringe filter 0.22 µm (Merck-Millipore). All the tubes were incubated at 37° C with gentle mixing inside a hybridization rotor for 5 to 30 min followed by FC analysis on a BD FACS Canto II system (BD Biosciences).

Measurement of EtBr fluorescence intensity was performed by flow cytometry with excitation wavelength set at 488 nm and the fluorescence emission at 585 nm. The data were analyzed by using FlowJo LLC software.

Figure 2.2: Steps followed for morphological quantitative analysis of *H. pylori* strains by CellTool software; (A) confocal image of *H. pylori* cells were executed by Adobe Photoshop 7, (B) The individual cell contours were aligned (C) Shape models were plotted based on the variance from mean, (D) Plot represent the normalized positions for all individual cells (E) Plot represent the mean model of the cell population.

Quantitative-PCR and gene expression analysis

The method for qRT-PCR analysis was described previously [129]. Briefly, using TriZOL, (Invitrogen) RNA was isolated from 10^8 cells of *H. pylori* strains. Subsequently, 3 µg of RNA was converted to cDNA using random hexamers and SuperScript-III (Invitrogen) according to the manufacturer's instructions. For qRT-PCR, 40 ng of the first transcribed DNA strand was amplified by using SYBR® Fast qPCR Mix (Takara, Japan) with primers targeting *cds3*-F 5' CTAAACATGGCAGCTTGATCC 3', *cds3*-R 5' AATGGATTTCACCACCTTCC 3', *cds1*-F 5' GGATGAATTTTACGATTTGC 3', *cds1*-R 5' CCCTCTTCTTTTCTTCTTCAGG 3', *wzx*-F 5' AAACCTCAAAGACAACCACGAAG 3', *wzx*-R 5' CGACCGCTAAAATCAACAAG 3', *wecA*-F 5' ATGGTGCTTGGGTTTATGGTG 3', *wecA*-R 5' GGCTTTCTGGCGTTTTATTTTG 3' genes and *16S rRNA*-F 5' GGTAATCCGTAGAGATCAAGAG 3', *16S rRNA*-R 5' ACAACTAGCATCCATCGTTTAGG 3' as an internal control. For *luxS*, *H. pylori* strains were grown for 2 days in 2 ml of Brucella broth and RNA was isolated from planktonic and sessile bacterial cells and targeted with primers *luxS*-F 5' TTTGATTGTCAAATACGATGTGC 3', *luxS*-R 5' TGTGAGATAAAATCCCGTTTGG 3'.

Treatment of *H. pylori* cells with filamenting drug aztreonam

To induce bacterial cell elongation, 2 µg/ml of aztreonam antibiotic was added to Brucella agar medium and incubated at humidified microaerophilic conditions at 5% O₂ and 5% CO₂. *H. pylori* 48 hour culture was washed thrice by PBS (pH 7.0) containing 10% glycerol and the cells were adjusted to OD₅₅₀ 0.2. Cells were mounted on glass slides and imaged by confocal microscopy by employing transmitted light mode (Carl Zeiss Model: LSM 880).

RESULTS

Loss of CGs alter the morphology of *H. pylori*

To decipher the role of CGs on *H. pylori* morphology, the wild-type (*Hp76*), knock out (*Hp76Δ421*) and *Hp76Δ421* reconstituted strains morphologies were captured under confocal

microscope by employing transmitted light mode. *Hp76Δ421* indeed exhibited morphological deformities wherein most cells displayed coiled 'c'-shape as a dominant morphology along with coccoid and rod-shaped bacteria (Figure 2.3A), whereas *Hp76* strain exhibited the native helical shape (Figure 2.3B). Interestingly, the reconstitution of *Hp76Δ421* strain resulted in the recovery of the cell morphology (Figure 2.3C). To study the morphology of *Hp26695* strain in absence of cholesterol, *Hp26695* wild-type were grown either in the presence or absence of cholesterol. The confocal images revealed remarkable variation in morphology of *Hp26695* cells that were grown in absence of cholesterol (Figure 2.4A). The altered shapes that were observed included 'c' shape, rod and coccoid forms in contrast to the bacteria grown in the presence of cholesterol which exhibited normal helical shape (Figure 2.4B).

Furthermore, we performed quantitative morphological analysis of confocal microscopy images of wild-type (*Hp76*), knockout (*Hp76Δ421*) and *Hp76Δ421*-reconstituted strains using CellTool software package. It was revealed that the distribution of cell populations of *Hp76Δ421* according to the *x-size* and *y-size* of cell population was bimodal and notably the size of cells varied as a result of variable cell shapes, whereas the *Hp76* population distribution was narrower, due to the consistency of cell shapes (Figure 2.3D). Moreover, the aspect ratio which represents the width/length ratio of individual cell presented significantly uneven distribution of *Hp76Δ421* cell population due to inconsistencies and distortion in the shape of *Hp76Δ421* cells, mainly because of 'c' shaped cells compared to the wild-type cells which demonstrated native distribution for the aspect ratio (Figure 2.3E). Moreover, the morphology quantitative analysis of *Hp76Δ421* reconstituted strain shown that cells restored the wild-type like morphology and cell population distribution based on aspect ratio, *x-size* and *y-size* was comparable to the wild-type strain. To ensure that the morphological alteration was not strain specific. Similar morphological quantitative analysis was performed on *Hp26695* strains. Morphology analysis of *Hp26695*, *Hp26695Δ421* was in concordance with the results obtained in case of *Hp76* strains (Figure 2.4C & D).

In order to manifest the morphological changes of *Hp76*, *Hp76Δ421* and *Hp76Δ421* reconstituted strains, they were grown in the presence of aztreonam, an antibiotic that induces pronounced filamentation in *H. pylori* by inhibiting septal peptidoglycan synthesis. Under these conditions, the *Hp76Δ421* exhibited morphological changes such as loss of curvatures and stunted filamentation (Figure 2.3F) compared to wild-type cells which exhibited typical curvatures and elongated

filaments (Figure 2.3G). Remarkably, *Hp76Δ421* reconstituted strain restored the curvature and wild-type-like morphologies (Figure 2.3H).

Moreover, to confirm that the deletion of *hp0421* did not interfere with *csd1* and *csd3* expression, the genes that are responsible for the native curvature and length of *H. pylori*, we analyzed their relative mRNA expression using qRT-PCR of *H. pylori* wild-type and *hp0421* mutant strains. According to our observation there was no significant influence on the *csd1* and *csd3* mRNA expression levels due to the deletion of *hp0421* gene (Figure 2.4E & F). Overall, we observed adverse morphological changes of *H. pylori* upon deletion of *hp0421* or by cholesterol depletion in growth media which indicates that the lack of CGs remarkably impairs the morphology of *H. pylori*.

Figure 2.3: Deletion of *hp0421* gene perturbs *H. pylori* cell morphology; confocal microscopy profiles depicting morphological patterns of (A) *Hp76Δ421*, (B) *Hp76* and (C) *Hp76Δ421*-reconstituted strain. (D) Scatter plots arraying *Hp76*, *Hp76Δ421* and *Hp76Δ421*-reconstituted cells based on *x*-size and *y*-size analyses performed using CellTool software. (E) CellTool analysis output based on plots representing the distribution of *Hp76*, *Hp76Δ421* and *Hp76Δ421*-reconstituted cell populations according to the ‘aspect

Figure 2.4: Morphology of *H. pylori* entailing the absence of cholesterol in culture and upon deletion of *hp0421*; confocal microscopy images depicting *H. pylori* cultured in absence (A) and presence of cholesterol (B). Shown in (C) are the scatter plots arraying *Hp26695* and *Hp26695Δ421* cell populations by x-size and y-size as analyzed by CellTool. Graphical profiles (D) representative of the distribution of *Hp26695* and *Hp26695Δ421* cell populations according to the aspect ratio and as analyzed by CellTool are shown. RNA isolated from and the relative mRNA expression analyses of *Hp26695* and *Hp76* strain [54] g phase culture as quantified by qRT-PCR entailing gene loci *csd1* and *csd3* are shown in panels E and F. (ns denotes non-significant differences at $p \geq 0.05$).

The morphological changes following CG's absence are attributed to a 'c' shaped bacterial population

The flow cytometry analysis appears to be an efficient and rapid technique to detect the cell shape of *H. pylori* at population level [126]. As *H. pylori* is dependent on exogenous cholesterol for synthesis of CGs the strain *Hp26695* was grown under microaerophilic conditions with and without cholesterol to analyze the morphological changes by FC. Forward scatter (FSC) usually represent the cell size while side scatter (SSC) roughly correlates with cell complexity, granularity and the absorbance of cell wall. We observed that *Hp26695* strain cultured in the absence of cholesterol exhibited much higher FSC that corresponded with the increased bulk width of the bacterial cell, represented by 'c'-shaped cells compared to the cells cultured in presence of cholesterol. Moreover, *Hp26695* grown in the absence of cholesterol displayed slightly higher side scatter (SSC) value, which indicates that cells presented higher granularity or complexity (Figure 2.5A). Notably, *Hp26695* strain grown for 72 hours in the absence of cholesterol also displayed remarkably higher FSC and SSC values compared to those grown up to only 48 hours (Figure 2.5B). Furthermore, the mean values of FSC and SSC in both conditions were higher in *H. pylori* grown in the absence of cholesterol. To analyze the morphology of *hp0421* mutant, the *Hp26695* and *Hp26695Δ421* cell populations were acquired by flow cytometry. The strain *Hp26695Δ421* displayed higher FSC and SSC values in both 48 hours and 72 hour culture populations, in comparison to the wild-type strain (Figure 2.5C & D). Furthermore, the cell population morphology analysis for mice-adapted strain, *Hp76* strains were subjected for analysis by flow cytometry. As expected the *Hp76Δ421* exhibited higher FSC and SSC mean compare to *Hp76* which is in accordance with the observation recorded for *Hp26695* and *Hp26695Δ421* strains. Interestingly, the mean values of FSC and SSC in *Hp76Δ421* reconstituted cell population was similar to the results from *Hp76* cell population which indicates that *Hp76Δ421* reconstituted strain cells have restored the native morphology and cell wall integrity (Figure 2.6A and B). Taken together, these observations suggest that the alterations in morphology of *Hp26695Δ421* and *Hp76Δ421* or of wild-type strains cultured in the absence of cholesterol are due to the presence of 'c' shaped cell population which is also evident by the higher FCS values. Moreover, *H. pylori* that lack CGs displayed alteration in cell wall integrity and cell granularity which correlates with higher SSC values observed.

Figure 2.5: Flow cytometry analysis of *H. pylori* cell populations based on their shape; Representative contour plots of *H. pylori* populations depicted based on flow cytometry analyses. SSC on the y-axis and FSC as plotted on the x-axis are presented with mean and median. (A) *Hp26695* grown with or without cholesterol for 48 hours and (B) 72 hours. Similarly depicted are (un-supplemented) *Hp26695* and *Hp26695* Δ 421 (C) grown for 48 hours and (D) grown for 72 hours.

Figure 2.6: Morphology of *Hp76* strains presented by flow cytometry. Representative contour plots of *H. pylori* populations when analyzed by flow cytometry; FSC and SSC are shown on the *x-axis* and *y-axes*, respectively, with mean. *Hp76Δ421* displayed high FSC and SSC compared to the *Hp76* and *Hp76Δ421*-reconstituted strains grown for 48 (A) and for 72 hour (B).

DISCUSSION

H. pylori belongs to the Epsilon proteobacteria which display helical-shape as a default morphology. In this work, we analyzed the possible role of CGs in the maintenance of native helical-shape of *H. pylori*. CGs are one of the unique characters of *H. pylori* that are present adequately in *H. pylori* membrane [90]. Presence of membrane lipids is suggested to be an

important component that maintains eukaryotic cell structures and morphology [130]. Lipid presence in prokaryotes membrane is uncommon feature and only few organisms possess lipids in their cell envelop such as *Helicobacter pylori*, *Mycoplasma spp.* and *Borrelia burgdorferi* [131]. Given this, we observed that the presence of CGs is essential factor in maintenance of the native helical morphology of *H. pylori*, irrespective of the strain type and growth duration. Whereas, lack of CGs remarkably distorted the shape of *H. pylori* cells to variable shape and size, with coiled and 'c'-shaped cells being the dominant. A previous studies by Sycuro et al., observed similar morphological alterations like 'c' shaped and rod shaped cells upon deletion of *csds* genes, such as peptidoglycan endopeptidase genes *csd1* and *csd3* in *H. pylori* [120]. However, we found that there was no effect on the gene expression levels of *csd1* and *csd3* upon deletion of the *hp0421*. Moreover, CGs are one of the main constituents of *H. pylori* cell wall which comprise around 25% of the total cell wall lipids [92]. Given this, our results strongly suggests that depletion of CGs leads to alteration of lipid raft components of the *H. pylori* cell wall which disrupts its integrity. Since lipid rafts are required in maintaining the architecture of cell wall and order of cell wall domains, absence of the CGs may be linked to change in the normal helical shape of *H. pylori*. In fact, in a study on *Borrelia burgdorferi* when cell wall cholesterol was depleted by methyl- β -cyclodextrins (M β CD) without substitution by other sterols, as a result *Borrelia burgdorferi* was converted into coiled spirochetes [119]. These data support the previous observations which demonstrated that the GCs contents were altered when *H. pylori* morphology undergoes transformation from helical to coccoid form [122]. Our results are in line with this observation which supports that the lack of sterols alters the morphology of *H. pylori*. Moreover, the morphology analysis of suggests that the lack of CGs remarkably altered the size and curvature of *H. pylori* cells; these results point at the possibility that CGs are part of lipid rafts in the cell wall and they play a substantial role in maintaining the typical helical shape and size of *H. pylori* cells. It should be considered that the helical shape of *H. pylori* is a key stratgy in the process of invasion of gastric niches. This is of particular significance given the reports that the colonization rates in mice stomach by the helical rod-shaped *H. pylori* were higher compared to *csd1* and *csd3* mutants that were curved and rod-shaped [120]. Similarly, Wunder *et al.*, reported that *hp0421* mutant(s) failed to colonize C57BL/6 mice and were cleared from the gastric tissue [96]. These results demonstrate that the changes morphology in *H. pylori*, due to the absence of CGs negatively influence the colonization potential of *H. pylori*. We speculate that this could be a result of direct

or indirect interaction between the CGs and the peptidoglycans that altered the order of cell wall domains.

Chapter 3

Objective 2: To evaluate the roles of *H. pylori* CGs in cell wall permeability, antibiotic resistance, LPS profiles and biofilm formation.

INTRODUCTION

Cell-envelope is the shield that protect the bacterial cell and the first ²³ region of contact between pathogens and host. The organization of *H. pylori* cell envelope is identical to the other gram-negative bacteria. In vitro studies have revealed that *H. pylori* cell-envelop in general is negatively charged and it has a hydrophilic surface character [132]. Separation of outer and inner membranes of *H. pylori* has been reported to be difficult as they are very connected [133]. Furthermore, unlike *Escherichia coli* *H. pylori* (1-6)-anhydro-*N*-acetylmuramic acid and having peptidoglycan composed of a mucopeptides with pentapeptide side chain ending with glycine[134]. Similar to other bacteria the peptidoglycan synthesized in the cytoplasm followed by integration into the membrane by the penicillin-binding proteins (PBPs) [135]. Several genes that involve in synthesis of *H. pylori* peptidoglycan have been identified as cell shape determinants CsdS (explained in details in chapter 2).

Remarkably, *H. pylori* has a characteristic composition of lipids and fatty acids which is the major feature that excludes *H. pylori* from the genus *Campylobacter* [136]. The gas-liquid chromatography (GC) analysis of four strains of *H. pylori* fatty acid compositions resulted in identification of several fatty acids like palmitic acid, myristic acid, linoleic acid, and stearic. The most membrane abundant fatty acids was myristic acid (31 to 45%), followed by 19-carbon cyclopropane (20 to 24%) [137].

H. pylori has most abundantly (lipid by weight) phospholipids 73.4%, then 20.6% glycolipids, and is 6% neutral lipids. The main phospholipids are cardiolipin, phosphatidylethanolamine, and phosphatidylglycerol. CGs are uncommon in bacteria and animals, but they have been identified in 13 out of 15 *Helicobacter* species studied [92].

It has been observed that the mechanisms disturbing the properties of the bacterial outer membrane lipid bilayer itself will ¹⁶ have an influence on the Gram-negative bacteria sensitivity to certain types

of antibiotics. Like-wise, perturbing the bacterial LPS pattern such as targeting LPS synthesizing enzymes have rendered the bacterial sensitivity to certain hydrophilic and hydrophobic antibiotics, leading to the possibility of combinatorial drug therapy [138]. Several studies have determined the effects of permeabilizers on bacteria resistance to antibiotics. For instance, Sung W. J. et al., have investigated the effect of liposomal linolenic acid (LipoLLA) nanoparticles, which is a permeabilizing and effective bactericidal agents, against *H. pylori*. They observed that LipoLLA permeabilizes *H. pylori* membranes, and actively work in a dose-dependent manner [139]. Interestingly, Hildebrandt *et al.*, observed that *Hp26695* cultured in the absence of cholesterol develops an aberrant LPS which are determined by dephosphorylation of lipid A at the 1-position compare to the one grown in presence of cholesterol. *H. pylori* LPS usually presents Lewis Y and/or X antigens. The quantification of Lewis Y and Lewis X antigens by whole-cell ELISA shown that the expression of these genes markedly increased when 26695, SS1, or G27 strains were grown in cholesterol containing media [140]. Furthermore, *H. pylori* cultivated in the absence of cholesterol showed susceptibility to certain antibiotics, bile salts and ceragenins [104, 105].

MATERIAL AND METHODS

H. pylori cell wall fluidity analysis by flow cytometry

For cholesterol based selection, *Hp26695* strain was grown on chemically defined medium Ham's-F12 as explained in the previous chapter. The strains *Hp26695* wild-type, *Hp26695*Δ0421, *Hp76* strains were grown for 48-72 hours on Brucella agar (BD Biosciences). The staining and measurement procedures for EtBr influx were followed from a previous study with minor modifications [141]. Briefly, bacterial cells were suspended and washed thrice with PBS at pH 7.4 (Gibco, USA). A total of 10⁶ cells were resuspended in 1 ml PBS or in 1 ml PBS [containing 5 μg of EtBr filtered through a Millix-GV syringe filter 0.22 μm (Merck-Millipore, USA)]. All the tubes were incubated at 37° C with gentle mixing inside a hybridization rotor for 5 to 30 min followed by FC analysis on a BD FACS Canto II system (BD Biosciences). EtBr fluorescence intensity was measured by flow cytometry analysis with excitation wavelength set at 488 nm and the fluorescence emission at 585 nm. The data were analyzed by using FlowJo LLC software.

Quantitative-PCR and gene expression analysis

The method for qRT-PCR analysis was followed as described previously (Doddam, Peddireddy, & Ahmed, 2017). Briefly, RNA was isolated from 10⁸ cells of *H. pylori* strains by TRIzol (Invitrogen). Subsequently, 3μg of RNA was converted to cDNA using random hexamers and SuperScript-III (Invitrogen) according to the manufacturer's instructions. For qRT-PCR, 40 ng of the first transcribed DNA strand was amplified by using SYBR® Fast qPCR Mix (Takara) with primers corresponding to *wzx*-F 5' AAACTCAAAGACAACCACGAAG 3' *wzx*-R 5' CGACCGCTAAAATCAACAAG 3', *wecA*-F 5' ATGGTGCTTGGGTTTATGGTG 3' *wecA*-R 5' GGCTTTCTGGCGTTTTATTTG 3' genes and *16S-rRNA*-F 5' GGTAATCCGTAGAGATCAAGAG 3', *16S-rRNA*-R 5' ACAACTAGCATCCATCGTTTAGG 3' used as an internal control. For luxS, *H. pylori* strains were cultured in Brucella broth (BB) for 2 days and RNA was isolated from planktonic and sessile

bacterial cells ⁴⁹ using the primers *luxS*-F 5' TTTGATTGTCAAATACGATGTGC 3' *luxS*-R 5' TGTGAGATAAAATCCCGTTTGG 3'.

Determination of antibiotic resistance among *hp0421* mutant and *H. pylori* wild-type

Hp26695 and *Hp76* strains grown on Brucella agar medium were suspended and washed with PBS and resuspended in BHI broth media. About 50 µl of cell suspension which contains approximately 10⁸ *H. pylori* was spread on Brucella agar medium and antibiotic impregnated discs corresponding to colistin, amoxicillin, fosfomycin, clarithromycin, Azithromycin, Gentamycin, tetracycline, ciprofloxacin and rifampicin (HiMedia) were placed on the agar plate. Subsequently, based on the above screened antibiotics, the strips corresponding to clarithromycin ¹⁰ (0.016-256 mcg/ml), amoxicillin (0.016 - 256 mcg/ml) fosfomycin (0.064-1024 mcg/ml), polymyxin-B (0.016-256 mcg/ml), colistin (0.016-256 mcg/ml), tetracycline (0.016-256 mcg/ml) and ciprofloxacin (0.002-31 mcg/ml) were selected for MIC test. The E-MIC strips were placed on Brucella agar plates and incubated for 3 days. The susceptibility was defined by breakpoints defined as per Clinical and Laboratory Standards Institute (CLSI)[142].

Biofilm formation by *H. pylori hp0421* mutant strains

The biofilm formation assay was performed using a modified protocol as described previously [143, 144]. In brief, *Hp26695* and *Hp76* cells were collected from BHI agar and washed with PBS. Inoculums at an OD₅₅₀ of 0.2 were seeded in 12 well plates, each well contain 2ml of BB with 7% of decomplexed horse serum (Gibco) and sterilized glass coverslips were used to cover the wells and also to enhance the attachment of *H. pylori* at the air-liquid interface. The cultures were incubated under microaerophilic conditions at 37°C for 2 to 6 days. Subsequently, the coverslips were washed with PBS followed by 0.1% crystal violet staining. The coverslips

were further rinsed with PBS, dried and the associated dye was dissolved in acetone and ethanol (2:8) and the crystal violet dye absorbance was measured by microplate reader at 594 nm.

Lipopolysaccharides purification and visualization

Purification of lipopolysaccharides from *H. pylori* strains was performed according to the previously described method of Hong *et al.* with slight modifications [145]. Briefly, the bacterial lawns were collected and washed thrice in 1ml PBS (pH 7.4) and pelleted down at 10000 rpm for 10 min. The pellets were lysed with lysis buffer (60 mM Tris-HCl pH 6.8, 2% SDS) and incubated at 98° C for 10 min and the whole lysate protein was quantified by BCA bicinchoninic acid assay (Thermo Fischer Scientific). LPS were extracted by adding 45% hot phenol to the lysate, vortexed vigorously and incubated at 70° C for 30 min. The mixtures were centrifuged at 16000g for 15 min and the upper phase layer was collected in 2 ml tubes and LPS were precipitated by adding 75% cold ethanol and 10 mM sodium acetate. The tubes were then incubated at -20° C overnight followed by centrifugation at 16000g for 15 min. To remove DNA and RNA contaminants, 3 µl of buffer 2 (10 mM MgCl₂, 50 mM NaCl, 1 mM DTT, 10 mM Tris-HCl, pH 7.9@25°C) (NEB), 0.5 mg/ml DNaseI (amplification grade) (Sigma) and 0.5 mg/ml RNase A (Invitrogen) were added, incubated for 1 hour at 37° C and treatment with 0.5 mg/ml Proteinase K (Amresco) for 1 hr at 56° C. The LPS was re-extracted by adding 50% phenol followed by vigorous vortexing and centrifugation. The pellet was finally precipitated by cold ethanol, dissolved in 50 µl of deionized water and preserved at -80 °C. For visualization of LPS, 10 µl from each tube were loaded on 15% SDS gel and stained with dual silver stain [146]. The LPS units were been quantified by Limulus ameocyte lysate (LAL) chromogenic endotoxin quantitation kit (Pierce) according to the manufacturer's instructions.

Statistical analysis

The statistical analyses for Hp26695 strains were performed using student's *t-test* and one-way ANOVA followed by Tukey's multiple comparison tests for Hp76 strains. The data are presented as mean \pm the standard errors (of mean) from three independent experiments..

RESULTS

Lack of CGs enhanced *H. pylori* cell wall permeability

H. pylori CGs comprise around 25% of total cell wall lipids [92]. Hence, to study whether the depletion of CGs has any effect on *H. pylori* cell wall permeability, we measured the influx of ethidium bromide (EtBr) among wild-type and knockout strains by flow cytometry. Bacterial strains were incubated with EtBr and the median fluorescence intensity (MFI) was measured. We observed that *Hp26695* strain grown in absence of cholesterol showed higher MFI compared to the bacteria grown in the presence of cholesterol (Figure 3.1A), indicating a higher influx of EtBr in bacterial cultured in the absence of cholesterol. We also measured EtBr fluorescence intensity between the strains *Hp26695* and *Hp26695Δ421*; the MFI was considerably higher in *Hp26695Δ421* as compared to the wild type (Fig. 3.1B). To determine the kinetics of EtBr influx in *Hp26695* and *Hp26695Δ421* strains, we measured the MFI of EtBr influx at 5, 10 and 30 minutes time intervals. The MFI of *Hp26695Δ421* was significantly higher through all the time intervals compared to the MFI observed for *Hp26695* (P value <0.05) (Fig. 3.1C).

To check the cell wall fluidity of lag phase cultures, the *Hp26695Δ421* and *Hp26695* strains were cultured for 72 hours and were observed for EtBr influx. As expected, the MFI was found to be remarkably higher in *Hp26695Δ421* compared to the *Hp26695* (P value <0.05) (Fig. 3.1D & 3.2A). Furthermore, we observed that *Hp76Δ421* exhibited higher MFI compared to *Hp76* and *Hp76Δ421*-reconstituted strain (Fig. 3.1E and 3.2B). We also measured the MFI for *Hp76* strains in 72 hours cultures and found that the influx rate was considerably higher in *Hp76Δ421* compared to *Hp76* and *Hp76Δ421*-reconstituted strains (P value <0.05) (Fig. 3.1F, 3.2C and D). Overall, from these observations, we anticipate that the lack of CGs would likely perturbs the cell wall permeability of *H. pylori* by damaging the cell wall integrity.

Figure 3.1: Absence of cholesteryl glucosides increased *H. pylori* cell wall permeability: Flow cytometry analysis based on influx rates of EtBr as depicted in the form of PE-A histograms delineating the median fluorescence intensity (MFI) for (A) *Hp26695* grown in presence and absence of cholesterol. Also depicted are (B) influx rates of EtBr for *Hp26695* and *Hp26695Δ421* grown for 48 hours. Bars in panels C to F represent MFIs when analyzed by student's *t*-test and one-way ANOVA for different wild type, knockout and reconstituted strains (as annotated) when treated /incubated with EtBr for 5, 10 and 30 minutes using cultures grown either at 48 hours or 72 hours (* denotes $p<0.05$, ** denotes $p\leq0.01$ and *** denotes $p\leq0.001$).

FIG 3.2: The absence of cholesteryl glucosides caused increased cell wall permeability. PE-A histograms delineating the influx rates of EtBr represented as MFI for (A) *Hp26695* strains grown for 72 hours and incubated with EtBr for 30min, (B) *Hp76* strains grown for 48 hours and incubated with EtBr for 5min, (C) *Hp76* strains grown for 72 hours and incubated with EtBr for 5min, (D) *Hp76* strains grown for 48 hours and incubated with EtBr for 30min.

Cholesteryl glucosides perturbation in *H. pylori* renders bacteria sensitive to antibiotics

To decipher the effect of loss of CGs in *H. pylori* on antibiotics resistance, we determined the minimum inhibitory concentrations (MICs) of certain antibiotics entailing *Hp26695* and *Hp76*

strains. For this, the strains were grown on Brucella agar plates in the presence of MIC E-strips belonging to different antibiotics. *Hp26695* and *Hp76* strains were resistant to fosfomycin, polymyxin-B, colistin, tetracycline and ciprofloxacin. Moreover, *Hp26695Δ421* was more sensitive to amoxicillin compared to *Hp26695* while both strains were sensitive to clarithromycin. Interestingly, *Hp26695Δ421* and *Hp76Δ421* strains on the other hand, were found to be sensitive to all the above antibiotics tested (Figure 3.4A) and (Table 3.1). The increased sensitivity of *Hp26695Δ421* and *Hp76Δ421* strains was understandable as these strains demonstrated an increase in cell wall permeability due to the loss of CGs. Overall, it appears that the deletion of *hp0421* perturbs the cell wall integrity of *H. pylori* which in turn leads to increased susceptibility to all the antibiotics tested.

Lack of CGs disrupts LPS structure

In order to detect the changes in O-antigen expression due to CGs disruption, we isolated lipopolysaccharides from *Hp76*, *Hp76Δ421* and *Hp76Δ421*-reconstituted strain and visualized by silver stained SDS gel. Depletion of CGs resulted in the disruption of O-antigens as observed by silver staining of *Hp76Δ421* LPS in which the O-antigens were absent when compared to *Hp76* LPS profile. Consequently, the O-antigens and core LPS were partially restored in the *Hp76Δ421*-reconstituted strain (Fig. 3.3A). Moreover we investigated whether the deletion of *hp0421* in *Hp26695* and *Hp76* strains had any effect on the transcription of *wcecA* and *wzk* genes. We found no influence on *wcecA* and *wzk* mRNA expression levels of these two genes in both wild-type and *Hp26695Δ421* and *Hp76Δ421* (Fig. 3.3C and 3.3D). This observation rules out the possibility that the alteration in LPS profile was due to alterations in the expression of these O-antigen synthesis genes. Thus, the lack of CGs most likely disrupted the normal components of *H. pylori* LPS.

Table 3.1: MICs of wild-type, $\Delta 421$ mutants, and $\Delta 421$ -reconstituted *H. pylori* strains

Antibiotic. mcg/ml	<i>Hp26695</i>	<i>Hp26695$\Delta 421$</i>	<i>Hp76</i>	<i>Hp76$\Delta 421$</i>	<i>Hp76$\Delta 421$ recons</i>
Fosfomycin	≥ 1024 (R)	$\leq 1.5 \pm 0.5$ (S) ²⁶	≥ 1024 (R)	$\leq 0.064 \pm 2$ (S)	≥ 1024 (R)
Colistin	≥ 256 (R)	$\leq 12 \pm 3$ (S)	≥ 256 (R) ²⁶	$\leq 10 \pm 5$ (S)	≥ 256 (R)
Polymyxin B	≥ 256 (R)	$\leq 8 \pm 4$ (S)	≥ 256 (R)	$\leq 10 \pm 4$ (S)	≥ 256 (R)
Ciprofloxacin	$\leq 0.38 \pm 0.5$ (R)	$\leq 0.064 \pm 0.02$ (S)	$\leq 0.50 \pm 0.5$ (R)	$\leq 0.19 \pm 0.2$ (S)	$\leq 0.047 \pm 0.08$ (R)
Tetracycline	$\leq 10 \pm 3$ (R)	$\leq 0.01 \pm 0.02$ (S)	$\leq 0.50 \pm 0.1$ (R)	$\leq 0.01 \pm 0.09$ (S)	$\leq 0.38 \pm 0.18$ (R)
Amoxicillin	$\leq 0.47 \pm 0.01$ (S)	$\leq 0.016 \pm 0.01$ (S)	$\leq 0.016 \pm 0.01$ 0.01 (S)	$\leq 0.016 \pm 0.01$ (S)	$\leq 0.016 \pm 0.01$ (S)
Clarithromycin	≤ 0.001 (S) ²⁹	≤ 0.001 (S)	≤ 0.001 (S)	≤ 0.001 (S)	≤ 0.001 (S)

The letters in parentheses after the MIC indicate whether the strain is resistant (R) or sensitive (S) to the indicated antibiotic.

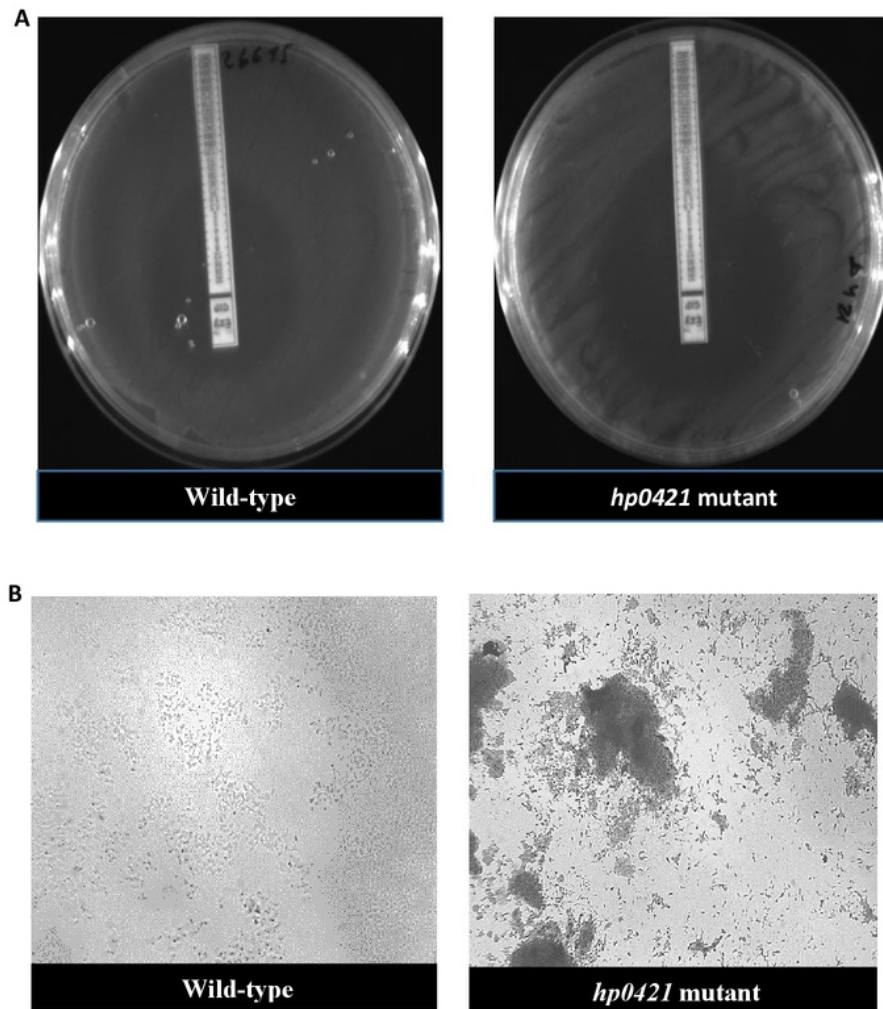


Figure 3.4: Lack of CGs in *H. pylori*: (A) Caused an increase in susceptibility against ciprofloxacin and (B) enhanced the aggregation of *H. pylori* on glass coverslip which were placed in broth media

Deletion of *hp421* enhances *H. pylori* cell aggregation

H. pylori produce biofilms on stomach mucosa in order to circumvent the gut's harsh environment and it was stated that the deletion of the *luxS* gene increases the biofilm formation [147]. We observed that *Hp26695Δ421* and *Hp76Δ421* tended to aggregate in the liquid cultures in contrast to the wild-type cultures that appeared turbid in their growth. So, we investigated the effect of *hp0421* deletion on the biofilm formation in *Hp26695* and *Hp76* strains. Biofilm formation was visualized under the microscope on glass coverslips (Figure 3.4B).

Hp26695Δ421 and *Hp76Δ421* demonstrated biofilm formation on the third day while wild-types formed biofilm on the fifth day. Moreover, crystal violet absorbance assay revealed the biofilm formation in *Hp26695Δ421* and *Hp76Δ421* to be significantly denser than in *Hp26695*, *Hp76* and *Hp76Δ421*-reconstituted strains (Figure 3.3B). The results showed that *Hp26695Δ421* and *Hp76Δ421* tended to aggregate and adhere strongly to the surface of the coverslip at the air-liquid interface. Hence, perhaps, the lack of CGs enhances aggregation of bacterial cells and promotes biofilm formation in *H. pylori*. Moreover, we analyzed the expression of the *luxS* gene in the above strains to check if its expression is affected by the deletion of *hp0421*. We observed that deletion of *hp0421* did not influence *luxS* mRNA expression levels in both wild-type and *Hp26695Δ421* and *Hp76Δ421* strains (Fig 3.3E).

Figure 3.3: Analysis of LPS expression and biofilm formation (A) (15%) SDS-PAGE gel double silver stained depicting profiles of LPS from *Hp76*, *Hp76Δ421* and *Hp76Δ421*-reconstituted strain; (B) bar graph representing quantification of biofilm formation by *H. pylori* after 5 days of incubation. (C, D) qRT-PCR analyses of *wecA* and *wzk* genes by using RNA isolated from wild-type (*Hp26695*, *Hp76*), knockout (*Hp26695Δ421*, *Hp76Δ421*), and *Hp76Δ421*-reconstituted strain(s) grown for 48 hr; (E) relative mRNA expression of *luxS* from 2 day old broth cultures (ns denotes non-significant difference(s), * denotes $p < 0.05$, ** denotes $p \leq 0.01$ and *** denotes $p \leq 0.001$).

DISCUSSION

Beside the substantial role of CGs in maintenance of *H. pylori* native helical morphology, the deletion of *hp0421* gene which results in loss of all CGs variants in the cell wall, which could lead to higher cell wall permeability. Likewise, when *H. pylori* 26695 strain was grown without cholesterol, the bacterial outer membrane permeability was significantly higher. Thus, this may indicates the critical role of CGs in the formation of intact cell wall units of *H. pylori* to maintain its integrity. In an alternative scenario, the CGs are probably required to preserve the tight pack of the outer membrane of *H. pylori*. Sterols in the membrane are believed to support the cell membrane integrity. For example, in *B. burgdorferi* the depletion of membrane cholesterol by M β CD and substitution with different sterol analogues increased the permeability of the membrane at varying levels based on the type of sterols, while the depletion of cholesterol without substitution with any sterols caused significant increase in the permeability of the membrane [119]. Also, in yeast, the deletion of essential genes of sterol biosynthesis was reported to increase the cell membrane permeability [148]. Our findings are in line with these and other reports and suggest that CGs interact with peptidoglycan domains to maintain the architecture of *H. pylori* cell wall. The permeabilization of *H. pylori* cell wall has far reaching implications for therapeutic interventions.

Further, we observed that *Hp76 Δ 421* exhibited aberrant LPS expression profile with loss of O-antigens and lack of core LPS. Our observations suggest that the perturbation of the architecture of *H. pylori* cell wall as a result to the lack of CGs reduced the LPS expression. On the other hand, this might have occurred due to the alterations in the structure of cell wall affecting the O-antigen biosynthesis enzymes that are present in the cell wall. It is relevant in this context that the deletion of *hp0421* did not affect the mRNA expression of essential LPS synthesis genes *wecA* and *wzk*. Alternatively, the alterations in the structure and composition of the cell wall due

to the lack of CGs may result in the dysregulation of the transfer of LPS units through membranes. Our observations appear to be in correlation with the report of Hildebrandt *et al.*, who observed that depletion of cholesterol leads to the development of aberrant LPS in *Hp26695*, which depends on lipid-A phosphorylation [140].

Furthermore, we observed that lack of CGs reverted the resistance of *H. pylori* to antibiotics. The increased susceptibility to the antibiotics due to the deletion of *hp0421* may be the result of permeabilization of the cell wall, facilitating antibiotics to penetrate passively through *H. pylori* cells. The bacterial cell wall is the first line of defense against antibiotics, detergents and host defense elements. The membrane/cell wall permeabilization could be an effective method to control bacterial infections by enhancing antibiotic action/delivery [138]. Secondly, our study suggest that disruption of LPS and/or influencing the outer membrane charge as a result to the lack of CGs decreased the resistance of *H. pylori* to certain antibiotics like polymyxin and colistin. Disruption of lipid A gene encoding *lp_{XEHP}*, in *H. pylori*, has been shown to dramatically decrease the polymyxin resistance from MIC > 250 µg/ml to MIC, 10 µg/ml [149]. Similarly, we believe that the deletion of *hp0421* might possibly affect the LPS structure thus influencing the outer membrane charge and cell wall integrity and eventually increasing the sensitivity of *H. pylori* to certain antibiotics. Inhibition of CGs synthesis may not kill the bacteria directly, but rather render the pathogens incapable of establishing successful infection by hindering their colonization potential and fitness advantage (resistance towards antibiotics).

Moreover, our study suggest that the tendency of *Hp26695Δ421* and *Hp76Δ421* to aggregate on the surface of coverslips is probably due to the changes in the properties of LPS. Modifications in LPS have been shown to enhance bacterial auto-aggregation and biofilm formation [150]. Alternatively, the changes in the cell wall properties and morphology may triggered stress-related

genes, including quorum sensing gene *luxS*. Similarly, the changes in the membrane structure of *Pseudomonas aeruginosa* were previously reported to alter quorum sensing [151]. However, according to our observation there was no changes in the mRNA expression levels of *luxS*.

Chapter 4

**Objective 3: To decipher the role of *H. pylori* CGs in
Mincle receptor regulation**

INTRODUCTION

The first line of body defense is the innate immunity that identifies any non self, non-specific molecular patterns of pathogens. One category of the innate immune receptors are C-type lectin receptors (CLRs) that contain members of transmembrane and soluble receptors. These receptors possess a carbohydrate recognition domain (CRD) as a characteristic feature or a homologous domain [152]. Furthermore, Transmembrane CLRs can function as pattern recognition receptors (PRRs), which mean that it has the ability to recognize and internalize a pathogen, and subsequently degrade and present the constituent molecules as an antigens which will be recognized by innate immune defense system and subsequently induce adaptive immunity [153]. One of plausible example of transmembrane CLRs that identify a wide range of foreign and self-molecule as part of innate immune response is Mincle [154]. One of the most studied molecules that are recognized by Mincle receptor is the 'cord factor' trehalose dibehenate (TDB) which is a part of *M. tuberculosis* membrane. TDB trigger a strong immune response and has potent immune modulating properties [155, 156].

Mincle is composed of 219 amino acids and a carbohydrate recognition domain (CRD) which is categorized under type II transmembrane protein which and present at its extracellular region that are present in various cells including macrophages, DCs and neutrophils [157]. The ligand binding site expressed on cell surface side, its ligand include cholesterol and protein, the signal transduces via the Fc receptor γ -chain molecule (FC- γ) with tyrosine- based activation motif immune receptor that has [158]. Mincle downstream signaling pathway involves activation of spleen tyrosine kinase (Syk) which subsequently activates Card9-Bcl10-MALT1 complex where the latter target (NF- κ B). Subsequently, the transcription factor NF- κ B induces the expression of various cytokines such as interleukin-6 (IL-6) and tumor necrosis factor (TNF), interleukin-10 (IL-10)

[159]. TNF and IL-6 responses act as a pro-inflammatory while induction of IL-10 is considered as anti-inflammatory and results in downregulation of IL-12p40 that interferes with pro-inflammatory cytokine secretion [160]. Induction of Mincle receptor triggers a defensive TH1 cell mediated immunity when induced by cord factor and initiates TH17 responses (Figure 4.1) [161]. Recently, there are number of studies that have shown that lipid derivatives induce Mincle signaling and trigger inflammatory responses [162, 163]. Moreover, Kiyotake R. et al., analysed ligands that trigger the human-Mincle by mass spectrophotometry (MS) and it revealed that free cholesterol, cholesterol crystals, cholesterol intermediate induced hMincle expression while endogenous steroids such as testosterone, cortisone, estradiol, progesterone, aldosterone, bile acid cholestanoic acid, and yeast ergosterol did not induce hMincle expression [163].

Mincle is a PRRs which recognizes the pathogen-associated molecular patterns (PAMPs) of bacteria and fungi mainly glycolipids [164]. Previously, it was shown that *H. pylori* induces Mincle expression and triggers anti-inflammatory responses through IL-10 production in order to escape clearance by the host immune system [165]

Figure 4.1: Signaling via Mincle, some of glycolipids ligands that induce Mincle and the signaling pathway through Mincle which triggers secretion of chemokines, cytokines, and activate T-cell immune responses [5].

MATERIAL AND METHODS

Culture of Macrophage cell lines

The human monocyte THP-1 cells and RAW 264.7 cells were obtained from National Centre for Cell Sciences, Pune, India. THP-1 cells were cultivated in RPMI-1640 medium and RAW 264.7 cells were cultivated in Dulbecco's Modified Eagle's Medium (DMEM) (Gibco) enriched with 10% (v/v) decompemented fetal bovine serum (FBS) (Invitrogen), 1% of 100X anti-mycotic/antibiotic solution which contains Amphotericin B, Penicillin, Streptomycin (Gibco) and were incubated in microaerophilic conditions with 5% O₂ and 5% CO₂ at 37°C. To differentiate THP-1 cells from monocytes to macrophages 50 ng/mL PMA (phorbol 12-myristate 13-acetate) were added (Sigma) and incubated for 48 hours. After cell differentiation and adherence, the culture media was replaced by fresh media with 10% decompemented FBS and was further incubated for another 12-24 hours before infection.

Infection assay

THP-1 cells and RAW 264.7 cell infection assay was modified from [165, 166]. Briefly, *H. pylori* strains lawns were collected from GC agar plates in 1X PBS and were washed twice with 1X PBS. Macrophage-like THP-1 cells in serum and antibiotic free RPMI-1640 medium were infected with *Hp26695* and *Hp26695*Δ421 strains (human-adapted strain) at multiplicity of infection (MOI) of 100 i for 12 hour. Similarly, RAW 264.7 cells were grown till they reached 70% confluency and infected by *Hp76* wild-type, *Hp76*Δ421 and *Hp76*Δ421-reconstituted strains (mice-adapted strain) for 12 hour.

Quantitative-PCR and gene expression analysis

The method for qRT-PCR analysis was described previously [129]. Briefly, RNA was isolated from 10^8 cells of *H. pylori* strains by TriZOL (Invitrogen). Subsequently, 3µg of RNA was converted to cDNA⁶ using random hexamers and SuperScript-III (Invitrogen) referring to the manufacturer's instructions. For qRT-PCR, 40 ng of the first transcribed DNA strand was amplified using SYBR[®] Fast qPCR Mix (TaKaRa) with primers corresponding to Mincle receptor expression in THP-1 cells by using primers Mincle-F²⁵ 5' AAACACAATGCACAGAGAGAGG 3', Mincle-R 5' ACACATCTGGTGATGAAACAGG 3', together with GAPDH-F 5' GAGTCAACGGATTGTCGT 3' GAPDH-R 5' GACAAGCTTCCCGTTCTCAG 3', as internal control. For RAW 264.7 cells the primers used were Mincle-F²⁴ 5' AGGAAGAAAGGCAGGAAAAAGG 3', Mincle-R 5' GAAACAGCCACTGAGAAACAGG 3', together with β-actin-F 5' GCTACAGCTTACCACCACAG 3', β-actin-R 5' GGTCTTACGGATCAACGTC 3' as internal control.

Statistical analysis

²¹ The statistical analyses were performed using student's *t-test* and one-way ANOVA followed by Tukey's multiple comparison tests. The data represented the mean and standard error mean of three independent experiments.

RESULTS

Mincle induction reduces in THP-1 and RAW 264.7 cells upon infection by *hp0421* mutants

THP-1 cells are human macrophage cells that express Mincle receptor. We observed that *Hp26695* wild-type strain significantly induced Mincle expression compared to uninfected cells when tested at 12 hour post infection. Moreover, Mincle relative mRNA expression in THP-1 cells infected by *Hp26695* Δ 421 was remarkably reduced compared to the cells that were infected by *Hp26695* wild-type. The difference was statistically significant as analyzed by student's *t*-test Mincle(Figure 4.2). Similarly, expression of Mincle relative mRNA expression was significantly induced upon infection by *Hp76* wild-type compared to uninfected RAW 264.7 cells. Furthermore, Mincle expression was reduced significantly in RAW 264.7 cells upon infection by *Hp76* Δ 421 strain compared to Mincle expression after infection with wild-type strain. Interestingly, infection of RAW 264.7 cells by *Hp76* Δ 421-reconstituted strain induced Mincle expression similar to the induction of Mincle by wild-type strain (Figure 4.3). Overall, infection of macrophage cells by *H. pylori* strains induces Mincle expression while infection by *hp0421* mutants demonstrated reduced Mincle expression compared to wild-type and reconstituted strains.

Figure 4.2: Deletion of *hp0421* in *Hp26695* resulted in decreased expression of Mincle receptor in THP1 cells; THP-1 cells were infected by *Hp26695* strains for 12 hours at MOIs of 100. Mincle relative mRNA expression levels were analyzed by qRT-PCR. The expression of *46* *ncle* gene was reduced significantly in THP-1 cells upon infection by *Hp26695*Δ*421* strains compared to wild-type as analyzed by student's *t*-test for wild type, knockout and un-infected(as annotated). ** denotes $p \leq 0.01$.

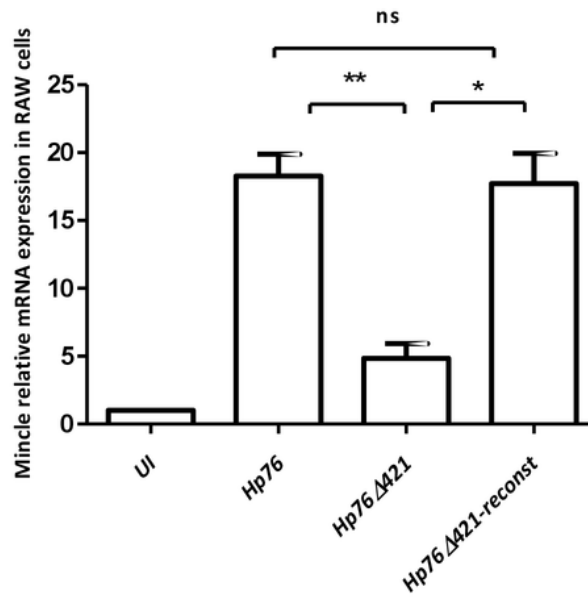


Figure 4.3: Deletion of *hp0421* in *Hp76* strain resulted in decreased expression of mMincle in RAW 264.7 cells; RAW 264.7 cells were infected by *Hp76* strains for 12 hours at MOI of 100. Mincle mRNA expression levels were detected by qRT-PCR. The expression of mMincle gene was reduced significantly in RAW 264.7 cells upon infection by *Hp76* Δ 421 strain compared to infection with wild-type and reconstructed strains. Data were analyzed by one-way ANOVA followed by Tukey's multiple comparison tests. (ns denotes non-significant difference(s), * denotes $p < 0.05$, ** and denotes $p < 0.01$).

DISCUSSION

Evading the responses of innate immune system is a key strategy in prolong colonization of *H. pylori*. *H. pylori* achieves this by its ability to regulate the host innate immune responses and their signaling pathways. Mincle, the C-type lectin receptors (CLRs) which are predominantly expressed by macrophages are critical in mounting host defense responses against the invading pathogens. Mincle receptor mainly recognizes the glycolipids present on the pathogens. *H. pylori* CGs are a glycolipids which are the characteristic feature of this bacterium. Our study suggest that may CGs work as a ligands in order to induce Mincle receptor expression in macrophages obtained from human and mice as it was evident from the *in vitro* experiments performed. The reduction of Mincle expression in mice-macrophages and human-macrophages upon infection by *hp0421* mutants that lack CGs indicates that the presence of CGs is required to upregulate Mincle expression in macrophage cells. Restoration of Mincle expression comparable to the Mincle expression level in cells infected with wild-type and *Hp76Δ421*-reconstituted provides a strong evidence that CGs could perhaps play an important role in induction of Mincle receptor. In line with this, previous studies have also demonstrated that the glycolipids present on some pathogens are responsible for Mincle receptor induction. For example Mycobacterial trehalose-6-6'-dimycolate (TDM) which is present on *M. tuberculosis* cell wall is a potent trigger that induces immune response upon interaction with Mincle receptor [167]. Furthermore, the glycolipid α -Glucosyl diacylglycerides from *Streptococcus pneumonia* was shown to induce Mincle expression in Mincle reporter cell line [168]. Overall, our results indicate that *H. pylori* CGs induces Mincle receptor response in animals and modulates host immune response through Mincle expression. These observations provide important insights into the innate immune responses mediated by *H.*

pylori which could be helpful in targeting immune based control of infections and *H. pylori* eradication strategies.

Role of cholesterol glucosylation in maintenance of *Helicobacter pylori* morphology, cell wall integrity and regulation of Mincle receptor response

ORIGINALITY REPORT

8%

SIMILARITY INDEX

3%

INTERNET SOURCES

7%

PUBLICATIONS

1%

STUDENT PAPERS

PRIMARY SOURCES

1

Dunne, Ciara. "Factors that mediate colonization of the human stomach by *Helicobacter pylori*", *World Journal of Gastroenterology*, 2014.

Publication

1%

2

"Molecular Pathogenesis and Signal Transduction by *Helicobacter pylori*", Springer Nature, 2017

Publication

1%

3

Helicobacter pylori, 2016.

Publication

1%

4

Ellen Hildebrandt. "Helicobacter pylori lipopolysaccharide modification, Lewis antigen expression, and gastric colonization are cholesterol-dependent", *BMC Microbiology*, 2009

Publication

1%

5

L. Zheng. "CcpA regulates biofilm formation

<1%

and competence in *Streptococcus gordonii* :
CcpA regulates biofilm formation of
S. gordonii", Molecular Oral Microbiology,
04/2012

Publication

6

www.ibpc.fr

Internet Source

<1 %

7

Li, Hong, Tingting Liao, Aleksandra W. Debowski, Hong Tang, Hans-Olof Nilsson, Keith A. Stubbs, Barry J. Marshall, and Mohammed Benghezal. "Lipopolysaccharide Structure and Biosynthesis in *Helicobacter pylori*", *Helicobacter*, 2016.

Publication

<1 %

8

www.ncbi.nlm.nih.gov

Internet Source

<1 %

9

edoc.ub.uni-muenchen.de

Internet Source

<1 %

10

Yilmaz Emre Gencay. "Sheep as an important source of *E. coli* O157/O157:H7 in Turkey", *Veterinary Microbiology*, 2014

Publication

<1 %

11

www.frontiersin.org

Internet Source

<1 %

12

Holgado, M Angeles, Martin-banderas, Alvarez-fuentes, Duran-lobato, Jose Prados, Melguizo,

<1 %

and Fernandez-arevalo. "Cannabinoid derivate-loaded PLGA nanocarriers for oral administration: formulation, characterization, and cytotoxicity studies", International Journal of Nanomedicine, 2012.

Publication

13

Hung-Jung Wang. "Helicobacter pylori cholesteryl glucosides interfere with host membrane phase and affect type IV secretion system function during infection in AGS cells : Cholesterol glucosylation influences membrane dynamics", Molecular Microbiology, 01/2012

Publication

<1 %

14

academic.oup.com

Internet Source

<1 %

15

www.reproduction-online.org

Internet Source

<1 %

16

Delcour, A.H.. "Outer membrane permeability and antibiotic resistance", BBA - Proteins and Proteomics, 200905

Publication

<1 %

17

Park, Hae-Ran, Sung-Kee Jo, and Sang-Gi Paik. "The NK1.1+T cells alive in irradiated mice play an important role in a Th1/Th2 balance", International Journal of Radiation Biology, 2006.

Publication

<1 %

18

M. Fukuda. " 1,4GlcNAc-capped mucin-type O-glycan inhibits cholesterol -glucosyltransferase from Helicobacter pylori and suppresses H. pylori growth", Glycobiology, 04/09/2008

Publication

<1 %

19

Spencer J. Williams. "Sensing Lipids with Mincle: Structure and Function", Frontiers in Immunology, 2017

Publication

<1 %

20

www.pathogenomics-era.net

Internet Source

<1 %

21

repub.eur.nl

Internet Source

<1 %

22

www-brs.ub.ruhr-uni-bochum.de

Internet Source

<1 %

23

Kazmierczak, B. I., K. Mostov, and J. N. Engel. "Interaction of Bacterial Pathogens with Polarized Epithelium", Annual Review of Microbiology, 2001.

Publication

<1 %

24

Submitted to University of Hong Kong

Student Paper

<1 %

25

jcb.rupress.org

Internet Source

<1 %

26

Anna Rzepkowska, Dorota Zielińska,

<1 %

Aleksandra Ołdak, Danuta Kołożyn-Krajewska.
" Organic whey as a source of strains with
selected technological and antimicrobial
properties ", International Journal of Food
Science & Technology, 2017

Publication

27

"MicroRNA Profiling", Springer Nature, 2017

Publication

<1 %

28

www.jyoungpharm.org

Internet Source

<1 %

29

link.springer.com

Internet Source

<1 %

30

repec.ioe.ac.uk

Internet Source

<1 %

31

Submitted to Mahidol University

Student Paper

<1 %

32

Yi-Ying Wu. " enhances tumor necrosis factor-
related apoptosis-inducing ligand-mediated
apoptosis in human gastric epithelial cells ",
World Journal of Gastroenterology, 2004

Publication

<1 %

33

Submitted to Napier University

Student Paper

<1 %

34

Nagar, Jignesh Patel, Praful Mohapatra,
Jogeswar Sharma, Manoranjan Pandya,

<1 %

Gaurav Umar, Malik Chatt. "Differential effects of dexamethasone and rosiglitazone in a sephadex-induced model of lung inflammation", Indian Journal of Pharmacology, March-April 2015 Issue

Publication

35

Liu, Ting, Ai-Ping Qin, Bin Liao, Hui-Ge Shao, Li-Juan Guo, Gen-Qing Xie, Li Yang, and Tie-Jian Jiang. "A novel microRNA regulates osteoclast differentiation via targeting protein inhibitor of activated STAT3 (PIAS3)", Bone, 2014.

Publication

<1 %

36

cancerbiomedcentral.com

Internet Source

<1 %

37

d-nb.info

Internet Source

<1 %

38

Coleman, James L., Alvaro Toledo, and Jorge L. Benach. "Borrelia burgdorferi HtrA: evidence for twofold proteolysis of outer membrane protein p66 : Proteolysis of p66 by HtrA in Borrelia", Molecular Microbiology, 2015.

Publication

<1 %

39

Christian Wunder, Yuri Churin, Florian Winau, Dirk Warnecke et al. "Cholesterol glucosylation promotes immune evasion by Helicobacter pylori", Nature Medicine, 2006

<1 %

40	www.scribd.com Internet Source	<1 %
41	lra.le.ac.uk Internet Source	<1 %
42	Submitted to University of Sheffield Student Paper	<1 %
43	www.biomedcentral.com Internet Source	<1 %
44	www.jimmunol.org Internet Source	<1 %
45	Submitted to Brunel University Student Paper	<1 %
46	www.plantphysiol.org Internet Source	<1 %
47	preview-ojrd.biomedcentral.com Internet Source	<1 %
48	A. X. Tran. "The Lipid A 1-Phosphatase of Helicobacter pylori Is Required for Resistance to the Antimicrobial Peptide Polymyxin", Journal of Bacteriology, 06/15/2006 Publication	<1 %
49	Kwak, Kyu-Won, Myung-Sae Han, Sung-Hee Nam, Ji-Young Choi, Seok-Hyun Lee, Young-	<1 %

Cheol Choi, and Kwan-Ho Park. "Detection of Insect Pathogen *Serratia marcescens* in *Protaetia brevitarsis seulensis* (Kolbe) from Korea", International Journal of Industrial Entomology, 2014.

Publication

50

ediss.sub.uni-hamburg.de

Internet Source

<1 %

51

Shiota, Seiji, Rumiko Suzuki, and Yoshio Yamaoka. "The significance of virulence factors in *Helicobacter pylori* : Virulence factors in", Journal of Digestive Diseases, 2013.

Publication

<1 %

52

www.spandidos-publications.com

Internet Source

<1 %

53

www.bioone.org

Internet Source

<1 %

54

preview-annals-general-psychiatry.biomedcentral.com

Internet Source

<1 %

55

Senthilkumar Palaniyandi, Arindam Mitra, Christopher D. Herren, Xiaoping Zhu, Suman Mukhopadhyay. "LuxS contributes to virulence in avian pathogenic *Escherichia coli* O78:K80:H9", Veterinary Microbiology, 2013

Publication

<1 %

Exclude quotes On

Exclude bibliography On

Exclude matches < 10 words